DEPARTMENT OF MINES AND ENERGY
GOVERNEMENT OF NEWFOUNDLAND AND LABRADOR

Contribution to Canada-Newfoundland Mineral Development Agreement 1984-89, a subsidiary agreement under the Economic and Regional Development Agreement. Project funded by the Geological Survey of Canada.

Energy, Mines and Resources Canada
Énergie, Mines et Ressources Canada

92-01232/

GEOLOGICAL SURVEY OF CANADA
BULLETIN 395

GEOLOGY OF THE LONG RANGE INLIER, NEWFOUNDLAND

J. Victor Owen

1991

©Minister of Supply and Services Canada 1991

Available in Canada through

authorized bookstore agents and other bookstores

or by mail from

Canadian Government Publishing Centre
Supply and Services Canada
Ottawa, Canada K1A 0S9

and from

Geological Survey of Canada offices:

601 Booth Street
Ottawa, Canada K1A 0E8

3303-33rd Street N.W.,
Calgary, Alberta T2L 2A7

A deposit copy of this publication is also available for reference
in public libraries across Canada

Cat. No. M42-395E
ISBN 0-660-13753-4

Price subject to change without notice

Cover photo

*Granulite of the Long Range gneiss complex
at Western Brook Pond*

Author's Address

Department of Geology
Saint Mary's University
Halifax, Nova Scotia
B3H 3C3

Critical Readers

H.H. Bostock
K.L. Currie

CONTENTS

1 Abstract/Résumé

2 Summary/Sommaire

4 Introduction
- 5 Access
- 5 Previous work
- 7 Topography and drainage
- 7 Glacial and surficial geology
- 7 Acknowledgments
- 7 Lithological subdivision of the Long Range Inlier

8 General Geology
- 8 The Long Range Gneiss Complex
  - 8 Lithology
    - 8 Quartzofeldspathic gneiss
    - 11 Pelitic gneiss
    - 14 Metacarbonate rocks
    - 14 Quartzite
    - 14 Mafic gneiss
    - 14 Schistose and phyllitic rocks
  - 15 Age relations
- 15 Plutonic rocks
  - 15 Geophysical expression
  - 15 The Taylor Brook gabbro complex
    - 15 Lithology
    - 18 Age relations
    - 18 Mineralogy
    - 18 Geochemistry
  - 18 Granitoid plutons
    - 19 The Lake Michel intrusive suite
    - 20 Lithology
      - 20 Charnockitic rocks
    - 23 "Intermediate" granite
    - 24 Leucocratic granitoid rocks
    - 25 Age relations
    - 25 Mineralogy
    - 26 Geochemistry
    - 28 The Potato Hill pluton
    - 28 Lithology
    - 30 Age relations
    - 32 Mineralogy
    - 34 Geochemistry
    - 34 Significance of the corona structures
    - 35 Petrography and geochemistry of other granitoid plutons
    - 38 Tectonic setting of the Grenvillian plutons
- 38 Late Proterozoic and Paleozoic rocks
  - 38 The Long Range dykes
    - 39 Petrography and mineralogy
    - 40 Age relations
    - 40 Geochemistry
  - 42 Porphyritic felsic dykes
  - 43 The Devils Room pluton
  - 46 Paleozoic supracrustal rocks
  - 47 Post-Coney Arm Group mafic dykes

48 Metamorphism
48 Metamorphism 1: Pre-plutonic stage
48 Age and metamorphic grade
48 Mineral chemistry
50 Metamorphic P-T conditions
51 Geobarometry
52 Geothermometry
54 Metamorphic fluids
54 Interpretation
56 Metamorphism 2: Syn-plutonic stage
56 Age and metamorphic grade
56 Metamorphic conditions
57 The metamorphic aureole of the Taylor Brook gabbro complex
57 Thermally metamorphosed pelitic gneiss
59 Metamorphism of the carbonate sequence
59 Metamorphism 3: Post-plutonic stage
59 Age and metamorphic grade
60 Metamorphic conditions
61 Metamorphism 4: Post-Long Range dyke stage

64 Structure
64 Proterozoic structures
67 Paleozoic structures

69 Economic geology
69 Gold
70 Copper
70 Heavy minerals
70 Phosphate
70 Quartz
70 Summary

70 Discussion
71 Proterozoic evolution
71 Paleozoic evolution
71 Correlations to the north
73 Correlations to the southwest

74 References

Appendices

79 Appendix I: Analytical methods
80 Appendix II: Microprobe mineral analyses
86 Appendix III: Bulk rock analyses

Tables

9 1. Modal composition of representative samples of quartzofeldspathic gneiss
19 2. Geochemistry of the Taylor Brook gabbro complex
19 3. Major rock units of the Lake Michel intrusive suite
23 4. Modal composition of the Lake Michel intrusive suite
26 5. Microprobe analyses of pyroxenes of diverse charnockitic plutons
27 6. Analyses and nomenclature of hornblende of the Lake Michel intrusive suite
28 7. Geochemistry and CIPW norms of the Lake Michel intrusive suite
34 8. Analyses of minerals of the Potato Hill pluton

35 9. Geochemistry and CIPW norms of the Potato Hill pluton
36 10. Geochemistry of diverse Grenvillian granitoid plutons
37 11. Geochemistry of the East Aides River pluton
41 12. Analyses of minerals (igneous phases) of the Long Range dykes
43 13. Geochemistry of the Long Range dykes
44 14. Interdyke compositional variation of the Long Range swarm
44 15. Isocon (composition-volume) data for the Long Range dykes
45 16. Petrogenetic modelling of the Long Range dykes
46 17. Geochemistry of felsic porphyry dykes
46 18. Analyses of minerals of the Devils Room pluton
48 19. Analyses of minerals of a Paleozoic mafic dyke
48 20. Mineral assemblages of the Long Range gneiss complex
51 21. Thermochemical data for thermobarometric equilibria
51 22. Compositional parameters and P-T determinations for coexisting gt-opx-pl-qz
52 23. Compositional parameters and P-T determinations for coexisting gt-cd-(sil-opx)
53 24. Compositional parameters and P-T determinations for coexisting gt-pl-sil-qz
54 25. Compositional parameters and P-T determinations for coexisting gt-bi
61 26. Analyses of garnet, biotite, and hornblende from deformed coronitic charnockite
62 27. Mineral analyses (metamorphic and relict phases) of the Long Range dykes
63 28. Model metamorphic reactions for the Long Range dykes
65 29. Summary of structural, metamorphic, and plutonic events in the Long Range Inlier

Illustrations

In pocket Map 1764A. Geology of the Long Range Inlier, Newfoundland
4 1. Regional geological setting for the Long Range Inlier
5 2. Distribution of Precambrian massifs in the Appalachian Orogen
6 3. Foot traverses and helicopter coverage
7 4. Glacial flow directions in the Long Range Inlier
8 5. Distribution of high grade mineral assemblages in the Long Range gneiss complex
9 6. Modal composition of quartzofeldspathic gneiss
10 7. Field photographs of quartzofeldspathic gneiss
12 8. Distribution of pelitic gneiss, quartzite, and marble
13 9. Field photographs of pelitic gneiss and quartzite
16 10. Geophysical data for the Long Range Inlier
16 11. Sketch map of the Taylor Brook gabbro complex
17 12. Field photographs and photomicrographs of the Taylor Brook gabbro complex
20 13. Distribution of Grenvillian plutonic rocks
20 14. Nomenclature of plutons in the Long Range Inlier
21 15. Sketch map of the Lake Michel intrusive suite
22 16. Field photographs of the Lake Michel intrusive suite
24 17. Modal composition of the Lake Michel intrusive suite and the Potato Hill pluton
24 18. Photomicrographs of charnockitic plutonic rocks
27 19. Composition of amphiboles from the Lake Michel intrusive suite and the Potato Hill pluton
28 20. AFM diagram for the Lake Michel intrusive suite
29 21. Variation diagrams for the Lake Michel intrusive suite
30 22. Trace element relations in the Lake Michel intrusive suite
31 23. Nb/La versus Th/La in the Lake Michel intrusive suite
31 24. P versus La and Zr plots for the Lake Michel intrusive suite
31 25. Sketch map of the Potato Hill pluton
32 26. Field photographs of the Potato Hill pluton
32 27. Photomicrograph of typical corona structure in charnockite of the Potato Hill pluton
38 28. Normative Qz-Ab-Or and An-Ab-Or diagrams for the East Adies River pluton and the Lake Michel intrusive suite

39 29. Trace element discrimination diagrams for the Lake Michel intrusive suite and the Potato Hill pluton
40 30. Ga/%Al plotted against alkalies and various high field strength elements in the Lake Michel intrusive suite and the Potato Hill pluton
41 31. Distribution of the Long Range dykes
42 32. Photographs and photomicrographs of a deformed and metamorphosed Long Range dyke
44 33. Isocon diagram for fresh and metamorphosed Long Range dykes
45 34. Photographs of a felsic porphyry dyke
46 35. Sketch map of the Devils Room pluton
47 36. Photographs of conglomerate and arkose at the basal unconformity of the Coney Arm Group
49 37. Photomicrographs of high grade mineral assemblages of the Long Range gneiss complex
50 38. Compositional profiles of garnet
52 39. Results of gt-opx-pl-qz geothermobarometry
54 40. Results of two-pyroxene geothermometry
55 41. Results of P-T determinations in the Long Range Inlier
56 42. Variation of garnet-biotite temperatures in metapelite flanking the Hooping Harbour satellite pluton
57 43. Sketch map of pelitic gneiss and metacarbonate rocks near the Taylor Brook gabbro complex
58 44. Photographs of pelitic gneiss near the Taylor Brook gabbro complex
60 45. Photographs of calc-silicate rocks from the marble sequence near the Taylor Brook gabbro complex
63 46. Nomenclature of calcic amphibole from a deformed Long Range dyke
63 47. Plot showing Ti versus Al(total) for calcic amphibole from a deformed Long Range dyke
64 48. Plot comparing tetrahedral Al ("Al^{iv}") and A-site Na+K for different generations of amphibole in metamorphosed Long Range dykes
64 49. Paleozoic(?) mylonite cutting the Taylor Brook gabbro complex
66 50. Multiply-folded leucocratic veins in migmatitic granitic gneiss
67 51. Distribution of faults and large northwest-trending folds in the Long Range gneiss complex
68 52. Field photographs of granitic pegmatite associated with shallow-dipping Paleozoic(?) faults at Devil Cove
69 53. Gold prospects in the Sops Arm area
72 54. Lithotectonic entities in the eastern Grenville Province

GEOLOGY OF THE LONG RANGE INLIER, NEWFOUNDLAND

Abstract

In northwestern Newfoundland, Proterozoic basement exposed in the Long Range Inlier comprises three lithostratigraphic groupings: (1) a high grade gneiss complex; (2) Grenvillian granitic-charnockitic plutons; and (3) latest Proterozoic (ca. 615 Ma) mafic dykes. The gneiss complex comprises granulite and amphibolite derived from protoliths at least 1550 Ma old. Metamorphic grade and temperature increase southwestward. Metamorphic pressure ranges from 5 to 8 kbar throughout the inlier. Northwest-trending large-scale folds dominate the structure of the gneiss complex. The age of these fold structures relative to the Grenvillian plutons is not certain.

The voluminous granitic-charnockitic plutons were emplaced at about 1056 Ma, and are approximately coeval with similar granitoid rocks in the Grenville Province of southern Labrador. Grenvillian plutonism in both regions terminated at about 970 Ma. These plutons delineate a 350 km wide Grenvillian magmatic belt south of a 225 km wide north-verging fold-and-thrust belt which is bounded to the north by the Grenville Front. The fold-and-thrust belt is composed of Labradorian (ca. 1650 Ma) crust which was reworked during the Grenvillian Orogeny (ca. 1000 Ma). A 30 km wide shear zone separates these two terranes in southeastern Labrador. The Grenvillian plutons occur in a structurally-high crustal block(s), implying that they were derived (at least in part) from thrust-induced anatexis of underlying Labradorian terranes presently exposed to the northwest. Biotite-hornblende granites in the Long Range Inlier have geochemical signatures consistent with an anatectic origin; however, coeval charnockitic rocks appear to have been derived at least in part from a depleted source (e.g., upper mantle or the refractory residue of previously melted crust). Both types of granitoids were deformed late during this plutonic episode (ca. 978 Ma).

Paleozoic orogenies resulted in mafic to felsic magmatism (e.g., the Devils Room pluton (ca. 390 Ma)), a structural and metamorphic overprint near the southeastern margin of the inlier, and the displacement of the massif toward the west. Displacement was accommodated by movement on an east-dipping thrust or reverse fault (Long Range frontal thrust) which separates the inlier from Paleozoic platform in the foreland to the west. Geophysical evidence suggests minimal horizontal displacement across this fault.

The economic potential of the inlier appears to be largely restricted to gold prospects in Grenvillian granite and nearby quartzofeldspathic gneiss and Paleozoic cover rocks near White Bay.

Résumé

Dans le socle protérozoïque du nord-ouest de Terre-Neuve, qui affleure dans la fenêtre de Long Range, sont présents trois groupements lithostratigraphiques: 1) un complexe gneissique fortement métamorphisé; 2) des plutons granitiques-charnockitiques du Grenvillien; et 3) des dykes mafiques du sommet du Protérozoïque (environ 615 Ma). Le complexe gneissique comprend des amphibolites et granulites dérivées de protolites âgés d'au moins 1550 Ma. Le degré de métamorphisme et la température augmentent vers le sud-ouest. La pression du métamorphisme se situe entre 5 et 8 kbar à travers toute la fenêtre. De grands plis d'orientation générale nord-ouest dominent la structure du complexe gneissique. L'âge de ces structures plissées par rapport à celui des plutons du Grenvillien est incertain.

Les volumineux plutons granitiques-charnockitiques ont été mis en place il y a environ 1056 Ma, et sont approximativement contemporains de roches granitoïdes similaires existant dans la province de Grenville du Labrador méridional. Dans les deux régions, le plutonisme du Grenvillien s'est terminé il y a environ 970 Ma. Ces plutons délimitent une ceinture magmatique d'âge grenvillien, de 350 km de large, au sud d'une zone de plissement et chevauchement de 225 km de large, s'inclinant vers le nord, limitée au nord par le front de Grenville. La zone de plissement et chevauchement se compose d'une croûte d'âge labradorien (environ 1650 Ma) qui a été remaniée durant l'orogénèse du Grenvillien (il y a environ 1000 Ma). Une zone de cisaillement de 30 km de large sépare ces deux terranes dans le sud-est du Labrador. Les plutons du Grenvillien apparaissent dans un bloc crustal surélevé; ils seraient donc peut-être le résultat (au moins partiellement) d'une anatexie, causée par les charriages, des terranes *labradoriens qui actuellement affleurent au nord-ouest. Les granites à biotite et hornblende de la fenêtre de Long Range montrent des signatures géochimiques concordant avec une origine anatectique ; cependant, des roches charnockitiques contemporaines semblent être en partie dérivées d'une source épuisée (p. ex., manteau supérieur ou résidus réfractaires d'une croûte antérieurement en état de fusion). Les deux types de roches granitoïdes se sont tardivement déformés durant cette épisode plutonique (environ 978 Ma).*

Les orogénèses survenues au Paléozoïque ont donné lieu à un magmatisme de caractère mafique à felsique (p. ex., la formation du pluton de Devils Room ; environ 390 Ma), à la surimpression structurale et métamorphique proche de la marge sud-est de la fenêtre, et au déplacement du massif vers l'ouest. Ce déplacement a été rendu possible par le mouvement le long d'une faille chevauchante ou d'une faille inverse de pendage est (chevauchement frontal de Long Range), qui sépare la fenêtre de la plate-forme paléozoïque située dans l'avant-pays à l'ouest. Les indices géophysiques suggèrent un rejet horizontal minimal de part et d'autre de cette faille.

Le potentiel économique de la fenêtre semble largement limité au gîte aurifère possible présent dans le granite et les gneiss quartzofeldathiques proches, qui sont d'âge grenvillien, et les roches de la couverture paléozoïque proches de White Bay.

SUMMARY

Gneissic and intrusive rocks of the Long Range Inlier correlate with Grenvillian rocks north of the Strait of Belle Isle on lithological and geochronological grounds. Both areas consist of a medium to high grade gneiss complex which was intruded first by granitoid plutons during the Grenvillian Orogeny (ca. 1056-970 Ma), and subsequently by northeast-trending tholeiitic dykes (615 Ma). Paleozoic orogenesis in the inlier is recorded by a low grade tectonometamorphic overprint and the emplacement of an Acadian granite (Devils Room granite; 390 Ma).

The inlier forms a structural culmination bounded to the southwest and northeast by structural depressions occupied by Taconic allochthons. Stratigraphic and structural contacts separate the inlier from Lower Paleozoic platformal rocks to the north and south. The western margin of the inlier is partly bounded by an east-dipping reverse or thrust fault (Long Range frontal thrust). Horizontal displacement on this fault appears to be minimal, since the geophysical signature of a large Grenvillian pluton in the inlier (Lake Michel intrusive suite) may be traced across the thrust. Vertical displacement of the inlier relative to the adjacent Grenville Province also appears to be minimal, since gneissic rocks on both sides of the Strait of Belle Isle yield similar pressure estimates from quantitative geobarometry.

The Long Range gneiss complex is dominated by biotite-bearing quartzofeldspathic rocks (orthogneiss?). Obvious paragneiss is restricted to narrow screens (≤ 1 km wide). Pelitic gneiss typically contains sillimanite, biotite, garnet and/or cordierite, graphite, and hercynite. In places, both quartzite and cordierite-garnet-biotite-orthopyroxene-graphite-bearing semipelitic gneiss are spatially associated with the pelites. Marble is virtually restricted to a pelite-calc-silicate rock sequence flanking a large mafic pluton (Taylor Brook gabbro complex).

SOMMAIRE

Les roches gneissiques et intrusives de la fenêtre de Long Range peuvent être mises en corrélation directe lithologiquement et géochronologiquement, avec des roches du Grenvillien au nord du détroit de Belle-Isle. Les deux régions sont constituées d'un complexe de nature moyennement à fortement gneissique, qui a été pénétré d'abord par des plutons granitoïdes pendant l'orogenèse grenvillienne (vers 1056 à 970 Ma), et plus tard par des dykes tholéiitiques de direction nord-est (615 Ma). L'orogenèse paléozoïque de la fenêtre se manifeste par une surimpression d'un métamorphisme diastrophique de faible degré et la mise en place d'un granite acadien (granite de Devils Room; 390 Ma).

La fenêtre forme une culmination structurale bordée au sud-ouest et au nord-est par des dépressions structurales remplies d'allochtones taconiques. Les contacts stratigraphiques et structuraux séparent la fenêtre de roches de plate-forme du Paléozoïque inférieur au nord et au sud. La marge ouest de la fenêtre est partiellement bordée par une faille inverse ou une faille chevauchante à pendange est (chevauchement frontal de Long Range). Le déplacement horizontal sur cette faille semble peu important, car la signature géophysique d'un grand pluton grenvillien situé à l'intérieur de la fenêtre (série intrusive de Lake Michel) peut être suivie en travers du chevauchement. Le déplacement vertical de la fenêtre par rapport à la province de Grenville contiguë semble être également peu important, car des roches gneissiques situées de chaque côté du détroit de Belle-Isle donnent des estimations analogues de pression obtenues par géobarométrie quantitative.

Des roches quartzo-feldspathiques à biotite (orthogneiss?) constituent le principal élément du complexe gneissique de Long Range. Des paragneiss évidents sont confinés dans des écrans étroits (≤ 1 km de large). Le gneiss pélitique renferme habituellement de la sillimanite, de la biotite, du grenat ou de la cordiérite, ou les deux, du graphite et de l'hercynite. Par endroits, du quartzite et du gneiss semipélitique à cordiérite, grenat, biotite, orthopyroxène et graphite, sont associés spatialement aux pélites. Le marbre est pratiquement confiné dans

Pre-Paleozoic metamorphic grade spans amphibolite to granulite facies, and increases toward the southwest. The amphibolite/granulite transition appears to be related to a temperature increase; metamorphic pressures ranges from 5 to 8 kbar (500-800 MPa) throughout the inlier. The role of fluid activities has not been determined.

Planar fabrics and lithological layering (e.g., paragneiss and quartzite screens) in the gneiss complex outline large northwest-plunging fold structures of uncertain age relative to the Grenvillian granitoid plutons.

The presence of ca. 1.0 Ga granitoid rocks characterizes the inlier and the southern part of the Grenville Province in Labrador (Pinware Terrane) as a Grenvillian magmatic belt tectonically analogous to the Higher Himalayas. The Grenvillian plutons are equigranular to megacrystic biotite-hornblende granites (sensu lato). Pyroxene-bearing ("charnockitic") granitoids occur in two composite intrusions (Lake Michel intrusive suite and Potato Hill pluton). Discrimination diagrams based on Y, Nb, and Rb suggest that the Grenvillian plutons are within-plate intrusions. Elevated Ga/Al ratios indicate A-type affinities. The most iron-rich intrusion (Potato Hill pluton) is garnetiferous. Charnockite in this composite intrusion contains garnetiferous corona structures interpreted to have formed during subsolidus cooling of the pluton. Garnet of probable magmatic origin occurs in equigranular hornblende-biotite granite in the Potato Hill pluton.

The Grenvillian plutons are massive to foliated. Foliation is defined by preferentially-oriented feldspar megacrysts, elongated clots of mafic minerals, and, in places, quartz ribbons. Foliation is generally concordant with planar structures in the gneissic country rock, but is regionally cut by the Long Range dykes. The largest intrusion, the Lake Michel intrusive suite (1500 km^2), has a concentric structure outlined by curviplanar plutons and kilometre-scale gneissic enclaves, and by foliation. Structural concordance with the country rock suggests diapiric emplacement of the intrusive suite.

The Long Range dykes were emplaced during initial rifting associated with the opening of the proto-Atlantic ocean. Despite a pronounced Paleozoic tectonothermal overprint in dykes in the eastern part of the swarm, primary geochemical signatures appear to have been preserved. Variations in the concentration of immobile incompatible elements (e.g., Nb, Zr, Ti) are better explained by fractional crystallization processes than by metasomatism.

The economic potential of the inlier appears to be largely restricted to gold mineralization associated with shear zones cutting basement and cover rocks in the White Bay area.

une série de roches pélitiques et calcosilicatées flanquant un grand pluton mafique (complexe gabbroïque de Taylor Brook).

Un métamorphisme pré-paléozoïque, allant du faciès des amphibolites au faciès des granulites, augmente vers le sud-ouest. Le passage du faciès des amphibolites au faciès des granulites semble être lié à une augmentation de température; la pression métamorphique varie de 5 à 8 kbar (de 500 à 800 MPa) à travers toute la fenêtre. On n'a pas déterminé le rôle joué par les fluides.

Des fabriques planaires et une foliation lithologique (p. ex., écrans de paragneiss et de quartzite), caractérisant le complexe gneissique, délimitent de grandes structures plissées plongeant vers le nord-ouest dont l'âge est incertain par rapport aux plutons granitoïdes du Grenvillien.

On considère la fenêtre et la partie sud de la province de Grenville au Labrador (terrane de Pinware) comme une zone magmatique du Grenvillien dont la tectonique est analogue au Grand Himalaya, à cause de la présence de roches granitoïdes, datant d'environ 1 Ga. Les plutons du Grenvillien sont constitués de granites (sensu lato) de nature isométrique à mégacristalline, à biotite et hornblende. Des granitoïdes à pyroxène (charnockitiques) se trouvent dans deux intrusions composites (série intrusive de Lake Michel et pluton de Potato Hill). Des diagrammes de discrimination fondés sur Y, Nb et Rb semblent indiquer que les plutons grenvilliens sont des intrusions se manifestant à l'intérieur des plaques. Les rapports élevés de Ga/Al indiquent des affinités de type A. L'intrusion la plus riche en fer (pluton de Potato Hill) est grenatifère. La charnockite de cette intrusion hétérogène renferme des structures coronotisées grenatifères qui, d'après l'auteur, se seraient formées au cours d'un refroidissement subsolidus du pluton. On trouve du grenat d'origine probablement magmatique dans le granite isométrique à hornblende et biotite du pluton de Potato Hill.

Les plutons grenvilliens sont massifs et feuilletés. Cette structure feuilletée est définie par des mégacristaux de feldspath à orientation préférentielle, des flocons allongés de minéraux mafiques et, par endroits, des rubans de quartz. La foliation concorde généralement avec des structures planaires des roches encaissantes gneissiques, mais est généralement traversée par les dykes de Long Range. La plus grande intrusion, la série intrusive de Lake Michel (1500 km^2), a une structure concentrique définie par des plutons curviplanaires et des enclaves gneissiques de taille kilométrique, et par la foliation. La concordance structurale avec les roches encaissantes laisse supposer une mise en place diapirique de la série intrusive.

Les dykes de Long Range ont été mis en place au cours de l'effondrement initial associé à l'ouverture de l'océan proto-Atlantique. Malgré une surimpression tectono-thermique prononcée au Paléozoïque dans les dykes de la partie est du groupe, des signatures géochimiques primaires semblent avoir été conservées. On explique mieux les variations de la concentration d'éléments incompatibles immobiles (p. ex., Nb, Zr, Ti) par des processus de cristallisation fractionnée que par le métamorphisme.

Le potentiel économique de la fenêtre semble être largement limité à une minéralisation en or associée à des zones de cisaillement traversant le socle et les roches de couverture de la région de White Bay.

INTRODUCTION

The Long Range Inlier is a massif of Proterozoic crystalline rocks which forms the core of the northern Long Range mountains in northwestern Newfoundland. The inlier is exposed in a northeast-trending rectangular area of approximately 9000 km^2 which is bounded by latitudes 49°20′ and 50°50′ (Fig. 1).

The Long Range Inlier is the northeasternmost of a series of basement massifs within the Appalachian Orogen (Fig. 2). It forms a structural culmination bounded to the southwest and northeast by structural depressions occupied by Taconic allochthons (Fig. 1; Williams and Erdmer, 1986), and is unconformably overlain by Lower Paleozoic platformal rocks on its southern and northern margins. Cambro-Ordovician clastic platformal rocks of the Coney Arm Group (Smyth and Schillereff, 1982) were deformed along the southeastern margin of the inlier prior to deposition of redbeds of the Carboniferous Deer Lake basin (Hyde, 1982). A moderately southeast-dipping fault (Long Range frontal thrust) separates the inlier from Cambro-Ordovician carbonate rocks to the west. The inlier was emplaced to its present structural position during the Middle Paleozoic (Devonian?; Cawood and Williams, 1986; Williams and Erdmer, 1986).

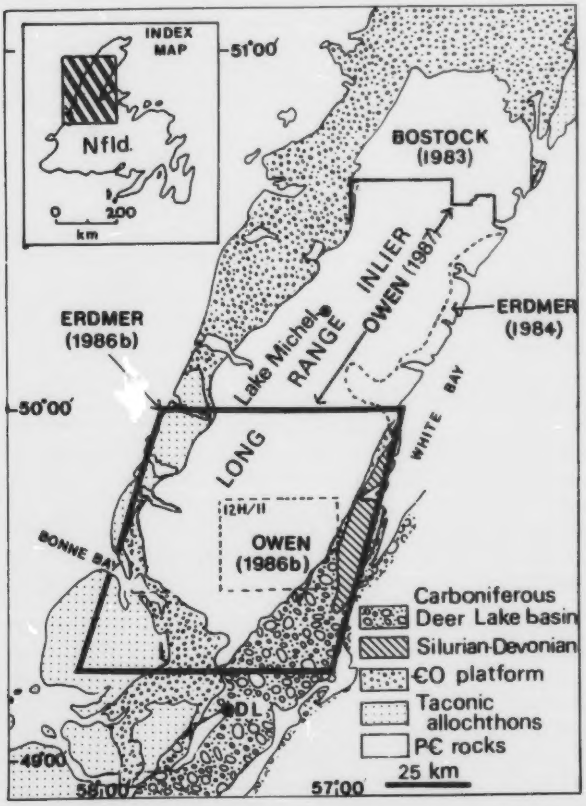

Figure 1. Regional geological setting of the Long Range Inlier, showing areas mapped by Geological Survey of Canada project geologists. DL-Deer Lake.

Although geological mapping of the Long Range Inlier dates back to the pioneering work of Alexander Murray (Murray and Howley, 1881), a systematic investigation of the massif was not undertaken until 1969, when the Geological Survey of Canada (GSC) initiated 1:125 000 scale mapping in the Strait of Belle Isle area. Hewitt Bostock's (1983) map of the northern part of the inlier accompanied a detailed description of the regional geology of this area.

Philippe Erdmer revived the northern Long Range project in 1984 as part of the Canada-Newfoundland Mineral Development Agreement (1984-1989) by mapping the White Bay coastal section, and investigating the Upper Humber River area in the south-central part of the inlier. Erdmer continued mapping in the southern part of the inlier in 1985, working in conjuction with J.V. Owen who conducted more detailed mapping in the Silver Mountain area (NTS 12H/11; Fig. 1). Erdmer's (1986a,b) 1:100 000 scale map of Sandy Lake map area (NTS 12H) covers the southern part of the inlier, including the Silver Mountain map sheet (Owen, 1986a,b). Mapping by Owen in the Lake Michel area (Owen, 1987; Owen et al., 1987) in the central part of the inlier completed the reconnaissance-scale coverage of the massif.

The primary objectives of the northern Long Range project under the Canada-Newfoundland Mineral Development Agreement (1984-1989) were threefold:

1) to produce a series of 1:100 000 scale maps identifying major geological units;
2) to describe the plutonic, metamorphic, and structural evolution of the area;
3) to identify and assess target areas of potential economic interest.

The extent to which these objectives have been met varies.

The accompanying 1:250 000 scale map is based on more detailed 1:50 000 to 1:100 000 scale maps prepared by Erdmer (1986b) and Owen (1986b, 1987), and on Bostock's (1983) 1: 125 000 scale map. Since no additional field data for Bostock's area were available during the preparation of this bulletin, the geology of the northern tip of the inlier has been greatly simplified to accommodate a revised legend. Readers should therefore consult Bostock (1983) for a more detailed description of that area.

The second objective has largely been met as a result of diverse topical studies in preparation, and published elsewhere, which address the isotopic age of gneissic and plutonic rock units (H. Baadsgaard, pers. comm., 1989), the metamorphic geology of the gneiss complex (Owen and Erdmer, 1986, 1989), the tectonic significance of Grenvillian plutons (Owen and Erdmer, in press), the effects of Paleozoic orogenesis on parts of the inlier (Erdmer and Owen, 1988), and the geochemistry of the Long Range dykes (Owen et al., 1989). The results of these studies are summarized herein.

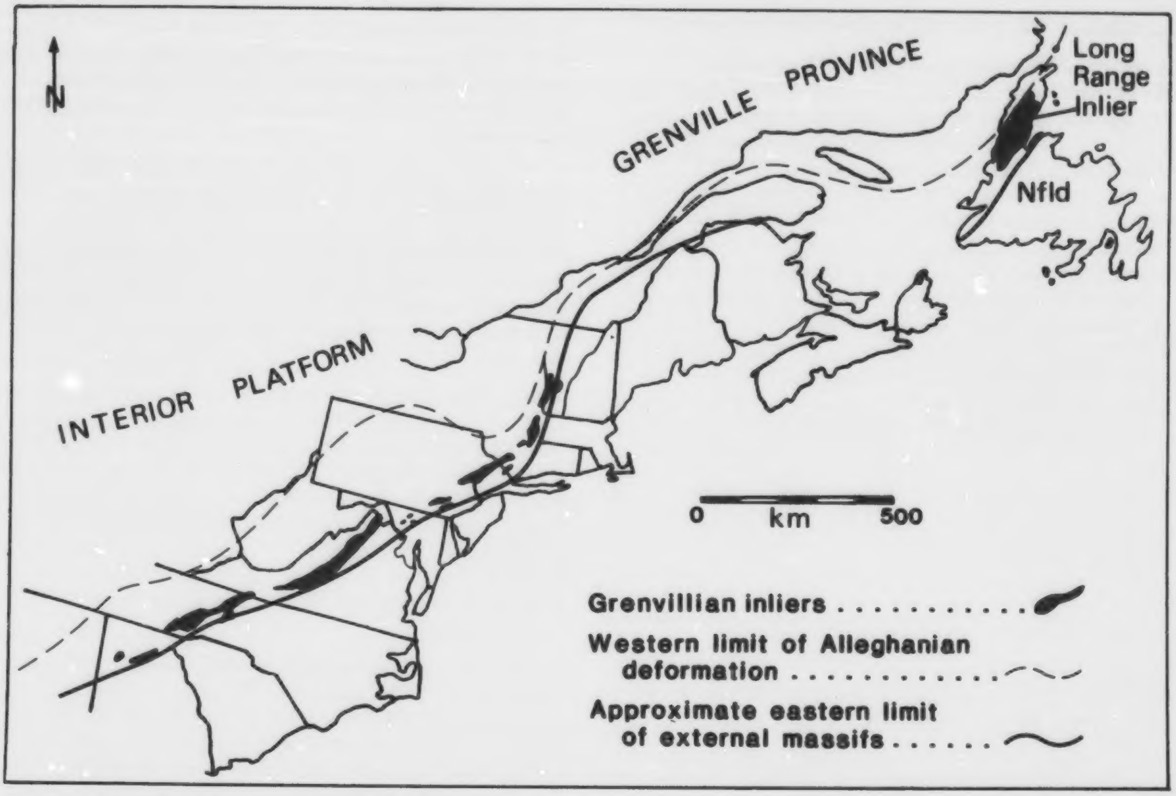
N
GRENVILLE PROVINCE
INTERIOR PLATFORM
Long Range Inlier
Nfld
0 km 500
Grenvillian inliers
Western limit of Alleghanian deformation
Approximate eastern limit of external massifs

Figure 2. Distribution of Grenvillian (sensu lato) massifs in the Appalachian Orogen (after Hatcher, 1983). Solid lines denote political boundaries.

The third objective was hampered by the regional scale of coverage, and by poor exposure in much of the inlier. The 1:250 000 scale map accompanying this bulletin is based, on average, on about one outcrop per square kilometre. Mapping in the southern 70% of the inlier was undertaken both by foot traverse and by helicopter "hopping"; detailed ground coverage is uneven, being largely restricted to fly camp localities and to river channels (Fig. 3).

Access

Until completion of this project, the Long Range Inlier remained the largest unmapped portion of insular Newfoundland. This reflects the relative inaccessibility of the northern Long Range mountains.

Road access is restricted to woods roads in the southern part of the inlier (e.g., along the Upper Humber River), and to the Cat Arm dam access road near Jackson's Arm. Many of the woods roads have not been maintained for several years. Bridges have been washed out and sections of woods roads are overgrown by alders and scrub brush. At time of writing, however, Corner Brook Pulp and Paper Company, Limited had constructed a new bridge across Taylor Brook, and had improved and extended existing woods roads in the Upper Humber River area, thereby facilitating access to some of the most diverse and interesting rocks in the inlier.

Although the inlier is well exposed along the western coast of White Bay, rugged topography restricts access inland. The only practical route to the highlands is by float plane and/or by helicopter. Many of the lakes in the inlier are small, shallow, and shoaly. Dark water makes visual estimation of their depth difficult, and access by float plane may be hazardous. Rivers within the inlier are shoaly and fast-flowing, and are virtually unnavigable (except by canoe, with frequent portages), particularly in the late summer.

Thick forest cover renders much of the southern and eastern parts of the inlier inaccessible to helicopter, although larger outcrops and swamps may be safely accessed, and tundra terrain in the highlands farther to the northwest is ideal for both helicopter-supported work and for foot traverse.

Previous work

The first geological investigations of the Long Range Inlier were restricted to coastal exposures in White Bay. Murray and Howley (1881, 1918) noted that gneissic rocks of the Laurentian system (i.e., of the Precambrian Shield) were

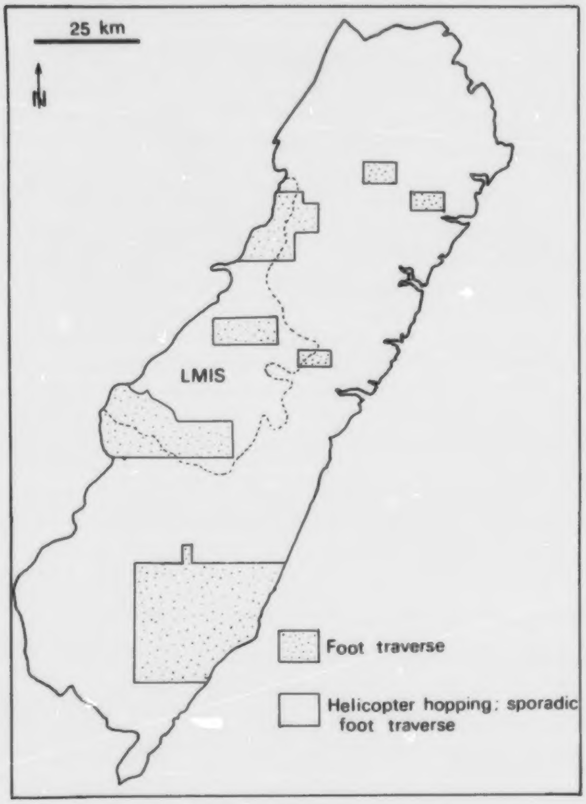

Figure 3. Foot traverses and helicopter coverage of the Long Range Inlier. The Lake Michel intrusive suite (LMIS) is drawn for reference. Foot traverse density for the northern part of the inlier (Bostock, 1983) is not known.

cut by northeast-trending mafic dykes, currently referred to as the Long Range dyke swarm. Attempts at subdividing the crystalline basement were initiated by Foley (1937), who recognized pre-Laurentian pelitic and quartzose rocks, Laurentian gneiss, post-Laurentian granitoid rocks, and mafic dykes in the interior of the inlier, and in coastal exposures on White Bay. He identified glauconite in arenaceous rocks of the Bradore Formation (Schuchert and Dunbar, 1934), which unconformably overlies the basement rocks, and noted the presence of northeast-striking shear zones near Great Harbour Deep, which he interpreted as thrust faults. Similarly-oriented thrusts were identified farther to the northeast by Betz (1939, 1943); these were interpreted to be Paleozoic in age. Foley (1937) suggested that regional structures in the basement rocks define a north-northwest-trending geanticline.

On the basis of three foot-traverses across the inlier, Fritts (1953) defined a Highlands Formation comprising mafic and felsic gneiss, schist, and porphyritic (megacrystic) granite as being distinct from the equigranular Cloud River granite, which he considered to be younger than the porphyritic granite owing to the more "altered" appearance of the latter. Noting the quartz-rich and "conglomeratic" nature of some of the gneissic rocks, he suggested that parts of the gneiss complex were derived from sedimentary protoliths.

Aircraft-supported reconnaissance mapping by Brinco geologists was initiated in the 1950s. Harrison and Johnson, in an unpublished report submitted in 1955, reported the presence of three generations of mafic dykes cutting the gneiss complex, and interpreted large porphyritic granite bodies as sills.

Contact relations between basement and cover rocks were investigated during regional mapping along the western part of the inlier by Oxley (1953), Nelson (1955), and Woodard (1957). These workers noted that basement was thrust over strongly deformed Lower Paleozoic platformal rocks, and concluded that the extent of structural reworking of both basement and cover increased toward the south in this area.

The first compilation map of the area was prepared by Clifford and Baird (1962). Their landmark map distinguished granitic rocks from basement gneiss, and outlined contacts with overlying sedimentary rocks. Metamorphic grade of the gneiss was reported as almandine-amphibolite facies; local evidence of higher metamorphic grade was provided by sillimanite. K-Ar (biotite) ages suggested a Grenvillian age of ca. 945 to 960 Ma for the equigranular and porphyritic granites (Cloud River and Leg Pond plutons, respectively).

Additional isotopic dating by Pringle et al. (1971) confirmed these Grenvillian ages. The largest of the granitoid plutonic complexes, originally termed the Portland Creek pluton and now known as the Lake Michel intrusive suite (Owen, 1987), yielded a Rb-Sr (whole rock) isochron age of 1130 ± 90 Ma, with a low initial ratio of 0.702 ± 0.004. A K-Ar (whole rock) age of 805 ± 35 Ma (Pringle et al., 1971) determined for the Long Range mafic dykes was revised to 605 Ma ($^{40}\mathrm{Ar}/^{39}\mathrm{Ar}$, whole rock, Stukas and Reynolds, 1974). Kamo et al. (1989) have recently reported a precise age of 615 ± 2 Ma (U-Pb (zircon, baddeleyite)) for a Long Range dyke from Labrador. The extrusive equivalent of the dykes, known as the Lighthouse Cove Formation, has been identified on Belle Isle (Williams and Stevens, 1969), and also occurs along the northeastern margin of the inlier.

Owing to its isolation, prospecting in the interior of the inlier has lagged behind mineral exploration surveys undertaken in the rest of Newfoundland. This is apparent from the fact that Mineral Occurrence Maps for the inlier (Newfoundland Department of Mines and Energy, Maps 85-30 (Port Saunders) and 83-60 (Sandy Lake)) identify few prospects. These include copper showings near Torrent River, a uranium anomaly or showing in the Lake Michel intrusive suite north of Inner Pond, and sources of building stone and limestone near fault zones along the southeastern margin of the inlier.

The recent discovery of anomalous gold concentrations in the Aspy pluton (formerly informally referred to as the French-Childs granite) and its host rocks, however, has sparked a renewed interest in the economic potential of the inlier (Tuach, 1986, 1987; Tuach and French, 1986; Saunders and Tuach, 1988).

Topography and drainage

The northern Long Range mountains are renowned in Newfoundland for alpine scenery. Crystalline rocks of the Long Range Inlier rise to elevations exceeding 600 m above the Cambro-Ordovician platformal rocks in the foreland to the west. The topography along the eastern part of the inlier is less dramatic, although relief attains 400 m near White Bay.

The major rivers of the inlier drain to the east and west. Rivers and streams flowing into the fjords along the western margin of the inlier have smaller watersheds, since they essentially drain high altitude plateaux. None of the rivers may be easily navigated for more than a few kilometres inland from the sea.

Glacial and surficial geology

A variety of surficial features testify to extensive glaciation of the inlier during the Pleistocene. Roches moutonnées, glacial striae, and chattermarks on glacially-polished surfaces indicate ice movement off the inlier in a radial fashion (Fig. 4), consistent with the orientation of fjords and deep bays transecting the periphery of the massif.

Local and erratic boulders are scattered over much of the inlier, particularly in the south, where they hamper navigation in lakes and rivers. Felsenmeer-covered terrain at higher altitudes in the west has been interpreted as comprising nunataks which projected above the ice cap during the latest period of glacial expansion ca. 11 000 years B.P. (Grant, 1969a). Grant (1977) distinguished the limits of successive glaciations in the west-central part of the inlier by documenting different types of weathering features.

Acknowledgments

Successful completion of the northern Long Range project would not have been possible without the support of colleagues at the Geological Survey of Canada and the Newfoundland Department of Mines and Energy. Continuity of the project was ensured by funds made available to the author through a Visiting Fellowship with the GSC. Thanks are due to Philippe Erdmer and Ken Currie, who have maintained unflagging interest in the project. Betty Manning kept financial aspects of the field work under control, and Jean van Berkel helped with logistics. Viking Helicopters, Limited and Newfoundland-Labrador Air Transport, Limited provided exemplary air transport into the mountains. Particular thanks are extended to my enthusiastic and capable field assistants: Sharon Baillie, Kim Bellefontaine, Janet Campbell, Frank Dennis, David Machin, and Steve Orr. Robert Marr assisted with point counting, photomicrography, and drafting.

Special thanks are extended to Hewitt Bostock, whose thorough review of the manuscript led to significant improvements in the final presentation.

Lithological subdivision of the Long Range Inlier

For the purposes of this report, crystalline rocks of the inlier are divided into three broad groupings, from oldest to youngest: (1) a high grade gneiss complex (minimum age: 1550 Ma; H. Baadsgaard, pers. comm., 1989); (2) massive to foliated plutonic rocks of Grenvillian age (ca. 1056 Ma; H. Baadsgaard, pers. comm., 1989); and (3) mafic dykes of the Long Range swarm (ca. 615 Ma; Kamo et al., 1989). The lithology and geochemistry of these rock groupings are outlined in the following sections, and their significance in reconstructing the metamorphic and structural evolution of the inlier is then highlighted. The economic potential of the inlier is considered on a commodity-by-commodity basis. The report concludes with a discussion of the position of the inlier vis-à-vis analogous basement rocks in southern Labrador and in the southern Long Range.

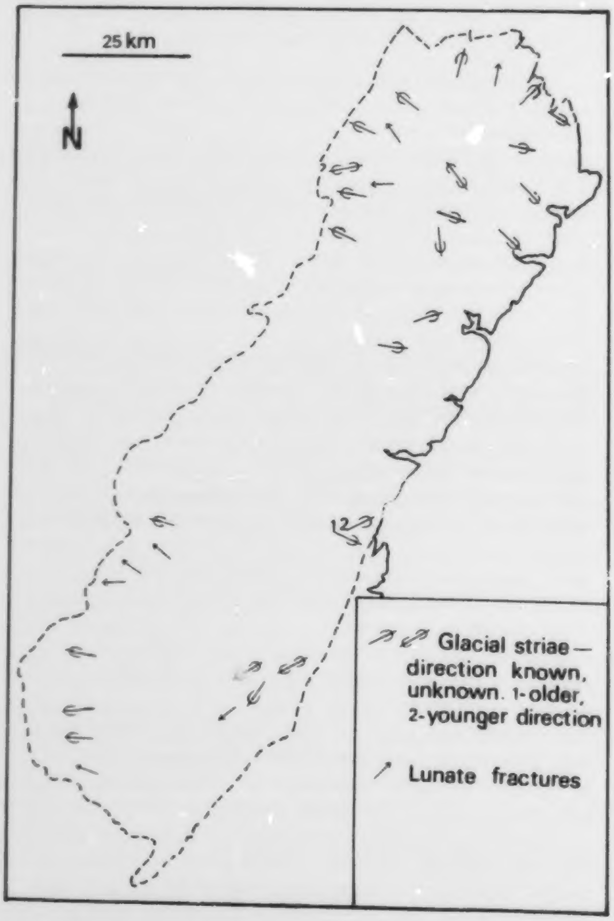
25 km
N
1
2
Glacial striae — direction known, unknown. 1-older, 2-younger direction
Lunate fractures

Figure 4. Glacial flow directions in the Long Range Inlier, as determined from striae, lunate fractures (chattermarks), and roches moutonnées. Figure incorporates data from Grant (1969b), Bostock (1983), Vanderveer and Taylor (1987), and Owen (1986b).

GENERAL GEOLOGY

The Long Range gneiss complex

Gneissic rocks underlie approximately 60 % of the inlier. The bulk of these are quartzofeldspathic rocks of granitic or granodioritic composition. The nature and age of the protolith(s) of these rocks are uncertain. Earlier workers (Foley, 1937; Bostock, 1983) considered them to be paragneiss, citing as evidence the local quartz-rich nature of these rocks, at least in the northern part of the inlier. Unequivocal metasedimentary rocks (i.e., pelite, quartzite (sensu stricto), and rare marble) form narrow screens within quartzofeldspathic gneiss. Collectively, these compose less than 5 % of the gneiss complex. The protoliths of the remaining quartzofeldspathic and mafic gneiss remain problematic, and their age relative to obvious paragneissic rocks is unclear. Noting the relative homogeneity of the quartzofeldspathic rocks dominating the central and southern parts of the inlier, Owen and Erdmer (1986) suggested that these rocks were derived from igneous protoliths.

Uranium-lead (zircon) data suggest that the (igneous?) protolith of quartzofeldspathic gneiss is at least 1550 Ma old (H. Baadsgaard, pers. comm., 1989). The time of metamorphism is not known, although crosscutting relations indicate that regional high grade metamorphism (M_1) predated the emplacement of the 1056 Ma granitic plutons. Metamorphic grade increases from medium to high grade southwestward along the length of the inlier. The distribution of metamorphic orthopyroxene provides a basis for crude subdivision of the basement complex into a granulite facies terrane in the central and southwestern parts of the inlier, and an amphibolite facies terrane farther to the northeast (Fig. 5). Bostock (1983) reported the presence of local orthopyroxene and mesoperthite in the northeastern part of the inlier (i.e., amphibolite terrane), and interpreted this as evidence that the area had locally attained granulite grade, but had subsequently been retrograded. Given this, and evidence for later, lower grade metamorphism elsewhere in the inlier, the boundary between these terranes may reflect prograde and/or retrograde events, and is not intended to delineate the location of an orthopyroxene-in isograd in the area.

Lithology

Quartzofeldspathic gneiss

Subdivision of quartzofeldspathic gneiss is based on modal and textural criteria. For granitoid rocks (sensu lato), Streckeisen's (1976) nomenclature is adopted. Several categories of gneissic granitoid rocks are distinguished on the accompanying map (Map 1764A, in pocket). These include quartz dioritic, tonalitic, and granitic-granodioritic variants. Their modes are listed in Table 1, and are depicted graphically in Figure 6.

Unit **Pqdn** is a leucocratic grey-green rock characterized by 5 to 10 mm ovoid aggregates (mafic "flecks") of hornblende and/or biotite (Fig. 7A). Orthopyroxene was identified at only one locality. Modally, the rock includes quartz dioritic, granodioritic, and granitic variants, and therefore overlaps the composition of other texturally- and/or mineralogically-distinct members of the gneiss complex. In this unit, quartz typically has a bluish cast, and occurs interstitial to oligoclase and perthitic microcline. Although not a banded gneiss, migmatitic textures are locally developed in this unit. The migmatites contain potassium feldspar- and quartz-rich layers up to about 10 cm wide. The leucosomes are bordered by hornblende- and biotite-rich seams. Polyphase deformation is indicated by the refolding of these leucocratic segregations and of mafic layers (e.g., deformed dykes) in the rock.

The flecky-textured gneiss occurs near the upper reaches of the Humber River, where it forms bands up to about 6 km wide within granitic-granodioritic gneiss (unit **Pgn**; see below) and is cut by equigranular biotite granite (unit **Pg**; see Fig. 62.5 in Owen, 1986a). The flecky gneiss cannot be followed northwestward along strike across the inlier.

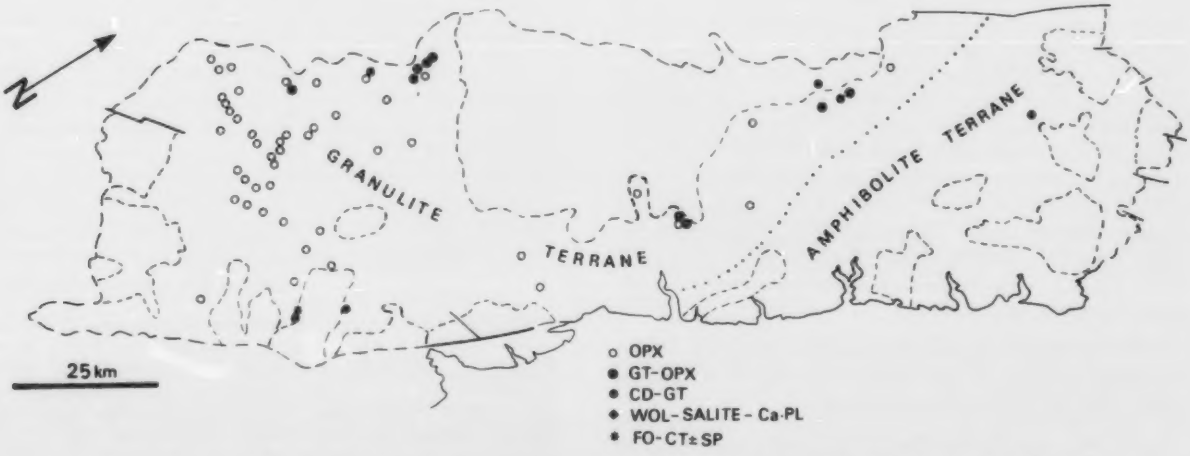

Figure 5. Distribution of high grade mineral assemblages in the Long Range gneiss complex. Dotted line separates the approximate location of widespread amphibolite facies assemblages from granulite to the southwest. Dashed lines outline plutons. Abbreviations as in Appendix II.

Table 1. Modal composition of representative samples of the quartzofeldspathic gneiss (orthogneiss?) of the Long Range gneiss complex. Data are rounded to nearest 1%. "tr" denotes trace concentrations (<0.5%). See Appendix II for abbreviations.

Unit and sample	qz	pl	Ksp	bi	hbl	opx	cpx	opq	accessory minerals
Ptn									
VO-86-310	16	57		1	6	14	3	2	zr, ap
2062	24	59	2	3		11		tr	ti
VO-87-193	9	70	8	2	3	5		2	
226	11	76	3		tr	5	3	2	
228	21	70	1	tr		6		tr	zr
287	11	71		3		15		tr	
Pqdn									
VO-85-962	18	57	11	12				1	
VO-87-111	35	16	44			5		tr	
Pgn									
VO-85-381	33	40	14	11				tr	ti
903	16	15	58		7		1	2	ti, ep, zr, ap
VO-86-211	25	38	17	16	tr			2	zr, ep, ap
412	16	27	52	5				tr	zr, ap, chl
VO-87-121	37	10	49	3				1	ti
124	38	17	40	2				1	mu
216	33	37	23	5		2		tr	
Pdn									
VO-86-258	1	61		9		17	10	2	

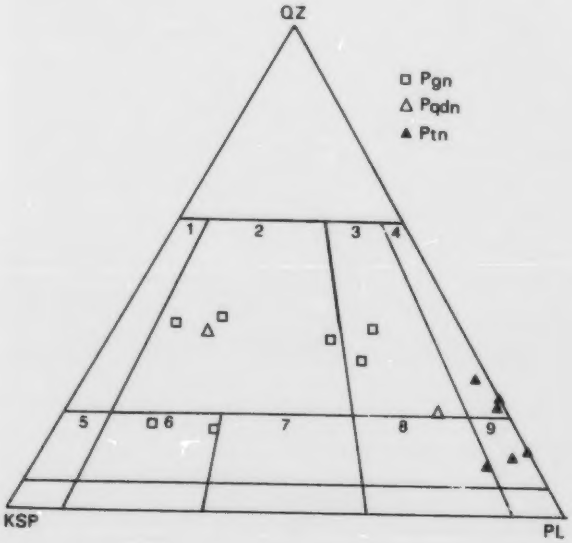

Figure 6. Modal composition of quartzofeldspathic and mafic rocks of the Long Range gneiss complex. Field boundaries after Streckeisen (1976): 1-alkali feldspar granite, 2-granite, 3-granodiorite, 4-tonalite, 5-quartz-alkali feldspar syenite, 6-quartz syenite, 7-quartz monzonite, 8-quartz monzodiorite, 9-quartz diorite.

Outcrops of the gneiss appear to terminate in the core of a large northwest-plunging antiform which deforms high grade granitic gneiss (unit Pgn) in the Gros Morne National Park area.

Granitic to granodioritic gneiss (unit Pgn) is volumetrically the most important unit of the gneiss complex. This unit typically consists of rose to tan coloured rocks; the rocks have a greenish-brown tinge where they contain orthopyroxene. Migmatitic textures are widespread, and include well-defined, biotite-seamed leucocratic veins (2-15 mm wide; Fig. 7B,C,D) as well as diffuse leucocratic segregations which in places constitute >50% of outcrop surfaces, imparting a diatexitic appearance to the rock. Like the leucosomes in the flecky quartz dioritic (to granodioritic) gneiss (unit Pqdn), these are potassium feldspar- and quartz-rich segregations which may approximate minimum melt compositions. The mesosome typically consists of oligoclase, microcline or perthitic microcline, quartz, and biotite, with local hornblende and rare garnet, clinopyroxene, and/or orthopyroxene. Zircon, apatite, and iron (titanium) oxides are common accessory minerals. Albite and epidote occur with chloritized biotite in some outcrops of granitic gneiss along the Upper Humber River in the southeastern part of the inlier, testifying to a greenschist-facies overprint. Texturally, unit Pgn consists of banded gneiss in the southern part of the inlier. Distinct banding is less evident in granitic-granodioritic gneiss farther to the north, where wispy mafic aggregates define the foliation (Fig. 7E).

Granitic gneiss adjacent to the southwestern margin of the Lake Michel intrusive suite locally contains potassium feldspar megacrysts and has a streaky texture (Fig. 7F). These features distinguish this rock from unit **Pgn**. The streaky-textured granitic gneiss (unit **Phgn**) is also mineralogically distinct. Hornblende is the dominant mafic mineral; it coexists with biotite, and locally, with garnet and/or orthopyroxene.

High-grade mineral assemblages are characteristic of granoblastic tonalitic (to quartz dioritic) gneiss (unit **Ptn**). This unit forms bands up to 1 km wide within granitic-granodioritic gneiss. In places, the tonalitic gneiss is spatially associated with pelite. The gneiss is a relatively fine grained (≤ 1 mm), grey to green-brown rock containing oligoclase and quartz, with clinopyroxene, orthopyroxene, biotite, and/or hornblende. Ilmenite is a common accessory mineral. Orthopyroxene is subordinate to clinopyroxene in two-pyroxene-bearing assemblages. Garnetiferous two-pyroxene assemblages are rare, and apparently developed only in iron-rich rocks characterized by disequilibrium textures (e.g., corona structures). Migmatitic fabrics occur only locally. These are represented by diffuse, relatively coarse grained tonalitic (i.e., oligoclase- and quartz-rich) segregations, which in places contain orthopyroxene, in contrast to biotite, pyroxene, and/or amphibole in the mesosome (Fig. 7G,H).

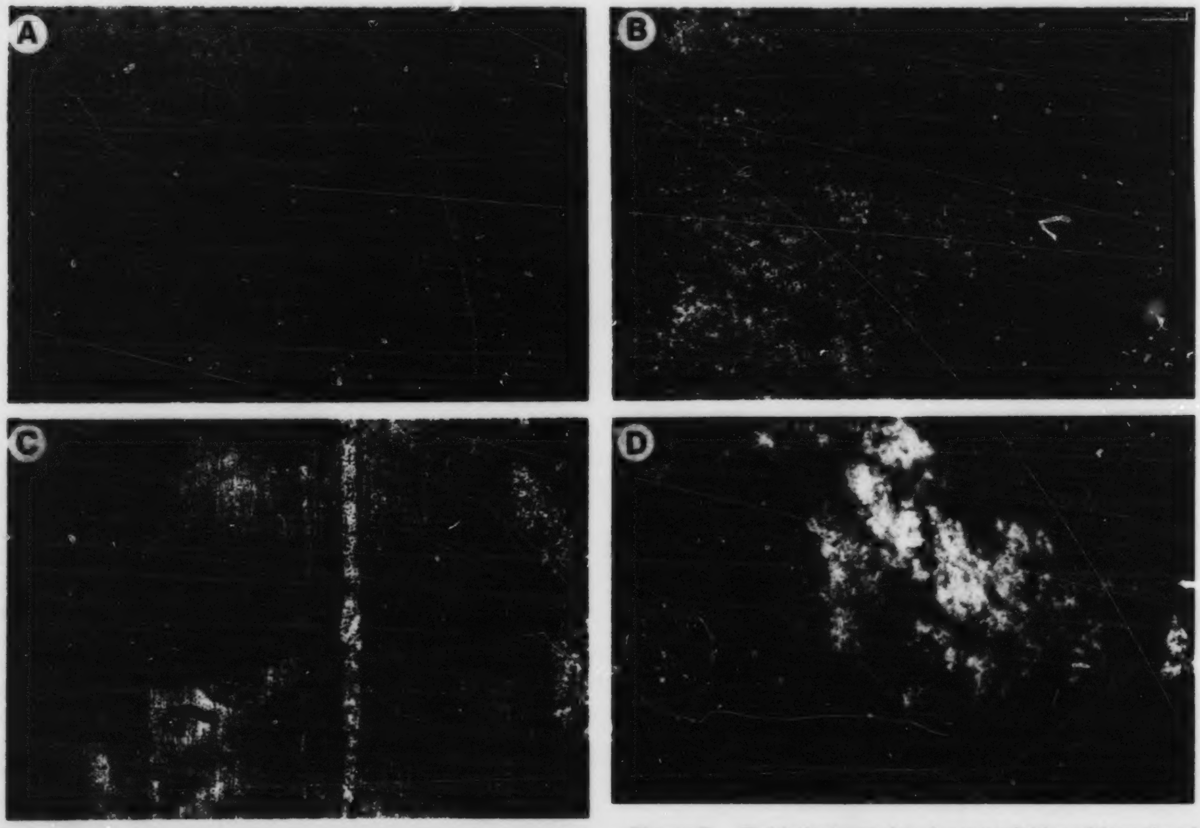

Figure 7. Field photographs of quartzofeldspathic rocks of the Long Range gneiss complex. A. Flecky quartz dioritic to granodioritic gneiss (unit **Pqdn**); scale bar is approximately 4 cm; B. migmatitic biotite granitic gneiss (unit **Pgn**) layered with 1 to 2 cm wide leucocratic segregations; scale bar is approximately 3 cm; C. biotite-seamed leucocratic segregations in granodioritic gneiss (unit **Pgn**); D. orthopyroxene porphyroblasts (rimmed by amphibole) in granitic leucosome in unit **Pgn**; E. nonmigmatitic biotite granitic gneiss (unit **Pgn**), with wispy biotite-rich aggregates (parallel to penknife), cut by uncorrelated granodioritic dykes (Grenvillian?); F. streaky-textured hornblende-, biotite-, garnet-, and pyroxene-bearing granitic gneiss (unit **Phgn**); G. migmatitic orthopyroxene-biotite-bearing tonalitic gneiss (unit **Ptn**); H. tonalitic leucocratic segregation studded with orthopyroxene porphyroblasts, in tonalitic gneiss (unit **Ptn**); I. pyroxene porphyroblasts in leucocratic segregations in hornblende-rich dioritic gneiss (unit **Pdn**). GSC photos 204932 7A to I.

In the east-central part of the inlier, biotite is the principal mafic mineral in narrow bands of grey quartz dioritic gneiss, which define a planar fabric in the rock. Orthopyroxene occurs locally as large (to 1 cm) porphyroblasts in quartz- and plagioclase-rich segregations. This variant is grouped on (modal) compositional grounds with the granoblastic tonalitic gneiss occurring farther to the west.

Dark grey biotite ± hornblende quartz dioritic schist (unit Pbs) is a texturally-distinct unit, characterized by a schistose fabric and by the presence of plagioclase megacrysts and lens-shaped plagioclase-rich aggregates, which impart a spotted appearance to the rock. Unit Pbs flanks tonalitic and pelitic gneiss immediately northwest of the Lake Michel intrusive suite. The northern extension of unit Pbs is not definitely known, but it may include the melanocratic gneiss unit of Bostock (1983).

Narrow bands of biotite schist too small to represent on the accompanying map (Map 1764A) occur locally in flecky quartz dioritic-granodioritic gneiss (unit Pqdn) in the Silver Mountain area. The biotite schist lacks plagioclase-rich patches characteristic of unit Pbs, and is not considered to be correlative with this unit.

Pelitic gneiss

Pelitic rocks are a minor but widespread component of the gneiss complex (Fig. 8). They typically are associated with quartzite, tonalitic gneiss, or banded mafic gneiss, and form narrow (≤ 1 km) bands enclosed by quartzofeldspathic gneiss or granitoid plutonic rocks. Quartzite is typically intercalated with the pelite on a centimetre to metre scale, and may be dominant, with pelite occurring as narrow screens within massive to banded, white to grey quartzite.

Pelite from the amphibolite terrane in the northeastern part of the inlier is mineralogically similar to that in the granulite terrane. The pelite contains oligoclase-andesine, quartz, biotite, garnet, sillimanite, and, in places, cordierite. Accessory phases include graphite, spinel, zircon, apatite, ilmenite, magnetite, pyrite and/or pyrrhotite, and rare chalcopyrite. White mica and sodic plagioclase occur locally due to late low-grade metamorphic events. The pelites exhibit layering resulting from primary compositional banding (e.g., quartz-rich layers) and from metamorphic differentiation or anatexis. Pelites and associated rocks are illustrated in field photographs in Figure 9.

Less aluminous metasedimentary gneiss (semipelite) is mineralogically similar to the pelites, but lacks sillimanite, and in places contains orthopyroxene. Plagioclase (oligoclase-andesine) is modally dominant over quartz and

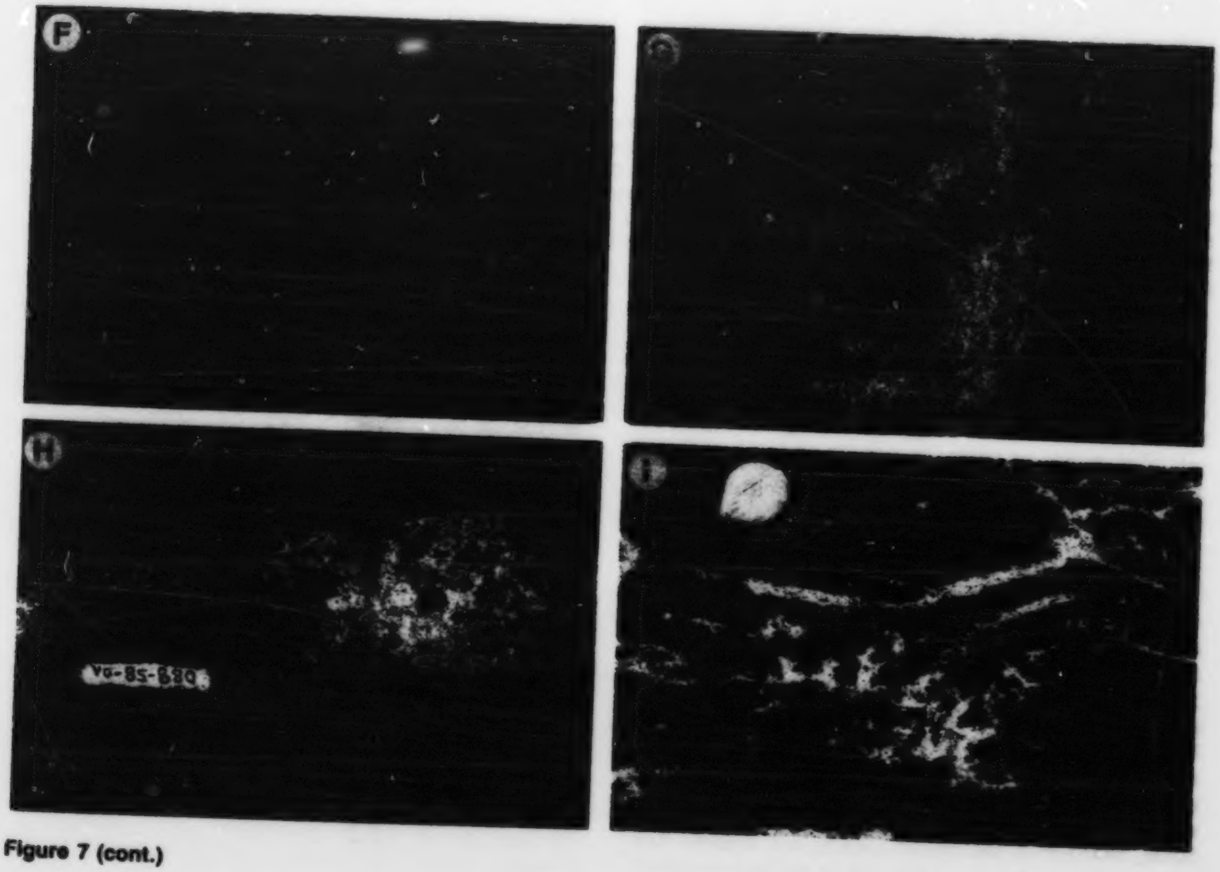

Figure 7 (cont.)

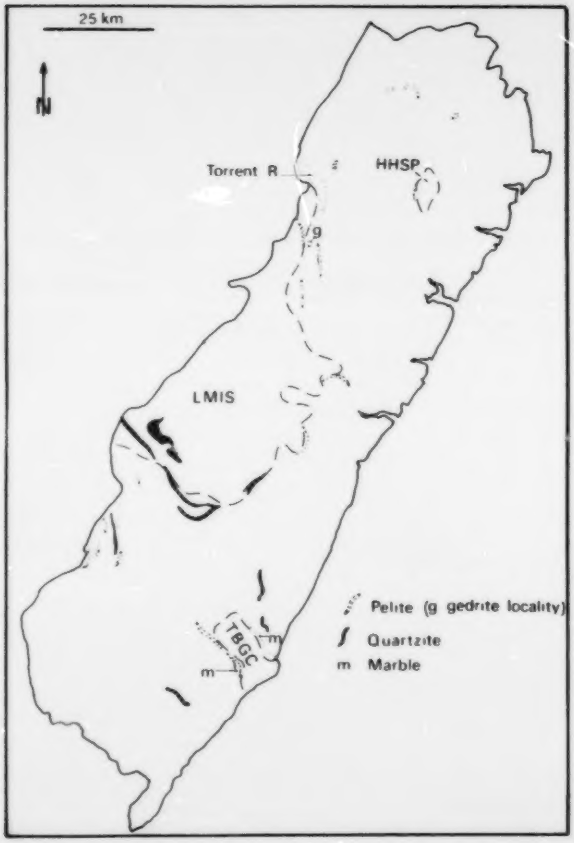

Figure 8. Distribution of pelitic gneiss, quartzite (orthoquartzite), and marble in the Long Range Inlier. The Lake Michel intrusive suite (LMIS), Hooping Harbour satellite pluton (HHSP), and Taylor Brook gabbro complex (TBGC) are shown for reference. The location of the Torrent River pelite sequence is indicated. Quartz-rich gneiss in the northern part of the inlier (Bostock, 1983) is not shown.

potassium feldspar. Mafic minerals include biotite, garnet, and cordierite, with accessory ilmenite and graphite; gedrite has been identified in one outcrop (see Fig. 8).

Major pelite sequences occur near the Taylor Brook gabbro complex, south of Inner Pond, east and northeast of the Lake Michel intrusive suite, on Torrent River, and along the western margin of the Hooping Harbour satellite pluton (Fig. 8).

Supracrustal rocks near the Taylor Brook gabbro complex include metacarbonate rocks in addition to pelite, and form a discontinuous envelope on the gabbro. The pelites in this sequence are interlayered on a metre scale with garnet- and orthopyroxene-bearing tonalitic gneiss (unit Ptn). Collectively, these rocks record the thermal effects of the gabbro. The pelite near the gabbro contains abundant cordierite, and is depleted in quartz, a characteristic feature of many high grade thermal aureole rocks (Pattison and Harte, 1985).

Farther to the west, north-trending bands of quartzite and pelite occur within the high grade granitic gneiss terrane in Gros Morne National Park. The pelites contain plagioclase (An_{32}), perthitic microcline, quartz, garnet, biotite, local cordierite and sillimanite, and accessory opaque minerals.

The migmatitic pelites south of Inner Pond are characterized by thin biotite ± sillimanite ± garnet ± graphite-rich layers and a diffuse, buff to rose, perthitic microcline- and quartz-rich leucosome (Fig. 9A). These pelites are spatially associated with homogeneous grey fine grained biotite + garnet + orthopyroxene ± hornblende-bearing tonalitic gneiss (unit Ptn), and with banded hornblende-, biotite-, and orthopyroxene-bearing dioritic gneiss (unit Pdn). These rocks form large gneissic enclaves enclosed by the Lake Michel intrusive suite.

The pelites east of the Lake Michel intrusive suite comprise a heterogeneous assemblage of rocks. Semipelitic rocks at this locality are green to steel-blue and consist of plagioclase (An_{24-32}), perthitic microcline, quartz, and biotite ± garnet ± orthopyroxene ± graphite. Associated with the semipelite is pale grey medium grained quartzite with thin pelitic bands containing perthitic microcline, quartz, sillimanite, garnet, biotite, and accessory graphite (Fig. 9B). The pelitic and semipelitic sequences at this locality are separated by fine grained grey biotite ± orthopyroxene-bearing tonalitic gneiss. Some of the semipelites are very similar to narrow bands (metre scale) of biotite- and garnet-bearing "granitic" gneiss which occurs locally in flecky textured, quartz dioritic to granodioritic gneiss (unit Pqdn) south of the Upper Humber River, in the Silver Mountain area. These were described as garnetiferous granitic gneiss by Owen and Erdmer (1986). Biotite in these rocks is a distinctive dark reddish-brown colour, and is clouded with a very fine grained opaque mineral, possibly ilmenite.

Massive to banded, white quartzite is a conspicuous component of the narrow pelitic sequence enclosed by the Lake Michel intrusive suite near its northern flank (Fig. 9C). This band of supracrustal rocks separates foliated megacrystic granite to the southwest from equigranular granite to the northeast. The pelites contain cordierite, sillimanite, garnet and biotite. In places, sillimanite forms skeletal ("hollow") needles enclosing quartz. The pelites are flanked on both sides by massive to banded white quartzite up to several tens of metres in width. Massive to banded hornblende-rich mafic gneiss with amphibole- or orthopyroxene-studded leucocratic segregations also occurs in the sequence.

Two north-trending bands of rusty-weathering pelitic gneiss occur in granitic gneiss near the northeastern flank of the Lake Michel intrusive suite. Microcline is subordinate to plagioclase (An_{22-24}) and quartz in these rocks. Biotite and garnet are the dominant ferromagnesian minerals; sillimanite occurs locally. Amphibole-bearing mafic enclaves (disrupted dykes?) have biotite-rich margins adjacent to the enclosing pelite, suggesting the small-scale mobility of alkalies and fluid phases during metamorphism.

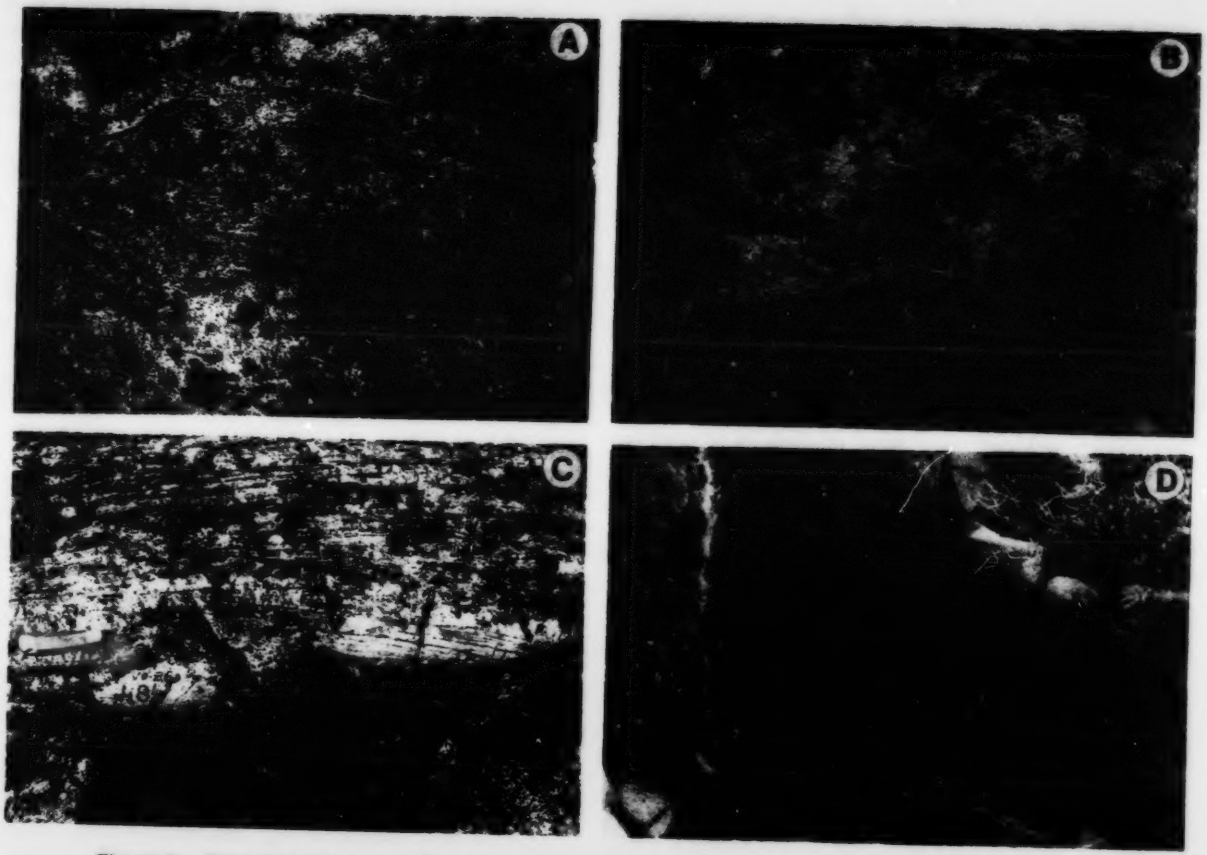

Figure 9. Field photographs of pelitic gneiss and quartzite in the Long Range Inlier. A. Migmatitic garnet-, sillimanite-, and biotite-bearing pelitic gneiss from a large enclave in the southern part of the Lake Michel intrusive suite (LMIS); B. narrow bands of sillimanite-, garnet-, and biotite-bearing pelitic gneiss in folded quartzite (supracrustal sequence adjacent to the eastern margin of the LMIS); C. layered pelitic gneiss and quartzite from a large enclave in the northern part of the LMIS; D. colour-banded quartzite, from a large enclave in the LMIS exposed on an island in Lake Michel. GSC photos 204932 9A to D.

Outcrops of rusty semipelite occur within a 2 km wide band of tonalitic gneiss flanking the northeastern margin of the Lake Michel intrusive suite. These are sodic plagioclase-(An$_{8-11}$) and quartz-rich rocks containing garnet, biotite, cordierite, and orthopyroxene or gedrite. Although coexisting in outcrop, orthopyroxene and gedrite have not been seen within the same thin section. The latter minerals are concentrated in thin lamellae (millimetre scale) in the rock.

Pelite exposed near Torrent River is spatially associated with tonalitic gneiss and with plagioclase-megacrystic biotite schist (unit Pbs). Like the pelites farther to the south, these are rusty-weathering migmatitic rocks which contain plagioclase (An$_{32-39}$), microcline, quartz, biotite, sillimanite, garnet, cordierite, and accessory ilmenite and spinel.

The pelites flanking foliated megacrystic granite of the Hooping Harbour satellite pluton (Bostock, 1983) are of particular interest since they appear to record the thermal overprint of this pluton. The pelites are migmatitic quartzofeldspathic rocks containing biotite, garnet, and sillimanite. A characteristic feature is the local presence of muscovite, both as large (to 1 cm) porphyroblasts in leucocratic segregations, and as fine grained flakes armouring sillimanite. There is no clear spatial relationship between the distribution of muscovite in the pelites and the proximity of the granite. Consequently, it is uncertain whether muscovite is a relic of the thermal aureole of the pluton, or formed during the subsequent regional metamorphic event responsible for the tectonic foliation developed in the granite. Evidence for a narrow thermal aureole around the pluton is provided by a rapid decline in metamorphic temperatures determined from the composition of coexisting garnet and biotite in pelite sampled across the sequence, away from the intrusion (see Metamorphism section, below). The metasedimentary rocks at this locality share affinities with other occurrences of pelites in the region, particularly with regard to the abundance of quartzite, which forms layers up to a few metres wide. Both pure and impure quartzite is present. The relatively pure quartzite is white or pale grey; it locally contains traces of feldspar and/or iron (-titanium) oxide. In addition to the latter minerals, impure quartzite also contains fine grained biotite and garnet. The garnet imparts a rose tint to the rock.

A number of pelite sequences occur in the northeastern part of the inlier. Like those farther south, these rocks are composed of quartz, oligoclase or more calcic plagioclase, potassium feldspar, biotite, and sillimanite, with local cordierite and garnet, and accessory spinel, opaque minerals, zircon, and apatite (Bostock, 1983). Andalusite coexists with sillimanite in pelites near the southeastern margin of the Leg Pond pluton, and in a pelitic enclave in the Cloud River pluton (Bostock, 1983). The andalusite apparently postdates sillimanite in these rocks.

Metacarbonate rocks

Metacarbonate rocks (unit **Pcs**) associated with pelite near the Taylor Brook gabbro complex include both relatively pure and impure varieties. Tan, grey, or white marble is a calcite-rich rock containing small amounts of phlogopite, forsterite, and/or diopside, with accessory graphite. Calc-silicate bands up to a few metres wide within the carbonate are dark grey to reddish, and contain abundant phlogopite, forsterite (partly serpentinized), and/or diopside, with accessory graphite, and local common (Mg) spinel. Calcite is the typical carbonate mineral, but dolomite is also present in some calc-silicate samples. Wollastonite, salite, scapolite, and bytownite coexist in one outcrop of foliated calc-silicate rock near the northeastern border of the Taylor Brook gabbro complex. Bands of quartzite and pelite up to a few metres wide occur locally in the marble-calc-silicate rock sequence.

Bostock (1983) described narrow (≤6 m wide) bands of calc-silicate gneiss from the northern part of the inlier as consisting predominantly of a pink, green, or grey-white, fine grained assemblage of diopside and quartz. Other minerals may include plagioclase (albite to bytownite), microcline, epidote, hornblende, garnet, chlorite, calcite, scapolite, vesuvianite, and rare olivine.

Quartzite

Large exposures of white to grey quartzite form prominent ridges in the southern part of the inlier. These quartzite ridges may be followed for several kilometres along strike, and are an important and conspicuous component of the gneiss complex in this area. The quartzite is generally massive. A weak colour banding or mineralogical layering defined by concentrations of feldspar or opaque minerals is locally evident (Fig. 9D). This is most apparent in an island-forming quartzite enclave within megacrystic granite of the Lake Michel intrusive suite (contacts not seen) at Lake Michel. Screens of sillimanite-bearing pelitic gneiss occur in a north-trending band of white quartzite northeast of the Taylor Brook gabbro complex.

Blue quartz is concentrated in foliation-parallel bands and discordant veins in equigranular granite and in small mafic bodies in the Silver Mountain area. In contrast to the metasedimentary quartzite, these probably represent hydrothermal veins related to the plutonic rocks.

Siliceous metasedimentary rocks in the northern part of the inlier contain from 40 to 90 % quartz, with lesser quantities of microcline, sodic plagioclase, biotite, and locally, hornblende, garnet, sillimanite, and clinopyroxene (Bostock, 1983).

Mafic gneiss

Massive to banded mafic gneiss (unit **Pdn**) is a minor but widespread component of the gneiss complex, with the largest mass occurring east of the Taylor Brook gabbro complex. Mafic gneiss consists essentially of hornblende and plagioclase (i.e., is amphibolite); pyroxene is also present locally.

Granoblastic mafic gneiss occurs as narrow (centimetre to metre scale) discontinuous bands within quartzofeldspathic gneiss throughout the inlier. These bands probably represent metamorphosed and deformed mafic dykes. Hornblende, andesine, and biotite are typical minerals; clinopyroxene and/or rare garnet occurs locally. In places (e.g., near the upper reaches of the Humber River), hornblende-rich mafic layers are migmatitic, with quartz-plagioclase segregations containing pyroxene porphyroblasts (Fig. 7I).

Schistose and phyllitic rocks

Schistose and phyllitic rocks occur at Torrent Cove (Canada Bay) and some 24 km farther south, near Fourché Point. Bostock (1983) described the rocks at Torrent Cove as constituting a 300 m wide belt of fine grained quartz-feldspar-mica phyllitic rocks (unit **Pqs**) structurally overlain in turn by aerially extensive, schistose mesocratic gneiss (unit **Psn**) and by a 200 m wide sequence of muscovite-chlorite schist and quartz-rich gneiss (**Pqs**; retrograded pelites?). Although grouped here, the phyllites and schists flanking the mesocratic gneiss are not identical, and were mapped as distinct units by Bostock (1983). Bostock described the phyllite as a fine grained crenulated rock containing albite, quartz, microcline, muscovite, chlorite, and epidote, with local biotite, amphibole, and garnet. The schistose mesocratic gneiss (unit **Psn**) forms a lens-like body of quartz, oligoclase, and subordinate microcline, with 5 to 15 % biotite and accessory muscovite, chlorite, and epidote. Lithologically, this unit may be similar to the schistose biotite quartz dioritic rock (unit **Pbs**) occurring to the west, although the latter unit is characterized by plagioclase megacrysts or crystal aggregates. At Torrent Cove, the mesocratic gneiss pinches out, and the quartz-rich micaceous phyllites and schists merge and become indistinguishable (Bostock, 1983).

This assemblage of schistose rocks dips shallowly to the southwest. It appears to have been derived at least in part from higher grade rocks of the Long Range gneiss complex. Bostock (1983) postulated that the phyllites at Torrent Cove formed as a consequence of the diapiric emplacement of the nearby Hooping Harbour pluton.

Quartz-rich schistose rocks at Fourché Point occur in a fault-bounded block flanked to the northwest by quartzofeldspathic gneiss, and to the southeast by granite. The rock is fine grained, and contains quartz "eyes" up to 2 mm in diameter set in a foliated quartz- and feldspar-rich micaceous matrix. Low metamorphic grade is indicated by the mineralogy of the schist, which includes albite, muscovite, biotite, epidote, chlorite, and pale green amphibole in various combinations. For convenience, the quartz-eye schist is grouped with micaceous schists and phyllites at Torrent Cove (unit **Pqs**), although this is not intended to imply a common protolith for all the schistose rocks in this area.

Age relations

The relative ages of the various lithological units of the gneiss complex have not been determined from field observations. Consequently, it is not known whether original contacts between paragneissic rocks and presumed orthogneiss (e.g., granitic-granodioritic gneiss, unit **Pgn**) were stratigraphic (i.e., basement-cover) or intrusive. The minimum age of the protoliths of quartzofeldspathic gneiss is 1550 Ma (U-Pb, zircon; H. Baadsgaard, pers. comm., 1989).

Despite their low metamorphic grade, the schistose rocks at Torrent Cove and Fourché Point appear to be Proterozoic, and are interpreted (Bostock, 1983) as including the retrograded equivalents of higher grade rocks of the Long Range gneiss complex. The minimum age of the Torrent Cove schists is provided by a K-Ar (muscovite) age of 843 ± 24 Ma (Wanless et al., 1973). This age determination supports, but does not prove Bostock's (1983) proposal that the Torrent Cove schists formed during (diapiric?) emplacement of the Hooping Harbour pluton. Schistose rocks at Torrent Cove and Fourché Point are locally cataclastic. Bostock (1983) noted that post-cataclastic biotite in the Fourché Point schist is petrographically similar to biotite from nearby gneissic rocks, which has yielded a K-Ar (biotite) age of 434 ± 18 Ma (Wanless et al., 1973). Bostock (1983) interpreted this as the minimum age of cataclastic fabrics in the schist.

Plutonic rocks

The Long Range gneiss complex hosts a variety of mafic and felsic plutonic rocks. The largest mafic pluton is the Taylor Brook gabbro complex, which comprises a suite of layered olivine- and pyroxene-bearing mafic rocks. Approximately 19 granitoid plutons occur in the inlier. Most of these have been isotopically dated and yielded Grenvillian ages; one pluton (Devils Room pluton) is Devonian (H. Baadsgaard, pers. comm., 1989).

Geophysical expression

The 1.0 Ga granitoid plutons in the inlier and adjacent Grenville Province have amoeboid to roughly circular shapes, and are associated with positive aeromagnetic anomalies (Gower and Loveridge, 1987; Owen and Erdmer, in press).

In the inlier, magnetic anomalies of magnitude 400 to 600 gammas are centred on the granitoid plutons (Fig. 10A), and in the case of the largest of these intrusions (the Lake Michel intrusive suite), faithfully record internal lithological and tectonic structures. An anomaly of similar magnitude is associated with the Taylor Brook gabbro complex. In both cases, the magnetic highs are attributed to the concentration of iron (-titanium) oxides in the plutonic rocks.

The southerly increase in Bouguer gravity values (Fig. 10B) appears to be unrelated to the distribution of the granitoid plutons. Weaver (1967) suggested that this Bouguer gravity gradient indicates the presence of mafic rocks beneath a relatively thin slab of Precambrian granitoid rocks near the southeastern margin of the inlier. Surface geology confirms the presence of mafic rocks in this area (the Long Range mafic dykes and the Taylor Brook gabbro complex). Bostock (1983) noted that the trend of the Long Range mafic dyke swarm is consistently at a high angle to the orientation of the regional gravity gradient. From this, he suggested that the gravity gradient is at least as old as the dykes (latest Proterozoic), and that thinned Grenvillian crust was preferentially rifted along the zone presently occupied by the dyke swarm.

The Taylor Brook gabbro complex

The Taylor Brook gabbro complex is an oblong mafic pluton with an exposed surface area of about 175 km^2. The gabbro exhibits a moderately to steeply dipping, concentric layered structure cut by pegmatitic gabbro (Fig. 11). The pluton occurs on the northeastern flank of an elongate gravity high of 35 mgals (Fig. 10B) centred over quartz dioritic-granodioritic gneiss. This anomaly may delineate the subsurface southwestward extent of the gabbro beneath the gneiss complex.

Lithology

The Taylor Brook gabbro complex comprises a wide variety of mafic rocks. Both textural and mineralogical heterogeneities are present, and these contribute to the igneous layering which is locally evident. Most typically, the gabbro is a medium grained (1-4 mm) mesocratic rock (colour index 35-50) (Fig. 12A), containing calcic plagioclase (labradorite), with olivine, augite, and orthopyroxene present in various combinations. Igneous (subophitic) texture is well preserved (Fig. 12B). Accessory minerals include biotite, ilmenite, and apatite. In places, ilmenite is symplectically intergrown with orthopyroxene. Where present, amphibole encloses (or in places completely replaces) pyroxene, and olivine is commonly partly serpentinized.

Primary (igneous) layering in the gabbro (unit **Pgb**) is developed on a centimetre to metre scale, and is defined by phase and/or grain-size variations. Layering dips moderately to steeply toward the centre of the intrusion (Fig. 11). The pegmatitic gabbro (unit **Ppgb**), which forms a small (ca. 5 km^2) stock-like body in the northern part of the complex, apparently correlates with pegmatitic mafic dykes that cut igneous lamination in the gabbro. The pegmatitic gabbro (Fig. 12C) is a massive rock containing large (up to 15 cm) brown pyroxenes which are generally mantled (or replaced) by amphibole. The pegmatitic gabbro is inferred to be a late phase of the intrusive complex.

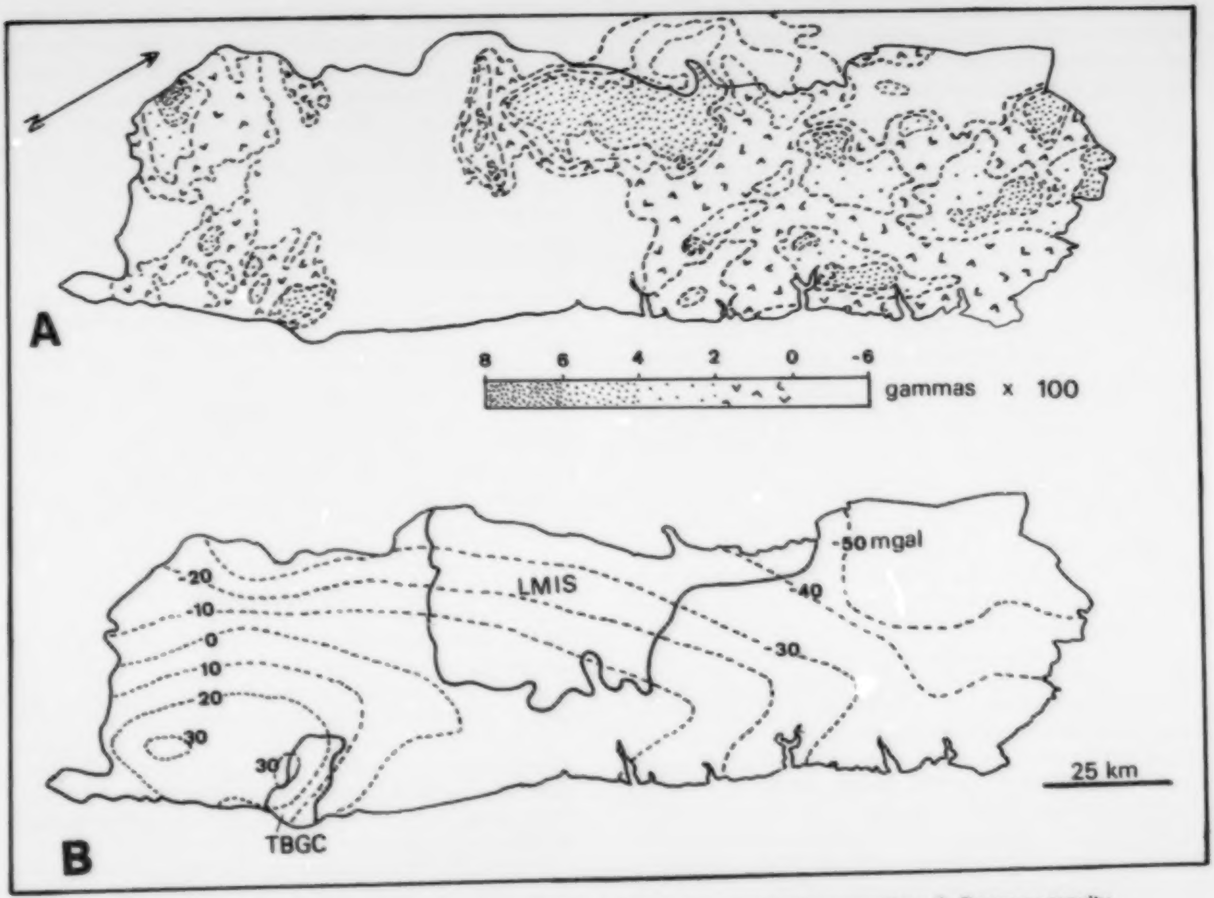
A
8
6
4
2
0
-6
gammas x 100
B
-20
-10
0
10
20
30
30
TBGC
LMIS
-50 mgal
-40
-30
25 km

Figure 10. Geophysical data for the Long Range Inlier. A. Aeromagnetic anomalies; B. Bouguer gravity anomalies. The Taylor Brook gabbro complex (TBGC) and Lake Michel intrusive suite (LMIS) are outlined in (B). The geophysical anomaly associated with the LMIS extends into the Cambro-Ordovician terrane west of the inlier in (A) (dashed lines). Geophysical data are from Williams and Haworth (1984a,b).

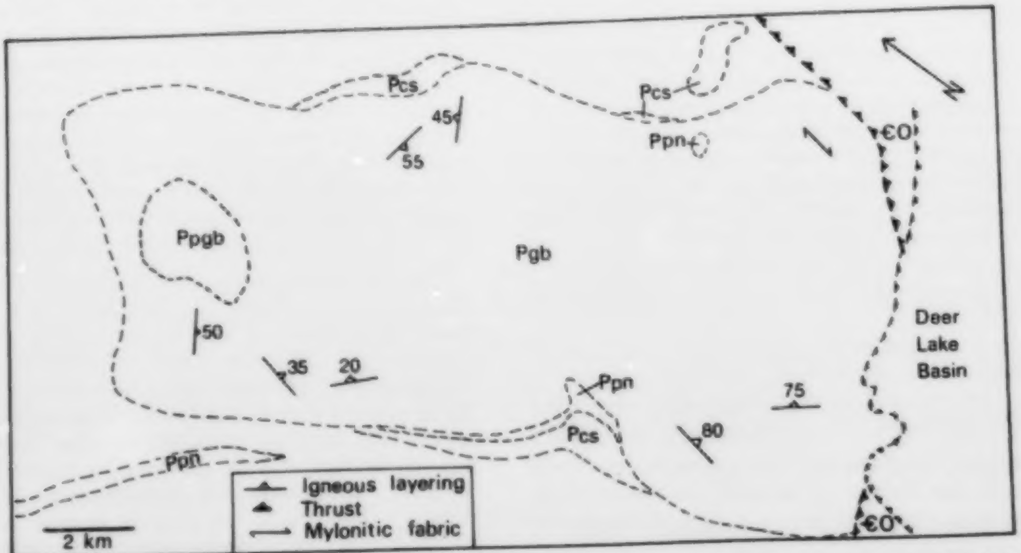
Pcs
45
55
Pcs
Ppn
€O
Ppgb
Pgb
Deer Lake Basin
50
35
20
Ppn
75
Pcs
80
Ppn
Igneous layering
Thrust
Mylonitic fabric
2 km
€O

Figure 11. Geological sketch map of the Taylor Brook gabbro complex. Major rock types are indicated (see Map 1764A for legend).

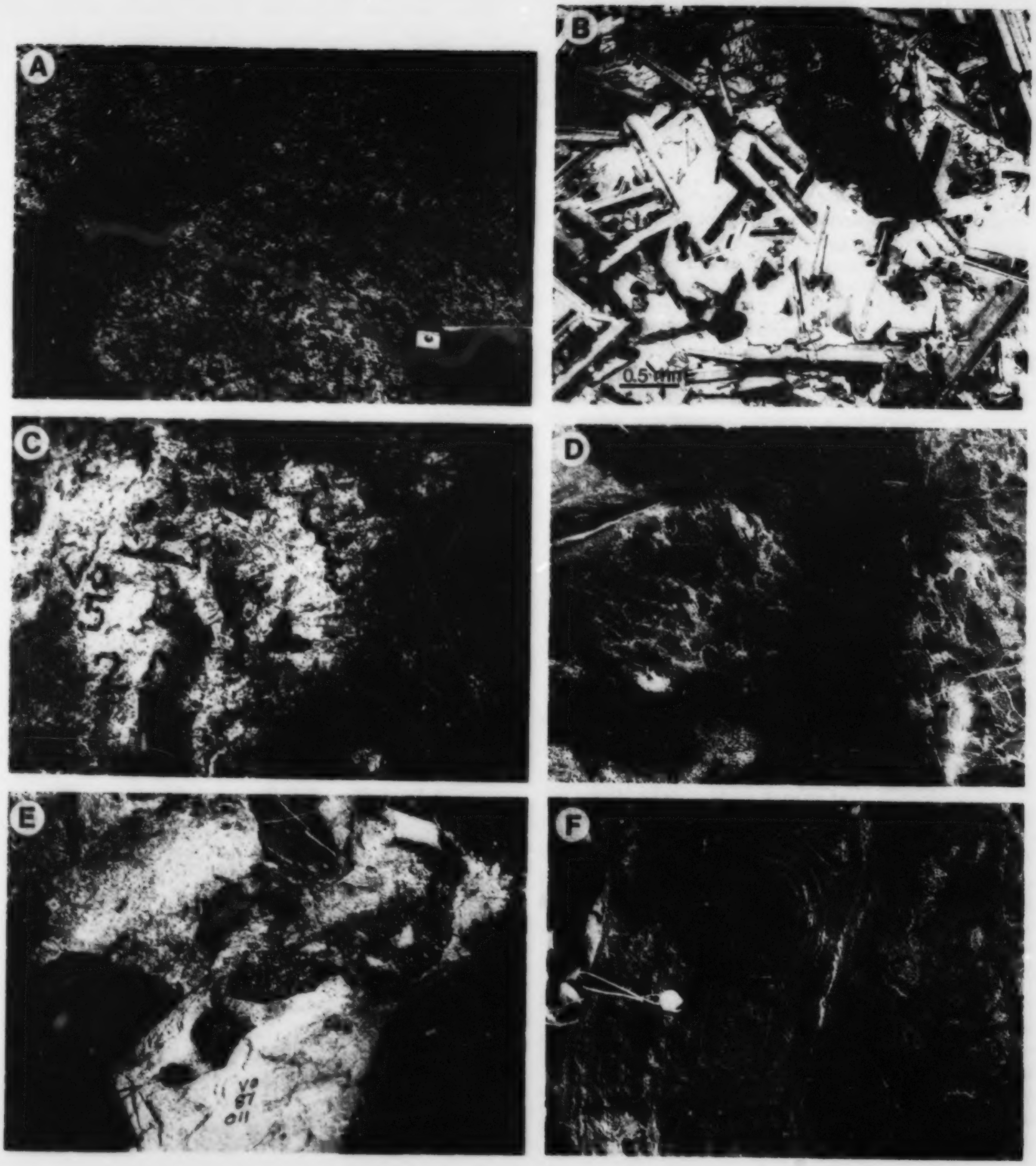

Figure 12. Photographs and photomicrographs of the Taylor Brook gabbro complex (TBGC). A. Augite and olivine gabbro; B.subophitic texture shown by two-pyroxene- and olivine-bearing gabbro (sample VO-85-007; crossed nicols); C. pegmatitic gabbro (unit Ppgb); D. relatively leucocratic pyroxene-bearing patches in mesocratic amphibole-bearing gabbro; E. heterogeneous assemblage of gabbro xenoliths in a granitic dyke cutting the TBGC; F. liesegang rings in weathered gabbro beneath the sub-Carboniferous unconformity along the southeastern margin of the inlier. GSC photos 204932 12A to F.

The heterogeneous nature of the intrusion is not restricted to outcrops displaying igneous layering. Several exposures of hornblende-bearing mesocratic gabbro along the woods road near the Upper Humber River contain diffuse patches of more leucocratic, relatively fine grained pyroxene-bearing diorite (Fig. 12D). Individual outcrops are described by Owen and Erdmer (1988).

Age relations

Since contact relations are poorly exposed, field observations provide few constraints on the age of the Taylor Brook gabbro complex. The gabbro certainly predates the Carboniferous, since submerged outcrops and boulders of the gabbro in Taylor Brook are veneered by conglomeratic redbeds of the Deer Lake Basin. Furthermore, three observations demonstrate that the gabbro postdates the gneiss complex: (1) northeast-trending mafic dykes mineralogically identical to the gabbro cut marble of the gneiss complex near the southwestern margin of the intrusion; (2) the gabbro is enclosed by a narrow metamorphic envelope (e.g., cordierite developed in nearby paragneiss); and (3) gneissic inclusions occur in gabbro boulders in the Upper Humber River.

The gabbro is cut by three types of dyke rocks: (1) fine grained felsic porphyry, which has tentatively been correlated with Silurian volcanic rocks to the east of the inlier (Erdmer, 1986a); (2) medium grained biotite granite of unknown age (Grenvillian?; Fig. 12E); and (3) a variety of mafic dykes. The latter include narrow northeast-trending rectiplanar metadiabase, which shows mineralogical similarities to Late Proterozoic dykes of the Long Range swarm (Owen and Machin, 1987), although it should be noted that mineralogically-similar mafic dykes with northeast trends cut Paleozoic cover rocks near the southeastern margin of the inlier (Owen and Edmer, 1988; see section on Late Proterozoic and Paleozoic rocks, below). Other rectiplanar dykes consisting of pegmatitic gabbro (mean grain size ~5-10 cm) cut primary (igneous) layering in the gabbro, and correlate to unit **Ppgb** in the northwestern part of the complex. These dykes contrast with narrow (centimetre-scale), fine grained mafic dykes with cuspate borders which were probably intruded into the complex while the gabbro was still incompletely crystallized (i.e., was a crystal mush).

The age of the gabbro relative to the Grenvillian granitoid plutons is not known. If the minor granitic dykes cutting the gabbro correlate to the Grenvillian plutons, then the gabbro must be older. This question will not be resolved until the isotopic age(s) of the granitic dykes is determined. Field relations nevertheless point to a Middle Proterozoic age for the Taylor Brook gabbro complex.

Mineralogy

Although the modal composition of the Taylor Brook gabbro complex varies widely, the primary mineralogy of gabbro is relatively simple. Typically, the gabbro contains olivine (Fo_{70-75}), augite, and/or hypersthene. In some samples, brown or green hornblendic amphibole encloses augite. Colourless fibrous amphibole (cummingtonite?) and secondary hornblende occur in some of the more altered gabbro samples. Plagioclase in the freshest samples is labradorite (An_{60-65}), and is generally not zoned. Plagioclase is relatively sodic (An_{30-40}) in altered (i.e., amphibole-rich) samples.

Geochemistry

Eight gabbro samples have been analyzed for major and selected trace elements (Table 2). The results demonstrate the tholeiitic nature of the complex. The wide range of compositions is consistent with the presence of igneous layering in the intrusion, and indicates that parts of the intrusion are highly fractionated. The most primitive sample (olivine-augite gabbro; VO-85-150) has Zr concentrations below detection limit (by XRF analysis), and contains 350 ppm Cr. The most evolved sample (two-pyroxene gabbro; VO-85-066-2) contains 160 ppm Zr and 30 ppm Cr.

Granitoid plutons

Granitoid plutons underlie approximately 35 % of the Long Range Inlier. Fourteen of these (including four plutons within the Lake Michel intrusive suite) have been dated by the U-Pb (zircon) method, and collectively yield a Grenvillian age of 1056 +4/-6 Ma (H. Baadsgaard, pers. comm., 1989). Zircon in some samples yields an age of 970 Ma, indicating that regional Grenvillian plutonism spanned a period of ca. 85 Ma. Granitoid plutons yielding isotopic ages between 1080 and 965 Ma are also widespread in the Grenville Province of southern Labrador and southeastern Quebec (Gower and Loveridge, 1987). These 1.0 Ga plutons delineate a Grenvillian magmatic belt in the Long Range Inlier and the adjacent Grenville Province (Owen and Erdmer, in press; Fig. 13; see also Fig. 54).

The voluminous plutons in this area demonstrate the importance of crustal accretion (or anatexis) during the Grenvillian Orogeny, a feature atypical of the Grenville Province near the foreland to the northwest. Equigranular and potassium feldspar-megacrystic biotite ± hornblende granite are the dominant Grenvillian plutonic rock types in the inlier. Mesoscopically, megacrystic biotite ± hornblende granite (unit **Pgk**) is identical in each pluton.

Individual plutons are named after nearby geographical localities (Fig. 14) and, where sufficient data are available, will be described below.

Mesocratic pyroxene-bearing granitoid rocks ("charnockite", sensu lato) occur in two composite Grenvillian plutons (the Lake Michel intrusive suite and the Potato Hill pluton) and in small satellite plutons near St. Pauls Big Pond. Megacrystic biotite ± hornblende-bearing granitic plutons include parts of the Lake Michel intrusive suite, and the Main River, Aspy, Little Cat Arm, Cat Arm River, Pigeon Cove, Leg Pond, Horse Chops, and Hooping Harbour (and satellite) plutons. Of these, all but the Main River and Hooping Harbour satellite plutons have been isotopically dated, and yield Grenvillian ages. Equigranular biotite ± hornblende-bearing granitic-granodioritic plutons

Table 2. Major and selected trace element geochemistry of the Taylor Brook gabbro complex. Trace elements in ppm. ns = not sought. See Appendix II for all other abbreviations. Total Fe as Fe_2O_3 in VO-85 samples.

	VO-85					VO-87		
	007	055	066-2	070	150	008	028-1	029
SiO_2	47.1	49.5	50.5	44.5	48.2	46.7	47.5	47.9
TiO_2	0.57	1.26	1.69	4.02	0.65	0.23	2.31	3.33
Al_2O_3	19.4	19.1	19.5	13.4	18.7	23.6	15.5	15.6
Fe_2O_3	7.25	9.18	9.35	18.2	7.10	1.0	4.4	4.1
FeO	ns	ns	ns	ns	ns	4.6	8.1	10.4
MnO	0.11	0.13	0.15	0.28	0.10	0.08	0.21	0.28
MgO	11.4	6.07	4.31	4.66	8.18	8.15	6.34	4.29
CaO	11.3	10.9	9.89	8.64	13.9	10.8	10.73	8.03
Na_2O	2.21	2.99	3.60	3.07	2.25	2.4	3.0	3.9
K_2O	0.15	0.40	0.53	0.59	0.09	0.20	0.24	0.44
P_2O_5	0.06	0.09	0.26	0.86	0.02	0.01	0.40	0.58
LOI	0.54	0.70	0.54	0.54	0.54	2.2	0.8	0.7
TOTAL	100.09	100.32	100.32	98.76	99.73	99.97	99.53	99.55
Ba	90	200	320	350	60	99	235	468
Rb	10	10	30	30	20	ns	ns	ns
Sr	390	550	510	400	520	556	428	478
Y	10	20	30	50	<10	ns	25	79
Zr	30	20	160	50	<10	19	56	130
Cr	190	180	30	<10	350	ns	ns	ns

Mafic mineralogy of analyzed samples:

VO-85-007:	ol-opx-cpx-hbl-bi	VO-87-008:	ol-cpx-opx-bi
-055:	opx-cpx-hbl-bi	-028-1:	cpx-opx-hbl-bi
-066-2:	opx-cpx-hbl-bi	-029:	opx-cpx-hbl-bi
-070:	opx-cpx-bi-hbl		
-150:	cpx-ol-hbl		

include parts of the Lake Michel intrusive suite, and the Cloud River, Killdevil Hill, Lomond River, Rex Lake, Fourché Harbour, and Camp Pond plutons. All yield Grenvillian isotopic ages, save the latter three, which have not been dated. Although mapping in southern Labrador is incomplete, available data indicate that Grenvillian plutons in this area are predominantly equigranular rocks which include monzonitic to syenitic variants (Gower and Loveridge, 1987).

The Lake Michel intrusive suite

The Lake Michel intrusive suite (Fig. 15) underlies an area of ca. 1500 km^2 and is composed of seven principal rock types (Owen, 1987; Table 3), including: (a) locally pyroxene-bearing, equigranular to sparsely plagioclase-megacrystic quartz monzodiorite to granite (unit **Pxg**; Fig. 16A); (b) locally pyroxene-bearing potassium feldspar-megacrystic granodiorite to granite (unit **Pxgk**; Fig. 16B); (c) potassium feldspar-megacrystic granite (unit **Pgk**; Fig. 16C); and (d) equigranular granite (unit **Pg**; Fig. 16D).

Table 3. Major rock units of the Lake Michel intrusive suite. Nomenclature for a 1:100 000 scale map of the intrusion (Owen, 1987) is given in quotation marks.

"Mesocratic granitoids"	
Pxg	medium grained hornblende + biotite ± pyroxene quartz monzodiorite-granite
Pxgk	potassium feldspar-megacrystic hornblende + biotite ± pyroxene-bearing granodiorite to granite, locally with a rapakivi texture
"Intermediate granitoids"	
Pgr	hornblende + biotite granite, sparsely potassium feldspar-megacrystic
"Leucocratic granitoids"	
Pgk	potassium feldspar-megacrystic biotite ± hornblende granite
Pgp	plagioclase-megacrystic hornblende + biotite granite to granodiorite
Ppg	medium grained biotite + hornblende granite, locally plagioclase-megacrystic
Pg	medium grained biotite + hornblende granite

Three additional texturally-distinct units are shown in Figure 15: (1) variably megacrystic granite (unit **Pgr**), which is texturally, mineralogically, and compositionally intermediate between the pyroxene-bearing granitoids and the more leucocratic granites; (2) plagioclase-megacrystic granite to granodiorite (unit **Pgp**); and (3) relatively fine grained, sparsely plagioclase-megacrystic granite (unit **Ppg**). Modal compositions of all units are listed in Table 4, and are portrayed in Figure 17A. The areal extent of unit **Pgp** is insufficient to permit its depiction on the accompanying 1:250 000 scale map (see Fig. 15 instead).

Elongate gneissic enclaves (e.g., pelitic gneiss and quartzite, Fig. 15), which in some cases separate different plutons within the intrusive suite, are continuous with the country rock; small inclusions are rare, but include amphibole-bearing diorite (restite?) and dioritic gneiss. The large elongate charnockitic (units **Pxg**, **Pxgk**) and gneissic bodies parallel (and contain) planar fabrics, which outline a nearly concentric structure in the complex (Fig. 10 and 15).

Lithology

Charnockitic rocks

The charnockitic units (**Pxg**, **Pxgk**) are mesocratic (colour index CI = 8-15), and occur as narrow (1-5 km wide)

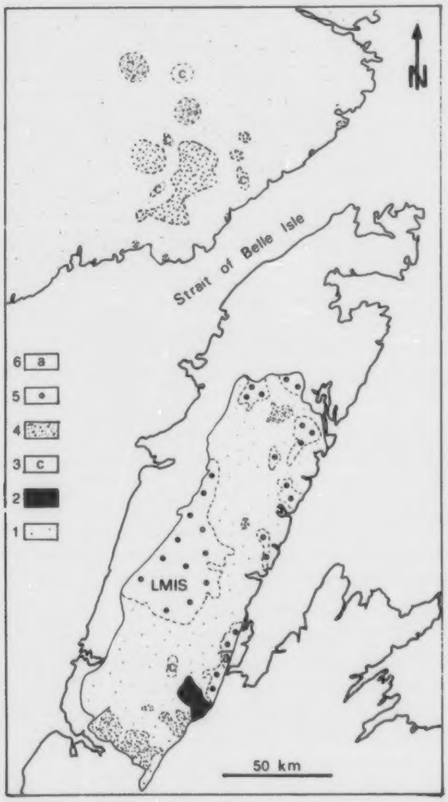

Figure 13. Distribution of plutonic rocks in the Long Range Inlier and adjacent Grenville Province of southern Labrador. 1-basement gneiss; 2-gabbro (Taylor Brook gabbro complex); 3-charnockite or mangerite (Grenvillian); 4-mostly equigranular granite (Grenvillian); 5-mostly megacrystic granite (Grenvillian); 6-Acadian granite (Devils Room granite). LMIS-Lake Michel intrusive suite. Only the three northernmost plutons shown in Labrador have been dated (Gower and Loveridge, 1987). Most of the plutons in the Long Range Inlier have been dated, and yield Grenvillian ages (H. Baadsgaard, pers. comm., 1989).

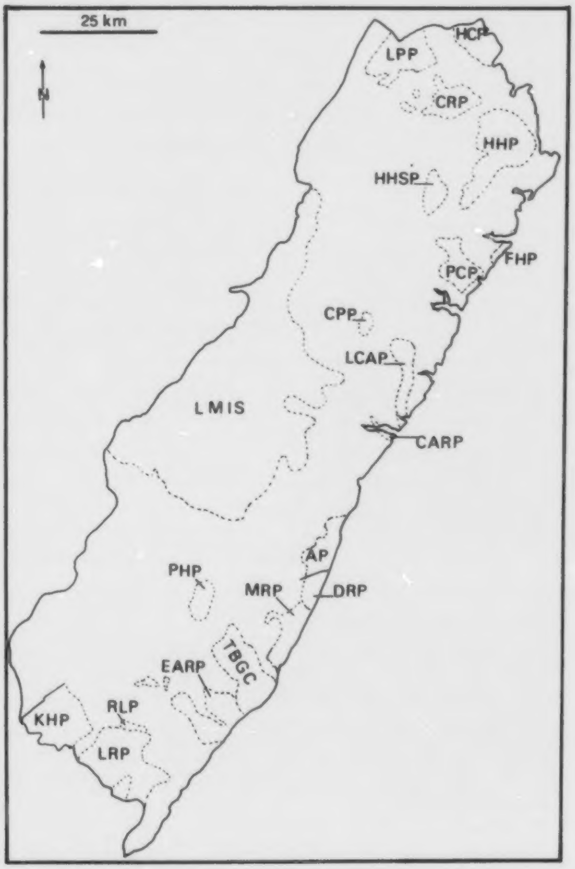

Figure 14. Nomenclature of plutons in the Long Range Inlier. HCP-Horse Chops pluton; LPP-Leg Pond pluton; HHP-Hooping Harbour pluton; HHSP-Hooping Harbour satellite pluton; PCP-Pigeon Cove pluton; CPP-Camp Pond pluton; CRP-Cloud River pluton; LCAP-Little Cat Arm pluton; CARP-Cat Arm River pluton; LMIS-Lake Michel intrusive suite; PHP-Potato Hill pluton; AP-Aspy pluton; DRP Devils Room pluton (Devonian); MRP-Main River pluton; TBGC-Taylor Brook gabbro complex; EARP-East Adies River pluton; RLP-Rex Lake pluton; KHP-Killdevil Hill pluton; LRP-Lomond River pluton; FHP-Fourché Harbour pluton. Small charnockitic plutons west of the PHP are not shown. Two small satellite plutons of medium grained biotite granite occur west of the EARP. Of the two small satellite plutons that lie west of the CRP, the southern one is the same rock type as CRP (equigranular granodiorite), and the northern one is a megacrystic granite.

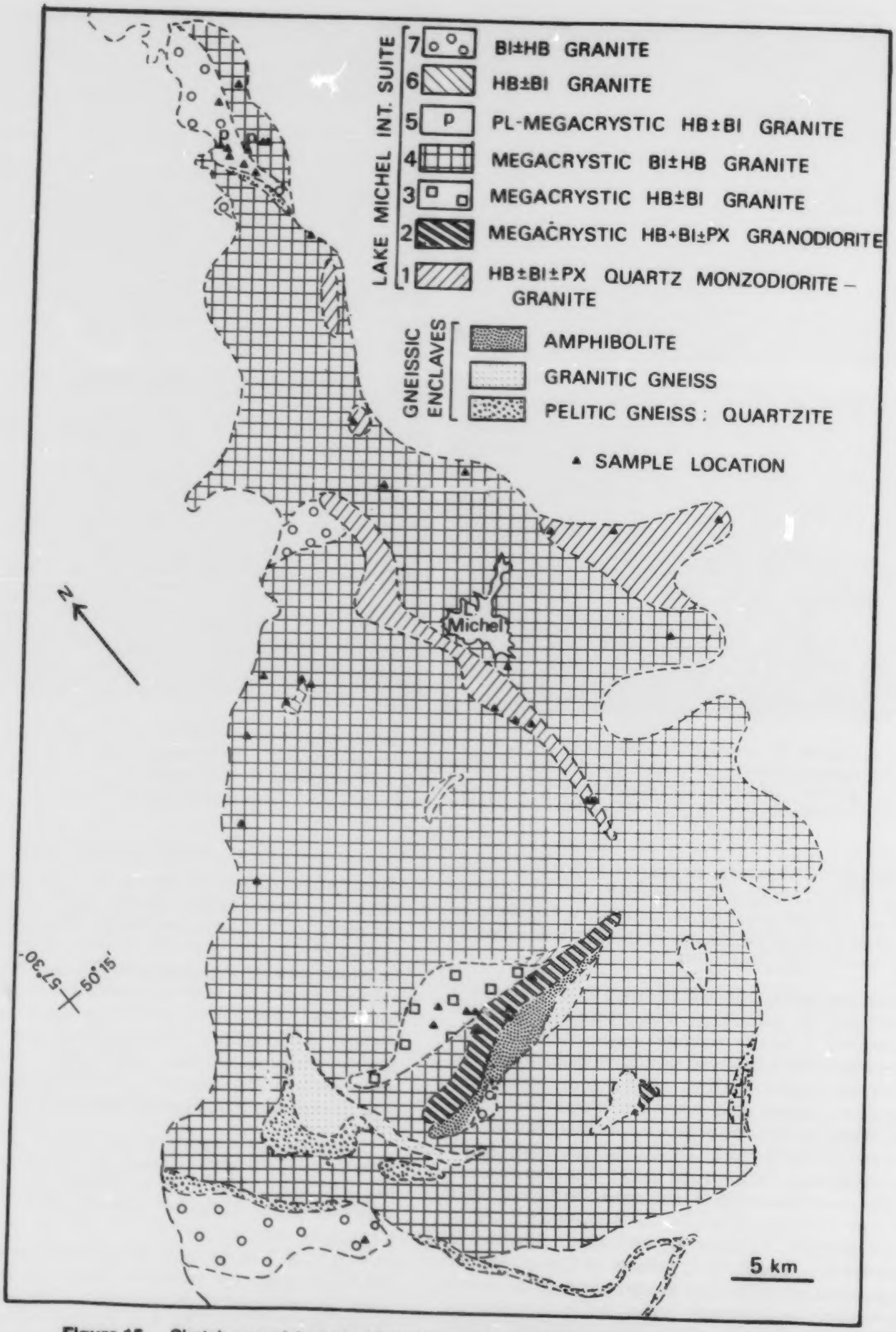

LAKE MICHEL INT. SUITE
7 BI±HB GRANITE
6 HB±BI GRANITE
5 PL-MEGACRYSTIC HB±BI GRANITE
4 MEGACRYSTIC BI±HB GRANITE
3 MEGACRYSTIC HB±BI GRANITE
2 MEGACRYSTIC HB+BI±PX GRANODIORITE
1 HB±BI±PX QUARTZ MONZODIORITE – GRANITE
GNEISSIC ENCLAVES
AMPHIBOLITE
GRANITIC GNEISS
PELITIC GNEISS ; QUARTZITE
▲ SAMPLE LOCATION
N
L. Michel
57°30'
50°15'
5 km

Figure 15. Sketch map of the Lake Michel intrusive suite. Unite numbers: 1 — Pxg, 2 — Pxgk, 3 — Pgr, 4 — Pgk, 5 — Pgp, 6 — Ppg, 7 — Pg. The gneissis enclaves include amphibolite (Pdn), granitic gneiss (Pgn), and pelitic gneiss (Ppn) and quartzite (Pqn).

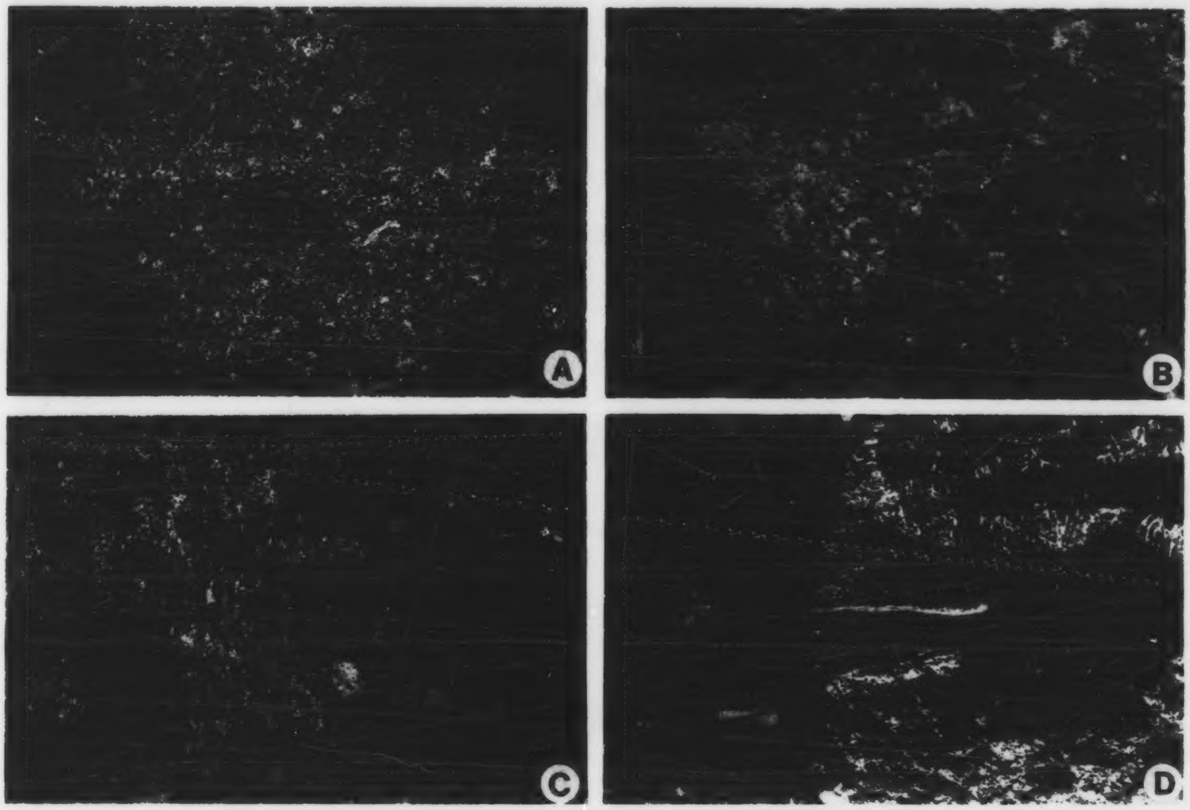

Figure 16. Field photographs of principal units of the Lake Michel intrusive suite. A. Equigranular hornblende biotite (± pyroxene) granodiorite (unit **Pxg**); B. rapakivi-textured hornblende-biotite (± pyroxene) granite (unit **Pxgk**); C. megacrystic biotite-hornblende granite (unit **Pgk**); D. dykes of equigranular biotite-hornblende granite (unit **Pg**) cutting megacrystic granite (unit **Pgk**). GSC photos 204932 16A to D.

elongate (up to 27 km long) bodies enclosed by leucocratic granite (CI = 5) (Fig. 15). Pyroxenes are only locally preserved, but are nevertheless sufficiently diagnostic of these rocks that their general description as "charnockites" (sensu lato) is warranted.

In outcrop, quartz monzodiorite (unit **Pxg**) is a medium grained, grey to green-grey rock. Although generally equigranular, it locally contains xenomorphic to idiomorphic oligoclase megacrysts up to 2 cm in diameter. The xenomorphic megacrysts have sutured grain boundaries, and in places enclose small potassium feldspar and quartz grains. Where present, the plagioclase megacrysts compose up to about 20 % of the rock. The groundmass is principally composed of mafic minerals and quartz. The plagioclase is generally partly saussuritized, and quartz commonly has a bluish cast. The rock is massive to well foliated, and in places is mylonitic. Pyroxene is preferentially preserved in the massive (i.e., undeformed) variants. In thin section, the mafic minerals generally occur in aggregates. Biotite forms subidiomorphic to idiomorphic grains, and in some samples is the predominant mafic mineral. Green hornblende occurs as subidiomorphic grains which in some samples enclose large (to 0.5 mm) well-formed apatite crystals. Pyroxenes form clusters of subidiomorphic grains. Both clinopyroxene and orthopyroxene may be present. In places, orthopyroxene partly encloses clinopyroxene, but grain boundaries are smooth and straight, and both phases appear to be stable. Relations between the amphibole and pyroxene vary. In two-pyroxene-bearing charnockite (e.g., sample VO-86-887; Fig. 18A), some pyroxenes are entirely enclosed by amphibole. Grain contacts are sharp and straight, and free of intervening quartz. This militates against reaction relations between these phases, and suggests instead that pyroxene and amphibole are stable.

In outcrop, the megacrystic granodiorite (unit **Pxgk**) is a buff coloured rock containing potassium feldspar megacrysts from 1 to 3 cm in diameter (rarely to 5 cm) which in places display a rapakivi texture. Plagioclase megacrysts occur locally. The megacrysts typically compose up to 40 % of the rock, but are locally more abundant (60 %), in which case the rock is better described as being coarse grained rather than megacrystic. The rock is massive to well-foliated. As with unit **Pxg**, pyroxene is rarely preserved in well-foliated samples. Hornblende is the dominant mafic mineral. It occurs as subidiomorphic, green or green-brown grains associated with biotite, ilmenite (or magnetite), apatite, and/or clinopyroxene. In samples VO-86-1217 and VO-86-4030, augite forms large (to 3 mm) grains, some of which are partly enclosed by hornblende. The hornblende has lobate grain boundaries, and is separated from the augite by quartz. This implies a reaction relation in which the clinopyroxene is partly replaced by amphibole and quartz. Some of the augite in both samples is altered to colourless to pale green amphibole (cummingtonite?).

The potassium feldspar in both charnockitic units is grid-twinned microcline. Microprobe analysis (see below) indicates that plagioclase is intermediate to calcic oligoclase. Accessory minerals include ilmenite (and/or magnetite), apatite (usually present as inclusions in hornblende or oxide minerals), zircon, and titanite. Compared with the more leucocratic members of the intrusive suite, the charnockitic rocks have a relatively high concentration (collectively approaching 2 or 3 volume percent) of accessory minerals.

"Intermediate" granite

The "intermediate" granite (unit **Pgr**) is a sparsely megacrystic rock with textural, mineralogical, and compositional characteristics of the charnockitic and more leucocratic granitoid rocks of the Lake Michel intrusive suite. The granite is pale rose in colour, and contains relatively small (1 cm), somewhat indistinct potassium feldspar megacrysts. In thin section, mafic minerals are seen to occur

Table 4. Modal composition of the Lake Michel intrusive suite. alt. px-altered pyroxene, tr-trace. See Appendix II for all other abbreviations.

	Ksp	pl	qz	bi	hbl	cpx	opx	alt. px	ilm and/ or mt	ap	sph	ep	zr	chl
Pxg														
050	22.5	38.7	12.6	2.0	16.6				4.1	1.5			tr	
802	11.7	43.4	26.3	10.2	4.0				3.2	1.2		tr		
811	16.7	40.5	25.9	6.8	3.7				2.1	3.0	0.5	0.4	0.4	
887	22.6	40.8	16.5		8.2	3.6	4.0		2.4	1.7			tr	
1174	22.2	36.9	20.4	1.7	11.8				4.4	2.3			tr	
1188	25.4	38.5	25.5	5.5	3.3				1.1	0.7				
Pxgk														
059	7.8	51.6	10.8	3.5	19.3				3.0	2.7	tr	tr	tr	
093	19.7	39.0	22.4	1.0	11.3			3.3	2.3	1.0			tr	
1217	25.0	44.6	9.3	1.8	13.3		0.9	2.5	1.9	0.7				
4030	24.1	41.6	9.2		15.3	5.9			1.8	1.7				
Pgr														
068	30.3	36.7	25.5	5.6					1.2	0.3				
076	26.2	39.8	20.2	8.1					3.4	1.7	1.2			
079	24.5	37.4	23.3	6.7	2.6				2.5	1.8				
1198	34.4	30.8	28.1	4.7	0.7				0.9	0.4				
4330	33.7	29.6	28.5	3.1	2.9				0.9	0.6		0.7		
Pgk														
044	42.8	13.8	41.6	0.3						0.6				
207	30.8	35.3	29.7	2.9					0.7	t				
443-1	37.6	27.8	25.3	2.4	4.1				0.4	0.4				1.9
864	45.1	30.9	19.0	1.1	2.0					0.6		0.6		
2079	53.2	18.5	25.7	1.9*					0.6	0.1				
2182	38.6	33.7	20.1	3.0	2.8				1.5	0.2				
4128	27.2	37.8	24.9	3.9	0.5				2.6	1.0	2.1			
Pgp														
445	20.7	49.8	23.9	0.3	2.3				0.4	tr				
469	30.2	34.3	20.8	2.2	9.0				1.5	1.9			tr	
Ppg														
209	28.3	37.5	16.7	0.6	11.0				4.8	1.1				
4134	30.9	32.1	17.0	7.2	3.9				4.2	2.4	2.2			
Pg														
443-2	37.9	34.8	16.0	8.6	2.3				0.4					
476	25.4	36.8	33.0	2.8					1.5	0.1				0.4
642	46.7	26.1	24.9	1.9	0.1									

* Biotite is chloritized

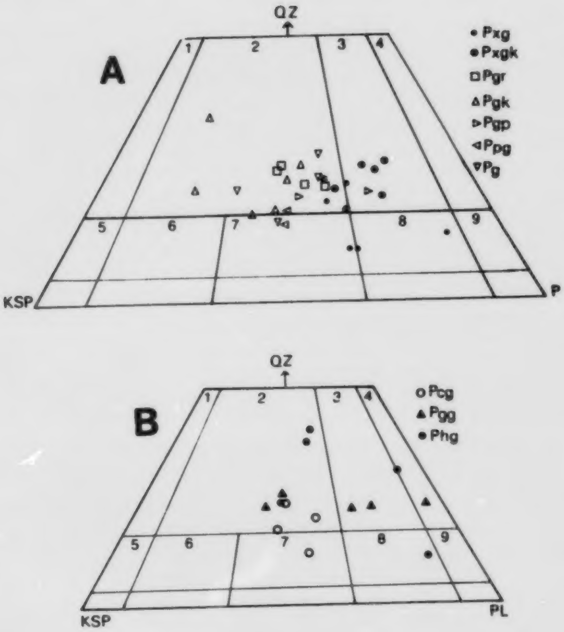

Figure 17. Modal composition of (A) the Lake Michel intrusive suite and (B) the Potato Hill pluton. Field boundaries after Streckeisen (1976): 1-alkali feldspar granite, 2- granite, 3-granodiorite, 4-tonalite, 5-quartz-alkali feldspar syenite, 6-quartz syenite, 7-quartz monzonite, 8-quartz monzodiorite, 9-quartz diorite.

in aggregates. Both biotite and green- to olive-brown hornblende are present as subidiomorphic grains up to 1.5 mm in diameter. As in the charnockites (units **Pxg**, **Pxgk**), accessory minerals are conspicuous, and include apatite, ilmenite (and/or magnetite), and large (to 1.5 mm) titanite grains. In one sample (VO-86-062), the titanites enclose an unidentified, nearly-isotropic high relief mineral containing (as determined by microprobe analysis) about 7% silica, 4% alumina, 55% TiO_2, 5% FeO (total Fe), and less than 0.5% each of lime and alkalies. Potassium feldspar in the granite is grid-twinned microcline. Plagioclase contains approximately 27% anorthite component (microprobe determination).

Leucocratic granitoid rocks

Leucocratic granitoids (colour index ≤5) are dominant in the Lake Michel intrusive suite. Aerially, the most extensive unit is megacrystic biotite-hornblende granite (**Pgk**). Lithologically-identical megacrystic granite occurs in several other Grenvillian plutons, particularly those in the northern part of the inlier (e.g., the Hooping Harbour, Pigeon Cove, and Little Cat Arm plutons).

The megacrystic granite is pale rose and weakly to well foliated, and contains preferentially-oriented, tabular or lens-shaped salmon-pink potassium feldspar megacrysts. The megacrysts range in size from about 1 to 3 cm (locally to 5 cm) and typically constitute from approximately 20 to 40% of the rock, although some sparsely megacrystic (5-10% megacrysts) rocks are included in this unit. Biotite and hornblende are the sole mafic minerals. Biotite is generally dominant. It forms clusters of subidiomorphic grains, and is often chloritized. Hornblende is green to brownish-green, and forms discrete grains or is associated with biotite. Potassium feldspar is grid-twinned microcline; plagioclase is calcic oligoclase. Myrmekite is common. The megacrystic granite contains small concentrations of apatite, magnetite (and/or ilmenite), and zircon.

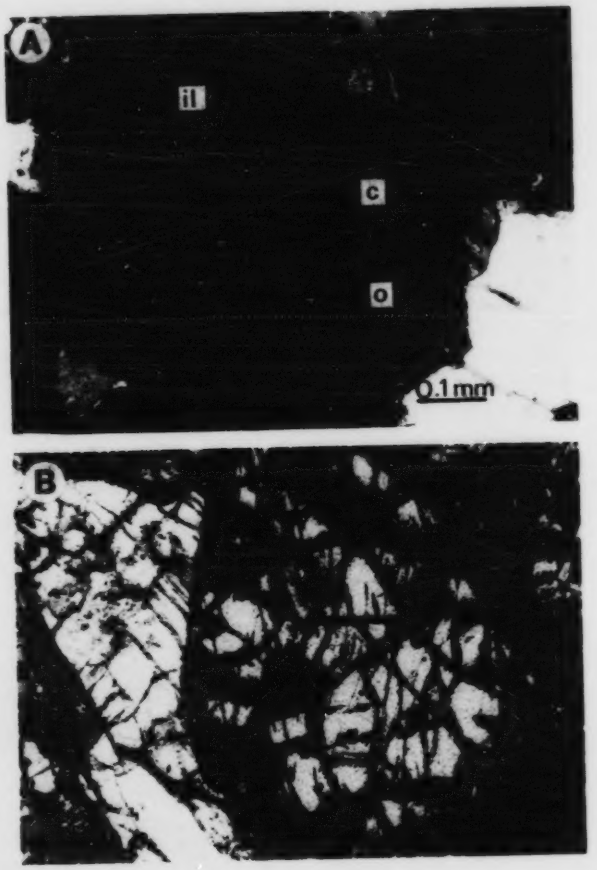

Figure 18. Photomicrographs of pyroxene-bearing granitoids. A. Two-pyroxene granodiorite (charnockite) of the Lake Michel intrusive suite (unit **Pxg**). o-orthopyroxene, c-clinopyroxene, il-ilmenite; sample VO-86-887; crossed nicols; B. coarse hypersthene in pyroxene monzonite (unit **Pom**; sample VO-87-163; plane polarized light).

Equigranular granite (unit **Pg**) is a relatively homogeneous, pale rose to tan rock. Biotite is the dominant mafic mineral. It occurs as subidiomorphic grains (0.5 to 1 mm) which are more-or-less evenly distributed in the rock. Hornblende, where present, occurs as green subidiomorphic grains. Both mafic minerals contribute to a weak foliation in the granite. Quartz, oligoclase, and microcline occur as granoblastic mosaics through which the mafic phases are dispersed. Potassium feldspar megacrysts occur locally; where present, they constitute less than 5 % of the rock. Apatite, magnetite (and/or ilmenite), and zircon are present in accessory concentrations.

Plagioclase-megacrystic granite (unit **Pgp**) is a distinctive rock containing sodic andesine (An_{33}) megacrysts up to 2 cm in diameter. In outcrop, the megacrysts are pale yellowish-green to dark grey, and occur as discrete well-formed crystals or as crystal clusters. Two morphological types of plagioclase megacrysts are present: (1) ovoid xenomorphic grains containing abundant graphic-quartz (cuniform) inclusions; and (2) (sub)idiomorphic quartz-free crystals. The fine grained (0.3 mm) matrix is rich in potassium feldspar and quartz, and in thin section has a granoblastic appearance resulting from evenly distributed, equant to lobate quartz grains, present both as inclusions in larger microcline grains, and as part of a polymineralic mosaic with microcline, biotite, green hornblende, and ilmenite (and/or magnetite). The mafic minerals form diffuse clusters riddled with quartz grains.

Plagioclase megacrysts characterize another minor granitoid unit in the intrusive suite. This rock (unit **Ppg**) differs from unit **Pgp** insofar as the plagioclase megacrysts (An_{25}) are smaller (5 mm), and are set in a slightly coarser grained (0.5-1 mm) matrix which contains oligoclase as well as quartz and microcline. A few salmon-pink microcline megacrysts are locally conspicuous. Green to olive-green hornblende and biotite occur as subidiomorphic to idiomorphic grains in varying proportions, and are fairly evenly distributed in the rock. Accessory minerals include ilmenite (and/or magnetite), apatite, and epidote.

Age relations

The relative age of only two of the seven members of the Lake Michel intrusive suite is known from field relations. Dykes of medium grained equigranular biotite-hornblende granite cut megacrystic biotite-hornblende granite (unit **Pgk**) in the northern part of the intrusion. These dykes are correlated with equigranular granite (unit **Pg**) which forms a large pluton approximately 1.5 km from the outcrop containing the dykes.

Possible inclusions of megacrystic charnockite (unit **Pxgk**) occur in sparsely megacrystic hornblende-biotite granite (unit **Pgr**) in the southern part of the intrusive suite; however, exposure was relatively poor in this outcrop and this observation should be considered inconclusive.

Regression of U-Pb (zircon) data for the charnockite (units **Pxg** and **Pxgk**), megacrystic granite (**Pgk**), and equigranular granite (**Pg**) yields an upper concordia-discordia intercept of 1023 +7/−5 Ma (2 sigma) and a lower intercept of 390 ± 42 Ma (H. Baadsgaard, pers. comm., 1989). Zircons from two samples and titanite from four megacrystic granite samples give concordant U-Pb ages of 970 ± 4 Ma. This apparently marks the terminal stages of Grenvillian granitoid plutonism in the inlier.

When the Lake Michel data are coupled with U-Pb (zircon) data for other granitic plutons in the inlier, the discordia line yields an upper intercept age of 1056 +4/−6 Ma. This is the preferred age for regional Grenvillian granitoid plutonism in the inlier (H. Baadsgaard, pers. comm., 1989).

Mineralogy

The mineralogy of the Lake Michel intrusive suite is rather simple. All rocks are massive to foliated, and contain biotite and/or hornblende, microcline, oligoclase, and quartz. Pyroxene is preserved only locally in charnockitic units.

Clinopyroxene in mesocratic charnockitic rocks (units **Pxg** and **Pxgk**) ranges in composition from $Wo_{39-42}En_{28-32}Fs_{26-32}$ (Table 5). It forms subidiomorphic to xenomorphic grains typically enclosed by amphibole.

Orthopyroxene coexisting with clinopyroxene in a single sample of medium grained mesocratic granodiorite (unit **Pxg**) is a ferrohypersthene of composition $Wo_2En_{35}Fs_{63}$. Orthopyroxene (hypersthene to ferrohypersthene) in other samples is replaced by amphibole.

Amphibole forms green to olive-brown xenomorphic or subidiomorphic grains. Amphibole compositions (Table 6) have been recalculated to 23 oxygens, with all cations excluding Ca, Na, and K normalized to 13, and Fe^{3+} estimated by charge balancing. These are calcic amphiboles, with A-site alkalies totalling 0.6 to 0.8 per formula unit (p.f.u.), and with $X_{Fe^{3+}}$ ($=Fe^{3+}/(Fe^{3+} + Fe^{2+})$) ranging from 0.1 to 0.4. The "13exCNK" scheme adopted here is appropriate for many calcic amphiboles (Robinson et al., 1982). Using this method, amphibole compositions determined for all units cluster in the magnesian hastingsitic hornblende field of Leake (1978) (Fig. 19), implying that the intrusive suite has alkaline affinities. It should be noted that amphibole nomenclature is sensitive to the recalculation scheme by which cations are cast into different structural sites, and amphibole from the intrusive suite is variously classified as ferroan pargasitic hornblende or tschermakite (etc.) if other crystal-chemical schemes are used (Table 6).

Biotite shows a range in X_{Mg} from 0.2 to 0.6 in the mesocratic units, and 0.3 to 0.8 in the leucocratic units. TiO_2 varies between 1.5 and 3.8 weight percent in the mesocratic granites, and up to 4.3 weight percent in the leucocratic granites.

Plagioclase in the mesocratic samples is slightly more calcic (An_{23-30}) than plagioclase in the leucocratic rocks (An_{16-26}). The composition of the most sodic oligoclase (determined by electron microprobe) lies within the peristerite gap, implying unusual crystallization conditions for some samples of leucogranite.

Andesine megacrysts (An_{33}) occur locally in the granitic rocks. Although plagioclase typically is not zoned, plagioclase rims in some samples are slightly more sodic (by up to 3 % Ab) than their cores.

Accessory minerals include apatite, ilmenite, magnetite, and zircon, locally with titanite or epidote. These phases

Table 5. Microprobe analyses of pyroxenes from the Lake Michel intrusive suite (units **Pxg** and **Pxgk**), the Potato Hill pluton (unit **Pcg**), and orthopyroxene monzonite (unit **Pom**). End member compositions determined by the method of Lindsley and Anderson (1983). A two-pyroxene temperature of 734°C for VO-86-887 was determined by the method of Davidson and Lindsley (1985). Oxygen basis = 6. Abbreviations as in Appendix II. Total Fe as FeO.

Unit:	Pxg		Pxgk		Pom	Pcg	Pcg	
	VO-86-887		VO-86-4030	VO-86-1217	VO-87-163	VO-87-0408	VO-87-0408	
	cpx	opx	cpx	cpx	opx	opx	cpx core	cpx rim
SiO_2	49.81	48.84	51.59	50.71	52.63	47.71	48.64	49.60
TiO_2	0.17	0.08	0.16	0.19	0.05	0.22	0.19	0.06
Al_2O_3	1.40	0.56	1.32	2.32	1.08	0.55	1.17	0.65
Cr_2O_3	0.01	0.02	0.00	0.02	0.00	0.00	0.02	0.01
FeO	17.94	37.36	15.94	16.84	22.16	44.05	27.26	22.03
MnO	0.73	0.16	0.48	0.53	0.68	0.97	0.49	0.45
MgO	8.43	10.72	10.13	8.82	22.16	6.54	5.52	5.84
CaO	20.62	0.87	20.27	19.52	0.57	1.33	16.61	20.68
Na_2O	0.38	0.02	0.52	0.41	0.00	0.12	0.42	0.36
	99.5	98.6	100.4	99.4	99.3	101.5	100.3	99.7
Si	1.953	1.992	1.974	1.965	1.974	1.965	1.955	1.978
Al^{iv}	0.047	0.008	0.026	0.035	0.026	0.035	0.045	0.022
Al^{vi}	0.018	0.019	0.034	0.071	0.022	—	0.010	0.009
Ti	0.005	0.002	0.005	0.006	0.001	0.007	0.006	0.002
Cr	—	0.001	—	0.001	—	—	0.001	—
Fe	0.588	1.274	0.510	0.546	0.695	1.517	0.916	0.735
Mn	0.024	0.006	0.016	0.017	0.022	0.034	0.017	0.015
Mg	0.493	0.652	0.578	0.509	1.239	0.401	0.331	0.347
Ca	0.866	0.038	0.831	0.811	0.023	0.059	0.715	0.884
Na	0.029	0.002	0.039	0.031	—	0.010	0.033	0.028
Wo	42.1	1.9	42.0	38.9	1.2	3.0	35.0	44.0
En	28.3	33.2	31.8	29.5	63.4	20.5	18.4	18.9
Fs	29.7	64.9	26.3	31.6	35.4	76.4	46.7	37.1

occur in relatively high concentrations in the mesocratic granitoids (i.e., units **Pxg**, **Pxgk**, **Pgr**). Ilmenite and magnetite coexist in several samples of mesocratic granodiorite/charnockite; magnetite is the typical oxide phase in leucogranite (i.e., units **Pg**, **Pgk**).

Geochemistry

Forty-six samples of the Lake Michel intrusive suite were analyzed for major and selected trace elements. Mean bulk compositions and CIPW norms of the intrusive suite are listed in Table 7; the complete set of analyses is listed in Appendix III.

Broad dissimilarities in the modal composition of the mesocratic and leucocratic granitoids are reflected in their major and trace element compositions.

All units are metaluminous. Collectively, their composition defines an alkali-lime index of about 56. Most samples, particularly the leucogranites, plot in the calc-alkalic field on an AFM diagram (Fig. 20). Charnockitic rocks (units **Pxg**, **Pxgk**), "intermediate" granite (unit **Pgr**), and plagioclase-megacrystic granite (unit **Pgp**) are diopside-normative; relatively leucocratic biotite ± hornblende granite (units **Pgk**, **Ppg**, **Pg**) is corundum-normative (Table 7).

Although charnockite occurs locally, granitic-granodioritic rocks containing biotite ± hornblende ± ilmenite ± magnetite are dominant in the inlier. These granitoid rocks form widespread amoeboid bodies which were emplaced over a period of about 85 Ma (i.e., 1056 to 970 Ma). Contrasted mafic-felsic associations are absent. The Lake Michel intrusive suite has low molecular Al/(Ca/2 + Na + K) values (A/CNK ≤ 1.1), has elevated trace element concentrations, and contains amphibole (magnesian hastingsitic hornblende) with compositions indicative of alkaline affinities. These features do not lend themselves to standard granite-type classification schemes (e.g., Pitcher, 1983). The absence of mafic rocks (apart from the Taylor Brook gabbro complex, of unknown age) and the dominance of megacrystic hornblende- and biotite-bearing granites militate against an orogenic classification for the Grenvillian plutons, at least according to the criteria for I- and S-type granites listed by Pitcher (1983). On the other hand, some granitoids in the Lake Michel intrusive suite, particularly the charnockites, have elevated Ga/Al (see section on Tectonic Setting, below) which implies A-type characteristics (Collins et al., 1982; Whalen et al., 1987).

The Lake Michel intrusive suite displays classic linear trends on major element variation diagrams (Fig. 21). SiO_2 shows a strong negative correlation with TiO_2 (correlation

Table 6. Composition and nomenclature of amphibole from different units of the Lake Michel intrusive suite (see Fig. 15). Amphiboles are classified using different recalculation schemes (Robinson et al., 1982) following the nomenclature of Leake (1978). Total Fe as FeO.

Unit:	1	2	3	4	5	6	7
SiO_2	41.04	41.52	43.30	41.62	40.14	43.44	41.64
TiO_2	1.93	1.98	1.11	1.51	1.48	1.33	1.51
Al_2O_3	10.57	10.01	10.24	9.74	10.66	9.43	9.88
FeO	20.84	20.88	16.21	20.37	24.41	14.14	22.07
MnO	0.39	0.29	0.74	0.56	0.60	0.50	0.50
MgO	7.97	7.73	11.37	8.56	6.10	13.12	7.41
CaO	11.09	10.61	11.37	10.72	10.81	11.48	11.06
Na_2O	1.86	1.82	1.69	2.00	1.76	2.00	1.86
K_2O	1.66	1.49	1.61	1.48	1.63	1.56	1.49
	97.4	96.3	97.7	96.6	97.6	97.0	97.4
n	4	3	2	3	2	2	1

Nomenclature

	All Fe as Fe^{2+}	13exCNK	15exNa,K	15exK
Unit 1:	FPH	MHH	*	T
Unit 2:	FPH	MHH	*	TH
Unit 3:	EH	MHH	EH	TH
Unit 4:	FPH	MHH	*	TH
Unit 5:	FPH	MH	FPH	T
Unit 6:	EH	M-HH	EH	*
Unit 7:	FPH	MHH	*	TH

* — Calculation not possible (charge > 46)

n — Number of samples; generally 3 grains were analyzed per sample. Analyses were determined using a JEOL JXA-50A microprobe (see Owen and Erdmer (1989) for operating conditions).

Abbreviations: FPH-ferroan pargasitic hornblende, MHH — magnesian hastingsitic hornblende, M-HH — magnesio-hastingsitic hornblende, MH — magnesian hastingsite, T — tschermakite, TH — tschermakitic hornblende, EH — edenitic hornblende

coefficient = -0.92), CaO (-0.93), MgO (-0.93), FeO (-0.82), P_2O_5 (-0.82), and Zr (-0.79), a moderate negative correlation with Sr (-0.63) and Ba (-0.62), and a weak positive correlation with K_2O (+0.34) and Rb (+0.39). These patterns suggest that at least some of the plutons within the intrusive suite evolved from a common parent magma source.

Several lines of evidence suggest that the leucogranites were derived, at least in part, from crustal source components. For example, K/Rb ratios are close to crustal averages ("K/Rb main trend", e.g., Rao and Rao, 1988; Fig. 22C), indicating a composition typical of crustal granites, and Th/La, expected to be relatively high in crustal granites, varies between 0.04 and 1.3 (see Fig. 23 and Appendix III). On the other hand, the charnockites have overlapping, generally higher K/Rb ratios (=287-481), reflecting a relative depletion in Rb, and have smaller but overlapping Th/La ratios (=0.02-0.23, see Fig. 23). These trends may be more apparent than real, since scatter on Ba versus Rb, Ca versus Sr, Ba versus Sr, and K versus Rb plots (Fig. 22), particularly for the leucogranites, may simply indicate that the primary chemistry of these rocks has been disturbed by secondary processes. Although only the freshest samples were selected for analysis, it is noteworthy that epidote and chlorite are ubiquitous in the intrusive suite.

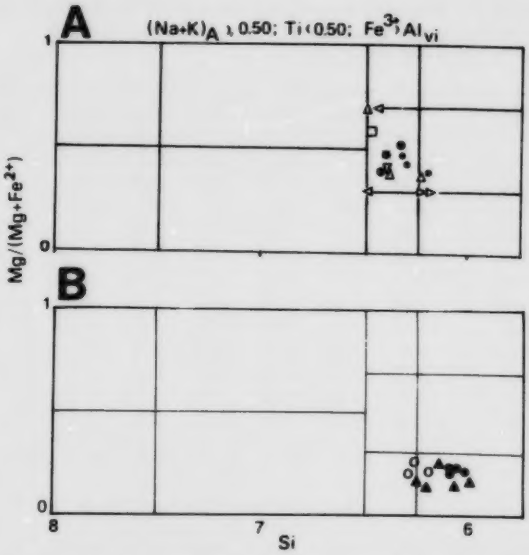

Figure 19. Composition of amphiboles from the Lake Michel intrusive suite (A) and the Potato Hill pluton (B). Field boundaries after Leake (1978). Amphiboles from the Lake Michel intrusive suite cluster in the magnesian hastingsitic hornblende field; amphiboles from the Potato Hill pluton straddle the boundary between hastingsite and hastingsitic hornblende. Crystal-chemical limits for the amphiboles are shown on top of the diagram. Symbols as in Figure 17.

For this reason, the concentration of relatively immobile elements (e.g., high field strength (HFS) elements) in the Lake Michel intrusive suite probably provides a more reliable basis for interpreting the origin of these rocks. The granitoids differ in their Nb/La ratio, which varies between 0.03 and 0.62 in the leucogranites, and between 0.24 and 0.89 in the charnockites (Fig. 23). The leucocratic and mesocratic granitoids define distinct fields on P_2O_5 versus La and P_2O_5 versus Zr plots (Fig. 24). Higher concentrations of P and Zr in the charnockites reflect higher modal apatite and zircon (respectively) in these rocks. Data for the intermediate pluton (unit **Pgr**) plot between the mesogranite and leucogranite fields, and minor leucogranite rock types (units **Pgp** and **Ppg**) plot outside the main leucogranite field, indicating a distinct petrogenetic history for these rocks. These features imply that the charnockites were derived either from partial fusion of the upper mantle, or from the refractory residue of previously partly melted crust (cf. Rogers, 1988), while a crustal origin is inferred for the leucogranites.

Isotopic data useful in evaluating the relative importance of mantle and crustal sources for the intrusive suite are unavailable. Although a low initial $^{87}Sr/^{86}Sr$ ratio of 0.702 ± 0.004 was determined by Pringle et al. (1971), it is not

Table 7. Mean bulk composition and CIPW norms of the Lake Michel intrusive suite. Trace elements in ppm. n = number of analyses.

Unit:	Pxg	Pxgk	Pgr	Pgk	Pgp	Ppg	Pg
SiO_2	63.3	62.4	65.2	70.8	66.5	60.9	71.3
TiO_2	1.33	1.34	1.10	0.55	0.85	1.55	0.39
Al_2O_3	14.0	14.8	14.2	13.7	14.4	14.0	14.4
Fe_2O_3	2.66	1.85	2.98	1.61	2.05	4.85	1.28
FeO	4.36	5.10	2.43	1.82	3.05	3.10	1.79
MnO	0.12	0.10	0.08	0.04	0.08	0.12	0.05
MgO	1.24	1.46	1.07	0.49	0.80	1.55	0.54
CaO	3.91	3.97	3.30	1.52	2.84	4.03	1.81
Na_2O	3.05	3.56	3.15	3.15	3.15	3.20	4.13
K_2O	3.79	3.54	4.39	5.27	4.41	4.11	3.78
P_2O_5	0.67	0.58	0.59	0.26	0.36	0.75	0.21
LOI	0.82	0.79	0.80	0.63	0.95	0.73	0.51
	99.3	99.4	99.2	99.8	99.3	98.9	100.3
n =	10	6	6	11	2	2	8
Ba	1603	1131	1280	904	1114	2173	962
Nb	36	51	34	30	40	39	25
Rb	116	65	211	198	156	130	124
Sr	154	402	497	300	354	779	371
Y	72	49	89	48	53	100	69
Zr	704	650	558	380	579	859	291
Ga	25	22	23	20	11	23	20
La	97	67	109	108	105	163	75
Yb	6	5	9	4	5	8	3
				CIPW norms			
Ap	1.47	1.28	1.30	0.57	0.79	1.65	0.46
Il	2.53	2.55	2.10	1.05	1.62	2.95	0.74
Mt	3.87	2.69	4.33	2.34	2.98	5.91	1.86
Or	22.40	20.92	25.94	31.13	26.06	24.29	22.33
Ab	25.82	30.14	26.66	26.65	26.66	27.09	34.94
An	13.32	13.87	11.59	5.84	11.74	11.84	7.61
Di	1.42	1.72	0.74			2.54	
Hy	6.21	8.58	2.65	2.40	4.64	2.68	3.02
C				0.62	0.09		0.77
Q	21.40	16.90	23.13	28.59	23.81	18.46	28.02
Hm						0.79	

known which units were analyzed (**Pgk**?), consequently the implications for the charnockitic and granitic units are unclear.

Evidence of a mantle origin (or a depleted lower crustal source) for the charnockites and of a crustal origin for leucogranite does not necessarily imply independent petrogenetic histories. For example, it is possible that the leucogranite was derived from crustal material, melted during emplacement of the mantle-derived charnockitic magma; or it may have resulted from the contamination of charnockitic magma by crustal components. The available data do not favour either alternative.

The Potato Hill pluton

Charnockite of Grenvillian age is not restricted to the Lake Michel intrusive suite; it also occurs in a smaller (65 km^2) composite intrusion known as the Potato Hill pluton (Fig. 25). Three principal rock types have been identified (Fig. 17). The southern part of the intrusion consists of coronitic charnockite (Fig. 26A). The remainder of the intrusion consists of garnetiferous biotite ± hornblende granite (Fig. 26B,C,D) and megacrystic hornblende-biotite mesogranite (Fig. 26E). A satellite pluton of garnetiferous charnockite occurs west of the Potato Hill pluton. Like charnockite in the Potato Hill pluton, this pluton is coronitic.

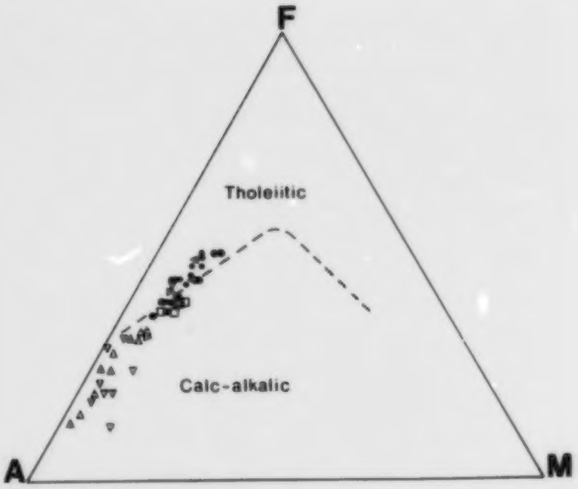

Figure 20. AFM diagram for the Lake Michel intrusive suite. Dashed line separating tholeiitic from calc-alkalic compositions is after Irvine and Baragar (1971). Symbols as in Figure 17. See text for complete discussion.

Lithology

The coronitic charnockite (unit **Pcg**) is a massive to weakly foliated, tan weathering, brownish-green rock containing primary Fe-rich orthopyroxene (eulite), pale green clinopyroxene, and biotite. The coronitic textures are plainly evident on the weathered surface, and represent a variety of disequilibrium assemblages. The coronas most typically comprise partial envelopes of hornblende, quartz, and garnet which enclose eulite (Fig. 27). The orthopyroxene core of the corona structure typically is twinned. The garnets are well formed, and contain symplectic intergrowths of quartz. Other corona types include hornblende and garnet rims on ilmenite (and/or magnetite) and clinopyroxene.

Massive to weakly foliated, buff weathering garnetiferous granite (unit **Pgg**) occupies the central part of the Potato Hill pluton. The garnetiferous granite is rose coloured on the fresh surface. Garnets have three associations in the granite: (1) as individual grains or grain aggregates up to about 1 cm across, irregularly distributed in the granite (Fig. 26D); (2) as smaller crystals, concentrated with biotite and/or hornblende in narrow (ca. 10 cm wide) mesocratic bands (igneous layering ?) in the rock (Fig. 26B); and (3) as large (to 4 cm) well-formed crystals in leucocratic

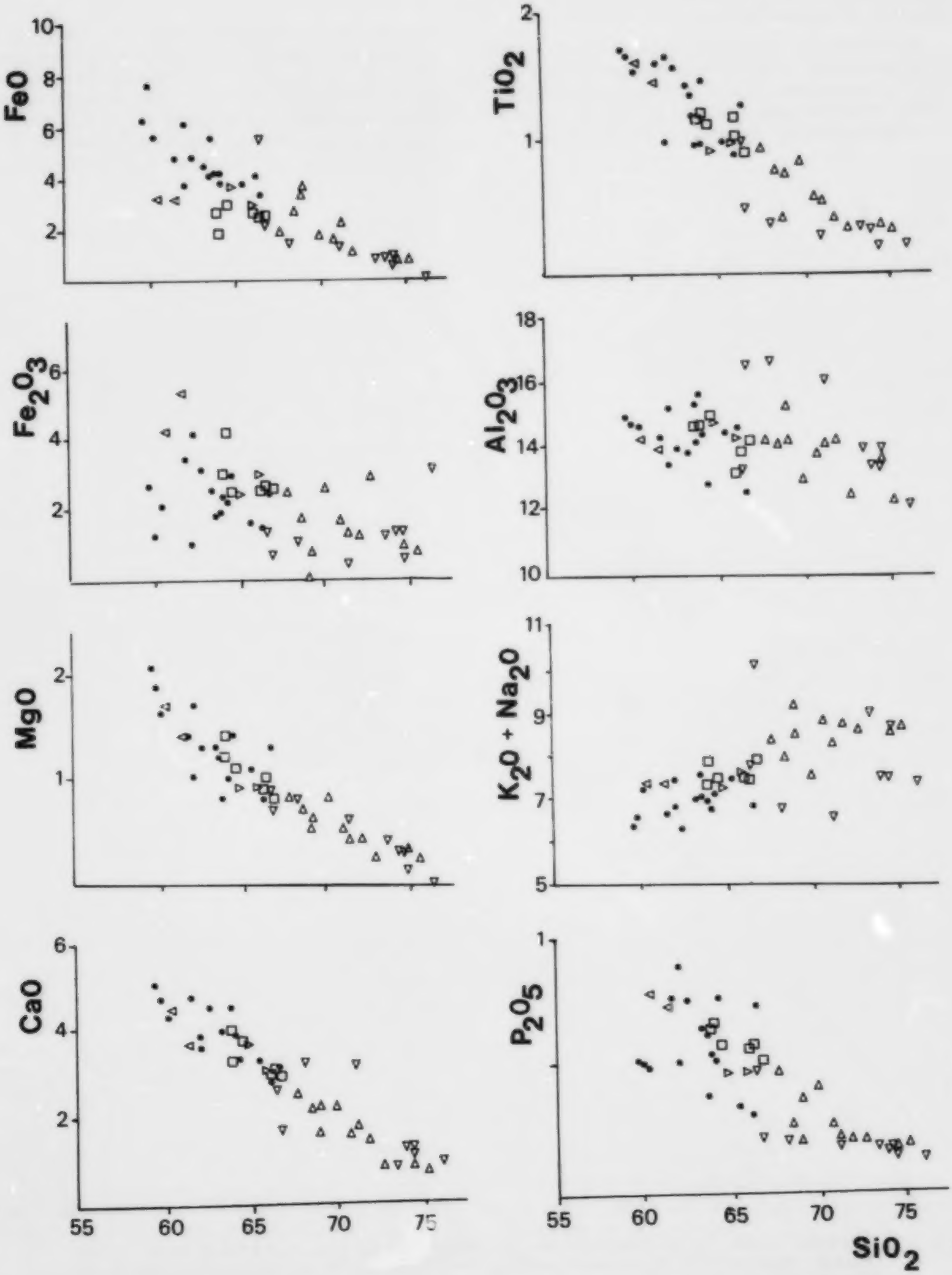

Figure 21. Variation diagrams for the Lake Michel intrusive suite (see text for complete discussion). Data in wt.%. Symbols as in Figure 17.

segregations (Fig. 26C). These features suggest a magmatic origin for the garnet (Owen and Marr, in press).

Well-foliated, potassium feldspar-megacrystic hornblende-biotite ± garnet mesocratic granite (unit **Phg**) occurs in the northern part of the pluton. The foliation is defined by oriented potassium feldspar megacrysts and the enclosing hornblende-, biotite-, and quartz-rich matrix.

Age relations

Contacts between the three members of the Potato Hill pluton were not observed, consequently, the relative ages of these units are not known from field relations. U-Pb data for zircon from the charnockite (unit **Pcg**) coupled with data for the other Grenvillian granitoid plutons defines a chord yielding an upper intercept age of about 1056 Ma. It will be seen below that all three members of the pluton share a

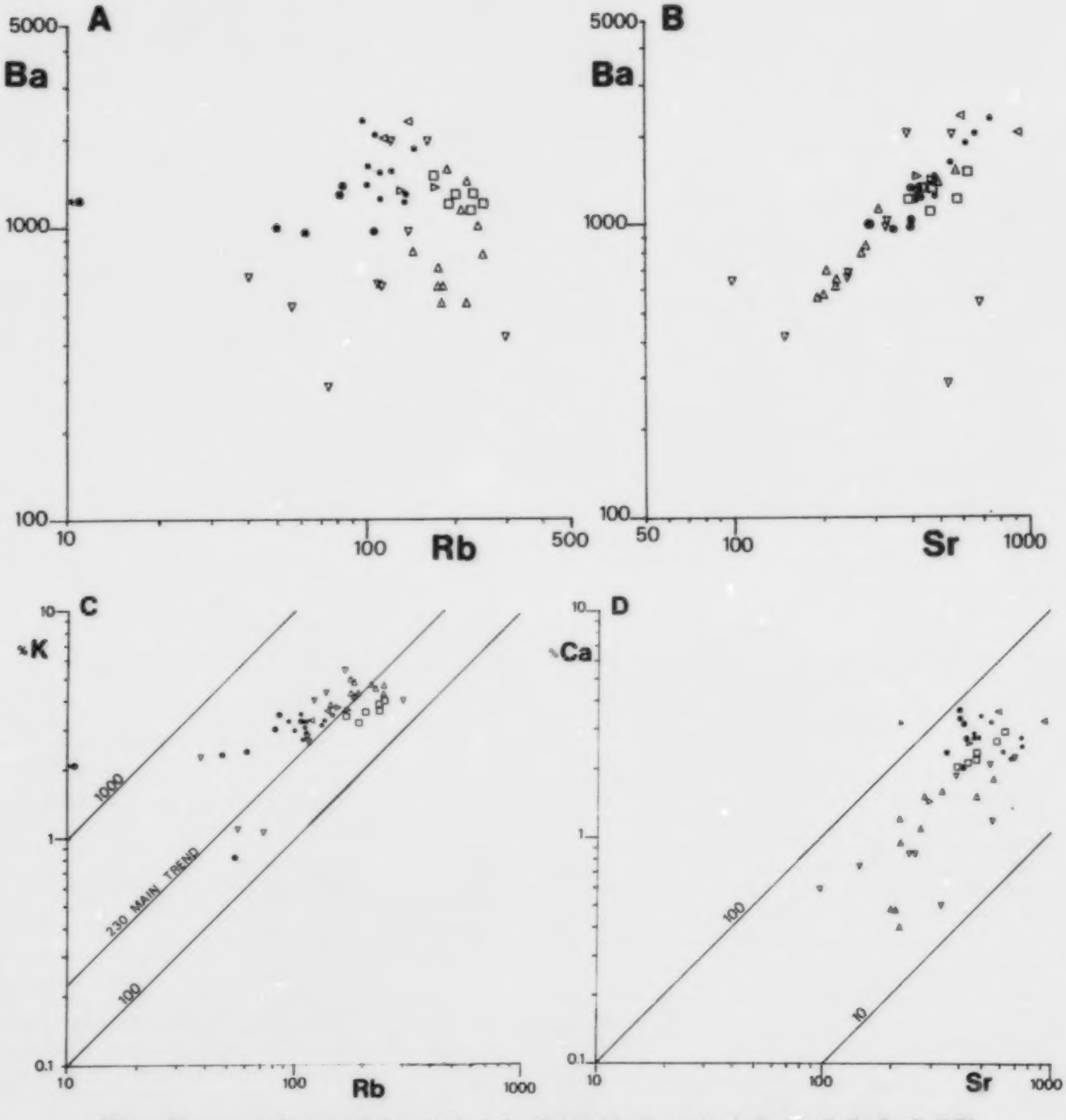

Figure 22. Trace element relations in the Lake Michel intrusive suite. A. Ba-Rb; B. Ba-Sr; C. K-Rb; D. Ca-Sr. "Main trend" in (C) indicates typical concentrations of K/Rb in crustal granites. Data in ppm. Symbols as in Figure 17.

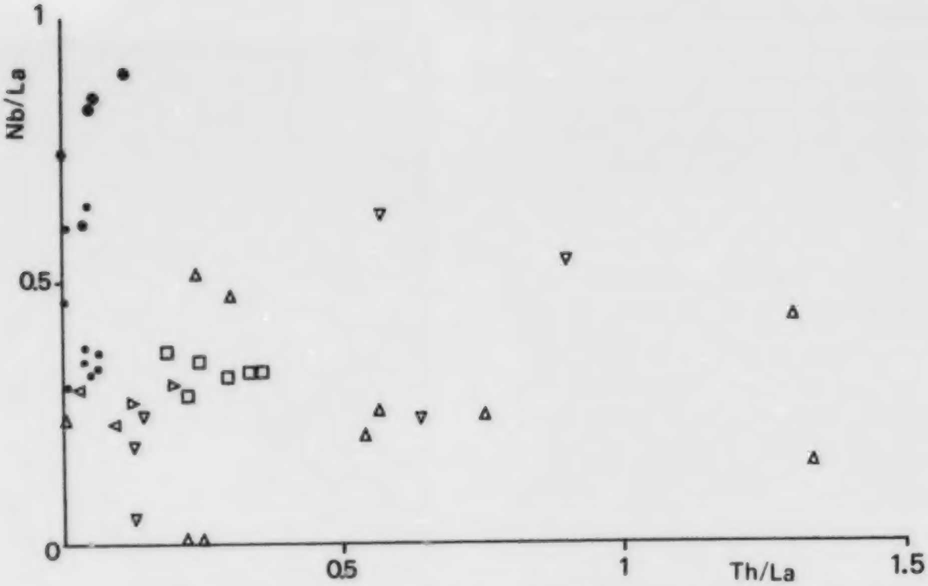

Figure 23. Nb/La versus Th/La in the Lake Michel intrusive suite. Symbols as in Figure 17.

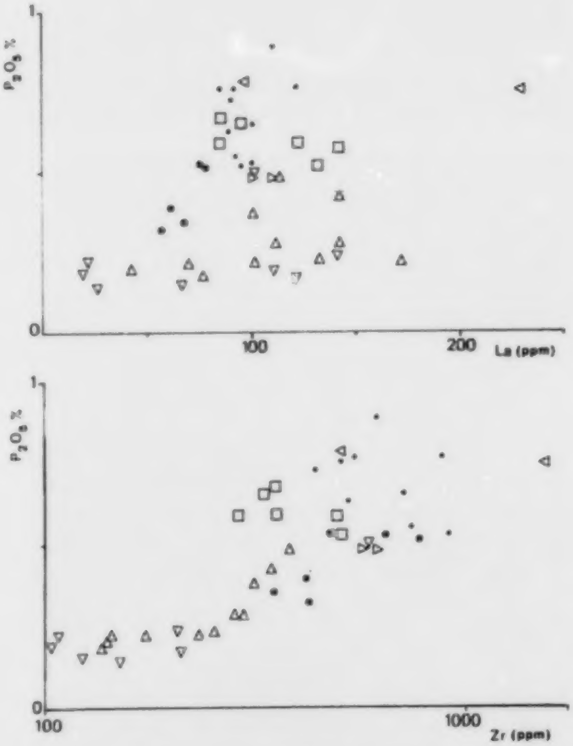

Figure 24. P_2O_5 versus La and Zr plots for the Lake Michel intrusive suite. Symbols as in Figure 17.

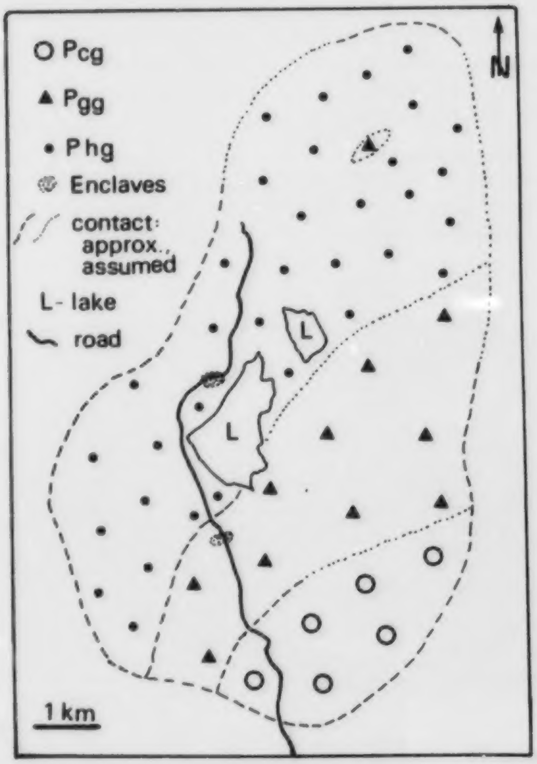
○ Pcg
▲ Pgg
• Phg
Enclaves
contact: approx., assumed
L - lake
road
N
L
L
1 km

Figure 25. Sketch map of the Potato Hill pluton. See Map 1764A legend for rock types.

distinctive geochemical signature (e.g., elevated Fe/Mg, Zr, and Ba concentrations), and therefore are probably comagmatic.

Inclusions of granitic and dioritic gneiss occur locally in mesocratic megacrystic granite exposed in roadcuts on the north-trending woods road accessing the pluton.

Mineralogy

The Potato Hill pluton has a distinctive mineralogy, which is reflected in the major and trace element geochemistry of the intrusion. Despite modal differences between the three units identified in the complex, mineral species are compositionally similar in each unit. Most characteristic is the iron-rich nature of the ferromagnesian minerals, and the relatively high concentrations of zircon and apatite. Representative analyses of mafic minerals are listed in Table 8.

Green hornblende is present in all units. It mantles pyroxene and ilmenite in coronitic charnockite (unit **Pcg**), and forms subidiomorphic grains in garnetiferous granite (unit **Pgg**) and megacrystic mesogranite (unit **Phg**). These are iron-rich amphiboles, with X_{Fe} varying between 0.73 and 0.82 in all units, and with A-site alkalies ranging from 0.69 to 0.82 (following the 13exCNK normalization scheme, with Fe^{3+} estimated by charge balancing; Robinson et al., 1982). Following Leake's (1978) classification, these are hastingsites and hastingsitic hornblendes (Fig. 19), and thus are slightly more ferruginous than hornblende in the Lake Michel intrusive suite.

Although texturally diverse, garnet in the coronitic charnockite and garnetiferous granite (units **Pcg** and **Pgg**, respectively) shows a limited range of compositions (Table 8), being Fe- and Ca-rich. These garnets contain 70 to 73 %

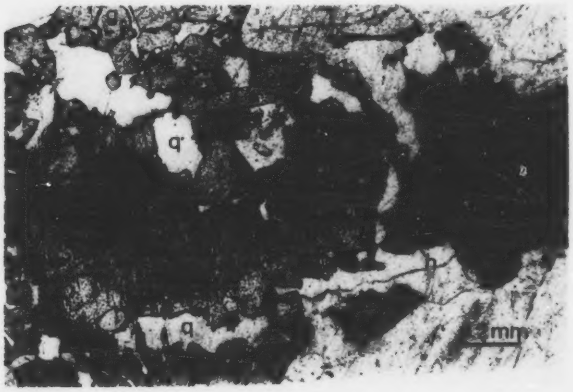

Figure 27. Photomicrograph of typical corona structure in charnockite of the Potato Hill pluton (unit **Pcg**). A central core of twinned eulite (o) is enclosed by partial rims of hornblende (h), quartz (q), and garnet (g) with symplectic quartz intergrowths. Note large zircons (z). Sample VO-87-040A1; plane polarized light.

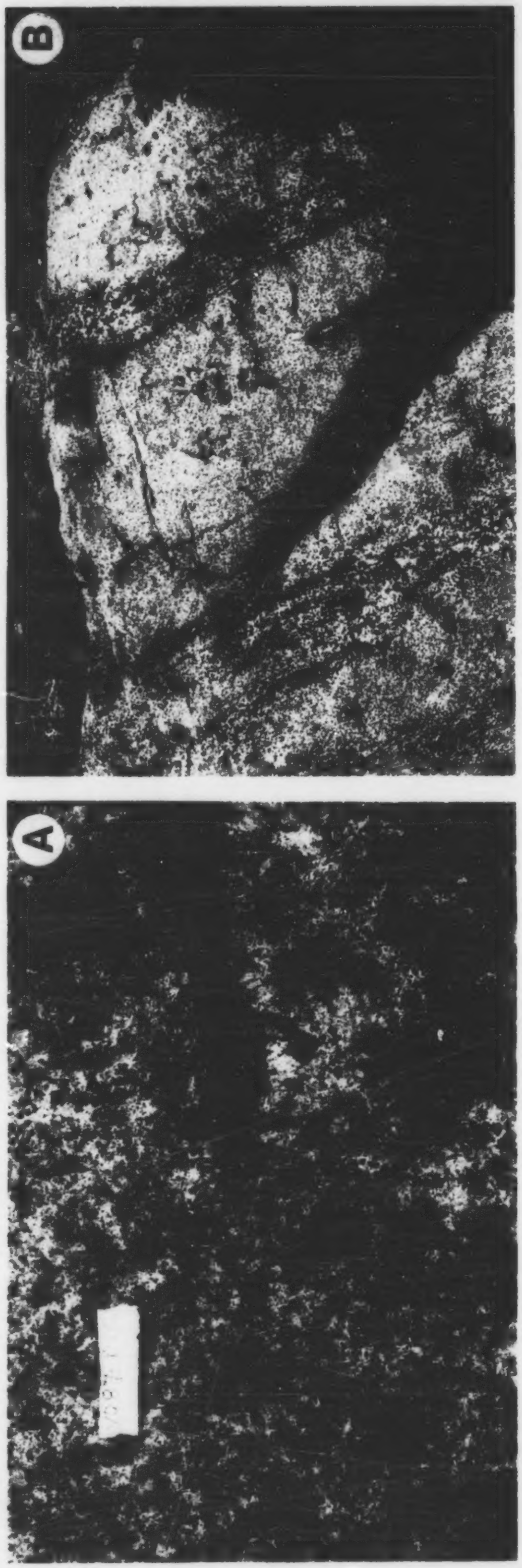

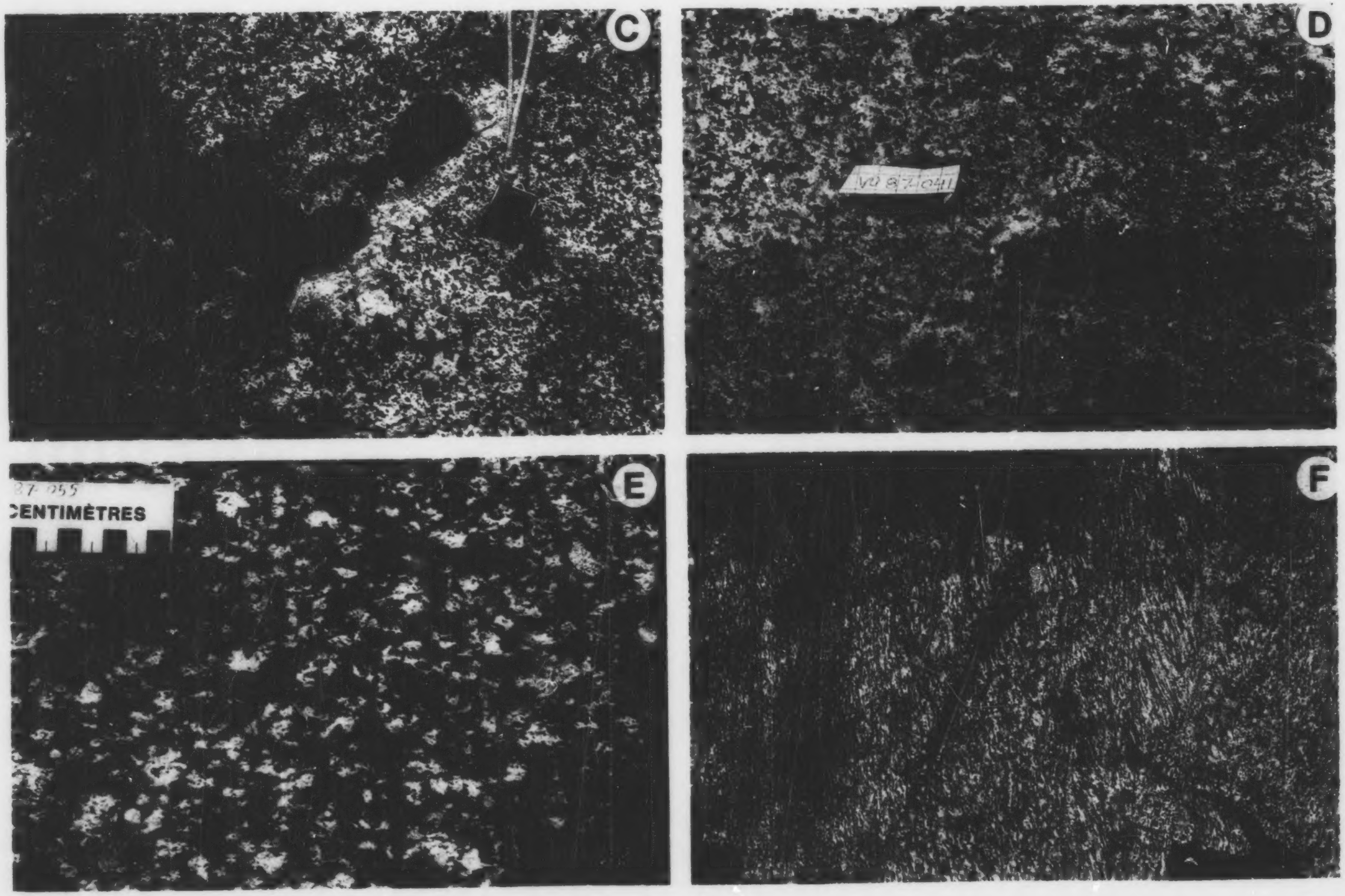

Figure 26. Field photographs of the Potato Hill pluton A. Coronitic charnockite (unit Pcg); B. mesocratic (biotite-hornblende-garnet-rich) banding in garnetiferous granite (unit Pgg); C. large garnets in leucocratic segregation in garnetiferous granite (unit Pgg); D. matrix garnet in biotite granite (unit Pgg); E. foliated mesocratic megacrystic hornblende-biotite granite (unit Phg); F. composite planar fabric developed in retrograded charnockite (unit Pcg) near the southern border of the pluton. GSC photos 204432 26A to F.

Table 8. Mean mineral analyses from representative samples of the Potato Hill pluton. Abbreviations as in Appendix II. Total Fe as FeO.

	*Coronitic charnockite (Pcg)			**Garnetiferous granite (Pgg)			***Mesocratic granite (Phg)		
	opx	hbl	gt	hbl	bi	gt	hbl	bi	gt
SiO_2	47.51	40.10	37.54	38.72	32.95	37.59	38.80	33.64	36.63
TiO_2	0.15	1.71	0.14	1.03	2.21	0.09	1.25	3.94	
Al_2O_3	0.41	10.66	20.28	11.17	15.42	20.31	12.42	15.35	20.58
FeO	42.83	25.28	32.14	28.32	31.24	25.87	27.43	29.05	24.13
MnO	0.86	0.26	1.61	0.71	0.51	5.70	0.73	0.57	8.69
MgO	6.83	4.60	1.33	2.45	3.08	0.70	3.30	4.10	0.40
CaO	1.01	11.08	7.79	11.16	0.07	9.89	11.35	0.14	9.03
Na_2O	0.09	1.67		1.57	0.08	0.07	1.53	0.16	
K_2O	0.09	1.67		1.40	8.64	0.09	1.69	9.16	
	99.8	97.0	101.0	96.4	94.2	100.3	98.5	96.1	99.5
Oxygen Basis:	6	23	12	23	22	12	23	22	12
Si	1.981	6.387	3.009	6.314	5.438	3.018	5.387	6.170	2.981
Al^{iv}	0.019	1.613	—	1.686	2.562	—	2.613	1.830	0.019
Al^{vi}	0.001	0.389	1.916	0.461	0.438	1.922	0.285	0.498	1.965
Ti	0.005	0.205	0.008	0.126	0.274	0.005	0.474	0.149	
Fe	1.493	3.368	2.154	3.862	4.312	1.737	3.890	3.648	1.642
Mn	0.030	0.035	0.109	0.098	0.071	0.388	0.077	0.098	0.599
Mg	0.424	1.092	0.159	0.595	0.758	0.084	0.978	0.782	0.049
Ca	0.045	1.891	0.669	1.950	0.012	0.851	0.024	1.934	0.787
Na	0.007	0.516		0.496	0.026	0.011	0.050	0.472	
K	0.005	0.339		0.291	1.819	0.009	1.871	0.343	

* sample VO-87-040A1
** sample VO-87-041 (analyst: R. Marr)
*** sample VO-87-086 (analyst: R. Marr)

almandine, 20 to 24 % grossular, and minor (3-5 %) pyrope and spessartine. Garnet associated with schistose fabrics in deformed and retrograded charnockite near the southern margin of the pluton is compositionally distinct (higher Mn, lower Fe) from that in its protolith. Large garnets in the garnetiferous granite are not zoned. In places, hornblende-mantled garnet in the mesocratic layers in the garnetiferous granite show a decrease in Mg and an increase in Mn toward the rim. Idiomorphic garnet associated with corona structures in the charnockite is not zoned. Rare garnet occurring in megacrystic hornblende-biotite mesogranite (unit **Phg**) has a relatively high Mn content, and is depleted in Fe (i.e., 53 % almandine, 2 % pyrope, 26 % grossular, 20 % spessartine).

Brown biotite forms subidiomorphic grains in units **Pgg** and **Phg**; it occurs as an accessory phase in the matrix of the charnockite. X_{Fe} in biotite ranges from 0.75 to 0.87; TiO_2 varies between 2 and 4 weight percent.

Plagioclase is calcic oligoclase to sodic andesine (An_{27-34}).

Accessory minerals include zircon, apatite, and ilmenite. The zircon and apatite are well formed and large (up to 1 mm), and collectively compose close to 1 % of each unit in the pluton.

Geochemistry

The mean bulk composition and CIPW norms for the three units composing the intrusion are listed in Table 9; the complete set of analyses is listed in Appendix III.

Although lithologically distinct, the Potato Hill pluton displays several compositional features already described for the Lake Michel intrusive suite. Like the latter, the Potato Hill pluton is a hypersthene- (and diopside-) normative, metaluminous intrusion. Collectively, the composition of the three units defines an alkali-lime index of about 54 (versus 56 in the Lake Michel intrusive suite). The presence of hastingsitic hornblende suggests alkaline affinities for the intrusion, a feature already noted for the Lake Michel intrusive suite. Like the latter, the Potato Hill pluton is characterized by low molecular A/CNK values (A/CNK = 0.79 to 0.96), but has higher HFS and low ion lithophile (LIL) element concentrations, with up to 1700 ppm Zr, 70 ppm Nb, 150 ppm Y, and 3900 ppm Ba.

Significance of the corona structures

Among the Grenvillian plutons, garnetiferous assemblages, including those within corona structures, are unique to the Potato Hill pluton. Corona structures in metaplutonic rocks have traditionally been attributed to either a metamorphic imprint subsequent to emplacement of the pluton, or to subsolidus cooling. The presence of garnets likely

Table 9. Mean bulk composition and CIPW norms of the Potato Hill pluton. Trace elements in ppm.
n = number of analyses.

Unit:	Pcg	Pgg	Phg
SiO_2	62.9	64.0	60.7
TiO_2	1.06	0.98	1.54
Al_2O_3	15.6	13.2	13.6
Fe_2O_3	1.33	2.23	2.07
FeO	5.07	7.00	7.70
MnO	0.14	0.22	0.18
MgO	0.50	0.75	1.24
CaO	4.03	2.90	4.23
Na_2O	3.30	2.30	2.85
K_2O	4.35	4.47	3.74
P_2O_5	0.31	0.16	0.43
H_2O	0.40	0.80	1.15
Total	99.0	99.0	99.4
n =	3	3	6
Ba	3461	3250	1787
Nb	27	22	50
Rb	86	115	96
Sr	527	322	324
Y	58	55	115
Zr	1432	1458	1402
Ga	25	23	25
Zn	183	263	261
Ni	8	<5	<5
V	<5	<5	28
Cr	<5	<5	<5
		CIPW norms	
Ap	0.69	0.35	0.95
Il	2.05	1.91	2.98
Mt	1.97	3.30	3.06
Or	26.09	26.87	22.48
Ab	28.33	19.80	24.55
An	15.11	12.71	13.37
Di	2.70	0.76	4.42
Hy	6.66	11.50	11.29
Q	16.41	22.80	16.89

reflects the iron-rich nature of the pluton or elevated pressure conditions. Similar corona structures in iron-rich mafic granulites in southern India have been interpreted to be products of subsolidus cooling of granulites (Manna and Sen, 1974). Preliminary interpretation of the corona structures suggests that they formed nearly isochemically via ionic communication between different corona reaction sites. The flux of iron appears to have been critical to the formation of the corona structures. Sodium was apparently lost to the system (Marr, 1989; Owen and Marr, in press).

Available isotopic age determinations are pertinent to an interpretation of the origin of the corona structures in the Potato Hill pluton. U-Pb (zircon) data indicate an emplacement age of ca. 1056 Ma for the pluton. Titanite from coeval granitoid plutons and from the basement gneiss complex collectively yield a metamorphic age of 978 Ma, which dates a widespread tectonothermal event in the Long Range Inlier. West- to northeast-trending schistose fabrics developed along the southern margin of the pluton (Fig. 26F) may be readily attributed to this event, since similarly-oriented fabrics of the same metamorphic grade (amphibolite facies) are locally evident elsewhere in the southern part of the inlier. The corona structures are obliterated in high strain zones near the southern margin of the pluton, consequently they predate formation of these (ca. 978 Ma?) schistose fabrics. They are therefore tentatively attributed to subsolidus cooling of this iron-rich pluton shortly after emplacement.

It is noteworthy that garnetiferous corona structures occur in one sample (VO-86-110) of granodioritic gneiss associated with tonalitic gneiss (unit Ptn) in the high grade terrane just south of the Lake Michel intrusive suite. The corona structures consist of necklaces of idiomorphic garnet enclosing clinopyroxene or ilmenite. Although well developed, the coronas are formed sporadically in the rock, and the majority of matrix pyroxene and ilmenite grains have not developed garnet rims. The garnets are petrographically and compositionally similar to those in coronitic charnockite of the Potato Hill pluton. They contain wormy quartz intergrowths, and are rich in almandine (71 %), with subordinate grossular (21 %), and minor pyrope (2 %) and spessartine (5 %). Both pyroxenes are iron-rich; X_{Fe} in clinopyroxene is 0.83, and X_{Fe} in orthopyroxene is 0.87 (eulite) (see Appendix II). Coronas in this sample are interpreted to have formed during the cooling of exceptionally iron-rich two-pyroxene granulite following peak metamorphic conditions. The occurrence of these coronas in the gneiss complex supports a subsolidus cooling origin for coronas in the Potato Hill pluton. It should be noted, however, that the relative age of coronas in the pluton and the gneiss is not known.

Petrography and geochemistry of other granitoid plutons

Petrographic and analytical data for the remaining granitoid plutons are relatively sparse, but will be summarized here. Grenvillian ages have been determined for most of these plutons. Chemical analyses are listed in Table 10.

Plutons from the northern part of the inlier are described by Bostock (1983). These comprise megacrystic and equigranular, biotite- and hornblende-bearing granitoid rocks. Bostock (1983) mapped seven plutons in this area, including the northern tip of the Lake Michel intrusive suite. He noted that megacrystic granite was the dominant rock type in the Leg Pond, Horse Chops, and Hooping Harbour (and its satellite) plutons. Bostock (1983) classified these rocks as quartz monzonite, based on visual estimation of modes. These plutons are texturally more heterogeneous than equigranular biotite-quartz monzonite of the Cloud River pluton. Principal minerals are quartz, microcline, oligoclase, biotite, and hornblende; accessory minerals include white mica, chlorite, epidote, titanite, magnetite, and apatite, with rare zircon, allanite, and pyrite. Potassium feldspar megacrysts are locally evident. Bostock (1983) noted that the Cloud River pluton contains 20 to 30 % quartz and roughly equal proportions of plagioclase and potassium feldspar; using Streckeisen's (1976) nomenclature, this is a granite.

The Fourché Harbour pluton was described by Bostock (1983) as an equigranular granite containing chlorite, biotite, or stilpnomelane and epidote. Parts of the pluton carry

Table 10. Geochemistry of diverse Grenvillian granitoid plutons. Data for BK70 and BK69 samples are compiled from Bostock (1983). ns = not sought. Total Fe as Fe_2O_3 in VO-85 samples. Trace elements in ppm.

	Lomond River pluton		Leg Pond pluton			Hooping Harbour pluton		
	VO-85-587	VO-85-1020	BK-70-157	BK-70-136	BK-70-158	BK-70-336	BK-69-308	BK-70-119
SiO_2	60.7	61.7	61.4	63.3	68.5	61.0	67.5	69.0
TiO_2	0.96	0.91	1.80	2.32	0.86	1.34	1.00	1.04
Al_2O_3	15.3	14.7	13.1	12.3	14.7	16.6	14.5	13.7
Fe_2O_3	7.59	7.05	4.2	4.2	1.9	3.1	2.5	2.5
FeO	ns	ns	5.0	5.4	2.6	1.7	1.6	2.0
MnO	0.17	0.15	0.15	0.14	0.11	0.07	0.11	0.05
MgO	1.09	1.14	1.5	1.6	0.7	2.0	0.7	1.4
CaO	4.93	4.52	3.9	4.1	1.7	3.2	1.7	2.2
Na_2O	3.56	3.55	2.8	2.2	3.0	3.3	3.0	2.6
K_2O	3.41	3.90	3.1	2.8	5.0	5.9	5.0	4.7
P_2O_5	1.11	0.90	0.98	1.07	0.31	0.90	0.31	0.40
LOI	0.93	1.00	0.7	1.1	0.5	0.6	0.5	0.5
	100.3	100.1	98.6	100.5	99.9	99.4	99.7	100.1
Ba	1926	2020	1000	870	1400	2500	2700	540
Rb	80	120	ns	ns	ns	ns	ns	ns
Sr	650	630	390	270	270	1100	580	540
Nb	40	70	ns	ns	ns	ns	ns	ns
Y	120	170	ns	ns	ns	ns	ns	ns
Zr	1680	1530	1500	1700	800	1200	1500	1300
Ga	35	32	ns	ns	ns	ns	ns	ns
La	ns	ns	280	250	170	310	550	410
Ce	ns	ns	850	830	nd	730	910	850

a cataclastic fabric. Fluorite is locally present in the granite. Apart from its association with breccia zones in the Devonian Devils Room pluton (Erdmer, 1986a), fluorite has not been observed in any other granitic plutons in the inlier. The Fourché Harbour pluton is cut by pegmatite and granitic dykes, and by two sets of mafic dykes, including the northeast-trending Long Range dykes and uncorrelated diabase dykes with east-west trends.

The Lomond River pluton is a buff, coarse grained to megacrystic biotite ± hornblende granodiorite. Biotite forms 1 to 2 mm, brown subidiomorphic flakes, as well as aggregates of 0.1 mm green-brown flakes. In places, biotite coexists with, and is partly enclosed by, fine grained green amphibole. Accessory minerals include medium grained (0.5 mm) apatite, titanite, zircon, allanite, and opaque minerals. Fine grained epidote is in part a breakdown product of plagioclase. The mode of one sample of the granodiorite is as follows: quartz (24 %), plagioclase (49 %), microcline (8 %), biotite (14 %), and hornblende (3 %), as well as the aforementioned accessory minerals.

The dominant rock type of the Killdevil Hill pluton is massive to foliated, biotite ± hornblende granite. Subordinate biotite-hornblende granodiorite is also present. The granodiorite is mesoscopically identical to that composing the Lomond Hill pluton.

The Main River pluton is a well-foliated megacrystic biotite ± hornblende granite mesoscopically indistinguishable from other Grenvillian megacrystic granites. The pluton carries a north- to northeast-trending tectonic fabric which may be attributed, at least in part, to Paleozoic orogenesis. Like the schistosity developed in the Long Range dykes (see below), this is a low grade fabric defined by elongate clots of recrystallized and partly chloritized mafic minerals and epidote.

The Cat Arm River, Little Cat Arm, Aspy and Pigeon Cove plutons are massive to foliated biotite-hornblende granites which are mesoscopically identical to megacrystic granite of the Lake Michel intrusive suite. As in the Lake Michel intrusive suite, the size, proportion, and shape of feldspar megacrysts varies considerably within each pluton. Equigranular biotite granite occurs near the northeastern margin of the Little Cat Arm pluton.The Aspy pluton is extensively epidotized.

The Camp Pond pluton comprises relatively leucocratic (CI = 2), white weathering, tan to rose biotite granite. A small body of megacrystic mesocratic hornblende-biotite granodiorite similar to unit **Pxgk** occurs near the northwestern border of the pluton. The main part of the pluton is grouped with equigranular granite of the Lake Michel intrusive suite (unit **Pg**).

The East Adies River pluton differs from other equigranular plutons in the inlier insofar as it is intimately associated with migmatitic granodioritic and granitic gneiss. The age of the pluton has not been determined.

The granite is massive to foliated; foliated variants grade into the migmatitic gneiss. Two satellite plutons of the granite occur to the west of the main body. These are coarser grained and less altered than fine grained epidotized biotite granite in a small pluton (Rex Lake pluton) flanking the Lomond River pluton immediately to the south.

The East Adies River pluton is leucocratic (CI = 2), and contains abundant microcline (locally perthitic) and quartz, subordinate plagioclase, accessory apatite and zircon, and clots of xenomorphic brown biotite and green amphibole. Biotite also occurs as mantles on opaque minerals (ilmenite?), and as rare subidiomorphic flakes.

Mesoscopically, the granite is similar to biotite-seamed leucocratic segregations in nearby migmatitic gneiss; both contain grey to blue-grey quartz.

Compared with members of the Lake Michel intrusive suite, the East Adies River pluton is relatively rich in alkalies and silica, and is depleted in lime, Fe, and Mg (Table 11). These features are consistent with the potassium feldspar-rich and leucocratic nature of the intrusion.

Petrographic similarities with leucosomes in the surrounding gneiss, and the leucocratic nature of the granite suggest that the East Adies River pluton resulted from the ponding of silicate melt generated by regional anatexis. In this regard, it is noteworthy that the pluton apparently overlies the subsurface continuation of mafic rocks of the Taylor Brook gabbro complex, which, as noted above, has a high grade thermal aureole. If derived by anatexis from the surrounding gneiss complex, the granite should be compositionally similar to leucocratic segregations in the migmatitic gneiss, and have major and trace element characteristics of anatectic granites (e.g., low concentrations of incompatible elements; see Sawyer, 1987). It is noteworthy that an anatectic origin has been proposed for Grenvillian granites in southern Labrador (Gower, 1988). However, most analyses for both the East Adies River pluton and the Lake Michel intrusive suite diverge from minimum melt compositions when plotted on normative quartz-albite-orthoclase and anorthite-albite-orthoclase diagrams (Fig. 28). Furthermore, the hypothesis that the East Adies River pluton resulted from partial melting of country rock above subsurface mafic rocks associated with the Taylor Brook gabbro complex requires that both plutons yield similar isotopic ages. Data required to evaluate this hypothesis are presently unavailable. Consequently, an anatectic origin sensu stricto for these intrusions remains to be demonstrated.

A small pluton (ca. 5 km^2) of massive, buff, coarse grained monzonite (unit **Pom**) occurs about 7 km southeast of Parsons Pond. The rock contains idiomorphic hypersthene crystals (Fig. 18B) up to 1 cm in diameter, which coexist with subidiomorphic oligoclase (An_{22}) and microcline. Accessory minerals include opaques, biotite, zircon, and apatite. In the single thin section made of the monzonite, quartz is restricted to myrmekitic intergrowths with feldspar. The orthopyroxene is locally partly retrograded to phyllosilicate. A microprobe analysis of the pyroxene is given in Table 5. The age of the monzonite is not known.

For the most part, the plutons depicted in Figure 14 are well-defined bodies which can readily be distinguished from the gneissic country rock in the field. However, some plutonic complexes such as the East Adies River pluton include gneissic rocks which cannot be distinguished at regional map scales. Bostock (1983) identified four hybrid bodies which collectively underlie about 100 km^2 of the area south of Leg Pond in the northern part of the inlier. He described the hybrid rocks (unit **Pgnk**) as being composed of equigranular to megacrystic quartz monzonite or granite interbanded with or containing enclaves of layered gneiss. Bostock included part of the northern tip of the Lake Michel intrusive suite, which he described (Bostock, 1983, p. 28) as consisting of "megacrystic to massive granitic rocks that contain large lenses or bands of leucocratic to melanocratic gneiss and some quartz-rich gneiss". Remapping of this part of the suite (Owen, 1987) has shown that the "massive" (equigranular) and megacrystic granites in this area form distinct bodies which locally contain amphibolite enclaves, and which are separated, in part, by a large screen of quartzite, cordierite-bearing pelitic gneiss, and subordinate mafic gneiss. This

Table 11. Major and trace element geochemistry of the East Adies River pluton. Trace elements in ppm.

VO-85-:	366	370	764	862	950	980	991
SiO_2	74.8	74.6	69.7	69.7	76.2	73.3	74.1
TiO_2	0.17	0.29	0.34	0.14	0.22	0.10	0.19
Al_2O_3	13.4	12.6	15.4	15.9	13.2	14.6	13.3
Fe_2O_3	0.60	1.30	1.05	0.49	0.30	0.80	1.12
FeO	0.7	0.8	0.8	0.1	0.1	0.05	0.6
MnO	0.03	0.03	0.02	0.01	0.01	0.01	0.03
MgO	0.23	0.36	0.83	0.36	0.13	0.14	0.69
CaO	1.15	0.87	1.35	0.33	0.83	1.06	0.51
Na_2O	4.12	3.68	3.43	3.10	4.02	3.69	4.81
K_2O	4.22	5.00	6.04	8.32	4.37	6.01	4.11
P_2O_5	0.04	0.05	0.10	0.02	0.02	0.02	0.05
LOI	0.39	0.31	0.54	0.62	0.39	0.31	0.39
	100.1	100.2	100.0	99.8	100.0	100.2	100.1
Ba	930	760	2010	4480	1350	230	400
Rb	110	250	180	220	90	270	100
Sr	150	100	870	1430	260	170	70
Y	30	70	<10	<10	<10	10	60
Zr	170	260	30	<10	140	100	170
Nb	20	20	10	20	10	<10	10
Ga	21	21	17	16	17	18	19

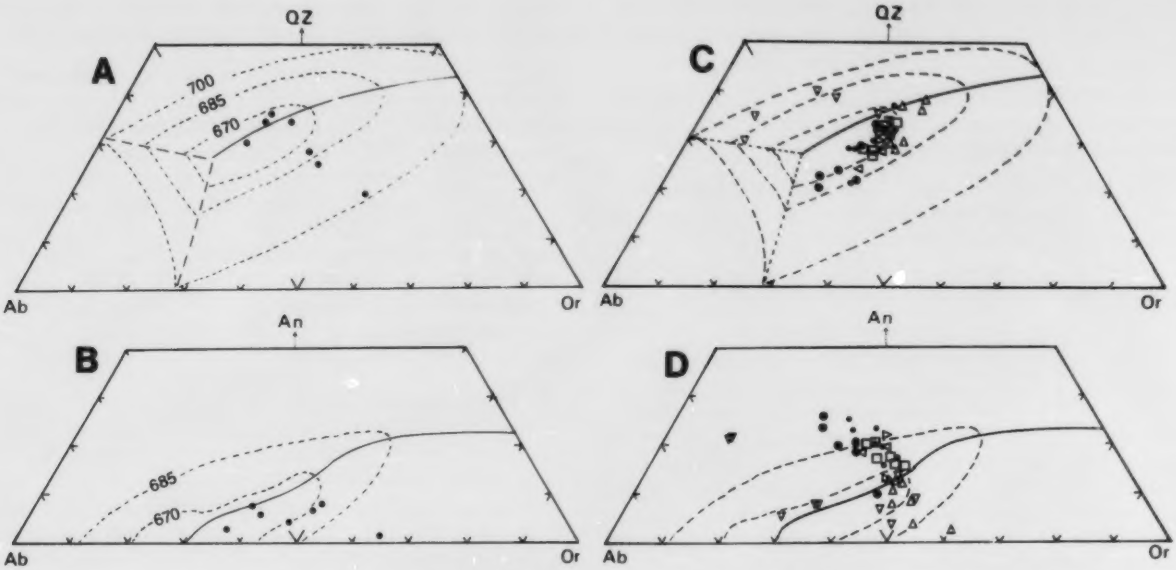

Figure 28. Normative Qz-Ab-Or and An-Ab-Or diagrams for the East Adies River pluton (A, B) and the Lake Michel intrusive suite (C, D; symbols as in Fig. 17). Isotherms and the cotectic line experimentally determined for the system An-Ab-Or-Qz-H_2O at 5 kbar P_{H_2O} are shown (Winkler, 1979).

suggests that more detailed mapping may reveal the presence of discrete plutons within the other hybrid bodies farther to the north.

Tectonic setting of the Grenvillian plutons

The tectonic setting of the Grenvillian plutons is evaluated by trace element discrimination diagrams appropriate for granitoid rocks (Pearce et al., 1984). Analyses of granitic and charnockitic rocks in the Lake Michel intrusive suite and the Potato Hill pluton plot in the within-plate field on the Nb versus Y and Rb versus (Y+Nb) fields (Fig. 29). I-, M-, and S-type granitoids typically plot in the volcanic-arc field near the triple junction with the within-plate and ocean ridge or collisional granite fields (Whalen et al., 1987), rendering distinction of granite types by this method equivocal.

Elevated Ga/Al ratios (Fig. 30) support a within-plate setting for both plutonic complexes. Although not definitive, the available data nonetheless exclude the likelihood that the Grenvillian granitoids were emplaced in a destructive continental margin-type setting (i.e., Andean margin), and suggest instead an encratonic setting.

Owen and Erdmer (in press) compared the eastern Grenville Province (including the Long Range Inlier) to the foreland part of the Himalayan Orogen (i.e., south of the Indus suture; cf. Dewey and Burke, 1973; Windley, 1986). Differences in the composition of plutonic rocks in both orogens (e.g., two-mica-bearing S-type leucogranites in the Higher Himalayas versus biotite-hornblende ± pyroxene granites in the Long Range Inlier and the adjacent Grenvillian Province of Labrador) reflect contrasts in the role of basement and cover rocks (where present) in granitoid petrogenesis. The foreland part of the Grenville orogen in eastern Labrador comprises a north-verging fold-and-thrust belt north of structurally-higher nappes containing the Grenvillian granitoid plutons (e.g., in the Long Range Inlier and in southernmost Labrador). According to cross-sections presented by Allègre et al. (1984), the foreland fold-and-thrust belt including leucogranite-sheeted nappes in the Higher Himalayas) south of the Indus suture is approximately 350 km wide. The Grenvillian counterpart of this terrane, from the Grenville Front southward through the Long Range Inlier (see Discussion section below, and Fig. 54) is considerably wider (minimum of 580 km). Despite differences in scale, the geometry of the foreland region of both orogens, in which the locus of granitoid plutonism is centred on nappes high in the thrust sequence, is striking.

Late Proterozoic and Paleozoic rocks

A variety of post-Middle Proterozoic rocks have been identified in the Long Range Inlier. These are: (1) mafic dykes, including the Long Range swarm; (2) porphyritic felsic dykes; (3) the Early Devonian Devils Room granite; and (4) undeformed clastic rocks which overlie parts of the basement complex.

The Long Range dykes

The Long Range dykes comprise a swarm of northeast-trending tholeiites concentrated near the northeastern margin of the Long Range Inlier (Fig. 31). Similarly-oriented mafic dykes occur in the Grenville Province of southeastern Labrador, and on Belle Isle, where the dykes feed mafic flows of the Lighthouse Cove Formation (Strong and Williams, 1972). The Lighthouse Cove Formation (unit Pb) is also exposed along the northeastern flank of the Long Range

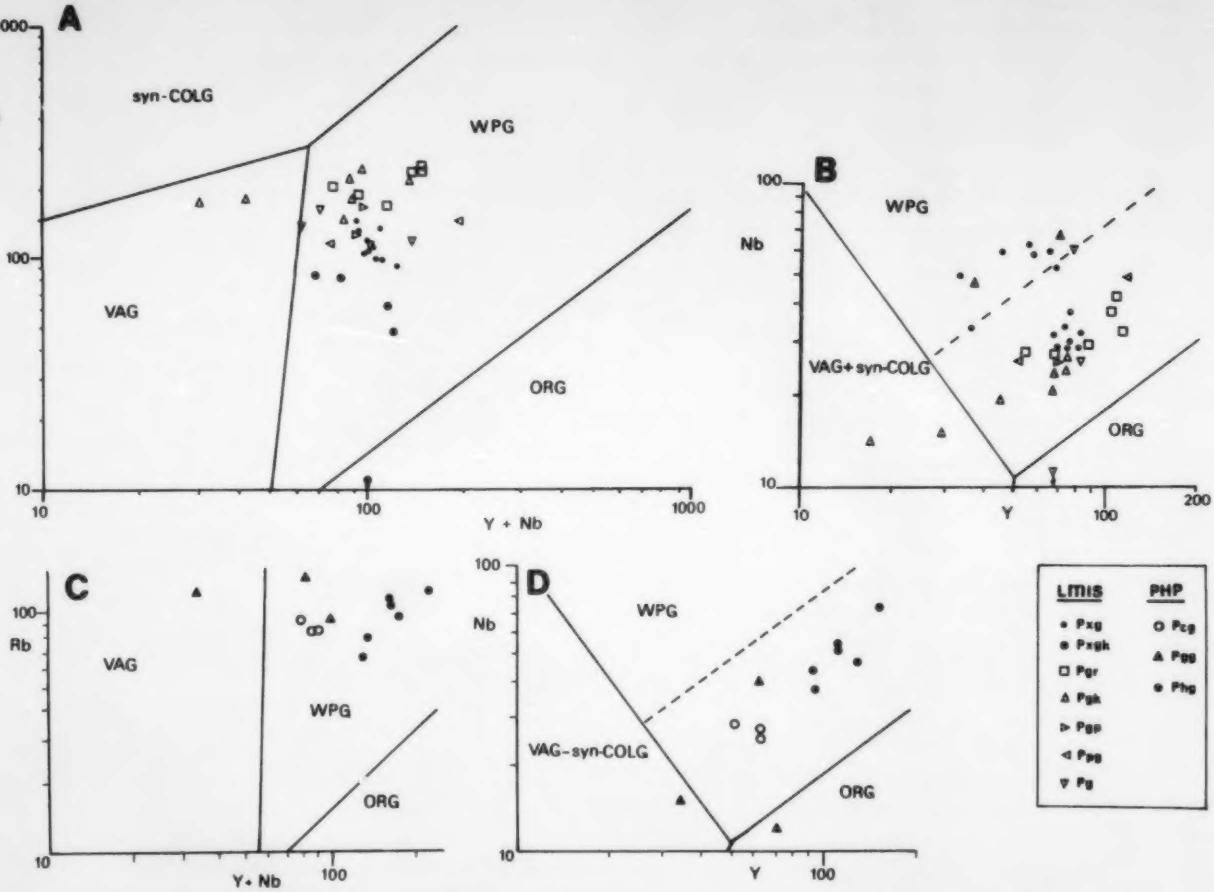

Figure 29. Trace element discrimination diagrams (after Pearce et al., 1984) for the Lake Michel intrusive suite (A and B) and the Potato Hill pluton (C and D). WPG-within-plate granites; ORG-ocean-ridge granites; VAG-volcanic arc granites; COLG-collision granites. Dashed line in (B) and (D) represents the upper compositional boundary for ORG from anomalous oceanic ridge segments.

Inlier. Emplacement of the Long Range dykes and contemporaneous basaltic volcanism in the Strait of Belle Isle area is attributed to initial rifting of the proto-Atlantic ocean (Strong and Williams, 1972; Strong, 1974). The dykes have been dated at 605 Ma by the $^{40}Ar/^{39}Ar$ method (Stukas and Reynolds, 1974), and have recently yielded a precise U-Pb (zircon, baddeleyite) age of 615 Ma (Kamo et al., 1989).

In the inlier, individual dykes are up to about 50 m in width, and may be traced up to at least 5 km along strike. Compositionally-similar but relatively narrow (≤ 1 m wide) northeast-trending mafic dykes have been described from the Silver Mountain area, well to the south of the main concentration of dykes (Owen and Machin, 1987). These dykes are too small to portray on Figure 31 or on the accompanying 1:250 000 scale map. Their distribution has been shown by Owen and Machin (1987, Fig. 29.1). The largest concentration of these dykes occurs in the western part of the Taylor Brook gabbro complex.

Petrography and mineralogy

The primary mineralogy of the Long Range dykes includes augite (mean composition: $Wo_{35}En_{48}Fs_{17}$; Table 12), normally-zoned calcic plagioclase (typically An_{55} to An_{39}), ilmenite, and accessory biotite, apatite, and rare pigeonite. These dykes are subophitic, and have well-defined chilled margins. Clinopyroxene is rimmed by a narrow fringe of calcic amphibole. Ilmenite in places is enclosed by fine grained biotite. Quartz is locally present as myrmekitic intergrowths with plagioclase. Apatite forms long acicular crystals. Pigeonite was noted in one sample, where it occurs as small (≤ 0.1 mm) xenomorphic grains nucleated on larger augite crystals. Both zoned and unzoned plagioclase is present; unzoned plagioclase is compositionally similar (mean An_{54}) to the cores of zoned plagioclase grains (mean rim composition, An_{39}).

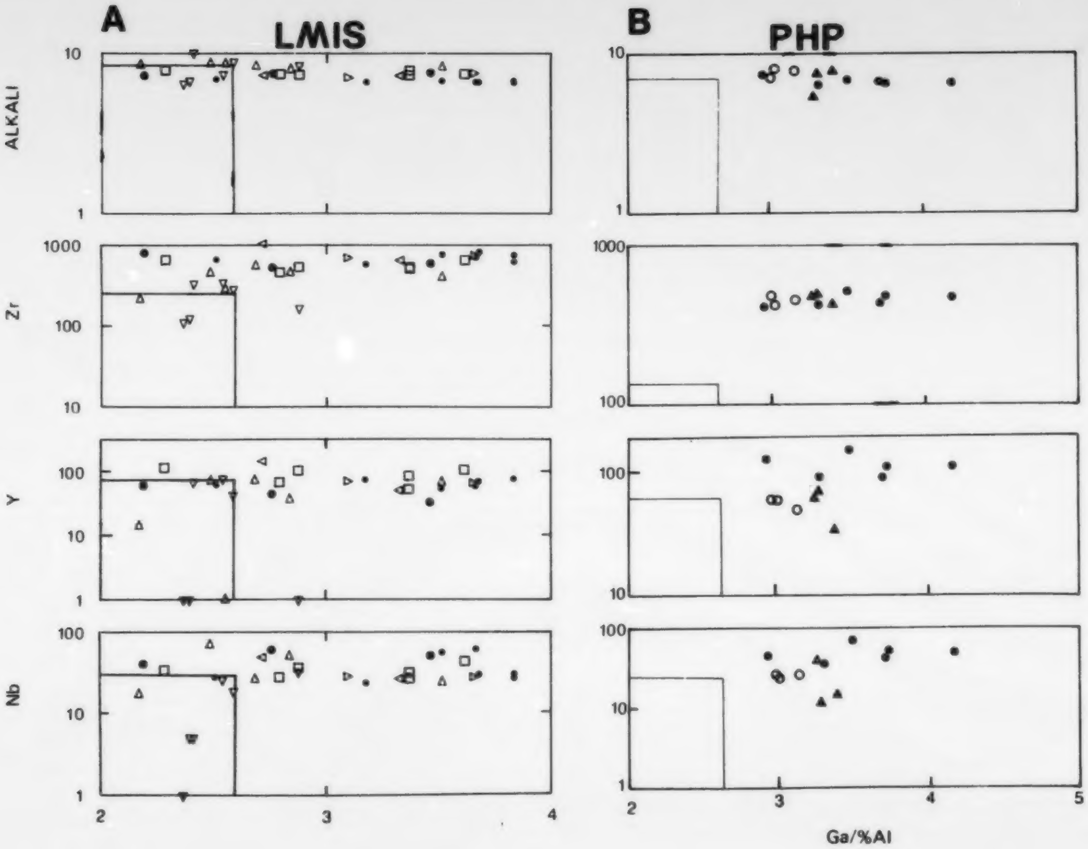

Figure 30. Ga (ppm)/%Al plotted against alkalies and various high field strength elements in (A) the Lake Michel intrusive suite (LMIS), and (B) the Potato Hill pluton (PHP). The rectangular area in each diagram encloses the typical composition of I-, M-, and S-type granites (Whalen et al., 1987). Symbols as in Figure 17.

Toward the east, the primary mineralogy is progressively replaced by metamorphic assemblages (Fig. 32) comprising calcic amphibole, relatively sodic plagioclase, titanite, epidote, biotite, and quartz (Bostock, 1983). By virtue of the age of the dykes (latest Proterozoic), the metamorphic imprint is interpreted to be Paleozoic. The deformed dykes therefore record the effects of Appalachian orogenesis in the inlier.

Textural relations suggest that the dykes were recrystallized during two low-strain events and a final high-strain event. Metamorphic grade in each case is low (greenschist to epidote amphibolite facies).

Age relations

The Long Range dykes cut the Long Range gneiss complex and several of the Grenvillian granitoid plutons (e.g., the Pigeon Cove pluton and the Lake Michel intrusive suite). Age relations with the Devonian Devils Room pluton are not known from field observations; however, the dykes are considered to be approximately 225 Ma older, since they yield an isotopic age of 615 Ma (Kamo et al., 1989).

Geochemistry

Since all of the dykes show at least incipient metamorphic effects, it is possible that the composition of even the "freshest" has been modified during recrystallization. The author has documented primary and secondary (metamorphic) features of the dyke swarm (Owen et al., 1989), based on a suite of samples collected from a southeast-northwest transect near Pigeon Cove (Fig. 31, inset). Samples containing relict igneous assemblages have a more evolved tholeiitic composition than the metamorphosed dykes. This becomes apparent through a comparison of inter- and intra-dyke compositional variations. The relevant data are presented in Tables 13 and 14. Both weakly and thoroughly metamorphosed dykes appear to be compositionally homogeneous; however, considerable inter-dyke compositional variations are evident. Standard deviations

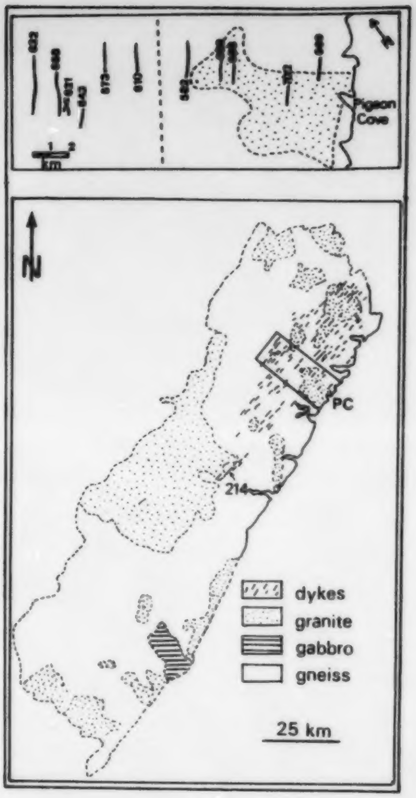

Figure 31. Distribution of the Long Range mafic dyke swarm. Narrow dykes in the southern part of the inlier are too small to be depicted (see Owen and Machin, 1987). Inset shows the location of dykes sampled in a transect near Pigeon Cove (PC); stippling denotes Pigeon Cove pluton. Dashed line represents the easternmost limit of widely-preserved igneous pyroxenes in the dykes. Arrow shows location of dyke 214 (see text).

for the mean compositions of both fresh dyke 622 and variably metamorphosed dyke 610 (see Fig. 31, inset) are low for most elements; Fe^{3+}/Fe^{2+} shows the most variation, possibly a reflection of analytical uncertainty.

Thoroughly metamorphosed and variably strained dyke 214 (Fig. 31) is similarly homogeneous (Bellefontaine, 1987), but is relatively depleted in high field strength (HFS) elements (e.g., Ti, Nb, Zr). A similar apparent depletion in Ti, Zr, Nb, and Y (and enrichment in MgO*; $MgO^* = MgO/(MgO + FeO_t)$ characterizes highly strained dykes from the eastern part of the sampling transect (i.e. dykes 702 and 669). Compositional variations in the concentrations of selected trace elements (Ti, Zr, Nb, Y) and MgO* between other dykes are summarized in Table 14. The data point to considerable inter-dyke variations in the concentrations of Ti and Zr among the westernmost dykes. Geochemically, these are among the least mobile of elements (Lesher et al., 1986); they are also among the elements expected to be concentrated in more evolved rocks in tholeiitic magma series.

Table 12. Mean microprobe analyses of igneous phases of the Long Range dykes. FeO* = FeO(total). n = number of analyses.

	clino-pyroxene	plagioclase		ilmenite
		core	rim	
SiO_2	52.58	55.78	59.41	
TiO_2	0.79			46.95
Al_2O_3	2.60	28.45	26.55	
FeO*	9.95	0.67	0.62	50.19
MnO	0.24			1.46
MgO	15.95			
CaO	18.50	11.03	8.19	
Na_2O	0.32	5.22	6.95	
K_2O		0.13	0.19	
	100.93	101.28	101.91	98.6
n =	15	13	7	3
Oxygen basis:	6	8	8	6
Si	1.931	2.487	2.613	
Al	0.113	1.496	1.376	
Ti	0.022			1.861
Fe	0.306	0.025	0.023	2.213
Mn	0.007			0.065
Mg	0.873			
Ca	0.728	0.527	0.386	
Na	0.320	0.451	0.593	
K		0.007	0.011	

The apparent depletion of HFS elements in the metamorphosed samples may record the preferential mobility of these elements under unusual geochemical conditions, or may be an artifact of primary compositional variation.

Quantification of the apparent mobility of various elements between thoroughly metamorphosed dykes has been undertaken using the isocon method of Grant (1986). By this approach, composition-volume relations derived by Gresens (1967) are expressed as linear equations which compare the concentration of different components in the protolith (C_i^o) and its deformed (and/or altered) equivalent (C_i^a). An isocon is simply a line of equal elemental concentration. Concentration changes are expressed relative to model isocons (constant mass, volume, or a chosen relatively immobile element), or to a best-fit isocon defined by a linear array of elements in C_i^o - C_i^a space. The results for the Long Range dykes are listed for model and best-fit isocons in Table 15, and are depicted graphically in Figure 33.

Isocon analysis of the bulk rock data requires an unreasonably large degree of mobility for most major and trace elements. For example, both the constant mass and constant volume isocons require a gain of 55 to 60 % H_2O, with a minor (ca. 10 %) increase in Al, Fe^{3+}, Mg, Na, and Y, and a 20 to 65 % decrease in Ti, Fe^{2+}, P, V, Cu, Zn, Ga, Ba, Nb, and Zr. Similarly unreasonable results are provided by two potential best-fit isocons depicted in Figure 33.

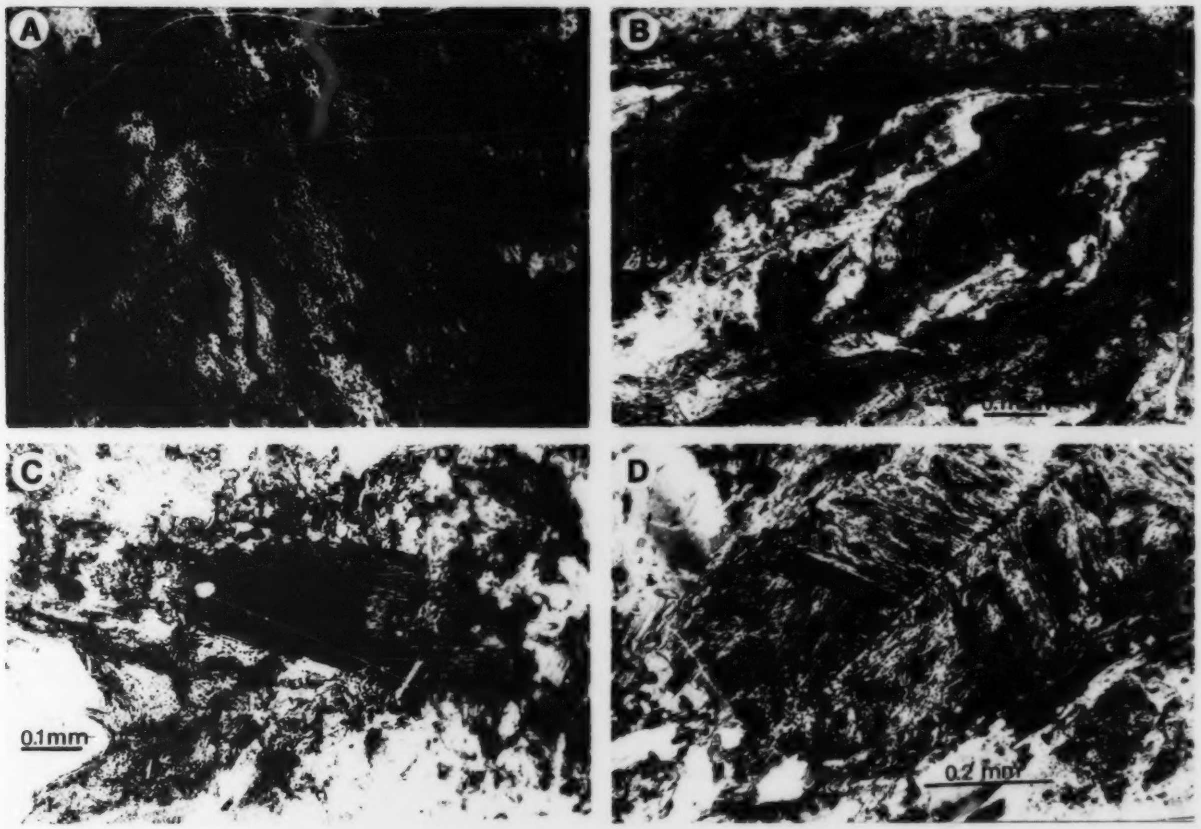

Figure 32. Photographs of a deformed and metamorphosed Long Range dyke (dyke 214; Fig. 31). C-S fabric in (A) outcrop and (B) thin section; C. early brown hornblende mantled by green hornblende; D. actinolite (a) pseudomorph after twinned augite, with a partial mantle of green hornblende (h). All photomicrographs taken with plane polarized light. GSC photos 204932 32A to D.

The available data do not favour either the best-fit or the model isocons, and suggest instead that compositional differences between the "fresh" and metamorphosed dykes reflect primary compositional variations rather than metasomatism.

The hypothesis that the apparent depletion of HFS elements in the recrystallized dykes is a primary feature, reflecting a more primitive composition, is supported by petrogenetic modelling calculations (Table 16). The mean of the three most primitive samples (from easternmost dykes 702 and 669) were used to model element concentrations in samples from the most evolved dyke (622) through mass balance (major elements) and Rayleigh fractionation (trace elements) calculations (paper in preparation by author). A reasonably good fit for the mass balance modelling (R^2 = 0.46) suggests that the evolved rocks were derived from a primitive magma through the removal of 56 % of the magma as plagioclase, augite, and olivine in the proportions 58:35:7. Trace element concentrations in the evolved rocks were modelled using these phase proportions and percent fractionation values. The similarity between the calculated and observed evolved composition in terms of most trace element concentrations supports the crystal fractionation model (Table 16). These data suggest that most of the variation in composition between the eastern dykes (most primitive and most thoroughly metamorphosed) and western dykes can be explained by magmatic crystal fractionation processes. Metamorphism of the Long Range dykes is therefore interpreted to have proceeded nearly isochemically (cf. Strong, 1974), and principally involved hydration and oxidation.

Porphyritic felsic dykes

Fine grained porphyritic felsic dykes cut the Taylor Brook gabbro complex near its southern margin. The same felsic porphyry is deformed with Paleozoic cover rocks within the Doucers Valley fault complex (Lock, 1972) immediately to the southeast of the inlier. The distribution of these dykes has been documented by Owen (1986a,b) and Owen and Erdmer (1988).

The porphyry is a tan to rose, very fine grained rock containing well-formed quartz and potassium feldspar

Table 13. Mean bulk compositions of fresh ("igneous") and altered ("metamorphosed") dykes of the Long Range swarm. Intra-dyke variations are shown for dykes 622, 610, and 214. sd = standard deviation; n = number of analyses; ns = not sought.

	ALL SAMPLES									
	"Igneous"		"Metamorphosed"		"Ign" Dyke 622		"Partly Met" Dyke 610		"Met" Dyke 214	
		sd		sd		sd		sd		sd
SiO_2	48.4	0.6	48.7	0.7	48.4	0.4	48.9	0.5	49.1	0.3
TiO_2	2.52	0.45	1.85	0.23	3.06	0.25	2.44	0.34	1.94	0.08
Al_2O_3	13.5	1.0	14.9	0.6	12.52	0.49	13.4	0.5	14.6	0.2
Fe_2O_3	2.91	0.67	3.21	0.80	2.97	0.67	3.12	1.02	3.73	0.38
FeO	11.55	0.99	8.97	0.69	12.68	0.28	11.18	0.72	8.97	0.41
MnO	0.22	0.02	0.20	0.02	0.24	0.01	0.22	0.01	0.20	0.01
MgO	5.65	0.50	6.37	0.44	5.19	0.13	5.79	0.46	6.12	0.09
CaO	10.28	0.59	10.87	0.84	9.64	0.26	10.32	0.47	10.47	0.49
Na_2O	2.13	0.11	2.35	0.33	2.15	0.06	2.06	0.14	2.51	0.29
K_2O	0.53	0.12	0.53	0.14	0.62	0.15	0.48	0.14	0.59	0.11
P_2O_5	0.27	0.05	0.19	0.02	0.32	0.02	0.25	0.05	0.20	0.01
H_2O^+	1.02	0.22	1.61	0.49	1.12	0.23	0.89	0.20	2.02	0.18
	98.98		99.75		98.9		99.67		101.5	
mean density	3.05		3.01	g cm^{-3}	ns		ns		ns	
n =	30		12		6		8		8	
Rb	25	10	24	9	33	12	26	8	21	8
Sr	187	20	199	26	195	10	171	27	186	22
Ba	134	34	118	25	167	12	119	24	133	12
Zr	163	35	123	26	198	17	164	32	133	10
Nb	28	9	10	8	37	5	29	10	6	3
Y	29	11	33	15	35	10	26	5	42	10
Cr	89	34	96	47	72	12	90	26	78	13
Ni	70	24	71	10	67	11	69	14	70	4
Cu	234	56	130	78	278	10	232	65	103	74
Zn	127	25	97	14	140	6	124	9	101	14
Ga	18	17	14	1	16	1	14	1	ns	
V	425	74	330	24	453	40	435	79	326	12

phenocrysts (1-4 mm in diameter; Fig. 34A) set in a plagioclase- and quartz-rich, white-mica-bearing matrix which in places is spherulitic (Fig. 34B). Amphibole phenocrysts were observed at one locality. The quartz phenocrysts typically are embayed. Modally, the rock approximates a dacite; compositionally, it is a rhyolite (Table 17). The presence of groundmass spherulites and the embayed nature of the quartz phenocrysts suggests that these dykes are hypabyssal intrusions. Although the age of the porphyry is not known, these features tend to support Erdmer's (1984) proposal that the porphyry correlates with volcanic members of the Silurian Sops Arm Group described by Smyth and Schillereff (1982).

The Devils Room pluton

The youngest isotopically-dated pluton in the inlier is the Devils Room granite (Heyl, 1937; Smyth and Schillereff, 1982; Dunford, 1984). Coeval granitoid rocks occur in the Gull Lake intrusive suite, which cuts lower Paleozoic supracrustal rocks southeast of the inlier (Smyth and Schillereff, 1982). U-Pb (zircon) data for the Gull Lake and Devils Room granitoid rocks (H. Baadsgaard, pers., comm., 1989) yield an upper intercept age of 398 +21/-7 Ma. Titanite gave a concordant age of about 390 Ma. These data indicate an Early Devonian age for these rocks. Preliminary $^{40}Ar/^{39}Ar$ dating supports this interpretation. Megacrystic granite from the Devils Room pluton yielded a concordant $^{40}Ar/^{39}Ar$ (biotite) age of 384 Ma, indicating cooling through a blocking temperature of about 300°C at this time (Reynolds et al., 1988). A preliminary fission track date of 187 ± 14 Ma for apatite from the same sample suggests that the pluton was not buried at depths exceeding 3 km since the Middle Jurassic (Reynolds et al., 1988).

The Devils Room pluton is partly fault-bounded, but clearly cuts across all tectonic fabrics in the adjacent country rock (Erdmer, 1986a). The intrusion is well to the south of the bulk of the Long Range dykes, but the isotopic data clearly indicate that the pluton is approximately 225 Ma younger than the dykes.

The bulk of the pluton consists of massive megacrystic biotite ± hornblende granite which grades into equigranular two-mica granite toward the centre of the intrusion. The two-mica granite forms an oval body approximately 1.5 km in diameter.

Table 14. Inter-dyke variations in TiO_2 (wt.%); Zr, Nb, and Y (ppm); and MgO* in Long Range swarm near Pigeon Cove. Standard deviations (sd) are given where the mean was determined for ≥3 samples. See Figure 31 for dyke locations. n = number of analyses.

	Relatively fresh dykes							
	622		658	621	643		573	
		sd				sd		sd
TiO_2	3.06	0.25	1.90	2.65	1.99	0.12	2.46	0.16
Zr	198	32	100	160	137	15	163	32
Nb	37	6	15	20	20	10	23	6
Y	35	15	30	30	23	6	27	15
MgO*	0.25		0.31	0.26	0.33	0.27		
n =	6		2	1	3		3	
	Metamorphosed dyke		More thoroughly metamorphosed dykes					
	610		582	659**	668		702	669
		sd				sd		
TiO_2	2.44	0.34	2.78	2.30	2.88	0.21	1.52	1.47
Zr	164	32	170	155	183	15	70	90
Nb	29	10	30	35	23	6	10	15
Y	26	5	50	25	27	21	20	15
MgO*	0.29		0.27	0.31	0.26		0.40	0.41
n =	8		1	2	3		1	2

* MgO* = MgO/(MgO + FeO_t)

** Contains minor relict clinopyroxene

Table 15. Concentration changes ($\Delta C_i/C_i$) in the altered Long Range dykes corresponding to three model isocons and the Ti-Zr best-fit isocon.

	Constant			Ti-Zr best-fit
	alumina	mass	volume	
Nb	−0.68	−0.64	−0.65	−0.52
Cu	−0.50	−0.44	−0.45	−0.25
P_2O_5	−0.36	−0.30	−0.30	−0.05
TiO_2	−0.33	−0.27	−0.28	—
Zr	−0.31	−0.25	−0.26	—
Zn	−0.31	−0.24	−0.25	0.02
FeO	−0.29	−0.22	−0.23	0.05
V	−0.29	−0.22	−0.23	0.05
Ga	−0.29	−0.22	−0.23	0.05
Ba	−0.20	−0.12	−0.13	0.18
MnO	−0.17	−0.09	−0.10	0.22
Rb	−0.13	−0.04	−0.05	0.29
SiO_2	−0.09	0.01	−0.01	0.35
K_2O	−0.09	0.00	−0.01	0.35
Ni	−0.08	0.01	0.00	0.35
CaO	−0.04	0.06	0.04	0.42
Sr	−0.03	0.06	0.05	0.43
Cr	−0.02	0.08	0.06	0.45
Fe_2O_3	0.00	0.10	0.09	0.48
Na_2O	0.00	0.10	0.08	0.48
Al_2O_3	—	0.10	0.09	0.48
Y	0.03	0.14	0.12	0.53
MgO	0.02	0.13	0.11	0.51
H_2O	0.43	0.58	0.56	1.12

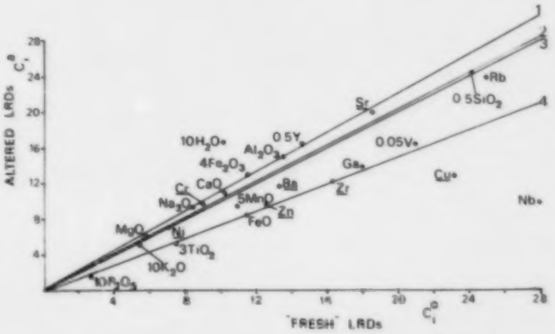

Figure 33. Isocon diagram comparing the mean bulk composition of relatively fresh (pyroxene-bearing) Long Range dykes (LRDs) and their metamorphosed equivalents (see Table 15). Components are scaled as indicated (underscored trace elements are plotted in 0.1 ppm). 1-constant alumina isocon; 2-constant mass isocon; 3-constant volume isocon; 4-best-fit high field strength element (Ti, Zr) isocon.

The outer part of the megacrystic granite is mylonitized, and is partly enclosed by a narrow (ca. 100 m) band of amphibolite (Dunford, 1984) consisting of hornblende, quartz, albite(?), and accessory titanite, rutile, biotite, and opaques. The concentric form of the intrusion is mimicked by inward-dipping joints (Fig. 35), which delineate a ring-like structure clearly evident on aerial photographs.

An unusual feature of the pluton is the local presence of narrow steeply-dipping bands of silicified fluorite-bearing breccia. These are well exposed on the forestry road following the north bank of Main River (see Owen and Erdmer, 1988). The breccias are interpreted to result from hydraulic fracturing (Erdmer, 1986a). Megacrystic biotite-hornblende granite transected by the breccia zones contains brown biotite, idiomorphic green hornblende, and normally-zoned plagioclase (An_{24-14}). Analyses of the mafic minerals are presented in Table 18.

Table 16. Petrogenetic modelling of the Long Range dykes. Mean compositions of the most primitive ("parent") and evolved ("daughter") dyke samples (n = 3) used in mass balance and Rayleigh fractionation calculations are listed.

	Parent Analysis	Daughter Analysis	Calculated Daughter
SiO_2	49.08	49.38	49.42
TiO_2	1.52	3.19	3.15
Al_2O_3	16.36	12.51	12.44
FeO	10.52	15.96	15.84
MnO	0.17	0.26	0.31
MgO	7.33	5.28	5.30
CaO	12.48	9.72	9.65
Na_2O	2.00	2.17	2.72
K_2O	0.39	1.20	0.83
P_2O_5	0.15	0.34	0.35
Rb	33	37	72
Sr	233	193	215
Ba	83	167	163
Zr	83	210	185
Nb	13	40	29
Y	17	37	38
Cr	151	77	18
Ni	77	73	39
Ga	13	16	16
V	317	460	449

Major element oxides are presented as weight percent volatile free, with total Fe as FeO. Major elements of calculated evolved composition were determined from mass balance calculations as described in Bryan et al. (1969). Phases removed are plagioclase (AV-5, Papezik and Hodych, 1980), augite (Appendix, Papezik et al., 1988), and olivine (CQ-2, Greenough and Papezik, 1986) in proportions 58:35:7 with 44% of the magma remaining. $R^2 = 0.46$. Trace elements modelled using Rayleigh fractionation law (e.g. Gast, 1968) with phases, phase proportions, and fraction of melt remaining as given from mass balance calculation. Partition coefficients used for Rb, Sr, Ba, Zr, Nb, Y, Cr, Ni, Ga, and V in plagioclase: 0.08, 1.85, 0.30, 0.02, 0.02, 0.02, 0.01, 0.04, 1.00, 0.08; in clinopyroxene: 0.00, 0.08, 0.00, 0.01, 0.01, 0.01, 10.00, 2.75, 0.50, 1.50; in olivine: 0.00, 0.01, 0.01, 0.01, 0.01, 0.01, 1.92, 12.00, 0.06, 0.05. Partition coefficients from Evans (1978), Frey et al. (1974), and Philpotts and Schnetzler (1970).

The relation of these cataclastic breccias to the mylonitic fault zones bordering the intrusion is not known. Dunford (1984) reported that the mylonite is mineralogically similar to its protolith (megacrystic granite), but is impoverished in sphene and opaque minerals, and microcline is not perthitic. Compositionally, the mylonite has higher Si/K and Si/(Ca+Na) ratios than the protolith. Faulting therefore appears to have been accompanied by silicification. Mylonite derived from the adjacent gneiss complex contains brown to green biotite and idiomorphic garnet.

Major element data for 70 samples of the pluton have been reported by Dunford (1984). The mean composition of the megacrystic granite is presented in Table 18. Dunford (1984) noted that lithological zonation *is manifested by an*

Figure 34. Photographs of felsic porphyry dykes. A Field aspect, showing quartz and feldspar phenocrysts; B. photomicrograph, showing feldspathic spherulites in the matrix of an embayed quartz phenocryst (sample VO-85-010; plane polarized light). GSC photos 204932 34A to B.

enrichment in Na and Ca relative to K toward the centre of the intrusion.

Paleozoic supracrustal rocks

The Long Range Inlier is surrounded by a variety of Paleozoic clastic and chemical sedimentary rocks, with which both structural and stratigraphic relations are evident. In the foreland to the west, these include cover rocks of the western Newfoundland platformal sequence (Cumming, 1983), and clastic rocks of the Humber Arm Allochthon

Table 17. Mean major and selected trace element composition of felsic porphyry dykes (n = 4). Also shown are CIPW norms. sd = standard deviation.

Majors (wt. %)			Traces (ppm)			CIPW norms	
		sd			sd		
SiO_2	74.6	0.5	Ba	223	239		
TiO_2	0.09	0.04	Rb	315	111	ap	0.05
Al_2O_3	13.9	0.5	Sr	23	32	il	0.12
Fe_2O_3	0.57	0.16	Nb	33	9	or	25.82
FeO	0.06	0.00	Ga	22	5	ab	39.95
MnO	0.06	0.04	Y	38	19	an	3.30
MgO	0.14	0.03				hy	0.23
CaO	0.70	0.20				c	0.36
Na_2O	4.73	0.72				q	28.69
K_2O	4.38	0.30				hm	0.57
P_2O_5	0.02	0.01					
H_2O^+	0.45	0.06				A	92.17
						F	6.39
	99.63					M	1.44

Table 18. Mean major element composition of the megacrystic phase of the Devils Room granite (from Dunford, 1984), and microprobe analyses of biotite and hornblende from megacrystic granite. ns = not sought; nr = not reported. Abbreviations as in Appendix II.

	Mean bulk comp.	VO–88–2003	
		bi	hbl
SiO_2	73.5	37.27	42.30
TiO_2	0.19	2.56	1.33
Al_2O_3	14.14	14.30	8.40
Cr_2O_3	ns	0.02	0.02
Fe_2O_3	1.08	ns	ns
FeO	ns	18.23	17.08
MnO	0.04	0.47	0.48
MgO	0.35	11.24	10.45
CaO	0.89	—	11.49
Na_2O	nr	0.09	1.99
K_2O	4.69	9.45	0.79
P_2O_5	0.06	ns	ns
	95.7	93.6	94.3
Oxygen basis:		22	23
Si		5.766	6.641
Al^{iv}		2.234	1.359
Al^{vi}		0.374	0.196
Cr		0.002	0.002
Ti		0.298	0.157
Fe		2.359	2.243
Mn		0.067	0.064
Mg		2.591	2.445
Ca		—	1.933
Na		0.027	0.606
K		1.865	0.158

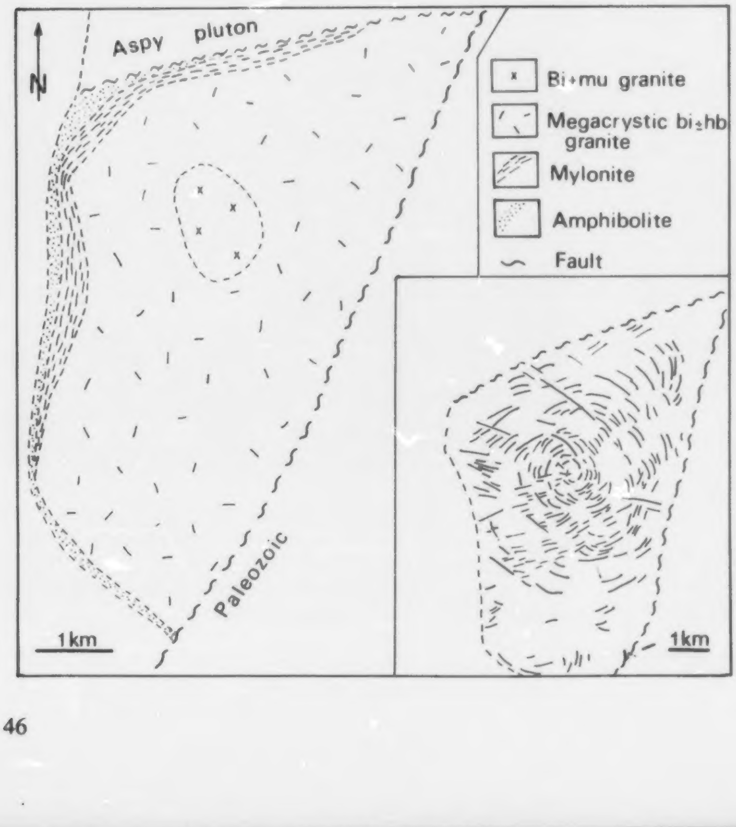

Figure 35. Sketch map of the Devils Room pluton. Inset shows distribution of concentric joints in the intrusion (after Dunford, 1984).

(Williams, 1973, 1975). Unconformably overlying Grenvillian basement are Cambro-Ordovician cover rocks which comprise, from oldest to youngest, the Bradore, Forteau, and Hawke Bay formations (Schuchert and Dunbar, 1934), the St. George and Table Head groups (Schuchert and Dunbar, 1934), and the Goose Tickle Formation (Cooper, 1937; Knight, 1985a,b). The Humber Arm Allochthon structurally overlies the cover rocks, and in this area comprises Cambro-Ordovician rocks of the Cow Head Group (Kindle and Whittington, 1958; Williams et al., 1985), the Lower Head Formation (Williams et al., 1985), and the Cape Cormorant Formation (Klappa et al., 1980).

Arkosic rocks of the Bradore Formation unconformably overlie basement near the northwestern margin of the inlier. A thickness of 45 to 60 m has been reported for the Bradore Formation in this area (Nelson, 1955; Bostock, 1983). East of Hawkes Bay, flat-lying exposures of the Bradore Formation have a minimum thickness of ca. 35 m. Contact with the underlying equigranular granite of the Lake Michel intrusive suite was not observed by the author. The lowest exposed lithology is a reddish conglomerate to conglomeratic arenite, which contains elongate rounded grey quartz pebbles. The conglomerate is overlain in turn by reddish arkose containing salmon-coloured feldspar chips, in places with quartz pebbles; grey crossbedded orthoquartzite or feldspathic quartzarenite; and, above a ca. 20 m gap in exposure, fine grained greenish arkose with knobby pink feldspathic patches which weather in positive relief.

Both stratigraphic and structural contacts separate the inlier from Paleozoic clastic and carbonate rocks along its southeastern margin. Supracrustal rocks in this area comprise four groupings: (1) Cambro-Ordovician platformal rocks of the Coney Arm Group (Smyth and Schillereff, 1982); (2) Cambro-Ordovician rocks of the Southern White Bay Allochthon (Williams, 1977) (also referred to as the Coney Head Allochthon; Erdmer, 1986b); (3) Silurian volcaniclastic, clastic, and carbonate rocks of the Sops Arm Group (Smyth and Schillereff, 1982); and (4) Carboniferous conglomerates and redbeds of the Deer Lake Basin (Hyde, 1982). Middle Paleozoic intrusive rocks include mafic to felsic rocks of the Gull Lake intrusive suite, which is coeval with the Devils Room granite. The Gull Lake plutons were emplaced into the Sops Arm Group after regional deformation during the Late Silurian (Tuach et al., 1988).

Basal conglomerate and arenite of the Coney Arm Group (Beaver Brook Formation, Lock, 1969; Smyth and Schillereff, 1982) unconformably overlie the Aspy pluton. The unconformity is well exposed along the Cat Arm Dam access road. The conglomeratic rocks contain an unsorted assemblage of feldspar chips and granitoid rock fragments (Fig. 36A). Arenite directly overlying the granite is a fine grained grey-green rock containing 1 mm magnetite crystals (Fig. 36B). Conglomeratic channel fills are locally evident in the basal arenite.

Clastic rocks of the Coney Arm Group flanking the inlier east of Taylor Brook are deformed within the Doucers Valley fault complex (Lock, 1972). These metasedimentary schists are quartz- and plagioclase-rich rocks containing biotite, white mica, and rare andalusite (sericitized). Mafic rocks deformed within the fault zone contain the greenschist facies assemblage chlorite, albite, and epidote.

Metasedimentary schists of the Coney Arm Group are overlain by flat-lying redbeds of the Deer Lake Basin, which onlaps the southeastern corner of the inlier near the Taylor Brook gabbro complex. Conglomeratic rocks are polymict, containing a heterogeneous assemblage of unsorted mafic and felsic plutonic rocks and gneiss. The contact with the underlying basement complex apparently is not exposed in this area; however, conglomerate veneers on displaced gabbro blocks in Taylor Brook indicate stratigraphic, not structural, relations with the underlying basement. The Taylor Brook gabbro complex is deeply weathered beneath the unconformity. Liesegang rings are developed in an outcrop of the reddish, weathered gabbro exposed on the Taylor Brook road (see Fig. 12F).

Post-Coney Arm Group mafic dykes

Northeast-trending mafic dykes cut the Coney Arm Group near Jackson's Arm. Their age is not known. A dyke exposed in roadcuts near Little Coney Arm is transected by

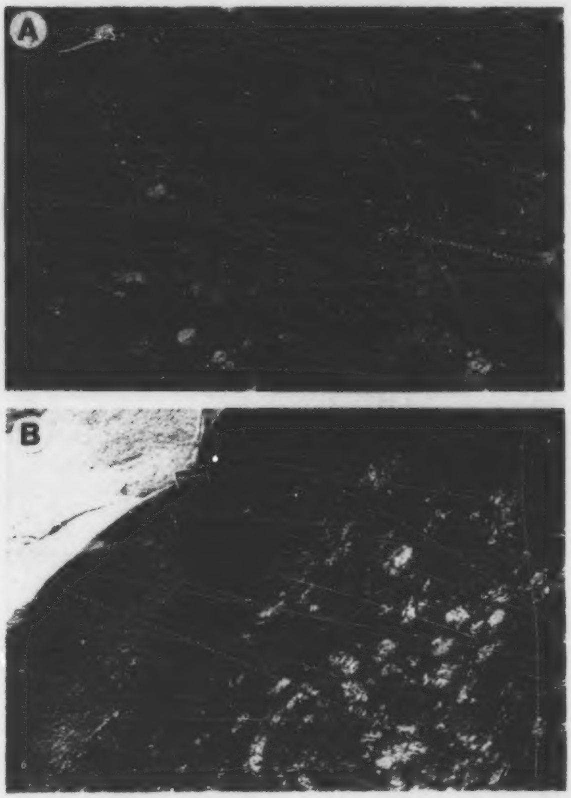

Figure 36. Field photographs of the basal unconformity of the Coney Arm Group, overlying megacrystic granite (Aspy pluton). A. Polymict conglomerate (note fragments of the underlying granite); B. magnetite-bearing arkose. GSC photos 204932 36A to B.

a shallowly northwest-verging thrust of suspected Carboniferous age (Owen and Erdmer, 1988). The field relations therefore suggest a post-Middle Ordovician age (Late Devonian?) for these dykes. The dykes are up to several metres in width and are steeply dipping.

The dyke exposed in roadcuts near Little Coney Arm is petrographically similar to Long Range dykes described above. It contains 1 mm long, normally-zoned plagioclase tablets ($An_{63\text{-}45}$) which are partly enclosed by augite. The augite is partly replaced by actinolite. Biotite and ilmenite are accessory phases. Mineral analyses are presented in Table 19. These data indicate that the composition of the primary and metamorphic assemblage in this sample is very similar to that of the Long Range dykes (cf. Tables 12, 27). Similarities with the Long Range dykes make regional correlation of northeast-trending dykes in the central and southern parts of the inlier suspect; both Late Proterozoic and Middle Paleozoic dykes may cut basement in this area.

METAMORPHISM

The Long Range Inlier exhibits a prolonged metamorphic history punctuated by intrusive events. Four broadly-constrained metamorphic events have been identified. The oldest event (Metamorphism 1, abbreviated as "M_1") predates emplacement of the Grenvillian plutons, and produced the amphibolite to granulite facies rocks of the Long Range gneiss complex. The gneiss complex was thermally recrystallized in narrow zones adjacent to plutons (synplutonic metamorphism; "M_2"). A period of regional amphibolite facies metamorphism ("M_3") affected the inlier after intrusion of the Grenvillian granites, but prior to emplacement of the Long Range dykes. Finally, the Long Range dykes and their host rocks were locally deformed and metamorphosed during Paleozoic orogenies ("M_4").

Table 19. Microprobe analyses of clinopyroxene, plagioclase, and amphibole from a northeast-trending Paleozoic mafic dyke near Little Coney Arm. Abbreviations as in Appendix II. Total Fe as FeO.

	VO-88-2001			
	cpx	pl core	pl rim	amph
SiO_2	47.40	51.81	56.24	54.36
TiO_2	2.33			0.10
Al_2O_3	5.60	29.53	26.38	1.32
Cr_2O_3	0.11			
FeO	9.40	0.54	0.49	11.96
MnO	0.13			0.13
MgO	12.94			15.91
CaO	21.12	13.24	9.50	12.62
Na_2O	0.69	4.28	6.55	0.27
K_2O				
	99.7	99.6	99.3	99.6
Oxygen basis:	6	8	8	23
Si	1.790	2.373	2.555	7.873
Al_{iv}	0.210	1.595	1.413	0.127
Al_{vi}	0.039			0.098
Cr	0.003			
Ti	0.066			0.011
Fe	0.297	0.021	0.019	1.449
Mn	0.004			0.016
Mg	0.728			3.434
Ca	0.855	0.650	0.463	3.434
Na	0.051	0.380	0.577	0.076
K				

Metamorphism 1: Pre-plutonic stage

Age and metamorphic grade

Crosscutting relations indicate that most of the features of the gneiss complex described above developed during a period of regional high grade metamorphism predating emplacement of the Grenvillian granitoid plutons. Regional variations in metamorphic grade, increasing from amphibolite to granulite facies toward the southwest, are attributed to this event (M_1). The age of this event is constrained by the minimum age of protoliths of quartzofeldspathic gneiss of presumed igneous origin determined by the U-Pb (zircon) method (1550 Ma; H. Baadsgaard, pers. comm., 1989) and the intrusive age (1056 Ma) of the voluminous Grenvillian granitoid plutons.

The gneiss complex comprises a variety of mineral assemblages useful in estimating the physical conditions of metamorphism.

Mineral chemistry

The composition of pressure- and temperature-sensitive metamorphic mineral assemblages was determined by electron microprobe analysis for use in geothermobarometry. Microprobe operating conditions and the accuracy and precision of the analytical data are outlined in Appendix I. Mineral analyses are presented in Appendix II. Typical assemblages are listed in Table 20, and are illustrated in Figure 37.

Table 20. Typical mineral assemblages of the Long Range gneiss complex. See Appendix II for abbreviations.

Pelite
Ksp-qz ± pl($An_{2\text{-}37}$)-sil-gt-bi ± cd ± gp ± hc
pl($An_{8\text{-}11}$)-qz-sil-cd-opx ± Ksp ± gd ± hc
pl($An_{28\text{-}35}$)-qz-Ksp-sil-cd-gt-bi ± hc
pl($An_{40\text{-}46}$)-gt-cd-bi-hc ± opx ± qz

Semipelite
gt-bi-qz-pl($An_{5\text{-}40}$)-Ksp ± opx ± gp

Marble; Calc-silicate rock
ct-fo-di-ph ± sp + gp
wol-sl-pl(An_{74})-ct-scp ± gp

Tonalitic-granitic gneiss
opx ± cpx-pl($An_{22\text{-}45}$)-qz ± bi ± Ksp
opx-gt-pl($An_{20\text{-}45}$)-Ksp-qz
bi-Ksp-pl($An_{16\text{-}28}$)-qz- ± hbl ± gt

Metabasite
opx ± cpx-pl($An_{18\text{-}70}$) ± hbl ± bi

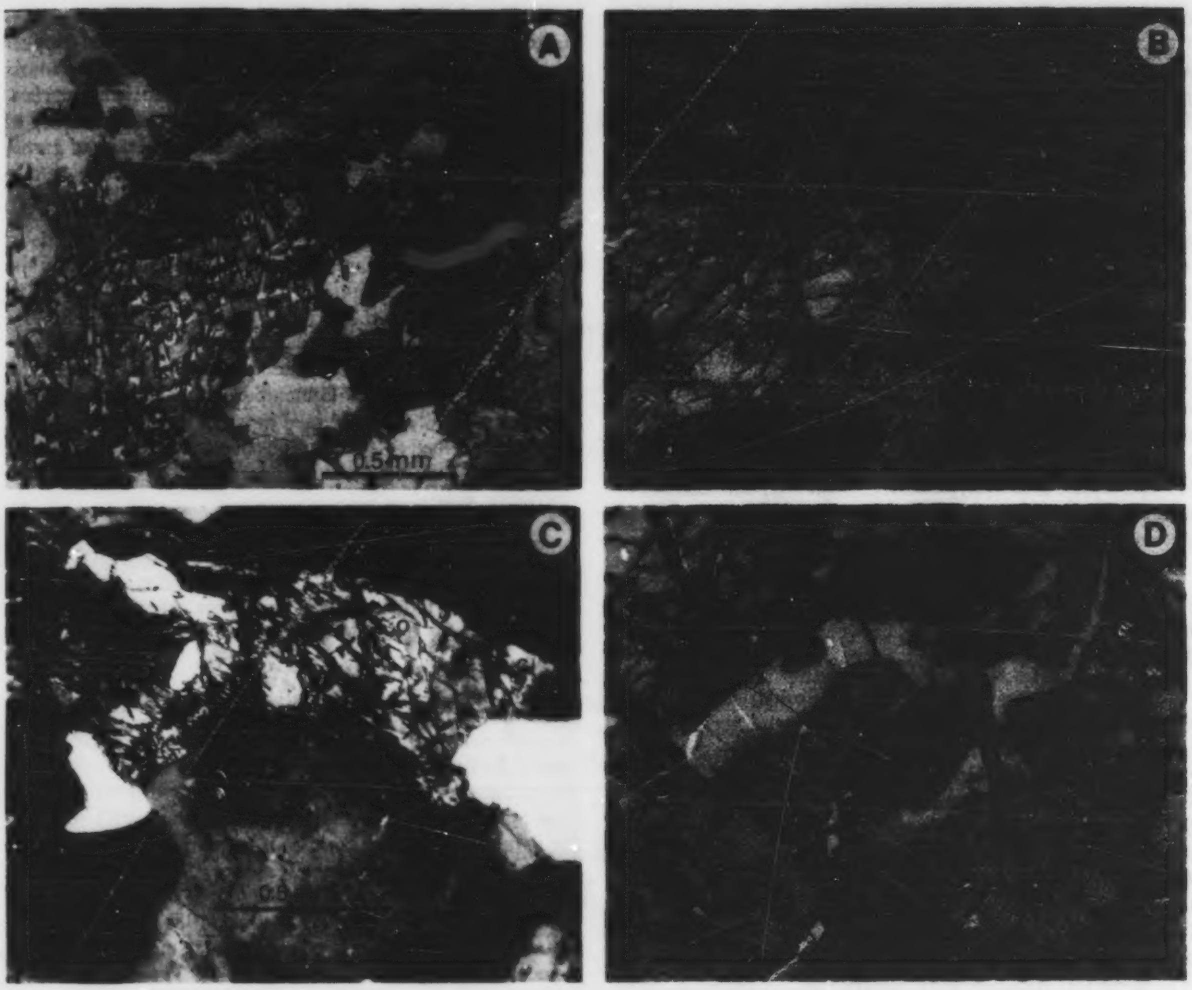

Figure 37. Photomicrographs of high grade mineral assemblages from the Long Range gneiss complex. A. Symplectic sillimanite-quartz intergrowth (s) adjacent to garnet (g) porphyroblast in pelitic gneiss (unit Ppn), from large paragneissic enclave in the northern Lake Michel intrusive suite (sample VO-86-484-2; plane polarized light (ppl)); B. garnet (g), sillimanite (s), plagioclase, quartz, and biotite in pelitic gneiss near Torrent River (VO-86-2279; ppl); C. orthopyroxene (o) and clinopyroxene (c) in tonalitic gneiss (unit Ptn) from the southern part of the inlier (VO-85-415; crossed nicols); D. garnet (g), orthopyroxene (o), and biotite (b) in tonalitic gneiss sampled south of the Lake Michel intrusive suite (VO-86-111; ppl). Note symplectic biotite-quartz intergrowth (retrograde) near orthopyroxene (arrow).

Garnet porphyroblasts generally 0.1 to 2 mm (maximum 1 cm) across occur locally in most quartzofeldspathic rocks of the gneiss complex. The garnets have "plateau" compositional profiles, with homogeneous cores, and narrow rims enriched in Fe/Mg and, in some samples, Ca and/or Mn (Fig. 38). All garnets are Fe-rich (no garnets were observed in metacarbonate rocks, sensu stricto).

Garnet with the lowest Mn and Ca contents occurs in pelitic gneiss. Garnet from cordierite-bearing pelite is rich in almandine (60-82 %) and pyrope (14-36 %), with subordinate grossular (1-3 %) and spessartine (0-6 %). The pyrope and almandine contents of garnet rims in contact with cordierite vary by <3 % of the garnet core composition. The grossular content of garnet coexisting with sillimanite, plagioclase, and quartz in pelitic gneiss ranges from 1 to 3 %. Garnet coexisting with orthopyroxene, plagioclase, and quartz in granitic and tonalitic gneiss, and in semipelites, is rich in almandine (65-72 %), with variable pyrope (7-27 %) and grossular (4-19 %) contents, and minor spessartine (1-3 %). In some samples, orthopyroxene or clinopyroxene, and ilmenite, are enclosed by coronitic garnet with symplectic quartz intergrowths. Garnet shows a range of compositions in rocks in which biotite is the other ferromagnesian mineral. Garnet from biotite-bearing gneiss contains up to 25 % spessartine and 13 % grossular. Garnet rims adjacent to biotite are enriched in almandine and spessartine by up to 6 % (with a corresponding decrease in pyrope). Matrix garnets (i.e., those separated from other ferromagnesian minerals by quartz and feldspar) may also show a core to rim increase in Fe/Mg, or are not zoned.

Pyroxene is ubiquitous as small porphyroblasts (0.1-1 mm) in quartzofeldspathic gneiss, semipelite, and metabasite. Although two-pyroxene and garnet-orthopyroxene assemblages occur, no texturally stable two-pyroxene-garnet or clinopyroxene-garnet occurrences were noted.

Orthopyroxene in garnetiferous granulite is hypersthene to ferrohypersthene, with Mg/(Mg+Fe) between 0.25 and 0.54. It contains 0.7 to 4.7 weight percent alumina, the highest values being in pyroxene from semipelite. Pyroxene rims in contact with garnet have higher Mg/Fe ratios than their cores. Orthopyroxene coexisting with clinopyroxene is hypersthene to ferrohypersthene, with X_{Mg} between 0.54 and 0.62. Eulite (X_{Mg} = 0.15-0.18) is present in two gneiss samples.

Clinopyroxene is typically subordinate to orthopyroxene in quartzofeldspathic gneiss. Clinopyroxene coexisting with hypersthene is augite with X_{Mg} between 0.64 and 0.73, and 20 to 22 weight percent CaO.

Cordierite occurs variously as porphyroblasts and as fine grained mosaics with hercynite replacing garnet and sillimanite. Pinitization is slight or absent in the analyzed samples. Cordierite porphyroblasts have cores with X_{Mg} of 0.59 to 0.87; rims touching garnet have X_{Mg} of 0.66 to 0.72. The optical characteristics of cordierite have been determined in five samples. In three samples, cordierite is optically positive, with $2V_x$ ranging from 92 to 106°, implying elevated CO_2 in cordierite channel fluids ($n^{cd}_{H_2O} < 0.3$; Armbruster and Bloss, 1980). Cordierite in a large pelitic screen within the LMIS is water-rich (sample VO-86-484-1; $n^{cd}_{H_2O} > 0.5$). Anhydrous cordierite occurs within the thermal aureole of the Taylor Brook gabbro complex (sample VO-85-024). Cordierite in the regionally metamorphosed pelites thus appears to be CO_2-rich, in contrast to water-rich and anhydrous cordierite in pelites near granitic and gabbro intrusions, respectively.

Biotite is an essential mineral in most of the gneiss complex. Brown to reddish biotite (TiO_2 up to 5.5 weight percent) occurs in granulite. In most samples the most magnesian biotite forms rounded inclusions within garnet, or subidiomorphic flakes flanking garnet, and increases in X_{Mg} have been noted in biotites within 2 or 3 mm of garnet porphyroblasts.

Sillimanite is the characteristic aluminosilicate in the inlier, although Bostock (1983) reported sericitized andalusite in pelites bordering a Grenvillian granitic pluton in the northern part of the inlier. The sillimanite contains small amounts of iron (≤ 0.2 % Fe_2O_3). It forms needles up to 3 mm long in narrow bands associated with, and in places enclosed by, garnet and biotite. Fibrolite is locally present in feldspar or garnet. Sillimanite in pelite flanking granitic plutons is locally retrogressed to white mica. Underschultz (1986) described two generations of sillimanite in sericitized pelite along the southeastern margin of the Lake Michel intrusive suite.

Metamorphic P-T conditions

Metamorphic P-T conditions have been estimated using the standard state, free energy relation:

$$\Delta G^\circ = -RT\ln K - \Delta V(P-1)$$

where R is the gas constant, T the temperature, K the equilibrium constant, ΔV the volume change on reaction, and P the pressure. Thermochemical data for the applicable equilibria are presented in Table 21. Owing to the controversy surrounding activity-composition (a/X) relations in garnet, particularly concerning mixing on the almandine-grossular join (Anovitz and Essene, 1987; Geiger et al., 1987) and the almandine-pyrope join (O'Neill and Wood, 1979; Hoinkes, 1986; Geiger et al., 1987), the activity of garnet components has been estimated using the quaternary model of Hodges and Royden (1984). This model adopts nonzero interaction parameters only for W_{CaMg} (Newton and Haselton, 1981), an assumption that has proven reasonable for low Ca-Mn garnets in high grade terranes (e.g., Newton, 1983). The author has used the anorthite-plagioclase activity-composition relations recommended by

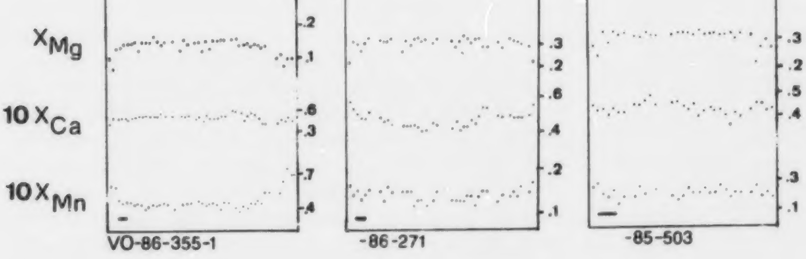

Figure 38. Rim-to-rim compositional profiles of garnet in pelitic, semipelitic, and granitic gneiss. VO-86-355-1, unit Ppn; VO-86-271, unit Ppn; VO-85-503, unit Pgn. Scale bar = 0.2 mm.

Newton (1983), and the ideal two-site mixing model for orthopyroxene suggested by Wood and Banno (1973). Ideal Fe-Mg mixing in biotite (Mueller, 1972) has been assumed, and nonideal mixing in cordierite has been corrected for using Bhattacharya et al.'s (1988) recently published interaction parameter ($W_{Fe\text{-}Mg}$) for this mineral. Distribution coefficients of the various thermobarometric equilibria have been modified accordingly. The results presented below are taken from Owen and Erdmer (1989).

Geobarometry

Moderate metamorphic pressures are suggested by the presence of sillimanite in pelitic gneiss, and by the apparent absence of coexisting garnet and clinopyroxene in quartz-free rocks.

This is confirmed by several geobarometers. Perkins and Chipera's (1985) calibration of the garnet-orthopyroxene-plagioclase-quartz geobarometer (R1, Table 21) yields pressures of 6.4 to 8.2 kbar (core compositions; Table 22) in

Table 21. Thermochemical data for thermobarometric equilibria. alm-almandine, an-anorthite, ann-annite, cd-cordierite, en-enstatite, fs-ferrosilite, gros-grossular, pyr-pyrope, phl-phlogopite, qz-quartz, sil-sillimanite.

	Equilibrium	ΔG (J)	ΔV (J/MPa) (25°C, 1 bar)
R1	an + en = 1/3gros + 2/3pyr + qz	−49360 + 102.45T	67.89
R2	1/2Fe-cd = 1/3alm + 2/3sil + 5/6qz	14477 + 9.33T	−2.5527
R3	1/2Fe-cd + fs = alm + 3/2qz	−20460 − 28.16T	−3.2899
R4	3an = gros + 2sil + qz	−42066 − 130.127T	−5.4584
R5	alm + phl = pyr + ann	32818 − 23.849T	−0.2414
R6	3pyr + fs = 3alm + en	34058 − 9.874T	0.2720
R7	Fe-cd + pyr = Mg-cd + alm	12916 + 5.615T	−0.075

References:

R1-Perkins and Chipera (1985)
R2-Bhattacharya (1986, reaction A)
R3-Bhattacharya (1986, reaction D)
R4-Goldsmith (1980), Holdaway (1971), Froese (1988)
R5-Perchuk and Lavrent'eva (1983)
R6-Sen and Bhattacharya (1984)
R7-Perchuk et al. (1985)

Table 22. Compositional parameters and pressure-temperature determinations of coexisting garnet - orthopyroxene-plagioclase - quartz. c-core, r-rim. P: Perkins and Chipera (1985; Mg-reaction); T: Sen and Bhattacharya (1984). Unique P-T estimates were derived by solving for P and T simultaneously (values were rounded off to nearest 50 bars and 5°C).

	garnet				opx	Pl		
	X_{Mg}	X_{Fe}	X_{Ca}	X_{Mn}	X_{Mg}	X_{An}	P kbar	T° C
VO-85-								
946c	0.242	0.655	0.082	0.021	0.521	0.388	7.80	790
r	0.229	0.686	0.065	0.020	0.526	0.388	5.95	690
VO-86-								
111c	0.208	0.697	0.072	0.022	0.488	0.347	6.70	725
r	0.181	0.711	0.083	0.025	0.497	0.347	5.75	620
113-2c	0.103	0.683	0.190	0.024	0.317	0.450	7.95	820
r	0.072	0.693	0.210	0.025	0.317	0.450	5.00	620
115c	0.078	0.744	0.145	0.033	0.285	0.306	6.35	685
r	0.065	0.742	0.164	0.029	0.298	0.306	5.00	570
279c	0.239	0.702	0.045	0.014	0.534	0.241	6.65	675
r	0.206	0.731	0.047	0.016	0.521	0.241	5.65	600
291c	0.254	0.686	0.048	0.012	0.513	0.308	7.20	790
451-2c	0.319	0.654	0.008	0.019	0.543	0.109	7.20	875
825-3c	0.199	0.737	0.037	0.027	0.427	0.224	7.00	810
VO-87-								
157-2c	0.265	0.636	0.078	0.021	0.554	0.382	8.15	785
175c	0.179	0.622	0.186	0.013	0.474	0.799	6.50	795
r	0.169	0.626	0.189	0.015	0.484	0.809	5.70	730
232c	0.159	0.593	0.188	0.059	0.528	0.460	6.50	645
r	0.147	0.601	0.193	0.059	0.541	0.471	5.35	570

most samples. Newton and Perkins' (1982) calibration yields similar pressures (5.5 to 7.5 kbar) for the same samples. The composition of garnet rims touching orthopyroxene yields pressures up to 3 kbar lower than contiguous cores, with correspondingly lower temperatures determined by Fe-Mg exchange between both minerals (Fig. 39; see below). This indicates that cooling accompanied regional decompression.

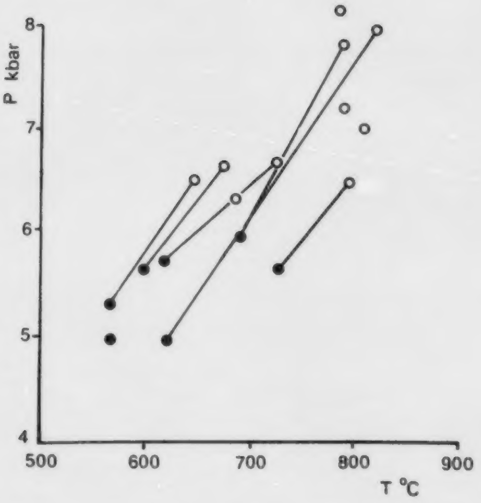

Figure 39. Results of garnet-orthopyroxene-plagioclase-quartz geothermobarometry from samples of the Long Range gneiss complex (tonalitic and semipelitic gneiss). Open symbols-core compositions; black symbols-rim compositions.

The cordierite-garnet-sillimanite-quartz geobarometer (R2; Bhattacharya, 1986, reaction A) indicates pressures ranging from 5.0 to 6.5 kbar (Table 23). Bhattacharya's (1986) calibration of the cordierite-orthopyroxene-quartz barometer (R3) yields a pressure of 6.4 kbar in one sample (VO-86-451-2).

The sillimanite-garnet-plagioclase-quartz barometer (R4, Table 24; see Froese, 1988) has a high degree of uncertainty owing to problems in attaining experimental reversals, the temperature sensitivity of the end-member equilibrium, and the low concentration of grossular in garnet from pelitic assemblages (Bohlen and Lindsley, 1987). This barometer is particularly unreliable for relatively low temperature (<700°C) assemblages containing sodic oligoclase or albite due to difficulties in establishing a/X relations for plagioclase of this composition (Ashworth and Evirgen, 1985). Sillimanite-bearing pelite containing calcic oligoclase or andesine yields relatively low pressures of 3 to 5 kbar. Although considered to be unreliable due to the extremely low concentration of grossular ($X_{gros} < 0.05$) in garnet, similar pressures were derived from pelite from the Grenville Province of southern Labrador (see below).

Errors associated with these geobarometers range from about ± 1.0-1.5 kbar for garnet-cordierite and garnet-orthopyroxene equilibria to at least ± 2 kbar for the garnet-plagioclase-Al_2SiO_5-quartz barometer (Bohlen and Lindsley, 1987). Bearing this in mind, it is concluded that the amphibolite and granulite-facies gneisses crystallized at ca. 5 to 8 kbar.

Geothermometry

On the basis of the regional distribution of high grade assemblages (Fig. 5), it is anticipated that the highest metamorphic temperatures should be derived from samples from

Table 23. Compositional parameters and P-T determinations for garnet + cordierite (± sillimanite ± orthopyroxene)-bearing pelitic gneiss from the Long Range Inlier and southern Labrador. r-rim, c-core; anhyd-anhydrous. P, T determined by simultaneous solution of the garnet-cordierite geothermometer (Perchuk et al., 1985) and the cordierite-garnet-sillimanite-quartz geobarometer (Bhattacharya 1986, reaction A) except for sample VO-86-451-2 (cordierite-garnet-orthopyroxene-quartz geobarometer; Bhattacharya 1986, reaction D). Results are rounded off to nearest 100 bar, 5°C.

		garnet				cordierite		P kbar	T°C
		X_{Mg}	X_{Fe}	X_{Ca}	X_{Mn}	n_{H_2O}	X_{Mg}		
VO-85-									
024	c:	0.230	0.683	0.034	0.052	anhyd	0.674	6.7	755
	r:	0.223	0.686	0.032	0.059		0.719		673
VO-86-									
451-2	c:	0.313	0.655	0.012	0.020	<0.3	0.768	6.4	705
484-2	c:	0.161	0.797	0.031	0.012	>0.5	0.642	6.4	645
	r:	0.162	0.797	0.030	0.011		0.676	6.4	600
PE-85-									
157A	c:	0.360	0.602	0.033	0.005	<0.3	0.812	6.0	700
BK-70-									
323A	c:	0.144	0.808	0.024	0.023	<0.3	0.610	5.0	650
	r:	0.135	0.818	0.025	0.022		0.661	5.3	570

the southern part of the inlier. Some high temperature assemblages in this area are spatially related to the Taylor Brook gabbro complex. These include forsterite + calcite + spinel and wollastonite + salite + bytownite in carbonate rocks, and silica-depleted cordierite + garnet + andesine + hercynite-bearing migmatites derived from pelitic gneiss. These assemblages apparently delineate the thermal aureole of exposed parts of the intrusion.

Metamorphic temperatures have been estimated from the composition of coexisting garnet-biotite, garnet-orthopyroxene, garnet-cordierite, potassium feldspar-plagioclase, and clinopyroxene-orthopyroxene. These assemblages are commonly in disequilibrium, consequently temperature estimates for individual samples may be imprecise.

For example, only 24 of approximately 70 garnet-biotite-bearing samples from the inlier were found to contain matrix biotite with compositions sufficiently homogeneous to permit the reliable application of this thermometer. Despite problems of down-temperature re-equilibration and significant between-calibration discrepancies, the garnet-biotite thermometer can document relative regional temperature variations, particularly if textural controls on garnet-biotite compositions are considered (Indares and Martignole, 1985). The experimental calibration of Perchuk and Lavrent'eva (1983; R5) apparently provides the most precise and accurate results (Chipera and Perkins, 1988). Temperatures determined for mineral core compositions vary from about 615 to 700°C in the northeastern part of the inlier, to nearly 800°C farther to the southwest (Table 25).

Application of the garnet-orthopyroxene geothermometer (R6) to eleven samples of tonalitic and semipelitic gneiss provides a broad range of temperatures, even for samples taken within a small area. Temperatures determined using Sen and Bhattacharya's (1984) thermodynamic calibration range from 645 to 820°C for mineral core compositions; rim compositions yield temperatures up to 200°C lower (Table 22; Fig. 39). Lee and Ganguly's (1988) experimental calibration yields temperatures ranging from 715 to 870°C (core compositions). Anomalously high temperatures (875 and 922°C; Sen and Bhattacharya (1984) calibration) were derived from cordierite-bearing semipelite in which orthopyroxene and garnet are not in contact.

The most precise temperature estimates are provided by the garnet-cordierite thermometer (R7). For each sample, temperature estimates using calibrations by Thompson (1976), Holdaway and Lee (1977), and Perchuk et al. (1985) vary by ± 10 to 40°C, and only the results of the latter calibration are reported here (Table 23). Temperatures range from 530 to 705°C for core compositions, the higher temperatures being from the granulite terrane in the southwestern part of the inlier. Rim compositions give temperatures 40 to 80°C lower than cores. Pelitic gneiss flanking mafic rocks of the Taylor Brook gabbro complex yields a temperature of 765°C. Thermal effects related to this mafic pluton are considered in more detail below.

Exsolution features compromise the applicability of the two-feldspar geothermometer (Haselton et al., 1983); however, the reintegrated composition of fine bead perthitic microcline may be determined by using a defocused microprobe beam. Using this approach, four gneiss samples selected over a wide area yield temperatures ranging from 550 to 645°C, even in the southern samples. Down-temperature re-equilibration of feldspar compositions may influence the results of certain barometers, e.g., the 5 to 8 kbar pressures determined from garnet-orthopyroxene-plagioclase-quartz barometry should be regarded as minimum values.

Most calibrations of the two-pyroxene thermometer yield anomalously high results when applied to metamorphic rocks (cf. Bohlen and Essene, 1979; Bohlen et al., 1985). Davidson and Lindsley's (1985) calibration calculates the equilibrium two-pyroxene temperature, as well as the composition of the model low Ca pyroxene for a given clinopyroxene, thereby providing a semiquantitative means

Table 24. Compositional parameters and pressure estimates of coexisting garnet-plagioclase-sillimanite-quartz in pelitic gneiss.

	garnet				pl		
	X_{Mg}	X_{Fe}	X_{Ca}	X_{Mn}	X_{An}	Given *T(°C)	*P(kbar)
PE-85-157A	0.356	0.604	0.033	0.007	0.323	700	5.1
VO-86-164-3	0.251	0.717	0.011	0.021	0.151	700	3.8
355-6A	0.128	0.687	0.030	0.156	0.250	650	4.2
2279	0.372	0.594	0.026	0.008	0.305	675	4.1
BK-70-323A	0.209	0.748	0.027	0.016	0.269	615	3.0

*T estimated from garnet-cordierite or garnet-biotite thermometry of same or nearby sample.
*P after method of Goldsmith (1980) and Froese (1988).

of evaluating the extent of disequilibrium between coexisting pyroxenes. Since the equilibrium temperature of coexisting metamorphic pyroxenes is known to be inversely proportional to their wollastonite content (Lindsley, 1983), the author has compared X_{Wo} in model and analyzed orthopyroxenes with the temperatures determined by Davidson and Lindsley's (1985) method. Temperatures vary systematically; the highest result from pyroxene pairs in apparent disequilibrium (Fig. 40). In only 3 of 16 samples is the discrepancy in X_{Wo} less than 40 %; 2 of these samples yield temperatures of ca. 720°C. A significantly higher temperature (834°C) was determined for the third sample, adjacent to the TBGC. The relatively high temperature in this sample is interpreted to record the thermal imprint of the Taylor Brook gabbro complex.

Metamorphic fluids

The widespread preservation of graphite in pelitic and semipelitic gneiss testifies to elevated X_{CO_2} in metamorphic fluids accompanying high grade metamorphism of the gneiss complex. This is consistent with the high CO_2 contents in the channel fluids of cordierite from regionally metamorphosed rocks.

Interpretation

It is concluded from the thermobarometric data that high grade gneisses throughout the Long Range Inlier equilibrated at pressures of 5 to 8 kbar. Metamorphic temperatures, although less narrowly constrained, range from 550 to 700°C in the north to 700 to 800°C farther to the south (Fig. 41), consistent with the regional distribution of amphibolite and granulite facies assemblages. For the most

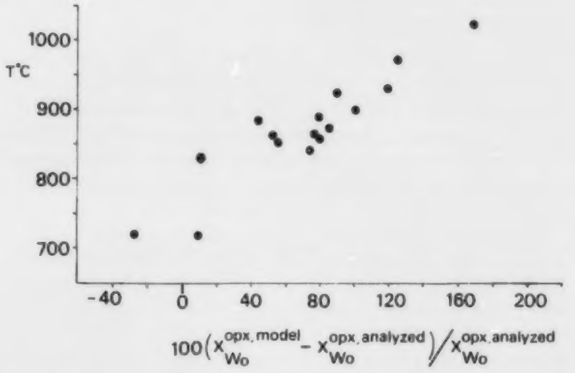

Figure 40. Results of two-pyroxene geothermometry (Davidson and Lindsley, 1985) from samples of the Long Range gneiss complex (chiefly tonalitic gneiss). See text for discussion.

Table 25. Compositional parameters and temperature estimates of coexisting garnet and biotite in quartzofeldspathic gneissic rocks of the Long Range Inlier. *Perchuk and Lavrent'eva (1983), for P = 6 kbar, and using a ternary garnet model for calculating Kd. Ti and Al^{vi} in biotite were calculated using an oxygen basis of 22.

	garnet				biotite			*T (°C)
VO-85-	X_{Mg}	X_{Fe}	X_{Ca}	X_{Mn}	X_{Mg}	Ti	Al^{vi}	
503	0.303	0.638	0.038	0.021	0.530	0.311	0.467	785
574	0.379	0.575	0.033	0.013	0.622	0.315	0.510	770
617	0.100	0.742	0.138	0.021	0.360	0.516	0.234	794
659-1	0.317	0.640	0.032	0.010	0.540	0.578	0.369	739
685	0.382	0.580	0.027	0.010	0.644	0.304	0.542	745
879	0.300	0.610	0.075	0.014	0.551	0.587	0.219	770
VO-86-								
111	0.206	0.698	0.074	0.022	0.514	0.590	0.132	680
271	0.296	0.649	0.043	0.012	0.578	0.552	0.210	723
279	0.262	0.684	0.038	0.016	0.557	0.506	0.276	700
291	0.254	0.686	0.048	0.012	0.562	0.478	0.261	706
451-2	0.319	0.654	0.008	0.019	0.640	0.393	0.366	675
484-2	0.161	0.797	0.031	0.012	0.461	0.370	0.606	643
825-2	0.128	0.779	0.047	0.046	0.438	0.349	0.350	619
2277-2	0.159	0.767	0.036	0.038	0.435	0.474	0.525	672
VO-87-								
157-2	0.259	0.643	0.077	0.020	0.518	0.764	0.090	755
232	0.173	0.585	0.190	0.052	0.465	0.706	0.092	729
BK-70-								
40B	0.239	0.696	0.045	0.019	0.587	0.337	0.642	648
323A	0.136	0.814	0.026	0.023	0.449	0.396	0.755	615

part, these assemblages have survived subsequent metamorphic events related to the emplacement (M_2) and deformation (M_3) of Grenvillian granitoid rocks, and polyphase recrystallization (M_4) during the Paleozoic. Mineral zoning patterns, particularly in garnet, nonetheless suggest polybaric down-temperature partial re-equilibration (to amphibolite facies) of the gneiss complex. This may be attributed either to uplift and cooling following the early high grade event, and/or to subsequent lower grade events (M_2 to M_4).

A comparison of mineral core-and-rim P-T data determined using the garnet-orthopyroxene(-plagioclase-quartz) thermobarometer indicates a fairly steep P-T-time path. These data define uplift curves for the inlier with slopes ranging from 9 to 19 bars/°C (Fig. 39), with a mean of 14 bars/°C. This result is attended by a high (but undetermined) error, resulting from thermobarometric calibration uncertainties, and from difficulties in establishing reliable petrographic and geochemical equilibrium criteria. In the present example, two points on the P-T-t curve have been estimated for each sample by "matching" core-core and rim-rim compositions of coexisting orthopyroxene and garnet (Fig. 39).

Implicit in this is the assumption that the relatively homogeneous ("plateau") cores of contiguous grains equilibrated during peak T conditions (probably at somewhat lower than the maximum pressure experienced by the rock). Mineral core compositions apparently equilibrated (or were quenched) at 6 to 8 kbar over a wide range of temperatures. Mineral rims were quenched in a relatively restricted P-T field (Fig. 39). Despite the range of P-T recorded by garnet and orthopyroxene compositions, the similarity of the dP/dT slopes defined by each sample supports the use of core and rim compositions in estimating the mean uplift curve of the inlier. The slope of the dP/dT curves depicted in Figure 39 is considerably steeper than

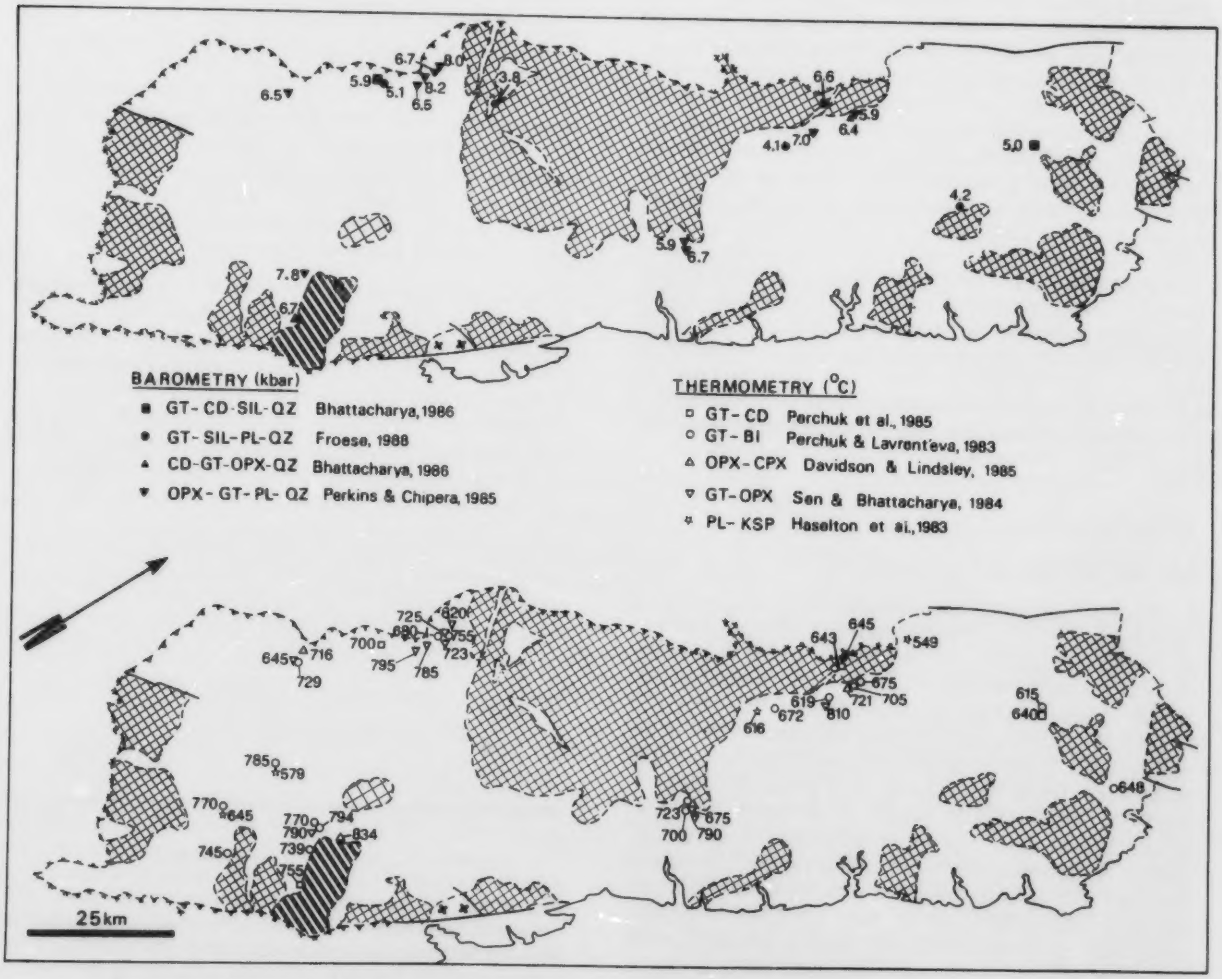
6.5
5.9
5.1
6.7
8.0
8.2
6.5
3.8
6.6
5.9
6.4
4.1
7.0
5.0
4.2
5.9
6.7
7.8
6.7
BAROMETRY (kbar)
■ GT-CD-SIL-QZ Bhattacharya, 1986
● GT-SIL-PL-QZ Froese, 1988
▲ CD-GT-OPX-QZ Bhattacharya, 1986
▼ OPX-GT-PL-QZ Perkins & Chipera, 1985
THERMOMETRY (°C)
□ GT-CD Perchuk et al., 1985
○ GT-BI Perchuk & Lavrent'eva, 1983
△ OPX-CPX Davidson & Lindsley, 1985
▽ GT-OPX Sen & Bhattacharya, 1984
☆ PL-KSP Haselton et al., 1983
645
716
729
700
795
785
725
820
680
755
723
643
645
549
675
619
672
810
721
705
616
615
640
785
579
648
770
645
770
794
790
834
739
745
755
723
675
700
790
25km

Figure 41. Results of P-T determinations in the Long Range Inlier. Pluton symbols: small square grid-equigranular or megacrystic granite; large square grid-charnockite or mesocratic granite; diagonal lines-gabbro; crosses-megacrystic granite (Acadian). Abbreviations as in Appendix II.

that determined for many other granulite terranes (e.g., the Adirondacks, dP/dT = 2 to 5 bars/°C; Bohlen et al., 1985; the Disappointment Hill complex (Newfoundland), dP/dT ~5 bars/°C; Owen and Currie, in press), and indicates relatively rapid exhumation of the Long Range Inlier during the Middle to Late Proterozoic and/or the effects of a late Grenvillian (ca. 978 Ma; Pb-Pb, titanite, H. Baadsgaard, pers. comm., 1989) tectonothermal overprint. Although the Adirondack massif apparently underwent near isobaric cooling, other parts of the Grenville Province show steep dP/dT curves similar to that determined for the Long Range. For example, Anovitz et al. (1988) report dP/dT values of 15 bar/°C for the Central Gneiss Belt in Ontario, and extremely rapid uplift (nearly isothermal) has been determined for sapphirine-bearing gneiss in the Wilson Lake area of central Labrador (Currie and Gittins, 1988). In the latter case, at least, rapid uplift may be related to Grenvillian thrusting.

An unresolved problem concerns the P and T conditions determined for garnet-, cordierite-, sillimanite-, and quartz-bearing assemblages. Core and rim compositions of contiguous cordierite and garnet in two of these samples define cooling curves with a shallow negative slope (dP/dT = -2 to -4 bars/°C). There is no compelling reason for rejecting these data and accepting instead the results of garnet-orthopyroxene-plagioclase-quartz thermobarometry. However, the results of garnet-cordierite barometry are viewed with caution, owing to the sensitivity of these equilibria to P_{H_2O}.

The timing of uplift is poorly known. An upper limit is provided by emplacement of the 615 Ma (Kamo et al., 1989) Long Range dykes, which acted as feeders to flows in the Strait of Belle Isle area, and indicate rifting of basement at shallow depth in the latest Proterozoic. Crystalline rocks on both sides of the Strait of Belle Isle thus occupied similar crustal levels, at least until the emplacement of the Long Range dykes.

Metamorphism 2: Syn-plutonic stage

Age and metamorphic grade

Evidence for a regional metamorphic event accompanying emplacement of the Grenvillian plutonic rocks is provided by the recrystallization of the nearby host rocks. Only lithologies of the appropriate bulk composition (notably pelites) appear to have been substantially affected. The effects of Grenvillian thermal metamorphism are most evident in the northern part of the inlier, and include (1) the formation of andalusite in pelite near the Leg Pond pluton (cf. Bostock, 1983, Fig. 42), and (2) the occurrence of muscovite (at least locally formed at the expense of sillimanite) in pelite adjacent to the Hooping Harbour satellite pluton. The spatial association of these assemblages with the Grenvillian plutons demonstrates that they are bona fide Grenvillian thermal effects. Bostock (1983) noted that the presence of late andalusite adjacent to plutons in the amphibolite terrane is diagnostic of low pressure (Abukuma-type) metamorphism. The replacement of early (M_1) sillimanite by white mica near the Hooping Harbour satellite pluton indicates recrystallization at conditions below the second sillimanite isograd (e.g., lower amphibolite facies).

Metamorphic conditions

Metamorphic conditions have been estimated in the thermal aureole of the Hooping Harbour satellite pluton. Pelite in the 250 m wide paragneiss sequence flanking the western margin of the pluton differs from regionally metamorphosed aluminous gneiss only in the presence of muscovite. It coexists with garnet, biotite, plagioclase (albite to oligoclase), quartz, garnet, microcline, and metastable(?) sillimanite. It is assumed in the following discussion that garnet and biotite in these rocks re-equilibrated, at least in part, due to the thermal effects of the adjacent pluton. Similar effects have been documented in high grade pelitic gneiss adjacent to granitoid rocks elsewhere (e.g., the thermal aureole of the Mistastin batholith; Owen, 1989).

Garnet-biotite thermometry applied to a suite of samples collected across the pelite sequence yields T estimates which decrease systematically from over 700°C to background values of 600 to 650°C (typical of the amphibolite terrane) over a short distance from the pluton (Fig. 42). The Hooping Harbour satellite pluton thus appears to have a narrow thermal aureole. From this, and given the paucity of obvious country rock recrystallization elsewhere in the inlier, it is apparent that the gneiss complex was not appreciably modified by widespread granitic plutonism.

It should nevertheless be noted that several variables control the extent of thermal metamorphism (e.g., composition and volume of individual intrusions, temperature of the country rock at the time of emplacement, and mechanism(s) of heat transfer). These variables, particularly intrusion size, may vary considerably. Furthermore, thermal aureoles in mineralogically-simple quartzofeldspathic gneiss may be cryptic, and may have been partly obliterated by subsequent metamorphic events (i.e., M_3 or M_4 metamorphism).

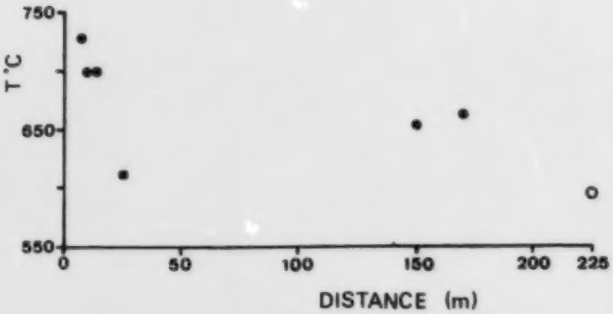

Figure 42. Variation of garnet-biotite temperatures (Perchuk and Lavrent'eva, 1983) across a metapelite sequence flanking the Hooping Harbour satellite pluton. Open symbol: temperature for high-Mn garnet-bearing metaquartzite.

The metamorphic aureole of the Taylor Brook gabbro complex

The Taylor Brook gabbro complex is partly enclosed by a high grade supracrustal sequence composed of marble and calc-silicate rock, pelitic gneiss, and minor quartzite. The mineralogy of the aluminous gneiss is atypical of pelite occurring elsewhere in the inlier, and is interpreted to record thermal effects of the adjacent mafic pluton (cf. Owen, in press). Salient features of the pelites and marbles introduced above are described in more detail forthwith.

Thermally metamorphosed pelitic gneiss

Pelites separate carbonate rocks from the gabbro along its southwestern margin. Pelite near the southwestern flank of the gabbro (location 1, Fig. 43) is depleted in quartz and sillimanite, and contains abundant cordierite. The contact with the gabbro is exposed on the old woods road along the Upper Humber River. A 2 m wide band of orthopyroxene-, garnet-, and biotite-bearing tonalitic gneiss (unit Ptn) separates the pelite from the gabbro. The gabbro next to the gneiss contains relict olivine and clinopyroxene kernels within green and brown amphibole; subophitic texture is preserved despite this alteration.

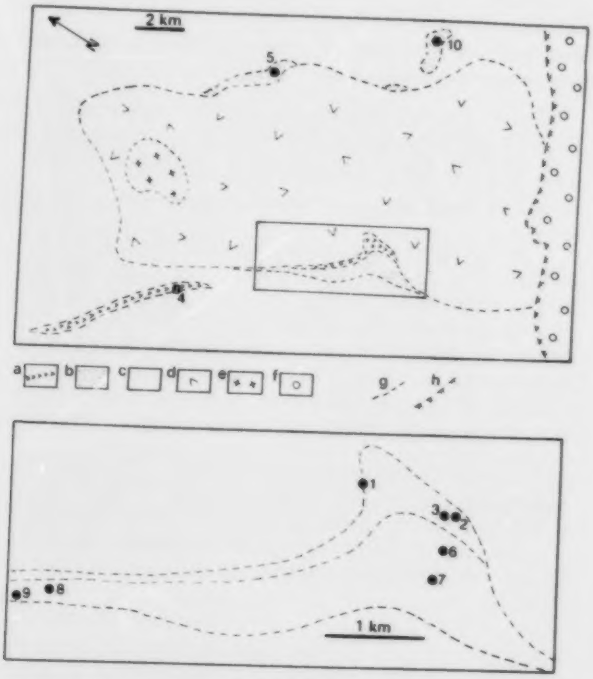

Figure 43. Sketch map of high grade pelitic gneiss and metacarbonate rocks near the Taylor Brook gabbro complex. Numbers refer to sample localities discussed in text. Symbols: a-pelitic gneiss (unit Ppn), b-metacarbonate rock (Pcs), c-granitic to granodioritic gneiss (undifferentiated), d-gabbro (Pgb), e-pegmatitic gabbro (Ppgb), f-conglomerate (Deer Lake Basin), g-geological contact (approximate), h-unconformity.

The pelite at this exposure is migmatitic (Fig. 44A). The diffuse leucocratic component is rich in andesine (An_{40-45}), and is studded with large garnet crystals and subordinate biotite. The plagioclase forms an interlocking network of (sub)idiomorphic crystals, and resembles an igneous phase. The idiomorphic shape of the garnets also suggests, but does not prove, an igneous origin. The dark blue-grey mesosome contains cordierite, biotite, andesine, spinel, magnetite, and rare andalusite. The cordierite forms relatively large (1 mm) xenomorphic to subidiomorphic grains in texturally-stable contact with garnet, and fine grained mosaics dusted with hercynite and magnetite. The andalusite is riddled with biotite, and appears to be metastable. Its presence nevertheless suggests that this is a low pressure thermal aureole.

One gneissic sample (VO-85-024) is mineralogically intermediate between the pelitic and tonalitic rocks. This sample, which contains abundant cordierite (Fig. 44B) and andesine (An_{40-45}), is layered with alternating garnet-rich and orthopyroxene-rich bands. Magnetite and hercynite cloud matrix cordierite. Optical data suggest that the cordierite is anhydrous (the cordierite is optically (+), with $2V_x$ near 90°; S. Perreault, pers. comm., 1987). This sample contains accessory quartz, which forms amoeboid patches interstitial to plagioclase. By analogy with similar microstructures described in anatectic migmatite (Vernon and Collins, 1988), this texture is interpreted as evidence for an igneous origin for at least some of the phases mentioned above, and nearly certainly for the plagioclase and quartz. This is consistent with the discordant nature of the leucocratic segregations (Fig. 44A), and the near elimination of quartz in outcrops near the gabbro (see Grant, 1985).

If migmatite near the gabbro is indeed anatectic, then K- and Si-rich eutectic liquids must have been removed, leaving fractionated, plagioclase-rich leucosomes. Spinel and quartz (where present) in the mesosome are not seen in contact. This probably reflects the Zn-poor nature of the spinel (<2 weight percent ZnO), since Zn stabilizes spinel in the presence of quartz at relatively low temperatures (Montel et al., 1986).

Pelite in an outcrop approximately 50 m from the gabbro (location 2, Fig. 43) is a layered quartzose rock with abundant cordierite and plagioclase (An_{28}). The rock is best described on a domainal scale. Quartz-rich layers (domain A) with plagioclase (An_{28}), cordierite, and fanning clusters of muscovite oriented nearly perpendicular to the foliation, are separated by relatively fine grained domains (domain B) containing foliation-parallel sillimanite, ragged flakes of biotite, chlorite, and muscovite, and minor plagioclase and quartz. In places, veins of the domain (A) assemblage cut the foliation which is defined in part by sillimanite. Biotite and, to a lesser extent, sillimanite appear to be metastable, being replaced by chlorite and muscovite. Well-formed cordierite in domain (A) appears to be in stable contact with sillimanite in adjacent domain (B); however, it is noteworthy that the cordierite- and sillimanite-rich domains are spatially distinct.

Textural criteria suggest that biotite and cordierite are replaced by muscovite and chlorite, possibly by the quartz-generating retrograde reaction:

$$\mathrm{cd + bi + (4\text{-}n)H_2O = mu + chl + 2qz} \qquad (1)$$

where n is the number of moles of water in cordierite.

Cordierite coexists with microcline, sillimanite, and accessory magnetite and hercynite in granoblastic pelite 100 m from the gabbro (location 3, Fig. 43). The rock is nearly devoid of phyllosilicates, containing only traces of biotite. This is a texturally-stable assemblage lacking evidence for specific reaction relations. However, the paucity of biotite in this sample, together with the absence of quartz and the embayed appearance of sillimanite, imply the quartz-consuming reaction:

$$\mathrm{6sil + 2bi + 9qz = 3cd + 2Ksp + (2\text{-}3n)H_2O} \qquad (2)$$

The persistence of sillimanite in the sample implies that the reaction was arrested due to the depletion of quartz and biotite. The presence of this quartz-deficient sample some 50 m from quartz-rich pelite at location 2 is somewhat enigmatic. It is possible that the gabbro is relatively close to location 3 as measured in a vertical section.

Texturally-unstable sillimanite and garnet coexist in quartzofeldspathic pelite at locality 4, approximately 0.8 km from the gabbro. Here, ragged sillimanite and garnet crystals are enclosed and separated by fine grained mosaics of cordierite and hercynite (Fig. 44C). Well-formed garnet is preserved where enclosed by plagioclase (An_{33}), perthitic microcline, or quartz. Ovoid patches of cordierite and hercynite are interpreted to coincide with former garnet (± sillimanite) sites. Clusters of subidiomorphic matrix biotite appear to stably coexist with cordierite.

These relations demonstrate that the garnet and sillimanite compose part of an early high grade assemblage (i.e., M_1) that was overprinted by a reaction of the type:

$$\text{garnet + sillimanite = spinel + cordierite} \qquad (3)$$

This reaction has a shallow positive slope in P-T space (Harris, 1981); spinel + cordierite is the lower pressure (and/or higher temperature) assemblage. Although reaction (3) may proceed by an isobaric temperature increase, an isothermal pressure decrease, or any other intermediate path, it is considered here to be related to thermal metamorphism by the gabbro, since the assemblage spinel + cordierite is diagnostic of pelitic rocks adjacent to the intrusion.

Two conclusions may be readily drawn from the pelitic assemblages: (1) the Taylor Brook gabbro complex has a narrow high grade thermal aureole, perhaps less than 1 km in width; and (2) earlier high grade assemblages are overprinted within the aureole. The latter statement implies that

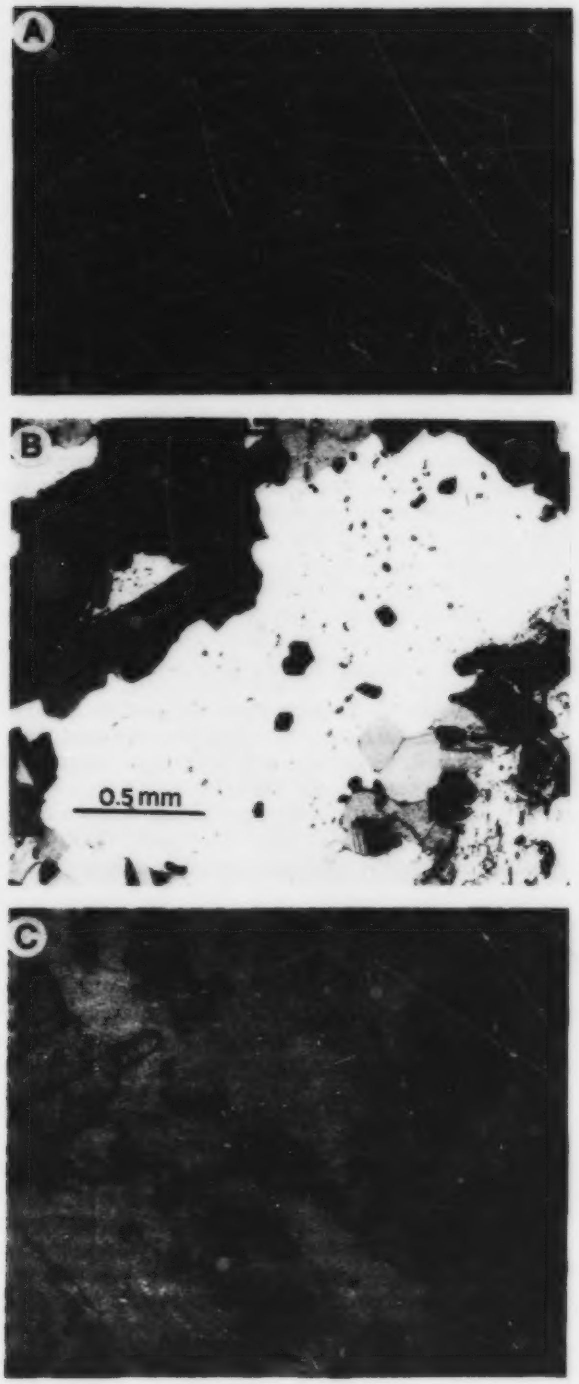

Figure 44. Photographs of pelitic gneiss near the Taylor Brook gabbro complex. A. Migmatitic aspect of pelitic gneiss in contact with the gabbro; B. Large cordierite porphyroblast (c) with hercynite and magnetite "inclusions" (sample VO-85-024, taken a few metres from contact with gabbro; crossed nicols); C. Photomicrograph showing textural evidence for the replacement of early (pre-gabbro) sillimanite (s) and garnet (g) by cordierite (c) and hercynite-rich spinel (h) associated with the thermal aureole of the gabbro (sample VO-85-659-1, taken 0.8 km from gabbro; plane polarized light). GSC photos 204932 44A to C.

the Taylor Brook gabbro complex postdates the M_1 metamorphic event. The heat source of the granulite facies terrane therefore remains problematic.

This need not present serious difficulties for the interpretation of the thermobarometric data reported above. The data appear to suggest that the amphibolite-granulite transition in the Long Range gneiss complex is approximately isobaric. However, given the imprecision and inaccuracy of current geobarometers (ca. 1-2 kbar), the narrow range of calculated paleopressures (5-8 kbar) may be misleading. The actual spread of values may be closer to 5 kbar than 3 kbar. Differential uplift of the granulites relative to the amphibolite terrane thus remains a distinct possibility. The thermobarometric data therefore do not conclusively favour either a magmatic underplating model (Bohlen, 1987) or more traditional structural depth—fluid fugacity controls on high grade metamorphism (Edwards and Essene, 1988) in the area. Regardless of the causes of high grade metamorphism, it should be noted that paleopressures determined from the Long Range gneiss complex fall in the typical range determined for granulite terranes worldwide (Bohlen and Lindsley, 1987).

Metamorphism of the carbonate sequence

As noted earlier, carbonate rocks sensu stricto in the inlier are apparently restricted to the supracrustal sequence that partially encloses the Taylor Brook gabbro complex. Consequently, comparison with marbles bearing only a regional metamorphic imprint is not possible. Furthermore, pelite separates the carbonate sequence from the gabbro along its southwestern margin, where exposure is best. Therefore, the attribution of particular mineral assemblages in the marble to thermal metamorphism is unwarranted except in the specific case where the contact between the gabbro and the carbonate sequence is exposed.

The carbonates are layered rocks, and include both "pure" and "impure" variants (Fig. 45A). The relatively pure marbles are calcite-rich rocks, with variable concentrations of forsterite, diopside, phlogopite, and accessory graphite. The impure calc-silicate rocks are, with two notable exceptions, mineralogically similar, but contain higher proportions of these silicate minerals, particularly phlogopite.

Relatively high temperature (and/or low P_{CO_2}) calc-silicate assemblages include (1) wollastonite-salite-bytownite (location 5, Fig. 43), and (2) forsterite-spinel-(calcite, phlogopite) (locations 6 to 9, Fig. 43; Fig. 45B,C). These assemblages occur at some distance (up to several hundred metres) from the nearest exposure of the Taylor Brook gabbro complex, consequently it is not known whether or not they predate emplacement of the gabbro. Low temperature assemblages (e.g., dolomite + chlorite) occur locally in marble exposed 2 km east of the gabbro (location 10, Fig. 43). These outcrops were previously portrayed as an outlier of Paleozoic cover rocks (Hibbard, 1983a). However, the local presence of higher temperature assemblages (e.g., diopside-phlogopite-microcline) in these outcrops invites correlation with the nearby marble of the gneiss complex, and suggests that the low grade assemblages result from a Paleozoic metamorphic overprint. Alternatively, marbles east of the gabbro may represent the remnants of a sedimentary sequence postdating the gneisses and predating the gabbro. Evaluation of this possibility is not possible since contact relations with the surrounding mafic and quartzofeldspathic gneiss are not exposed.

Contact relations with the gabbro have not been observed; however, the marble sequence is cut by narrow (≤ 1 m), northeast-trending mafic dykes exposed near the woods road following the northern bank of the Upper Humber River (location 9, Fig. 43). The orientation (N20°E) and mineralogy of these dykes suggest that they are apophyses of the Taylor Brook gabbro complex. The primary mineralogy of these dykes has been considerably modified by reaction with the country rock. The relict igneous assemblage includes olivine (Fo_{75}) and calcic plagioclase phenocrysts (An_{82}); augite appears to have been completely replaced by amphibole, a feature noted in nearby outcrops of the Taylor Brook gabbro complex. Groundmass plagioclase is more sodic (An_{30}) than the phenocrysts. Near the contact with the marble, one dyke contains hercynitic spinel enclosed by oligoclase (An_{28}) (and/or by scapolite, carbonate, and phlogopite). A narrow (1-3 mm) reaction rim containing fibroradial forsterite (Fig. 45D) and accessory titanite is developed near the dyke-carbonate interface. Diopside forms a reaction rim adjacent to another mafic dyke in the same outcrop. The carbonate country rock consists of calcite (± dolomite), forsterite, diopside, common spinel, phlogopite, and/or graphite.

The available data suggest that similar high temperature mineral assemblages developed in the carbonate sequence both prior to (i.e., M_1) and during emplacement of the gabbro. The similarity of the metamorphic grade of both events hampers their distinction.

Metamorphism 3: Post-plutonic stage

Age and metamorphic grade

Tectonic fabrics in many of the Grenvillian granitoid plutons are defined by aligned potassium feldspar megacrysts (where present), quartz lenses and ribbons, and aggregates of biotite, hornblende, and/or epidote. Plagioclase in these deformed granites is oligoclase (ca. An_{25}). Together with the mafic mineralogy, this implies that deformation accompanied medium grade metamorphism (i.e., lower amphibolite facies). These fabrics are attributed to the 978 Ma tectonothermal event identified by H. Baadsgaard (pers. comm., 1989).

Some plutons in the northeastern part of the inlier (e.g., the Hooping Harbour pluton) contain greenschist facies assemblages which may be related either to Grenvillian or Paleozoic deformation (H.H. Bostock, pers. comm., 1989).

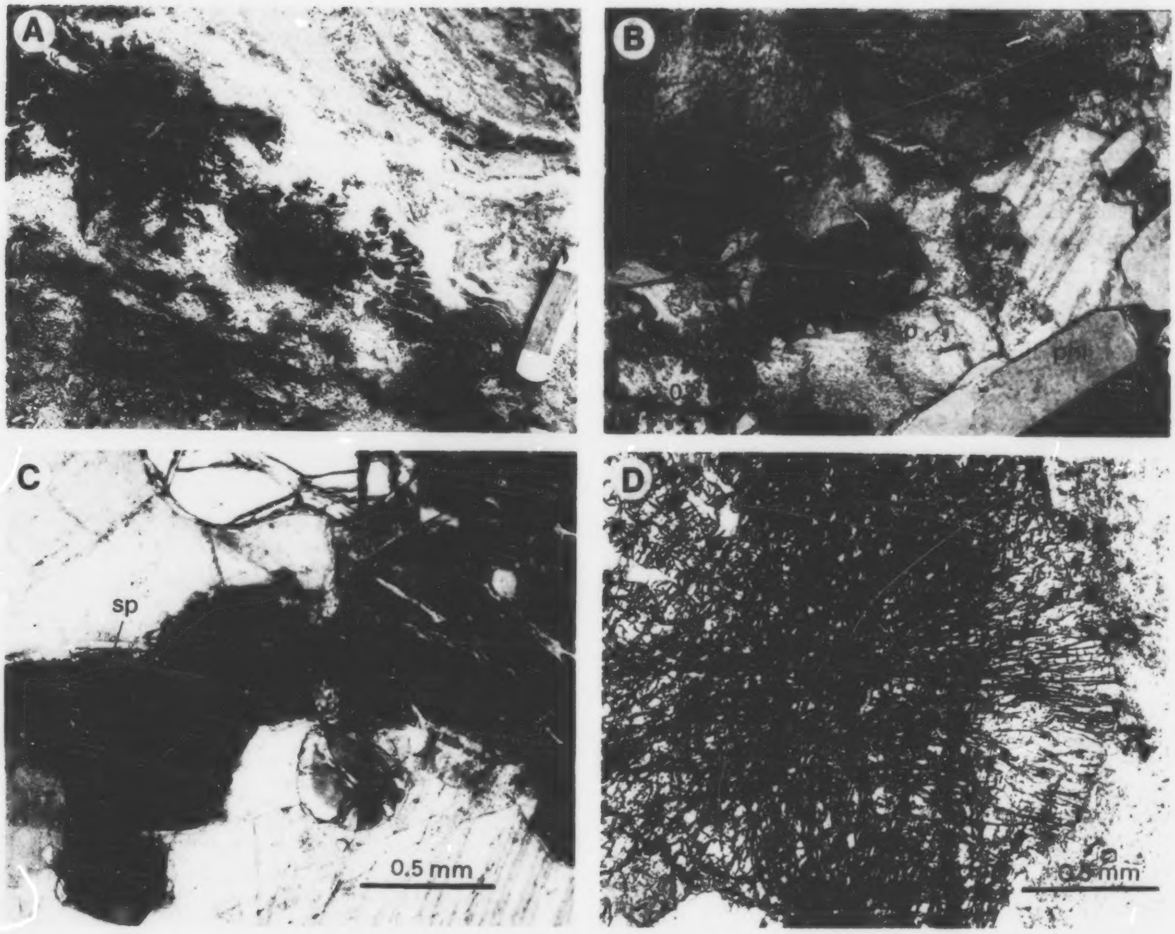

Figure 45. Photographs of calc-silicate rocks from the marble sequence near the southwestern flank of the Taylor Brook gabbro complex. A. Phlogopite-rich calc-silicate gneiss (dark layer) in impure marble; B. forsterite (fo), spinel (sp), and phlogopite (phl) in the adjacent carbonate rock (sample VO-87-001B, see (D); plane polarized light); C. spinel (sp) and forsterite (fo) in calc-silicate rock sampled 1 km from the gabbro (sample VO-85-074-3; crossed nicols); D. photomicrograph showing fibroradial forsterite near contact between marble and mafic dyke (sample VO-87-001B; plane polarized light). GSC photos 204932 45A to D.

Metamorphic conditions

Temperatures associated with M_3 metamorphism can be estimated from tectonic fabrics comprising T-sensitive assemblages which are known (or suspected) to predate emplacement of the Long Range dykes. Only one suitable candidate has been identified. A composite tectonic fabric occurs along the deformed and "retrograded" (to amphibolite facies) southern boundary of coronitic charnockite (unit Pcg) of the Potato Hill pluton (see Fig. 26F). Here, brownish-green charnockite containing orthopyroxene mantled by hornblende, quartz, and garnet is recrystallized to a rose-coloured gneissic assemblage comprising hornblende, biotite, garnet, oligoclase, quartz, microcline, and ilmenite. Owen (1986a) mapped the southern edge of the Potato Hill pluton as a foliated megacrystic granite; subsequent mapping by the author immediately to the north revealed that this rock was derived from the charnockite.

Application of the garnet-hornblende (Graham and Powell, 1984; Powell, 1985) and garnet-biotite (Perchuk and Lavrent'eva, 1983) geothermometers to one sample of the deformed charnockite (Table 26) yields temperatures of 705°C and 666°C, respectively. This is the only available estimate of M_3 metamorphic temperatures. Assemblages useful in determining metamorphic pressure have not been identified.

Metamorphism 4: Post-Long Range dyke stage

Textural overprinting relations amongst metamorphic minerals in the Long Range dykes demonstrate the involvement of parts of the inlier in polyphase Paleozoic orogenesis. Low metamorphic grade (greenschist to epidote amphibolite facies) of these events is confirmed by the mineralogy of deformed Cambro-Ordovician clastic rocks (i.e., two-mica-quartz-albite schist) and spatially associated mafic schist (chlorite-epidote-albite) near the southeastern flank of the inlier (Owen, 1986a; Owen and Erdmer, 1986).

Estimation of Paleozoic metamorphic conditions is hampered by the apparent absence of mineral assemblages suitable for quantitative thermobarometry. However, temporal variations in metamorphic grade may be qualitatively evaluated from the composition of calcic amphiboles (and coexisting minerals) in the Long Range dykes, and, to a lesser extent, from the mineralogy of Paleozoic rocks deformed near the southeastern margin of the inlier. The significance of the amphibole-bearing assemblages in the Long Range dykes will be considered first.

Compositionally-distinct calcic amphiboles trace the influence of Paleozoic metamorphism of the Long Range dykes. As many as three calcic amphiboles coexist in the metamorphosed dykes. In these samples, early olive-brown hornblende is rimmed by optically-continuous green magnesio- to ferro-hornblende (see Fig. 32C), or is enclosed by fibrous actinolite, with an outer rim of green hornblende or actinolitic hornblende. In some samples, including those containing primary augite, brown actinolite with elevated TiO_2 contents (to 1.5%) is interpreted to coincide with former brown hornblende sites. In places, actinolite replaces twinned clinopyroxene, and is mantled by green hornblende (see Fig. 32D).

Table 26. Garnet, biotite, and hornblende analyses for deformed coronitic charnockite (unit **Pcg**) of the Potato Hill pluton (sample VO-87-039-2). Abbreviations as in Appendix II. Total Fe as FeO.

	gt	bi	hbl
SiO_2	36.88	33.64	38.42
TiO_2	0.08	5.13	1.68
Al_2O_3	20.24	14.83	11.81
FeO	27.99	29.52	27.43
MnO	5.55	0.28	0.52
MgO	0.73	2.93	2.49
CaO	8.44		11.48
Na_2O		0.10	1.46
K_2O		9.22	1.40
	99.9	95.6	96.7
Si	2.989	5.421	6.225
Al^{iv}	0.011	2.579	1.775
Al^{vi}	1.923	0.239	0.481
Ti		0.622	0.205
Fe	1.897	3.979	3.717
Mn	0.381	0.038	0.071
Mg	0.088	0.704	0.601
Ca	0.733		1.993
Na		0.031	0.459
K		1.896	0.289

The three texturally-distinct calcic amphiboles are also compositionally distinct (Table 27). The olive-brown and green hornblendes straddle the boundary between the magnesio- and ferro-hornblende fields on Leake's (1978) diagram (Fig. 46). Their contrasting colour reflects higher Ti in the olive-brown hornblende (0.09-0.16) than the green hornblende rims (≤0.01; Fig. 47). Compared with the contiguous olive-brown hornblende core, the green hornblende is consistently less siliceous with similar or lower Mg/(Mg+Fe) (Fig. 46). The green hornblende rims mantling actinolite range from magnesio-hornblende to ferro-tschermakite, and show a wider range of Si contents for given Mg/(Mg+Fe) than their counterparts mantling olive-brown hornblende (Fig. 46).

These textural criteria indicate the sequential crystallization of calcic amphiboles commencing with olive-brown hornblende, then actinolite, and finally green hornblende. In low strain domains the amphiboles typically coexist with plagioclase similar in composition to igneous plagioclase preserved in the western dykes. Plagioclase core compositions range from An_{49} to An_{62}; some zoned grains are present with rim compositions of An_{14} to An_{33}. Owing to their calcic compositions, these are considered to be relict igneous grains, although their sodic rims probably reflect a metamorphic overprint since they are more sodic than the rims of zoned plagioclase (ca. An_{39}) in the western (igneous) dykes. The zoned plagioclase coexists in some samples with untwinned grains ranging in composition from An_{24} to An_{43}. Albite occurs in some samples from dyke 214 (Fig. 31).

Steeply-dipping, northeast-trending planar fabrics are locally developed in the eastern dykes and their host rocks, notably in dykes 214, 669, and 702 (Fig. 31). The mineralogy of the schistose dykes is similar to their low-strain equivalents except for the more extensive replacement of ilmenite by titanite. Variably-deformed gabbro in dyke 214 has been described in detail by Bellefontaine (1987). The overall mineralogy of this dyke indicates that peak strain occurred near the greenschist-amphibolite facies transition. C-S fabrics (Fig. 32A,B) and retort-shaped amphibole lozenges developed in a narrow (2 m wide) mylonite zone, which developed in the western chilled margin in this dyke, suggest that peak strain was associated with normal faulting (west side down). No kinematic indicators were observed in other deformed dykes, consequently it is not known if ductile normal faults are characteristic of the southeastern margin of the inlier as a whole.

Balanced reactions representing the sequential crystallization of calcic amphiboles are presented in Table 28. Initial recrystallization of the dykes yielded olive-brown magnesio/ferro hornblende, quartz, relatively sodic plagioclase, and an apparent excess of MgO and CaO (reaction 1, Table 28). Ilmenite and large calcic plagioclase grains in these samples are interpreted to be relict igneous phases. Subsequent recrystallization of the dykes involved arrested reactions yielding actinolite, albite (coexisting with relict igneous plagioclase), and titanite (enclosing relict ilmenite) (reaction 2), and later, during the high strain event, green hornblende and actinolitic hornblende, oligoclase, and titanite (reaction 3). Relics of earlier reactions preserved in the schistose rocks include olive-brown hornblende and actinolite. Epidote accompanies the product assemblages of reactions 2 and 3, but cannot be modelled here because of indeterminate ferric iron in the microprobe analyses.

The available data demonstrate that large tracts of the inlier were recrystallized during the Paleozoic. The polyphase nature of Paleozoic orogenesis is recorded in metastable mineral assemblages preserved in both deformed and undeformed Long Range dykes. However, apart from steeply-dipping, north- to north-northeast-trending schistose fabrics near White Bay, recognition of Paleozoic features within the country rock remains problematic.

Several workers have demonstrated that amphibole compositions are sensitive to changes in metamorphic P-T. Given the crystal-chemical complexity of amphiboles, those compositional parameters that are sensitive to P and/or T, but which are independent of the normalization scheme used to recalculate the mineral formula (cf. Robinson et al., 1982) are particularly useful. Hynes (1982) applied many of these criteria to amphiboles from known low and medium pressure terranes, and concluded that the Ti/Al(total) ratio is the most reliable monitor of metamorphic pressure. It should be noted that while these criteria are useful in tracing the evolving P-T history of a rock, they can only be used to quantify parts of the P-T-t path if at least one generation of amphibole is part of a thermobarometrically-calibrated assemblage.

The relatively titaniferous composition of the earliest amphibole (olive-brown hornblende) suggests crystallization at relatively low pressure (Spear, 1981; Hynes, 1982). The olive-brown hornblende was superseded first by a period of static (low strain) low grade metamorphism

Table 27. Mean microprobe analyses of metamorphic and relict igneous minerals from the Long Range dykes. n = number of analyses.

	1.	2.	3.	4.	5A.	5B.	6.	7.	8.	9.	10.
SiO_2	46.12	52.53	44.37	53.18	57.82	62.40	41.35	36.98	31.48	24.99	62.55
TiO_2	1.36	0.76	0.22	0.31			0.05	1.93	36.85	0.07	
Al_2O_3	6.38	3.02	13.14	3.82	26.47	25.01	23.77	16.75	2.02	20.24	23.20
FeO*	23.67	15.18	18.52	13.91	0.52	0.27	10.84	20.93	1.07	24.08	1.25
MnO	0.35	0.23	0.26	0.25			0.11	0.07	0.27		
MgO	7.87	13.27	7.91	13.44				9.38	0.23	15.78	
CaO	10.31	12.09	11.68	11.72	9.00	6.00	23.08		22.57		4.89
Na_2O	0.91	0.32	1.12	0.35	6.39	8.45		0.21		0.08	8.08
K_2O	0.63	0.06	0.47	0.10	0.11	0.08		8.90			0.38
	97.6	97.5	97.7	97.7	100.31	102.2	99.2	95.2	94.2	85.5	100.6
n =	12	14	4	3	4	4	2	1	1	1	
Oxygen basis:	23	23	23	23	8	8	13	22	20	36	
Si	7.085	7.670	6.639	7.721	2.587	2.714	6.252	2.827	3.292	5.390	2.757
Al^{iv}	0.915	0.330	1.361	0.279	1.396	1.282	—	1.173	0.250	2.610	1.205
Al^{vi}	0.240	0.190	0.957	0.375			4.239	0.336		2.535	
Ti	0.157	0.083	0.025	0.034			0.006	0.111	2.898	0.010	
Fe	3.041	1.854	2.318	1.689	0.019	0.010	1.371	1.338	0.094	4.344	0.045
Mn	0.046	0.028	0.033	0.031			0.015	0.005	0.002	0.049	
Mg	1.802	2.888	1.764	2.908			—	1.069	0.036	5.072	
Ca	1.697	1.892	1.873	1.823	0.431	0.280	3.741		3.090		0.230
Na	0.271	0.091	0.325	0.099	0.554	0.713		0.031	0.042	0.035	0.780
K	0.123	0.011	0.090	0.019	0.006	0.004		0.868			0.021

* Total iron as FeO.

1. brown/olive-brown hornblende
2. actinolite
3. green fabric-forming hornblende
4. green fabric-forming actinolitic hornblende
5A. plagioclase phenocryst (core)
5B. plagioclase phenocryst (rim) and matrix plagioclase
6. epidote
7. biotite
8. titanite
9. chlorite
10. fabric-forming plagioclase

(greenschist facies) represented by actinolite, and subsequently by the formation of green hornblende during a period of dynamic recrystallization (epidote amphibolite facies). This generalized interpretation is supported by various normalization-dependent plots, constructed such that amphibole compositions plotting near the origin reflect relatively low grade metamorphic conditions. For example, the Al^{iv} versus $(Na+K)^A$ diagram (Fig. 48; cf. Triboulet and Audren, 1988, Fig. 3 and 4) suggests that the youngest amphibole (green hornblende) is also of the highest grade.

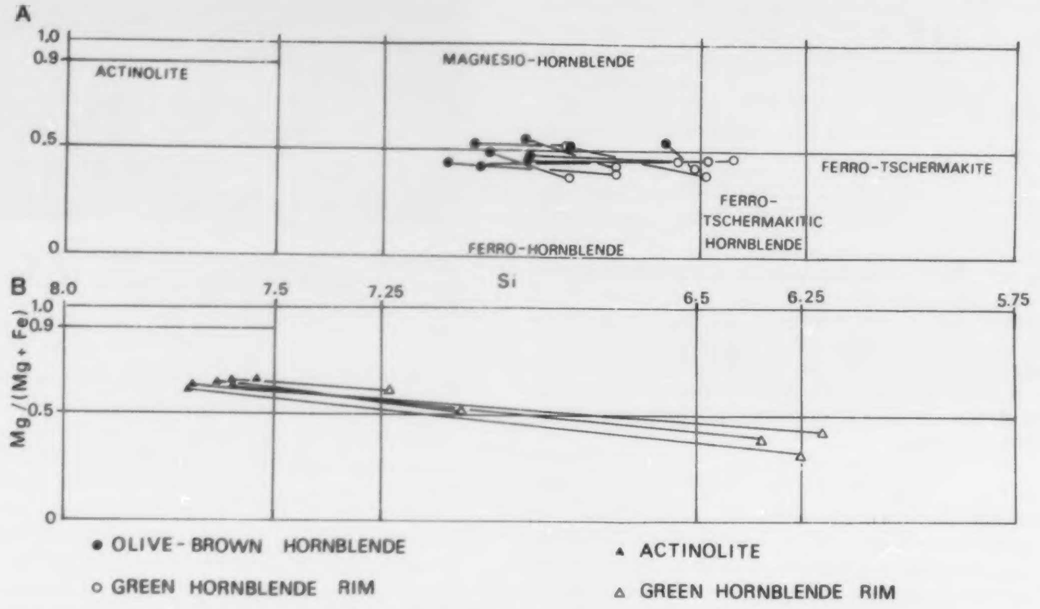

Figure 46. Nomenclature of calcic amphibole from dyke 214 (see Fig. 31). Tie-lines connect contiguous olive-brown and green hornblende in (A), and actinolite and green hornblende in (B). Fields after Leake (1978).

Table 28. Reactions illustrating the sequential metamorphic history of the Long Range dykes. The reactions were balanced using mean mineral compositions (Tables 12 and 27).

[1] cpx + 1.2 pl(1) + 0.1 FeO* =
0.7 hbl(1) + 1.2 pl(2) + 0.2 qz + 0.1 MgO + 0.1 CaO [pl(1)]

[2] hbl(1) + 9.1 qz + 6.0 pl(2) + 4.0 ilm + 2.7 CaO + 2.0 MgO =
15.2 act + 4.9 ti + 4.8 pl(4) [ilm, hbl(1), pl(1)]

[3] act + 0.4 pl(1) +0.03 ilm =
0.3 hbl(2) + 0.8 hbl(3) + 0.3 pl(3) + 0.04 ti + 0.01 qz [hbl(1), act]

* Total iron as FeO.

Cpx — igneous augite; pl(1) — rim composition, plagioclase phenocrysts (An_{39}); pl(2) — matrix plagioclase in low-strain metamorphosed dykes (An_{28}); pl(3) — albite (An_5); pl(4) — fabric-forming plagioclase (An_{24}); qz — quartz; hbl(1) — olive-brown magnesio/ferro hornblende; act — actinolite; ilm — ilmenite; hbl(2) — fabric-forming hornblende; hbl(3) — fabric-forming actinolitic hornblende; ti — titanite. [ ] — relict metastable phases.

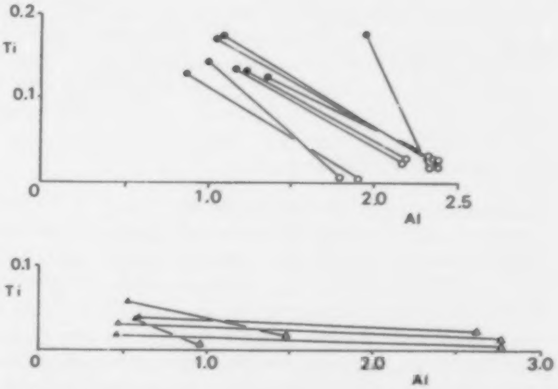

Figure 47. Plot showing Ti versus Al(total) for calcic amphibole from dyke 214 (see Fig. 31) expressed as per formula unit values based on 23 oxygen atoms. Symbols as in Figure 46.

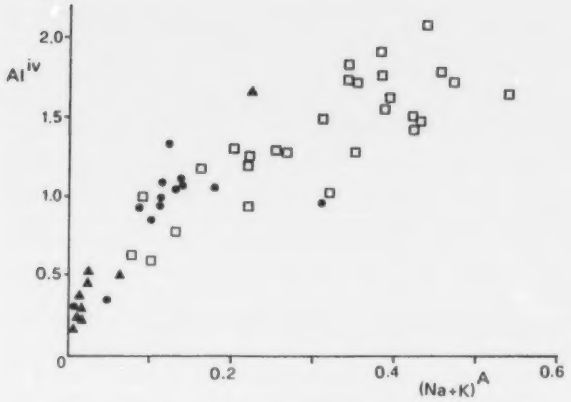

Figure 48. Plot (in ions per formula unit based on 23 oxygens) comparing tetrahedral Al ("Al^{iv}") and A-site Na+K ("(Na+K)^{A}") for the three different generations of amphibole in the metamorphosed Long Range dykes. Symbols: circle-titaniferous hornblende; triangle-actinolite; square-green hornblende. Diagram incorporates all amphibole analytical data, some of which were excluded from previous diagrams for clarity.

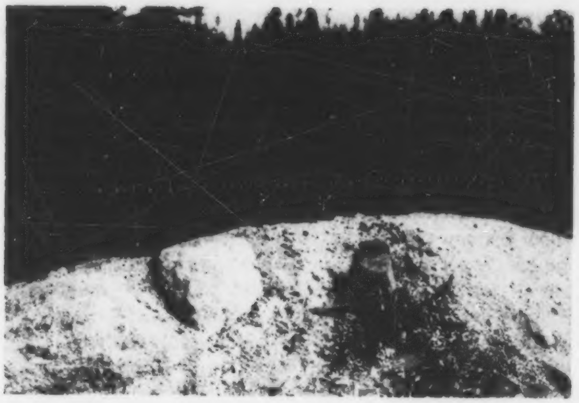

Figure 49. Rusty mylonite of probable Paleozoic age cutting the Taylor Brook gabbro complex. Hammer handle is 30 cm long. GSC photo 204932 49.

The amphibole-forming reactions prevalent near the greenschist-amphibolite facies transition are typically temperature-sensitive equilibria whose location in P-T space is controlled by f_{O_2}. Coexisting titanite and epidote in the metamorphosed dykes indicates oxidizing conditions, with -log f_{O_2} ~ 17-19 at moderate temperatures (Moody et al., 1983).

Evidence for oxidizing metamorphic fluids associated with northeast-trending schistose fabrics in this area is also provided by a narrow mylonite zone which transects the Taylor Brook gabbro complex along the old Taylor Brook road. At this exposure (Fig. 49; see also Fig. 11 for location of mylonite), the gabbro assemblage, comprising olivine (Fo_{73}), labradorite (An_{63}), augite, biotite, and ilmenite, has been altered within the mylonite zone to saussurite, minor chlorite, and unidentified fine grained opaque minerals (magnetite or ilmenite?).

Direct correlation of tectonothermal events between the inlier and the enclosing Paleozoic terranes is difficult, particularly given the structural discontinuities along the southeastern and western margins of the massif. The polymetamorphic history of the Paleozoic cover rocks is noteworthy in this regard. Although constraints are few, the presence of andalusite, replaced by sericite in pelitic schist of the Coney Arm Group(?), may track a similar metamorphic sequence already established from the Long Range dykes, i.e., an early, low pressure and low strain (burial?) event, followed by deformation at higher metamorphic grade.

STRUCTURE

Reconstruction of the structural evolution of the Long Range Inlier relies on the documentation of the geometry of different ages of structural elements developed in various rock units. The relative age of these features is established from structural overprinting relations, which record a relative sequence of deformational events, and from crosscutting igneous intrusions, which provide temporal markers recording (or separating) orogenic events. Structural features are considered to result from discontinuous deformation if they are temporally separated by, for example, an intrusive event. Grenvillian plutonic rocks which intruded the gneiss complex at 1056 to 970 Ma (H. Baadsgaard, pers. comm., 1989) may potentially be used to distinguish earlier Middle Proterozoic (or older) structures from Late Proterozoic (or younger) structures; mafic dykes of the Long Range swarm (ca. 615 Ma) serve as a time marker for distinguishing Proterozoic events from structures resulting from Paleozoic orogenesis. Structural, metamorphic, and plutonic events are summarized in Table 29.

Proterozoic structures

Although contact relations are generally lacking, it is apparent that Grenvillian granitic plutons postdate gneissic fabrics in the country rock. Evidence for this is provided by the absence of high grade mineral assemblages and of gneissic fabrics in the plutons, and from the observation that the granites are enveloped by regionally conformable fabrics, but are locally discordant (e.g., along the eastern margin of the Lake Michel intrusive suite).

Bostock (1983) divided the northern part of the inlier into five structural regions based on foliation orientation, faults, granitic plutons, and areas of sparse outcrop. He recognized three periods of northeast-trending, northwest-overturned folds (termed here F_1, F_2, and F_3). F_1 folds are associated with shallow southwest-plunging linear structures, and are attributed to the metamorphic maximum, which Bostock (1983) considered to be broadly synchronous with the emplacement of large hornblende-bearing (Grenvillian) granitic plutons. F_2 folding was accompanied by greenschist facies metamorphism, and occurred during or immediately following regional Grenvillian plutonism. F_3

Table 29. Summary of structural, metamorphic, and plutonic events in the Long Range Inlier. The table incorporates isotopic data from H. Baadsgaard (pers. comm., 1989) and Kamo et al. (1989), and geological information from Bostock (1983).

Age	Lithology	Deformation	Metamorphism
post-Carboniferous	uplift and erosion		
Carboniferous	deposition of Deer Lake Basin	block faulting	
Ordovician to Early Devonian	emplacement of Devils Room granite (390 Ma) (in part diapiric?)	thermal overprint of crystalline basement (recorded by Pb-Pb (titanite) ages of 978 Ma)	?
		emplacement of Ordovician allochthons; reverse faulting along southwestern margin of inlier	low grade schistosity "M_4"
Early Cambrian	deposition of Bradore and Forteau formations	normal faulting(?)	
latest Proterozoic	emplacement of Long Range dykes (615 Ma)	rifting	
		uplift and erosion	
Late Proterozoic	deposition of Bateau Formation	reverse faulting and rotation of fault blocks(?)	
late Middle Proterozoic		large northwest-trending folds**	
		schistosity in Grenvillian plutons; tight folding(?) (?ca. 978 Ma)	amphibolite facies "M_3" ca. 600°C
	emplacement of Grenvillian granitoid plutons	doming(?), diapirism(?), folding(?), local phyllonitization	low to medium grade; mild thermal overprint "M_2"
	?emplacement of Taylor Brook gabbro complex		thermal metamorphism of nearby gneissic rocks "M_2"
		folding of gneissosity(?)	
Middle Proterozoic	Long Range gneiss complex (ca. 1550 to 1056 Ma)	gneissosity, migmatites	amphibolite to granulite facies "M_1" (550 to 800°C; 5 to 8 kbar)
	deposition of supracrustal protoliths of paragneissic rocks and of schistose and phyllitic rocks (Torrent Cove and Fourché Point assemblages) and emplacement of protoliths of orthogneiss ($\geq$1550 Ma; Labradorian Orogeny?)		

* "M_1, "M_2" etc. refer to metamorphic events described in text

** minimum age

folds deform basement and supracrustal rocks on Belle Isle and in the Long Range. Bostock (1983) acknowledged that F_3 folds may involve both Late Proterozoic (Hadrynian) and Paleozoic deformation.

Northwest-trending folds of unknown age show contrasting structural style in different parts of the inlier, on Belle Isle, and in southern Labrador. In the northeastern corner of the Long Range (Northwest Brook region), these folds postdate the regional northeast-trending lineation, and were interpreted by Bostock (1983) to be related to the diapiric emplacement of nearby granite plutons (Horse Chops and Cloud River plutons). These folds are upright or are overturned to the southwest. Late northwest-trending open folds (F_4?) deform the regional lineation near White Bay.

Structural interference has apparently produced a regional dome-and-basin pattern in the northern part of the inlier. Bostock (1983) recognized a large dome structure north of Torrent River. The dome is defined by a concentric pattern of gneissosity developed in leucocratic gneiss (unit **Pgn**). It has a diameter of approximately 12 km. Bostock (1983) reported that the dome postdates two generations of linear structures associated with earlier folding episodes. It also appears to deflect a large east-west fold structure to the north, visible on aerial photographs (north part of air photo A20003-4). Structural data depicted on Bostock's (1983) 1:125 000 scale map are sparse in this area, but the fold appears to close to the east. This fold is considered here to be analogous to large northwest-trending folds which dominate the structural pattern of the gneiss complex to the south.

A possible structural basin occurs to the south of the Cloud River pluton. The concentric form of this structure is visible on aerial photographs (e.g., A20003-49), and is supported by Bostock's (1983) data. Dome and basin structures in this area may be related to the high concentration of granitic plutons.

Structural interpretation of the central and southern parts of the inlier is hampered by relatively poor exposure, which obscures critical contact and structural overprinting relations. Furthermore, the recognition in this area of features correlating to Bostock's (1983) F_1, F_2, and F_3 structures is difficult, since the regional correlation of fabrics simply on the basis of orientation is generally unreliable. Although correlation of individual structures remains problematic, the central and southern parts of the inlier nonetheless show a similar structural style to the northern part of the massif.

The earliest fold structures in the southern part of the inlier (Silver Mountain area) are open to tight folds in the gneiss complex (Owen, 1986a). Unlike Bostock's (1983) F_1 structures to the north, early folds in this area are not associated with well-developed linear fabrics. The original orientation of these folds is not known, since they have been transposed by northwest-trending planar fabrics associated with south-southeast- to southwest-plunging second-generation fold structures (Fig. 50). The northwest-trending planar fabric in this area developed, at least in part, after the emplacement of the Grenvillian granitoid plutons, which in places carry a similarly-oriented foliation.

Figure 50. Multiply-folded leucocratic veins in migmatitic granitic gneiss (unit **Pgn**). The second-generation folds have a well-defined axial planar schistosity. GSC photo 204932 50.

The gneiss complex throughout most of the inlier is dominated by large (wavelengths of several kilometres) upright northwest-trending folds (Fig. 51). A moderate northwest plunge is indicated by the orientation of minor fold structures, and from projected intersections of limbs of the major folds. The small-scale second-generation folds in the Silver Mountain area may be parasitic folds related to these larger structures.

The age of the northwest-trending folds relative to the Grenvillian granites is uncertain. Planar fabrics associated with these folds are rare, but occur, for example, in the Little Cat Arm pluton, which occupies the hinge area of a large northwest-trending fold. Northwest-trending planar fabrics in the country rock are cut by mafic dykes of the Long Range swarm, indicating that these folds formed before the latest Proterozoic.

The Grenvillian plutons are variably foliated. A steep northeast-trending greenschist to epidote amphibolite facies schistosity is developed in granites near White Bay. Since this schistosity also occurs in the Long Range dykes, it is attributed to Paleozoic deformation.

Farther west, where the Paleozoic overprint is insignificant, plutons typically carry a west- to northwest-trending planar fabric defined by feldspar megacrysts (where present), elongate quartz-rich domains, and biotite-hornblende aggregates. This fabric is clearly tectonic locally. Examples include: (1) coronitic charnockite (unit **Pcg**) of the Potato Hill pluton, which is transformed to well-foliated hornblende-biotite granite along its southern margin; and (2) deformed charnockitic rocks of the Lake Michel intrusive suite (units **Pxg**, **Pxgk**), which contain strained quartz ribbons and hornblende-rich aggregates developed at the expense of pyroxene. This fabric is attributed to the 978 Ma tectonothermal event defined by Pb-Pb (titanite) ages determined for samples of the Grenvillian granite and basement gneiss (H. Baadsgaard, pers. comm., 1989). This attribution is supported by the observation that tectonic fabrics in Grenvillian plutons well to the west of White Bay are locally

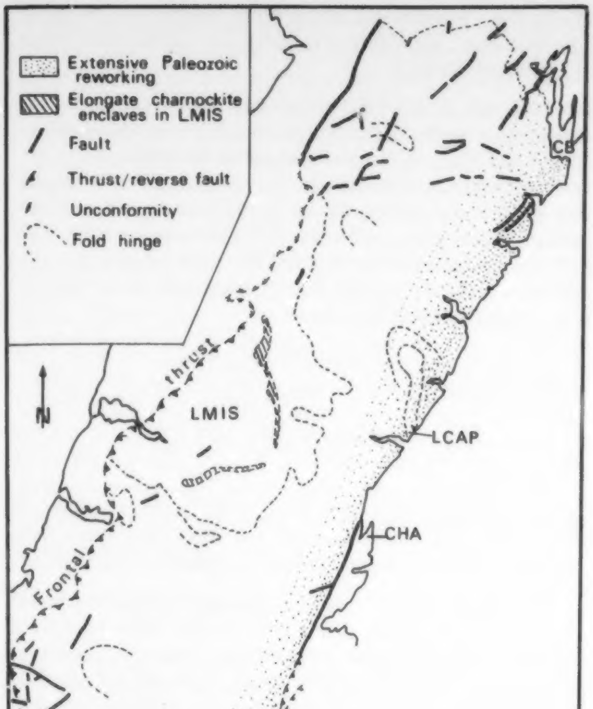

Figure 51. Distribution of faults and of large northwest-trending folds in the Long Range gneiss complex. The areal extent of widespread Paleozoic tectonic overprinting is also shown. CB – Canada Bay; CHA – Coney Head allochthon; LCAP – Little Cat Arm pluton; LMIS – Lake Michel intrusive suite.

cut by the Long Range dykes (e.g., the 20 m wide, north-northeast-trending mafic dyke exposed in the south-central part of the Lake Michel intrusive suite). These data suggest that metamorphism and deformation temporally overlapped the emplacement of some of the Grenvillian plutons.

As mentioned earlier, the Lake Michel intrusive suite has a nearly concentric structure outlined by large elongate bodies of charnockite and basement gneiss, and by planar fabrics. This structure may be related to either (1) emplacement mechanism, or (2) subsequent folding analogous to the large northwest-trending fold structures identified in the gneiss complex throughout the inlier (Fig. 51).

Supporting the first hypothesis are the observations that: (1) the foliation is parallel to internal and external pluton contacts (cf. Paterson et al., 1989); (2) schistose fabrics in the northern part of the Lake Michel intrusive suite are at a high angle to the axial surface of a well-defined northwest-trending fold in basement gneiss just to the east; and (3) the large west-northwest-trending fold outlined by the quartzite ridge at the southern margin of the intrusion is warped about the intrusion. Concentric structures are typical of many diapirically-emplaced granitoid plutons (e.g., Bateman, 1984).

Supporting the second hypothesis is the observation that the schistosity in some plutons is approximately parallel to the axial surface of large northwest-trending folds in the nearby country rock. The best example of this is the Little Cat Arm pluton, which occupies a large fold hinge.

Paleozoic structures

Textural and compositional evidence from metamorphosed Long Range dykes suggest polyphase deformation of the southeastern margin of the inlier during the Paleozoic.

The age of these events is uncertain. Within the inlier, Paleozoic orogenesis is largely bracketed to the interval 615 to 390 Ma by the emplacement ages of the Long Range dykes and the Devils Room granite. The similarity in metamorphic grade (greenschist facies) and of S-fabric orientations in deformed Cambro-Ordovician platformal rocks near the southeastern margin of the inlier provides a further constraint on the lower age of post-Long Range dyke events. Although the available data are broadly compatible with evidence for regional Acadian thrusting in the Canada Bay area (Knight, 1987), the correlation of Paleozoic structures in basement and cover rocks remains elusive.

Schistose and mylonitic fabrics in the Long Range dykes and their host rocks are clearly ductile features. The kinematic significance of these planar fabrics is not always clear, and a variety of movement senses is indicated by different fault zones containing reliable kinematic indicators. For example, the deformed margin of dyke 214 (see Fig. 31 for location) contains C-S fabrics that record normal faulting. On the other hand, small-scale structures in a shallowly north-dipping mylonite near the Cat Arm dam are indicative of south-directed thrusting (P. Erdmer, pers. comm., 1988). The age of this thrust is uncertain. The fault cuts a northeast-trending mafic dyke (Long Range dyke?), so it may be Paleozoic.

Shallow east-dipping brittle-ductile shear zones cut basement exposed in roadcuts on the junction to the Power House turnoff on the Cat Arm dam access road, near Devil Cove. A series of flat-lying granitic pegmatite dykes parallel these high strain zones (Fig. 52A). Since some of the pegmatites are deformed in the shear zones, while others aren't, these dykes may potentially be used to bracket the age of these faults. Reverse (top-to-west) translation is suggested by composite ductile fabrics (Fig. 52B) and by warping of the gneissosity across the fault surface. These shears are possibly structurally-deep analogues of a minor brittle thrust which cuts the northeast-trending Paleozoic dyke in phyllite of the Coney Arm Group (see Owen and Erdmer, 1988). These in turn may be splay faults from the Doucers Valley fault complex (Lock, 1972) which bounds the southwestern margin of the inlier.

The Doucers Valley fault complex is a major structural feature of the White Bay area. It separates Lower Paleozoic continental shelf (platformal) sediments to the west from

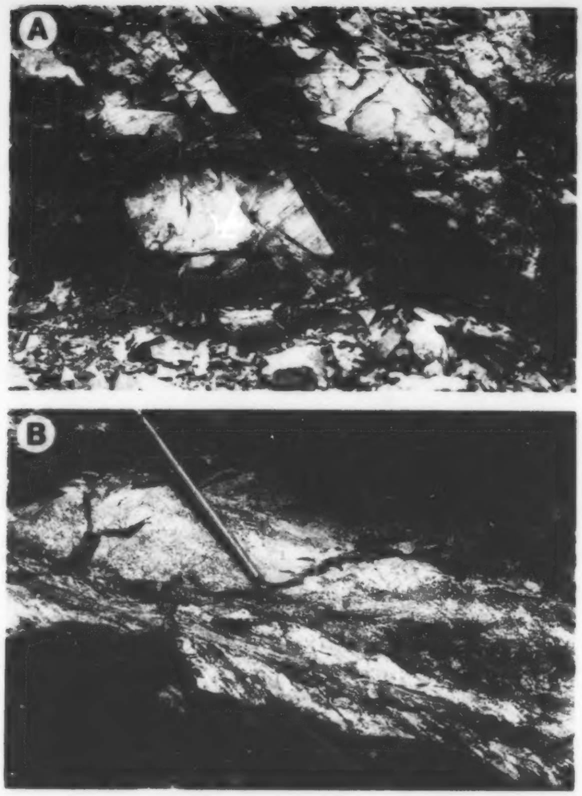

Figure 52. Field photographs of granitic pegmatite associated with shallow-dipping Paleozoic(?) faults at Devil Cove. A. Horizontal pegmatite sheets; hammer handle is 85 cm long; B. composite planar fabric in pegmatite, indicative of west-directed thrusting along a brittle-ductile fault zone. GSC photo 204932 52A to B.

continental slope and rise sediments and oceanic crust to the east (Williams, 1978; Tuach, 1987). Cambro-Ordovician arenites of the Coney Arm Group (Lock, 1969; Smyth and Schillereff, 1982) deformed within this high-strain zone have a well-developed greenschist facies schistosity which contains a moderately east-plunging, down-dip mineral lineation. A similarly-oriented, low grade schistose fabric occurs in nearby basement rocks (notably the Main River pluton). Fault-related composite schistose fabrics are developed in a northeast-trending band of felsic porphyry enclosed by the clastic rocks east of Taylor Brook. These C-S fabrics confirm a reverse (top to the northwest) sense of motion (Owen, 1986a) for the fault system as originally suggested by Lock (1972). Lock (1972) noted that these early penetrative planar fabrics (Ordovician?) were superseded by brittle features (i.e., cataclasite) associated with late deformation. Schistose rocks within the fault complex are unconformably overlain by redbeds of the Deer Lake basin. This places an upper age limit for major displacement on the fault in the Carboniferous; however, the Deer Lake Basin is brittly deformed in a northeast-trending fault (Wigwam fault; Hyde, 1982) in the southern part of the complex. The Wigwam fault parallels other late major faults (i.e., postdating Carboniferous sedimentary rocks) to the east (e.g., the Cabot and Green Bay faults; see review in Hibbard, 1983b).

Whereas ductile (and ductile-brittle) structures characterize the response of crystalline basement to Appalachian orogenies along the eastern margin of the inlier, the youngest structures identified near the foreland to the west are cataclastic (e.g., brittle faults). In this area, cataclasites are developed on a range of scales (millimetre to metre) in both gneissic and granitoid rocks. The age of the cataclasites relative to ductile and brittle-ductile structures in the eastern part of the inlier is not known.

Cataclasite derived from the Lake Michel intrusive suite forms steep northeast-trending zones near the western margin of the intrusion. Cataclastic fabrics developed in a small body of equigranular charnockite (unit Pxg) in the Lake Michel intrusive suite 8 km east of Eastern Blue Pond occur along strike of the Long Range frontal thrust where the latter disappears near Blue Mountain. These northeast-trending cataclasite zones may therefore represent the continuation of the Long Range frontal thrust in the interior of the inlier.

Conjugate sets of brittle faults with north-northeast and west-northwest trends in the Gros Morne Park area were interpreted by Erdmer (1986a,b) to have developed in response to movement by the underlying Long Range frontal thrust.

The Long Range frontal thrust separates the inlier from Cambro-Ordovician platformal rocks to the west. The thrust is exposed in a stream (West Brook) feeding Parsons Pond (see Grenier and Cawood, 1988, Fig. 3). At this locality, the thrust is a moderately-dipping (ca. 30-40°) brittle structure (P. Cawood, pers. comm., 1988). Bedding in the footwall carbonate rocks is overturned to the west. A nearby (ca. 500 m west) parallel thrust (Parsons Pond thrust) cuts parautochthonous platformal rocks and the overlying imbricated sequences of the Humber Arm allochthon (Cawood and Williams, 1986). The Parsons Pond and Long Range thrusts diverge northward, where the former fault is restricted to the parauthochthonous cover sequence, and the latter apparently is discontinuous to the north of Blue Mountain.

The continuity across the Long Range frontal thrust of the aeromagnetic anomaly associated with the Lake Michel intrusive suite (see Fig. 10A) suggests that horizontal west-directed movement was restricted in this area to a few kilometres at most. Although displacement on this fault appears to be minor and to decrease northward, unpublished seismic data suggest that the Long Range frontal thrust is a splay fault extending upward from a deeper master decollement.

The hypothesis that cataclasite zones in the western part of the inlier are related to movement on the Long Range frontal thrust (Erdmer, 1986a) requires that crystalline rocks in this area behaved as a relatively thin and rigid thrust slab. The thickness of crystalline rocks in the hanging wall at the time of thrusting is not known, but was probably small. In West Brook, the thrust cuts up through the 500 foot (ca. 150 m) topographic contour to within approximately

550 m of the maximum elevation of gneissic rocks exposed in this area. No lower Paleozoic sedimentary rocks are preserved in this area, so this value (550 m) represents a minimum thickness of crystalline rocks in the hanging wall immediately above the thrust as presently exposed. Farther north, however, the Bradore Formation (unit 1CB) lies unconformably atop parts of the Lake Michel intrusive suite and the Long Range gneiss complex. The nearly-horizontal unconformity beneath the Bradore Formation lies at an elevation of approximately 375 m. Assuming that the Bradore Formation originally extended southward to the West Brook area, a distance of 75 km, and that these sediments were deposited on a gently-sloping paleoerosion surface, basement rocks in the hanging wall above the northern part of the Long Range frontal thrust were probably not much more than about 1 km thick. If the current dip of this fault has not changed substantially since the Paleozoic (i.e., was about 35°), the thickness of the hanging wall would increase rapidly toward the east. This explains the virtual restriction of the cataclasite zones to a fairly narrow belt (ca. 10 km) along the western margin of the inlier.

ECONOMIC GEOLOGY

Exploration activity in the Long Range Inlier has focused on gold prospects recently identified in the Sops Arm-Jackson's Arm area near White Bay. Other showings of potential economic interest include iron and iron-copper sulphides associated with pelitic and mafic gneiss, heavy minerals (principally iron and iron-titanium oxides) concentrated in basal members of the Bradore Formation, aphanitic apatite (collophanite) associated with glauconitic rocks of the Bradore Formation, and massive quartzite of the gneiss complex.

Gold

Gold mineralization in the Jackson's Arm area was discovered in 1983 by C. Childs, a local prospector employed by Labrador Mining and Exploration Company, Limited. The gold in this prospect is associated with sparsely mineralized (pyrite, arsenopyrite) shear zones cutting the Aspy granite. Gold prospects were subsequently discovered in Cambro-Ordovician arenites of the Coney Arm Group.

The gold occurrences occur sporadically along a 20 km linear zone approximately parallel to the Doucers Valley fault complex (Fig. 53). There were 11 property holders in June 1987, but most of the known gold prospects occurred on properties held by BP Canada-Selco, Varna Gold, Inc., and Brinco. Based on 26 holes with a combined length of 3200 m, grade varied between 1.0 and 2.3 g Au/t (maximum of 44.8 g Au/t) over widths ranging from 3 to 47 m at intersection depths of 2 to 63 m (joint BP Selco-Varna Resources press release, 12 June 1987). These data indicate a large, low grade deposit. Economic viability is enhanced by the proximity of roads, sea lanes, and a hydroelectric power source. The shallow intersection depths favour open pit development.

The Jackson's Arm gold prospects are interpreted as epigenetic deposits associated with fault-related hydrothermal alteration (Tuach, 1986, 1987; Tuach and French, 1986; Tuach et al., 1988). Two stages of alteration have been identified by Saunders and Tuach (1988). Stage 1 (potassic) alteration resulted in the formation of microcline and sericite, thereby converting tonalitic and granodioritic protoliths (normative classification; see Saunders and Tuach, 1988, Fig. 3) to granite. Stage 2 (sodic) alteration produced fine grained albite with subordinate quartz, ankerite, siderite, and sericite. Stage 1 alteration apparently

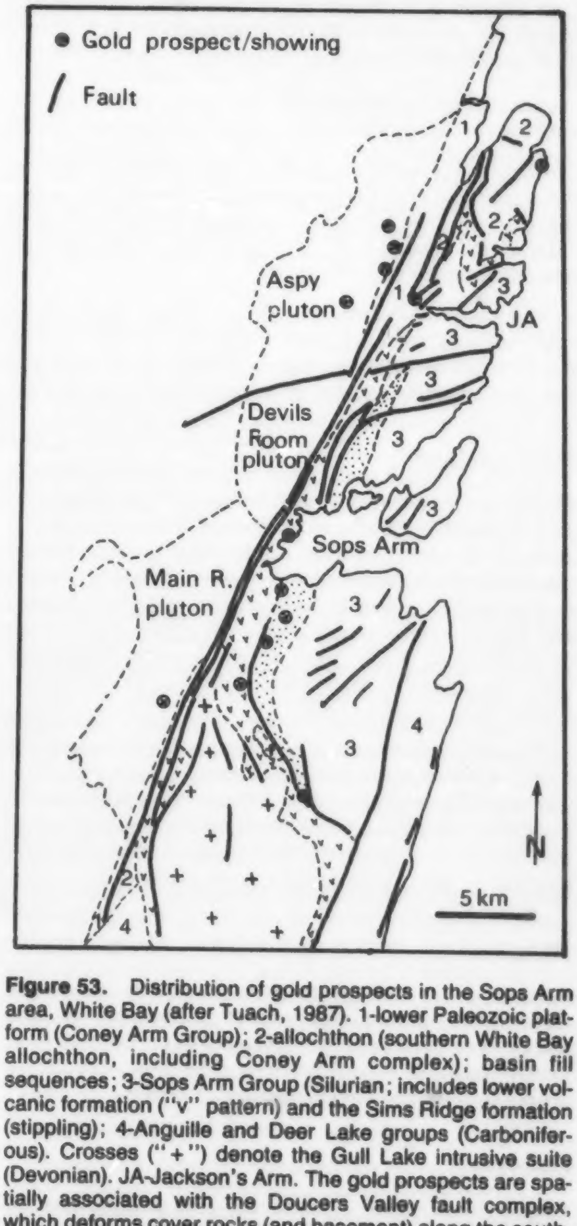

Figure 53. Distribution of gold prospects in the Sops Arm area, White Bay (after Tuach, 1987). 1-lower Paleozoic platform (Coney Arm Group); 2-allochthon (southern White Bay allochthon, including Coney Arm complex); basin fill sequences; 3-Sops Arm Group (Silurian; includes lower volcanic formation ("v" pattern) and the Sims Ridge formation (stippling); 4-Anguille and Deer Lake groups (Carboniferous). Crosses ("+") denote the Gull Lake intrusive suite (Devonian). JA-Jackson's Arm. The gold prospects are spatially associated with the Doucers Valley fault complex, which deforms cover rocks (and basement) along the southeastern flank of the inlier.

involved intergranular diffusion; stage 2 alteration is associated with hydraulic fracturing. Mineralizing fluids accompanied stage 2 alteration, which precipitated pyrite, arsenopyrite, and gold in fracture stockworks, veins, and shear zones. Gold forms micron-scale grains, typically enclosed by pyrite.

The age of the hydrothermal system is uncertain; however, the presence of alteration-related mineralization in Coney Arm Group arenites suggests a maximum age of Early Cambrian. Since the stockwork deposits are undeformed, mineralization may postdate the most recent major orogenic event (Acadian Orogeny) in the area (i.e., Late Silurian or younger) (C.B. McKenzie, unpublished manuscript presented to the Newfoundland Branch, Canadian Institute of Mining and Metallurgy, 1987).

Copper

Chalcopyrite occurs sporadically with pyrite and/or pyrrhotite in pelitic and (locally) mafic gneiss. Iron sulphides dominate over iron-copper sulphides. Nowhere was chalcopyrite observed to constitute greater than accessory concentrations in these rocks.

Chalcopyrite occurs with drusy quartz in vugs in amphibolite exposed in a roadcut along the northern side of the Upper Humber River (Owen, 1986a). A grab sample from this exposure yielded a Cu determination of 0.1%.

Heavy minerals

The basal (conglomeratic) unit of the Bradore Formation east of Hawkes Bay contains narrow (≤1 cm) laminae enriched in heavy minerals, principally ilmenite and/or magnetite. These laminae are concentrated in thin, discontinuous sandy horizons in the lower part of this conglomerate. The heavy-mineral concentrations occur in a zone not exceeding more than a metre or two in width. Analysis of one sample yielded background values of Pt and Au (I. Knight, pers. comm., 1988).

Ilmenite is a common accessory or minor mineral in the Taylor Brook gabbro complex. Although locally layered, igneous foliation appears to be defined by variations in the grain size and proportions of silicate minerals, and no oxide-rich layers were observed. The platinum group element potential of the gabbro remains to be evaluated.

Phosphate

Bostock (1983) reported the presence of aphanitic apatite (collophanite) in glauconitic beds of the Bradore Formation south of Leg Pond and east of Hawkes Bay. Although these locally constitute several percent of the rock, they do not appear to represent commercial concentrations.

Quartz

Discontinuous ridges of grey to blue-grey or white quartzite up to several tens of metres wide and up to about five kilometres long occur in the southern part of the inlier. The quartzite is rarely pure; feldspar and iron oxide (hematite?) occur in accessory concentrations.

Summary

While the base metal potential of the Long Range Inlier appears to be poor, its precious metal potential is much more promising. Gold prospects near Jackson's Arm may prove to be suitable for bulk mining methods. Although the age of the gold mineralization is not known, these prospects are spatially associated with Paleozoic fault systems, and developed in a variety of host rocks, including the Aspy granite and adjacent cover rocks. By analogy with the Jackson's Arm prospects, cataclasite and mylonite zones developed in Grenvillian granitoid plutons near White Bay (e.g., the Pigeon Cove pluton) and their gneissic host rocks merit further investigation.

The platinum group element potential of the Taylor Brook gabbro complex was being evaluated at the time of writing of this bulletin. No visibly obvious indicators of platinum group element mineralization were noticed during mapping of the gabbro.

Heavy minerals and phosphate in the Bradore Formation exposed east of Hawkes Bay appear to be of little economic interest. Precious metals have not been identified in the heavy mineral concentrations (I. Knight, pers. comm., 1988). The uranium potential of the Bradore Formation and the underlying granitic basement remains to be evaluated.

Quartzite of the basement complex is a potential source of silica. However, the quartzite locally contains visible impurities (feldspar, iron oxide), and may be less pure than quartzite prospects in central and western Labrador (Meyer and Dean, 1987).

DISCUSSION

The geological complexity of the Long Range Inlier reflects its polyorogenic history. The effects of five orogenies are evident (Erdmer and Owen, 1988):

1) high grade metamorphism of quartzofeldspathic rocks (minimum age 1550 Ma), pelite, and carbonate rocks during the interval 1550 to 1056 Ma;
2) emplacement and deformation of Grenvillian plutons at 1056 to 970 Ma;
3) uplift, rifting, and the emplacement of mafic dykes at 615 Ma;
4) thrusting during the Middle Paleozoic;
5) regional granitic plutonism (Devils Room granite) and a tectonothermal overprint at about 390 Ma.

Structurally, the inlier occupies a strategic position, being centred near the junction between the Appalachian and Grenvillian orogens, and it sheds light on tectonic events in both.

Proterozoic evolution

The Proterozoic evolution of the Long Range Inlier may be reconstructed (at least in part) from field data, isotopic age determinations (H. Baadsgaard, pers. comm., 1989), geothermobarometry of the gneiss complex, and the geochemistry of the Grenvillian plutons.

Neither the age of the protolith of the gneiss complex nor its earliest metamorphic imprint is well known. This represents a serious deficiency, since it prohibits reliable correlation with petrographically-similar gneiss elsewhere in the Appalachian orogen and in Labrador.

Although a well-established temporal framework is lacking, the relative ages of metamorphism, deformation, and plutonism determined from field relations and textural overprinting criteria provide the rudimentary elements of the early history of the inlier.

The southwestward-increasing metamorphic gradient in the inlier appears to be continuous, and to reflect increasing metamorphic temperatures. The highest temperatures were determined in granulites exposed west of the Taylor Brook gabbro complex. The contribution of the gabbro to the regional thermal budget in the inlier is not clear, although textural overprinting relations noted in nearby pelitic gneiss clearly demonstrate that the gneiss complex attained high grade (e.g., sillimanite + potassium feldspar in pelites) prior to emplacement of the gabbro. It is nevertheless worth noting that subsurface plutons have been invoked to explain thermal peaks in the Grenville Province of eastern Quebec (Perreault and Martignole, 1988).

The role of C-O-H fluid fugacities on the granulite-amphibolite transition in the northern part of the inlier also remains ambiguous. Regional variations in the composition of cordierite channel fluids suggest that metamorphic fluids may have influenced the distribution of the high grade assemblages (cf. Edwards and Essene, 1988).

The Grenvillian Orogeny involved regional granitoid plutonism (1056 to 970 Ma) and, subsequently, medium grade metamorphism and deformation. The significance of the Grenvillian plutons is considered in conjunction with correlative Grenvillian rocks in Labrador (see below).

The inlier was apparently inactive during the Late Proterozoic. No information is available for the 355 Ma period between late Grenvillian metamorphism (970 Ma) and the emplacement of the Long Range dykes (615 Ma).

Paleozoic evolution

Regional variations in structural style suggest that the Long Range Inlier acted as a buttress against west-directed thrusting in the southeast and as a thin competent slab along its western margin during the Paleozoic (Erdmer, 1986a). Penetrative deformation is restricted to the southeastern margin of the inlier, approximately 10 to 20% of the total area of the massif. Cover rocks in this region developed steeply-lineated schistose fabrics as they were "plastered" against basement during compression along an (approximately) east-west axis. Moderately to steeply east-dipping, low grade schistose and mylonitic fabrics in the inlier are tentatively attributed to this event. A steep normal fault represented by mylonite in one Long Range dyke (dyke 214, Fig. 31) may have formed during post-compression extension.

West- to northwest-verging brittle-ductile thrusts occur in both cover and basement near White Bay. These may be Carboniferous faults, since one thrust cuts a post-Acadian(?) mafic dyke in the Coney Arm Group (Cambro-Ordovician).

Steep conjugate cataclasite zones above the Long Range frontal thrust suggest that the foreland fringe of the massif is fairly thin, and is underlain by cover. The thickness of the inlier in the hanging wall is crudely constrained by the topographic elevation of flat-lying arkose of the Lower Cambrian Bradore Group. The southward extrapolation of the elevation of the unconformity beneath the Bradore Formation suggests that the Long Range frontal thrust cut within 1 km of the sub-Cambrian erosion surface. Geometrical relations at deeper structural levels are unknown, but will become apparent when the results of seismic profile surveys in the area are available.

Correlations to the north

Recent mapping of the eastern Grenville Province of Labrador by C.F. Gower has led to the recognition of several fault-bounded lithotectonic terranes (Gower and Owen, 1984; Gower et al., 1987; Gower et al., 1988). Southward from the Grenville Front, these are (Fig. 54): the Groswater Bay, Lake Melville, Hawke River, Mealy Mountains, and Pinware terranes. Each terrane comprises a characteristic assemblage of rock types of distinctive structural style, metamorphic grade, and/or isotopic age.

The Groswater Bay and Lake Melville terranes were derived from Labradorian crust (1710-1630 Ma; Thomas et al., 1986) which was extensively reworked during the Grenvillian Orogeny. Recent U-Pb dating by Schärer et al. (1986) has demonstrated that recrystallization of the Groswater Bay Terrane (ca. 970 Ma) predated Grenvillian reworking of the Lake Melville Terrane by 50 to 60 Ma. Quartzofeldspathic gneiss and mafic to felsic plutonic rocks occur in both terranes, although paragneiss is relatively common in the Lake Melville Terrane.

Anorthosite dominates the Mealy Mountains Terrane, whereas plutons in the Hawke River Terrane comprise a variety of mafic rocks. A large positive Bouguer gravity anomaly in the southern part of the latter terrane has been interpreted to result from the uplift of subsurface mantle material along or near the Gilbert River Shear Belt (Gower et al., 1987). This 30 km wide dextral shear zone defines the southern boundary of the Hawke River Terrane, and also marks the northern extent of widespread plutonic rocks of Grenvillian age in easternmost Labrador.

Terranes to the north and northwest of the Gilbert River Shear Belt were extensively reworked during the Grenvillian Orogeny. Deformation is represented by polyphase folding (e.g., three Grenvillian fold sets occur in the Grenville

Front; Owen et al., 1986) and by south-dipping thrust faults. The Groswater Bay, Lake Melville, and Hawke River terranes thus coincide with a 225 km wide (maximum), Grenvillian fold-and-thrust belt (Owen and Erdmer, in press; Fig. 54). The curviplanar disposition of the fold-and-thrust belt (i.e., convex toward the northeast) mirrors the eastward swing in the strike of the Grenville Front on the Labrador coast (Gower and Owen, 1984; Owen et al., 1986). Compared with the area south of the Gilbert River Shear Belt, the fold-and-thrust belt is lithologically and structurally complex, and apparently lacks major Grenvillian plutons.

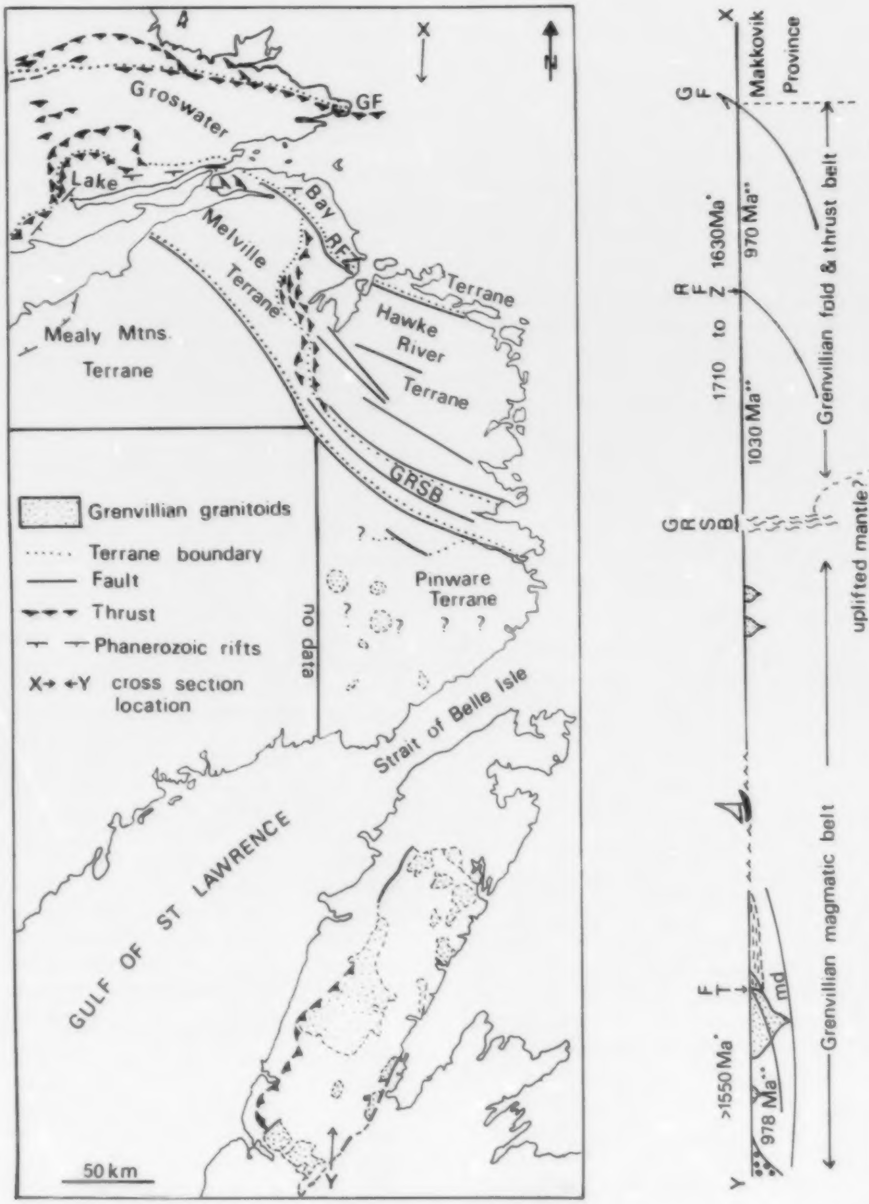
X
N
GF
Groswater
Lake
Bay
RFZ
Melville
Terrane
Terrane
Mealy Mtns
Terrane
Hawke
River
Terrane
GRSB
Pinware
Terrane
Grenvillian granitoids
Terrane boundary
Fault
Thrust
Phanerozoic rifts
X→ ←Y cross section location
no data
Strait of Belle Isle
GULF OF ST LAWRENCE
50 km
Y
X
Makkovik
Province
GF
RFZ
1710 to 1630Ma*
970 Ma**
1030 Ma**
Grenvillian fold & thrust belt
GRSB
uplifted mantle?
Grenvillian magmatic belt
FT
md
>1550 Ma*
978 Ma**
Y

Figure 54. Lithotectonic entities in the Grenville Province of eastern Labrador. GF-Grenville Front; GRSB-Gilbert River Shear Belt; RFZ-Rigolet fault zone. Cross-section symbols: circles-Deer Lake Basin; dashes-lower Paleozoic cover rocks; FT-Long Range frontal thrust; md-master décollement (Paleozoic); *age of crustal accretion; **age of Grenvillian reworking. Most of the granites indicated as Grenvillian have been isotopically dated (Gower and Loveridge, 1987; H. Baadsgaard, pers. comm., 1989).

Grenvillian granitoid plutons characterize more southerly terranes, which apparently occur in the upper part of a thrust stack imbricated northwestward during the Grenvillian Orogeny. This area, the Pinware Terrane, comprises orthogneiss and paragneiss, and mafic to felsic plutonic rocks, including Grenvillian plutons (Gower and Loveridge, 1987; Gower et al., 1988). Gower et al. (1988) noted that both the Pinware Terrane and the Long Range Inlier are similar insofar as both consist of quartzofeldspathic gneisses and (Grenvillian) granitoid plutonic rocks.

Although insufficient mapping has been undertaken in the Pinware Terrane to attempt direct lithological correlation with the Long Range Inlier, the presence of ca. 1.0 Ga granitoids in both areas characterizes this region as a Grenvillian magmatic belt outboard of the fold-and-thrust belt (Owen and Erdmer, in press). The minimum width of this magmatic belt, from the Gilbert River Shear Belt southward through the Long Range Inlier, is 350 km (Fig. 54).

The potential tectonic significance of this bipartite subdivision of the eastern Grenville Province becomes apparent when considering the geometry of Cenozoic orogens. By analogy with the Himalayas (cf. Dewey and Burke, 1973; Windley, 1986), the Grenvillian magmatic terrane may be the tectonic equivalent of nappes hosting S-type leucogranites in the Higher Himalayas, while the Grenvillian fold-and-thrust belt has a close analogue in the foreland region farther to the south. This model anticipates that at least some of the Grenvillian plutons were generated during anatexis of underthrust Labradorian crust. This hypothesis may be tested once the following information becomes available: (1) isotopic data for the Grenvillian plutons; (2) kinematics of the early history of the Gilbert River Shear Belt; and (3) uplift history (P-T-time curves) of individual terranes in the fold-and-thrust belt and the Grenvillian magmatic belt.

The location of a suture zone and a magmatitic arc-batholith expected toward the hinterland is not known. These features presumably occur (or occurred) well to the southeast of the Long Range Inlier, and may thus be buried beneath the Appalachians, or were rifted from North America following the Grenvillian Orogeny. The nature of the colliding (micro?) continental (and/or island arc) mass(es) on the hinterland side of the orogen is entirely unknown.

Correlations to the southwest

The Long Range Inlier is not the only occurrence of Proterozoic basement in the Appalachians of Atlantic Canada.

Proterozoic massif-type anorthosite and related rocks occur in the Indian Head (Walthier, 1949; Heyl and Ronan, 1954; Coleman-Sadd, 1974) and Steel Mountain (van Berkel, 1987) complexes 100 km southwest of the Long Range Inlier. South of Grand Lake, charnockite and granulite facies gneiss of the Disappointment Hill complex (Currie, 1987) is probably intruded by anorthositic rocks of the Steel Mountain complex. Lithological similarities with the Long Range Inlier led Currie (1987) to propose a Grenvillian age for these high grade rocks, although a preliminary U-Pb (zircon) age for the charnockite suggests an age of ca. 1500 Ma (K.L. Currie, pers. comm., 1989). Lithological comparison with the Long Range Inlier is considered in more detail below.

Grenvillian basement has recently been identified in the Cape Breton Highlands of Nova Scotia. The exposed basement complex in Cape Breton comprises felsic to mafic gneiss, monzodiorite, anorthosite, and syenite of the Blair River complex (Raeside et al., 1986). U-Pb (zircon) dating of the syenite yields a metamorphic age of ca. 1.04 Ga, and a poorly-constrained igneous age of 1.1 to 1.5 Ga (Barr et al., 1987).

On the basis of these data, Barr et al. (1987) correlated the Blair River complex to the Long Range Inlier and the Indian Head complex. Although Grenvillian syenite has been reported in southern Labrador (Gower and Loveridge, 1987), syenite has not been identified in the Long Range Inlier. Consequently, although basement in Cape Breton appears to be broadly coeval with the inlier, direct lithological ties between both terranes remain to be documented.

More striking is the lithological similarity between high grade gneiss of the Disappointment Hill complex and the Long Range Inlier. Where preserving its high grade mineralogy, quartzofeldspathic gneiss of the Disappointment Hill complex is a granoblastic rock containing orthopyroxene, biotite, and/or amphibole. Orthopyroxene-bearing metamafic bands are ubiquitous. Although the rock has the modal composition of tonalite or granodiorite, its protolith is uncertain. At Disappointment Hill, a 6 m wide band of pelite and associated charnockitic gneiss occurs within the tonalitic gneiss. The pelite consists of quartz, andesine (An_{35} to An_{38}), potassium feldspar, cordierite, biotite, garnet, ilmenite, and, in one sample, accessory sillimanite (derived from the breakdown of biotite) and ferrohypersthene. The charnockitic gneiss contains quartz, andesine (An_{33}), garnet, ferrohypersthene, biotite, potassium feldspar, ilmenite, and rare cordierite.

Identical assemblages occur in granulites of the Long Range gneiss complex to the north. The pelitic assemblage of cordierite, garnet, orthopyroxene, and quartz is particularly distinctive. This is not a common assemblage (cf. Powers and Bohlen, 1985). In the Long Range Inlier, it occurs in association with gedrite-bearing pelite near the northeastern flank of the Lake Michel intrusive suite. Thermobarometry of the assemblage at the latter locality yields a P-T estimate of 6.4 kbar and 705°C. Coexisting garnet and cordierite from the Disappointment Hill complex indicates P-T conditions of about 750°C and 4 kbar (Owen and Currie, in press). Together with the 1500 Ma age determined from both terranes, these data indicate that the Disappointment Hill complex is a shallow-level equivalent of the Long Range Inlier (cf. Currie, 1987). The Disappointment Hill complex therefore acts as a link between the inlier and Middle Proterozoic rocks exposed in Cape Breton, and demonstrates that different structural levels of Proterozoic basement rocks were uplifted by Paleozoic faulting along the length of the Long Range Mountains.

REFERENCES

Allègre, C.J., Courtillot, V., Tapponnier, P., Hirn, A., Mattauer, M., Coulon, C., Jaeger, J.J., Achache, J., Scharer, U., Marcoux, J., Burg, J.P., Girdeau, J., Armijo, R., Gariepy, C., Gopel, C., Li Tindong, Xiao Xuchang, Chang Chenfa, Li Guangqip, Lin Baoyu, Teng Jiwen, Wang Naiwen, Chen Guoming, Han Tonglin, Wang Xibin, Den Wanming, Sheng Huaibin, Cao Yougong, Zhou Ji, Qui Hongrong, Bao Peisheng, Wang Songchan, Wang Bixiang, Zhou Yaoxiu, and Ronghua Xu

1984: Structure and evolution of the Himalaya-Tibet orogenic belt; Nature, v. 307, p. 17-22.

Anovitz, L.M. and Essene, E.J.

1987: Compatibility of geobarometers in the system CaO-FeO-Al_2O_3-SiO_2-TiO_2 (CFAST): implications for garnet mixing models; Journal of Geology, v. 95, p. 633-645.

Anovitz, L.M., Essene, E.J., and Moecher, D.P.

1988: Pressure-temperature history of Ontario Grenville granulites (abstract); *in* Grenville Workshop 1988, Friends of the Grenville, Program with Abstracts, p. 7.

Armbruster, T. and Bloss, F.D.

1980: Channel CO_2 in cordierites; Nature, v. 286, p. 140-141.

Ashworth, J.R. and Evirgen, M.M.

1985: Plagioclase relations in pelites, central Menderes Massif, Turkey. II. Perturbation of garnet-plagioclase geobarometers; Journal of Metamorphic Geology, v. 3, p. 219-229.

Barr, S.M., Raeside, R.P., and van Breeman, O.

1987: Grenvillian basement in the northern Cape Breton Highlands, Nova Scotia; Canadian Journal of Earth Sciences, v. 24, p. 992-997.

Bateman, R.

1984: On the role of diapirism in the segregation, ascent and final emplacement of granitoid magmas; Tectonophysics, v. 110, p. 211-231.

Bellefontaine, K.A.

1987: A geochemical and petrographic study of the deformation, metamorphism, and alteration of a deformed mafic dyke from the Long Range dyke swarm, northwestern Newfoundland; B.Sc. thesis, St. Francis Xavier University, Antigonish, Nova Scotia, 91 p.

Betz, F., Jr.

1939: Geology and mineral deposits of the Canada Bay area, northern Newfoundland; Geological Survey of Newfoundland, Bulletin 16, 53 p.

1943: Late Paleozoic faulting in western Newfoundland; Geological Society of America Bulletin v. 54, p. 687-706.

Bhattacharya, A.

1986: Some geobarometers involving cordierite in the FeO-Al_2O_3-SiO_2 (+ H_2O) system: refinements, thermodynamics, calibration, and applicability in granulite facies rocks; Contributions to Mineralogy and Petrology, v. 94, p. 387-394.

Bhattacharya, A., Mazumdar, A.C., and Sen, S.K.

1988: Fe-Mg mixing in cordierite: constraints from natural data and implications for cordierite-garnet geothermometry in granulites; American Mineralogist, v. 73, p. 338-344.

Bohlen, S.R.

1987: Pressure-temperature-time paths and a tectonic model for the evolution of granulites; Journal of Geology, v. 95, p. 617-632.

Bohlen, S.R. and Essene, E.J.

1979: A critical evaluation of two-pyroxene thermometry in Adirondack granulites; Lithos, v. 12, p. 335-345.

Bohlen, S.R. and Lindsley, D.H.

1987: Thermometry and barometry of igneous and metamorphic rocks; Annual Reviews, Earth and Planetary Sciences, v. 15, p. 397-420.

Bohlen, S.R., Valley, J.W., and Essene, E.J.

1985: Metamorphism in the Adirondacks. I. Petrology, pressure and temperature; Journal of Petrology, v. 26, p. 971-992.

Bostock, H.H.

1983: Precambrian rocks of the Strait of Belle Isle area; *in* Geology of the Strait of Belle Isle area, northwestern insular Newfoundland, southern Labrador, and adjacent Quebec, Geological Survey of Canada, Memoir 400, p. 1-73.

Bryan, W.B., Finger, L.W., and Chayes, F.

1969: Estimating proportions in petrographic mixing equations by least-squares approximation; Science, v. 163, p. 926-927.

Cawood, P.A. and Williams, H.

1986: Northern extremity of the Humber Arm allochthon in the Portland Creek area, western Newfoundland, and relationships to nearby groups; *in* Current Research, Part A, Geological Survey of Canada, Paper 86-1A, p. 675-682.

Chipera, S.J. and Perkins, D.

1988: Evaluation of biotite-garnet geothermometers: application to the English River Subprovince, Ontario; Contributions to Mineralogy and Petrology, v. 98, p. 40-48.

Clifford, P.M. and Baird, D.M.

1962: Great Northern Peninsula of Newfoundland-Grenville inlier; Canadian Mining and Metallurgical Bulletin, no. 599, p. 193-223.

Coleman-Sadd, S.P.

1974: Iron deposits of the Indian Head Range; *in* Metallogeny and Plate Tectonics. A Guidebook to Newfoundland Mineral Deposits, edited by D.F. Strong, NATO Advanced Studies Institute, p. 150-158.

Collins, W.J., Beams, S.D., White, A.J.R., and Chappell, B.W.

1982: Nature and origin of A-type granites with particular reference to southeastern Australia; Contributions to Mineralogy and Petrology, v. 80, p. 189-200.

Cooper, J.R.

1937: Geology and mineral deposits of the Hare Bay area; Newfoundland Department of Natural Resources, Geology Section, Bulletin 9, 36 p.

Cumming, L.M.

1983: Lower Paleozoic autochthonous strata of the Strait of Belle Isle area; *in* Geology of the Strait of Belle Isle area, northwestern insular Newfoundland, southern Labrador and adjacent Quebec, Geological Survey of Canada, Memoir 400, p. 75-108.

Currie, K.L.

1987: A preliminary account of the geology of Harrys River map area, southern Long Range of Newfoundland; *in* Current Research, Part A, Geological Survey of Canada, Paper 87-1A, p. 653-662.

Currie, K.L. and Gittins, J.

1988: Contrasting sapphirine parageneses from Wilson Lake, Labrador; Journal of Metamorphic Geology, v. 6, p. 603-622.

Davidson, P.M. and Lindsley, D.H.

1985: Thermodynamic analysis of quadrilateral pyroxenes, Part II. Model calibrations from experiments and applications to geothermometry; Contributions to Mineralogy and Petrology, v. 91, p. 390-404.

Dewey, J.F. and Burke, K.C.A.

1973: Tibetan, Variscan, and Precambrian basement reactivation: products of continental collision; Journal of Geology, v. 81, p. 683-692.

Dunford, W.T.

1984: Geology of the Devils Room granite; B.Sc. thesis, Memorial University of Newfoundland, St. John's, Newfoundland, 121 p.

Edwards, R.L. and Essene, E.J.

1988: Pressure, temperature and C-O-H fluid fugacities across the amphibolite-granulite transition, northwest Adirondack mountains, New York; Journal of Petrology, v. 29, p. 39-72.

Erdmer, P.

1984: Summary of field work in the northern Long Range Mountains, western Newfoundland; *in* Current Research, Part A, Geological Survey of Canada, Paper 84-1A, p. 521-530.

1986a: Geology of the Long Range Inlier in the Sandy Lake map area, western Newfoundland; *in* Current Research, Part B, Geological Survey of Canada, Paper 86-1B, p. 19-27.

1986b: Geology of the Long Range Inlier in the Sandy Lake map area, western Newfoundland; Geological Survey of Canada, Open File 1310.

Erdmer, P. and Owen, J.V.

1988: The record of five orogenies in the Long Range Inlier of Newfoundland; *in* Geological Association of Canada/Mineralogical Association of Canada, Program with Abstracts, v. 13, p. A38.

Evans, J.L.

1978: An alkalic volcanic suite of the Labrador Trough, Labrador; M.Sc. thesis, Memorial University of Newfoundland, St. John's, Newfoundland.

Foley, F.C.

1937: Geology and mineral deposits of Hawke Bay-Great Harbour Deep area, northern Newfoundland; Geological Survey of Newfoundland, Bulletin 10, 22 p.

Frey, F.A., Bryan, W.B., and Thompson, G.
1974: Atlantic ocean floor: geochemistry and petrology of basalts from legs 2 and 3 of the Deep Sea Drilling Project; Journal of Geophysical Research, v. 79, p. 5507-5527.

Fritts, C.E.
1953: Geological reconnaissance across the Great Northern Peninsula of Newfoundland; Geological Survey of Newfoundland, Report 4, 22 p.

Froese, E.
1988: Discussion of "Metamorphic P-T conditions of the Kerala (South India) Khondalite Belt, a granulite facies supracrustal terrain"; Journal of Geology, v. 96, p. 383-384.

Gast, P.W.
1968: Trace element fractionation and the origin of tholeiitic and alkaline magma types; Geochimica et Cosmochimica Acta, v. 32, p. 1057-1086.

Geiger, C.A., Newton, R.C., and Kleppa, O.J.
1987: Enthalpy of mixing of synthetic almandine-grossular and almandine-pyrope garnets from high-temperature solution calorimetry; Geochimica et Cosmochimica Acta, v. 51, p. 1755-1763.

Goldsmith, J.R.
1980: The melting and breakdown reactions of anorthite at high pressures and temperatures; American Mineralogist, v. 65, p. 272-284.

Gower, C.F.
1988: Crustal formation and deformation in the Grenville Province of eastern Labrador; *in* Grenville Workshop 1988, Program with Abstracts, p. 11.

Gower, C.F. and Loveridge, W.D.
1987: Grenvillian plutonism in the eastern Grenville Province; *in* Radiogenic Age and Isotopic Studies. Report 1, Geological Survey of Canada, Paper 87-2, p. 55-58.

Gower, C.F. and Owen, V.
1984: Pre-Grenvillian and Grenvillian lithotectonic regions in eastern Labrador—correlations with the Sveconorwegian orogenic belt in Sweden; Canadian Journal of Earth Sciences, v. 21, p. 678-693.

Gower, C.F., Neuland, S., Newman, M., and Smyth, J.
1987: Geology of the Port Hope Simpson map region, Grenville Province, eastern Labrador; *in* Current Research, Newfoundland Department of Mines and Energy, Mineral Development Division, Report 87-1, p. 183-199.

Gower, C.F., Van Nostrand, T., and Smyth, J.
1988: Geology of the St. Lewis River map region, Grenville Province, eastern Labrador; *in* Current Research, Newfoundland Department of Mines, Mineral Development Division, Report 88-1, p. 59-73.

Graham, C.M. and Powell, R.
1984: A garnet-hornblende geothermometer: calibration, testing, and application to the Pelona Schist, southern California; Journal of Metamorphic Geology, v. 2, p. 13-31.

Grant, D.R.
1969a: Surficial deposits, geomorphic features, and late Quaternary history of the terminus of the Great Northern Peninsula of Newfoundland, and adjacent Quebec-Labrador; Maritime Sediments, v. 5, p. 123-125.
1969b: Late Pleistocene re-advance of Piedmont glaciers in western Newfoundland; Maritime Sediments, v. 5, p. 126-128.
1977: Altitudinal weathering zones and glacial limits in western Newfoundland, with particular reference to Gros Morne National Park; *in* Report of Activities, Part A, Geological Survey of Canada, Paper 77-1A, p. 455-463.

Grant, J.A.
1985: Phase equilibria in low-pressure partial melting of pelitic rocks; American Journal of Science, v. 285, p. 409-435.
1986: The isocon diagram—a simple solution to Gresens' equation for metasomatic alteration; Economic Geology, v. 81, p. 1976-1982.

Grenier, R. and Cawood, P.A.
1988: Variations in structural style along the Long Range Front, western Newfoundland; *in* Current Research, Part B, Geological Survey of Canada, Paper 88-1B, p. 127-133.

Greenough, J.D. and Papezik, V.S.
1986: Petrology and geochemistry of the early Mesozoic Caraquet dyke, New Brunswick, Canada; Canadian Journal of Earth Sciences, v. 23, p. 193-201.

Gresens, R.L.
1967: Composition-volume relationships of metasomatism; Chemical Geology, v. 2, p. 47-65.

Harris, N.
1981: The application of spinel-bearing metapelites to P/T determinations: an example from south India; Contributions to Mineralogy and Petrology, v. 76, p. 229-233.

Haselton, H.T., Hovis, G.L., Hemingway, B.S., and Robie, R.A.
1983: Calorimetric investigation of the excess entropy of mixing in analbite-sanidine solid solutions; lack of evidence for Na,K short-range order and implications for two-feldspar thermometry; American Mineralogist, v. 68, p. 398-413.

Hatcher, R.D.
1983: Basement massifs in the Appalachians: their role in deformation during the Appalachian orogenies; Geological Journal, v. 18, p. 255-265.

Heyl, G.R.
1937: Geology of the Sops Arm area, White Bay, Newfoundland; Newfoundland Department of Natural Resources, Geology Section, Bulletin 8, 42 p.

Heyl, A.V. and Ronan, J.J.
1954: The iron deposits of Indian Head area; *in* Contributions to the economic geology of western Newfoundland, Geological Survey of Canada, Bulletin 27, p. 42-62.

Hibbard, J. (compiler)
1983a: Geology of the Island of Newfoundland (1:1 000 000); Newfoundland Department of Mines and Energy, Map 83-106.

Hibbard, J.
1983b: Geology of the Baie Verte peninsula, Newfoundland; Newfoundland Department of Mines and Energy, Mineral Development Division, Memoir 2.

Hodges, K.V. and Royden, L.
1984: Geologic thermobarometry of retrograded metamorphic rocks: an indication of the uplift trajectory of a portion of the northern Scandinavian Caledonides; Journal of Geophysical Research, v. 89, p. 7077-7090.

Hoinkes, G.
1986: Effect of grossular-content in garnet on the partitioning of Fe and Mg between garnet and biotite; Contributions to Mineralogy and Petrology, v. 92, p. 393-399.

Holdaway, M.J.
1971: Stability of andalusite and the aluminum silicate phase diagram; American Journal of Science, v. 271, p. 97-131.

Holdaway, M.J. and Lee, S.M.
1977: Fe-Mg cordierite stability in high-grade pelitic rocks based on experimental, theoretical, and natural observations; Contributions to Mineralogy and Petrology, v. 63, p. 175-198.

Hyde, R.S.
1982: Geology of the Carboniferous Deer Lake Basin; Newfoundland Department of Mines and Energy, Mineral Development Division, Map 82-7.

Hynes, A.
1982: A comparison of amphiboles from medium- and low-pressure metabasites; Contributions to Mineralogy and Petrology, v. 81, p. 119-125.

Indares, A. and Martignole, J.
1985: Biotite-garnet geothermometry in granulite-facies rocks: evaluation of equilibrium criteria; Canadian Mineralogist, v. 23, p. 187-193.

Irvine, T.N. and Baragar, W.R.A.
1971: A guide to the chemical classification of the common volcanic rocks; Canadian Journal of Earth Sciences, v. 8, p. 523-548.

Kamo, S.L., Gower, C.F., and Krogh, T.E.
1989: Birth date for the Iapetus Ocean? A precise U-Pb zircon and baddeleyite age for the Long Range dikes, southeast Labrador; Geology, v. 17, p. 602-605.

Kindle, C.H. and Whittington, H.B.
1958: Stratigraphy of the Cow Head region, western Newfoundland; Geological Society of America Bulletin, v. 69, p. 315-342.

Klappa, C.F., Opalinski, P.R., and James, N.P.
1980: Ordovician Table Head Group of western Newfoundland: a revised stratigraphy; Canadian Journal of Earth Sciences, v. 17, p. 1007-1019.

Knight, I.

1985a: Port Saunders, Newfoundland, Mineral Occurrence Map; Newfoundland Department of Mines and Energy, Mineral Development Division, Map 85-30, scale 1:250 000.

1985b: Geological mapping of Cambrian and Ordovician sedimentary rocks of the Belleburns (12I/5 and 6), Portland Creek (12I/4) and Indian Lookout (12I/3) Map areas, Great Northern Peninsula, Newfoundland; *in* Current Research, Newfoundland Department of Mines and Energy, Mineral Development Division, Report 85-1, p. 79-88.

1987: Geology of the Roddickton (12I/16) map area; *in* Current Research, Newfoundland Department of Mines and Energy, Mineral Development Division, Report 87-1, p. 343-357.

Leake, B.E. (compiler)

1978: Nomenclature of amphiboles; Mineralogical Magazine, v. 42, p. 533-563.

Lee, H.Y. and Ganguly, J.

1988: Equilibrium compositions of coexisting garnet and orthopyroxene: experimental determinations in the system FeO-MgO-Al_2O_3-SiO_2, and applications; Journal of Petrology, v. 29, p. 93-113.

Lesher, C.M., Gibson, H.L., and Campbell, I.H.

1986: Composition-volume changes during hydrothermal alteration of andesite at Buttercup Hill, Noranda district, Quebec; Geochimica et Cosmochimica Acta, v. 50, p. 2693-2705.

Lindsley, D.H.

1983: Pyroxene thermometry: American Mineralogist, v. 70, p. 272-278.

Lindsley, D.H. and Anderson, D.J.

1983: A two-pyroxene thermometer; Proceedings of the 13th Lunar and Planetary Science Conference, Journal of Geophysical Research, Supplementary v. 88, p. A887-A906.

Lock, B.E.

1969: Silurian rocks of western White Bay area, Newfoundland; *in* North Atlantic Geology and Continental Drift, edited by M. Kay, American Association of Petroleum Geologists, Memoir 13, p. 433-442.

1972: Lower Paleozoic history of a critical area; eastern margin of the St. Lawrence Platform in White Bay, Newfoundland, Canada; 24th International Geological Congress, Montreal, Section 6, p. 310-324.

Manna, S.S. and Sen, S.K.

1974: Origin of garnet in the basic granulites around Saltora, W. Bengal, India; Contributions to Mineralogy and Petrology, v. 44, p. 195-218.

Marr, R.

1989: Petrography of a Grenvillian coronitic pluton in the Long Range Inlier, Newfoundland; B.Sc. thesis, Saint Mary's University, Halifax, Nova Scotia, 42 p.

Meyer, J.R. and Dean, P.L.

1987: Silica in western Labrador; *in* Current Research, Newfoundland Department of Mines and Energy, Mineral Development Division, Report 87-1, p. 71-76.

Montel, J.-M, Weber, C., and Pichavant, M.

1986: Biotite-sillimanite-spinel assemblages in high-grade metamorphic rocks: occurrences, chemographic analysis and thermobarometric interest; Bulletin Mineralogique, v. 109, p. 555-573.

Moody, J., Meyer, D., and Jenkins, J.E.

1983: Experimental characterization of the greenschist/amphibolite boundary in mafic systems; American Journal of Science, v. 283, p. 48-92.

Moore, J.M., Baer, A.J., and Davidson, A. (editors)

1986: The Grenville Province; Geological Association of Canada, Special Volume No. 31, 358 p.

Mueller, R.F.

1972: Stability of biotite: A discussion; American Mineralogist, v. 57, p. 300-316.

Murray, A. and Howley, J.P.

1881: Geological Survey of Newfoundland from 1864 to 1880; Edward Stanford, London, England, 536 p.

1918: Reports of Geological Survey of Newfoundland from 1881 to 1909; Robinson and Company, Ltd. Press, St. John's, Newfoundland, 725 p.

Nelson, S.J.

1955: Geology of Portland Creek, Port Saunders area, West Coast; Geological Survey of Newfoundland, Report 7, 58 p.

Newton, R.C.

1983: Geobarometry of high-grade metamorphic rocks; American Journal of Science, v. 283A, p. 1-28.

Newton, R.C. and Haselton, H.T.

1981: Thermodynamics of the garnet-plagioclase-Al_2SiO_5-quartz geobarometer; *in* Thermodynamics of Minerals and Melts, edited by R.C. Newton, A. Navrotsky, and B.J. Wood, Advances in Physical Geochemistry, v. 1, Springer-Verlag, New York, p. 131-147.

Newton, R.C. and Perkins, D.

1982: Thermodynamic calibration of geobarometers based on the assemblages garnet-plagioclase-orthopyroxene-(clinopyroxene)-quartz; American Mineralogist, v. 67, p. 203-222.

O'Neill, H.-St.C. and Wood, B.J.

1979: An experimental study of Fe-Mg partitioning between garnet and olivine and its calibration as a geothermometer; Contributions to Mineralogy and Petrology, v. 70, p. 59-70.

Owen, J.V.

1986a: Geology of the Silver Mountain area, western Newfoundland; *in* Current Research, Part A, Geological Survey of Canada, Paper 86-1A, p. 515-522.

1986b: Geology of the Silver Mountain area; Geological Survey of Canada, Open File 1279.

1987: Geology of the central part of the Long Range Inlier, western Newfoundland; Geological Survey of Canada, Open File 1505.

1989: Géologie de la région du Lac Lief (Territoire du Nouveau-Québec); Ministère de L'Énergie et des Ressources (Québec), ET87-18, 48 pp.

Owen, J.V.

in press: Cordierite + spinel parageneses in pelitic gneiss from the contact aureoles of the Mistastin batholith (Quebec) and the Taylor Brook gabbro complex (Newfoundland). Canadian Journal of Earth Sciences.

Owen, J.V. and Currie, K.L.

in press: The Disappointment Hill complex: Proterozoic granulites in southwestern Newfoundland; Transactions of the Royal Society of Edinburgh.

Owen, J.V. and Erdmer, P.

1986: Precambrian and Paleozoic metamorphism in the Long Range Inlier, western Newfoundland; *in* Current Research, Part B, Geological Survey of Canada, Paper 86-1B, p. 29-38.

1988: The Grenvillian Long Range Inlier of the Great Northern Peninsula, Newfoundland; Geological Association of Canada, Field Trip Guidebook (Trip B7), 36 p.

1989: Metamorphic geology and regional geothermobarometry of a Grenvillian massif: the Long Range Inlier, western Newfoundland; Precambrian Research, v. 43, p.79-100.

in press: Middle Proterozoic geology of the Long Range Inlier, Newfoundland: regional significance and tectonic implications; *in* Middle Proterozoic Geology of Proto-Laurentia-Baltica, edited by C.F. Gower, T. Rivers, and A.B. Ryan, Geological Association of Canada, Special Paper.

Owen, J.V., Campbell, J.E.M., and Dennis, F.A.R.

1987: Geology of the Lake Michel area, Long Range Inlier, western Newfoundland; *in* Current Research, Part A, Geological Survey of Canada, Paper 87-1A, p. 643-652.

Owen, J.V., Greenough, J.D., and Bellefontaine, K.A.

1989: Preservation of primary geochemical signatures in polymetamorphosed tholeiite: the Long Range dyke swarm, Newfoundland; Lithos, v. 24, p. 55-64.

Owen, J.V. and Machin, D.C.

1987: Petrography and geochemistry of some mafic dykes in the Long Range Inlier, western Newfoundland; *in* Current Research, Part A, Geological Survey of Canada, Paper 87-1A, p. 305-316.

Owen, J.V. and Marr, R.A.

in press: Contrasting garnet parageneses in a composite Grenvillian granitoid pluton, Newfoundland; Mineralogical Magazine, v. 54.

Owen, J.V., Rivers, T., and Gower, C.F.

1986: The Grenville Front on the Labrador coast; *in* The Grenville Province, edited by J.M. Moore, A. Davidson, and A.J. Baer, Geological Association of Canada, Special Paper 31, p. 95-106.

Oxley, P.

1953: Geology of Parsons Pond-St. Pauls area, west coast; Geological Survey of Newfoundland, Report 5, 53 p.

Papezik, V.S. and Hodych, J.P.

1980: Early Mesozoic diabase dikes of the Avalon Peninsula, Newfoundland: petrochemistry, mineralogy, and origin; Canadian Journal of Earth Sciences, v. 17, p. 1417-1430.

Papezik, V.S., Greenough, J.D., Colwell, J.A., and Mallinson, T.J.
1988: North Mountain basalt from Digby, Nova Scotia: Models for a fissure eruption from stratigraphy and petrochemistry; Canadian Journal of Earth Sciences, v. 25, p. 74-83.

Paterson, S.R., Vernon R.H., and Tobisch, O.T.
1989: A review of criteria for the identification of magmatic and tectonic foliations in granitoids; Journal of Structural Geology, v. 11, p. 349-363.

Pattison, D. and Harte, B.
1985: A petrogenetic grid for pelites in the Ballachulish and other Scottish thermal aureoles; Journal of the Geological Society of London, v. 142, p. 7-28.

Pearce, J.A., Harris, N.B.W., and Tindle, A.G.
1984: Trace element discrimination diagrams for the tectonic interpretation of granitic rocks; Journal of Petrology, v. 25, p. 956-983.

Perchuk, L.L. and Lavrent'eva, I.V.
1983: Experimental investigation of exchange equilibria in the system cordierite-garnet-biotite: *in* Kinetics and Equilibrium in Mineral Reactions, edited by S.K. Saxena, Springer, Berlin, Heidelberg, New York, p. 199-239.

Perchuk, L.L., Aranovich, L.Y., Podlesskii, K.K., Lavrent'eva, I.V., Gerasimov, V.Y., Fed'kin, V.V., Kitsul, V.I., Karsakov, L.P., and Berdnikov, N.V.
1985: Precambrian granulites of the Aldan shield, eastern Siberia, USSR; Journal of Metamorphic Geology, v. 3, p. 265-310.

Perkins, D. and Chipera, S.J.
1985: Garnet-orthopyroxene-plagioclase-quartz barometry: refinement and application to the English River Subprovince and the Minnesota River Valley; Contributions to Mineralogy and Petrology, v. 89, p. 69-80.

Perreault, S. and Martignole, J.
1988: High-temperature cordierite migmatites in the northeastern Grenville Province; Journal of Metamorphic Geology, v. 6, p. 673-696.

Philpotts, J.A. and Schnetzler, C.C.
1970: Phenocryst-matrix partition coefficients for K, Rb, Sr and Ba with applications to anorthosite and basalt genesis; Geochimica et Cosmochimica Acta, v. 34, p. 307-322.

Pitcher, W.S.
1983: Granite type and tectonic environment; *in* Mountain Building Processes, edited by K.J. Hsu, Academic Press, London, p. 19-40.

Powell, R.
1985: Regression diagnostics and robust regression in geothermometer/geobarometer calibration: the garnet-clinopyroxene geothermometer revisited; Journal of Metamorphic Geology, v. 3, p. 231-243.

Powers, R.E. and Bohlen, S.R.
1985: The role of synmetamorphic igneous rocks in the metamorphism and partial melting of metasediments, northwest Adirondacks; Contributions to Mineralogy and Petrology, v. 90, p. 401-409.

Pringle, I.R., Miller, J.A., and Warrell, D.M.
1971: Radiometric age determinations from the Long Range Mountains, Newfoundland; Canadian Journal of Earth Sciences, v. 8, p. 1325-1330.

Raeside, R.P., Barr, S.M., White, C.E., and Dennis, F.A.R.
1986: Geology of the northernmost Cape Breton Highlands, Nova Scotia; *in* Current Research, Part A, Geological Survey of Canada, Paper 86-1A, p. 291-296.

Rao, M.V.S. and Rao, V.D.
1988: Chemical constraints on the origin of the charnockites in the eastern Ghat mobile belt, India; Chemical Geology, v. 69, p. 37-48.

Reynolds, P.H., Zentilli, M., Jamieson, R.A., and Owen, J.V.
1988: Cooling history of the Long Range Inlier, Newfoundland: Argon/Argon and fission-track thermochronometry; *in* Lithoprobe East-report of transect meeting Oct. 21-22, 1988, held at Memorial University of Newfoundland, p. 37-40.

Robinson, P., Spear, F.S., Schumacher, J.C., Laird, J., Klein, C., Evans, B.W., and Doolan, B.L.
1982: Phase relations of metamorphic amphiboles: natural occurrence and theory; *in* Amphiboles: Petrology and Experimental Phase Relations, edited by D.R. Veblen and P.H. Ribbe, Mineralogical Society of America, Reviews in Mineralogy, v. 9B, p. 1-227.

Rogers, J.J.W.
1988: The Arsikere granite of southern India: magmatism and metamorphism in a previously depleted crust; Chemical Geology, v. 67, p. 155-163.

Saunders, C.M. and Tuach, J.
1988: K-feldspathization, albitization and gold mineralization in granitoid rocks: the Rattling Brook alteration system, western White Bay, Newfoundland; *in* Current Research, Newfoundland Department of Mines, Mineral Development Division, Report 88-1, p. 307-317.

Sawyer, E.W.
1987: The role of partial melting and fractional crystallization in determining discordant migmatite leucosome compositions; Journal of Petrology, v. 28, p. 445-473.

Schärer, U., Krogh, T.E., and Gower, C.F.
1986: Age and evolution of the Grenville Province in eastern Labrador from U-Pb systematics in accessory minerals; Contributions to Mineralogy and Petrology, v. 88, p. 64-71.

Schuchert, C. and Dunbar, C.O.
1934: Stratigraphy of western Newfoundland; Geological Society of America, Memoir 1, 123 p.

Sen, S.K. and Bhattacharya, A.
1984: An orthopyroxene-garnet thermometer and its application to the Madras charnockites; Contributions to Mineralogy and Petrology, v. 88, p. 64-71.

Smyth, W.R. and Schillereff, S.
1982: The pre-Carboniferous geology of southwest White Bay; *in* Current Research, Newfoundland Department of Mines and Energy, Mineral Development Division, Report 82-1, p. 78-98.

Spear, F.S.
1981: An experimental study of hornblende stability and compositional variability in amphibole; American Journal of Science, v. 281, p. 697-734.

Streckeisen, A.
1976: To each plutonic rock its proper name; Earth-Science Reviews, v. 13, p. 1-33.

Strong, D.F.
1974: Plateau lavas and diabase dikes of northwestern Newfoundland; Geological Magazine, v. 111, p. 501-514.

Strong, D.F. and Williams, H.
1972: Early Paleozoic flood basalts of northwestern Newfoundland: their petrology and tectonic significance; Proceedings, Geological Association of Canada, v. 24, p. 43-53.

Stukas, V. and Reynolds, P.H.
1974: ^{40}Ar/^{39}Ar dating of the Long Range dikes, Newfoundland; Earth and Planetary Science Letters, v. 22, p. 256-266.

Thomas, A., Nunn, G.A.G., and Krogh, T.E.
1986: The Labradorian Orogeny: evidence for a newly identified 1600 to 1700 Ma orogenic event in Grenville Province crystalline rocks from central Labrador; *in* The Grenville Province, edited by J.M. Moore, A. Davidson, and A.J. Baer, Geological Association of Canada, Special Paper, v. 31, p. 175-189.

Thompson, A.B.
1976: Mineral reactions in pelitic rocks. I. Predictions of P-T-X (Fe-Mg) phase relations. II. Calculation of some P-T-X (Fe-Mg) phase relations; American Journal of Science, v. 276, p. 425-454.

Triboulet, C. and Audren, C.
1988: Controls on P-T-t deformation path from amphibole zonation during progressive metamorphism of basic rocks (estuary of the River Vilaine, South Brittany, France); Journal of Metamorphic Geology, v. 6, p. 117-133.

Tuach, J.
1986: Metallogeny of Newfoundland granites—studies in the western White Bay area and on the southwest coast; *in* Current Research, Newfoundland Department of Mines and Energy, Mineral Development Division, Report 86-1, p. 27-38.
1987: Mineralized environments, metallogenesis, and the Doucers Valley Fault complex, western White Bay: a philosophy for gold exploration in Newfoundland; *in* Current Research, Report 87-1, Newfoundland Department of Mines and Energy, Mineral Development Division, p. 129-144.

Tuach, J. and French, V.A.
1986: Gold mineralization of possible late Precambrian age in the Jackson's Arm area (12H/15), White Bay, Newfoundland; *in* Current Research, Report 86-1A, Newfoundland Department of Mines and Energy, Mineral Development Division, Report 86-1.

Tuach, J., Dean, P.L., Swinden, H.S., O'Driscoll, C.F., Kean, B.F., and Evans, D.T.W.

1988: Gold mineralization in Newfoundland: a 1988 review; *in* Current Research, Newfoundland Department of Mines and Energy, Mineral Development Division, Report 88-1, p. 279-306.

Undershultz, J.

1986: Geology of a supracrustal slice in the Long Range Inlier, Cat Arm dam area, western Newfoundland; B.Sc. thesis, University of Alberta, Edmonton, Alberta, 30 p.

van Berkel, J.T.

1987: Geology of the Dashwoods Pond, St. Fintan's and Main Gut map areas, southwest Newfoundland; *in* Current Research, Part A, Geological Survey of Canada, Paper 87-1A, p. 399-408.

Vanderveer, D.G. and Taylor, D.M.

1987: Quaternary mapping — glacial-dispersal studies, Sops Arm area, Newfoundland; *in* Current Research, Newfoundland Department of Mines and Energy, Mineral Development Division, Report 87-1, p. 31-38.

Vernon R.F. and Collins, W.J.

1988: Igneous microstructures in migmatites; Geology, v. 16, p. 1126-1129.

Walthier, T.N.

1949: Geology and mineral deposits of the area between Corner Brook and Stephenville, western Newfoundland; Newfoundland Geological Survey, Bulletin 35, Part 1.

Wanless, R.K., Stevens, R.D., Lachance, G.R., and Delabio, R.N.

1973: Age determinations and geological studies, K-Ar isotopic ages, report 11; Geological Survey of Canada, Paper 73-2.

Weaver, D.F.

1967: A geological interpretation of the Bouguer anomaly field of Newfoundland; Dominion Observatory Canada, v. 25, p. 228-250.

Whalen, J.B., Currie, K.L., and Chappell, B.W.

1987: A-type granites: geochemical characteristics, discrimination and petrogeneses; Contributions to Mineralogy and Petrology, v. 95, p. 407-419.

Williams, H.

1973: Bay of Islands map area, Newfoundland; Geological Survey of Canada, Paper 72-34, 7 p.

1975: Structural succession, nomenclature and interpretation of transported rocks in western Newfoundland; Canadian Journal of Earth Sciences, v. 12, p. 1874-1894.

1977: The Coney Head Complex: another Taconic Allochthon in west Newfoundland; American Journal of Science, v. 277, p. 1279-1295.

Williams, H. (compiler)

1978: Tectonic lithofacies map of the Appalachian Orogen; Memorial University of Newfoundland, Map No. 1 (1:1 000 000).

Williams, H. and Erdmer, P.

1986: Long Range Inlier of western Newfoundland (abstract); Northeastern Section, Geological Society of America, Abstracts with Programs, v. 18, p. 75.

Williams, H. and Haworth, R.T. (compilers)

1984a: Magnetic anomaly map of Atlantic Canada; Memorial University of Newfoundland, Map No. 5 (1:2 000 000).

1984b: Bouguer gravity map of Atlantic Canada; Memorial University of Newfoundland, Map No. 6 (1:2 000 000).

Williams, H. and Stevens, R.K.

1969: Geology of Belle Isle—northern extremity of the deformed Appalachian miogeosynclinal belt; Canadian Journal of Earth Sciences, v. 6, p. 1145-1157.

Williams, H., James, N.P., and Stevens, R.K.

1985: Humber Arm allochthon and nearby groups between Bonne Bay and Portland Creek, western Newfoundland; *in* Current Research, Part A, Geological Survey of Canada, Paper 85-1A, p. 399-406.

Windley, B.F.

1986: Comparative tectonics of the western Grenville and western Himalaya; *in* The Grenville Province, edited by J.M. Moore, A. Davidson, and A.J. Baer, Geological Survey of Canada, Special Paper v. 31, p. 341-348.

Winkler, H.G.F.

1979: Petrogenesis of Metamorphic Rocks (4th edition); Springer-Verlag, New York.

Wood, B.J. and Banno, S.

1973: Garnet-orthopyroxene and orthopyroxene-clinopyroxene thermometry in simple and complex systems; Contributions to Mineralogy and Petrology, v. 42, p. 1109-124.

Woodard, H.H.

1957: Geology of Port Saunders-Castor River area, west coast; Geological Survey of Newfoundland, Report 10, 45 p.

APPENDIX I

Analytical methods

Mineral compositions in samples with BRA and VO-87 prefixes were determined using a JEOL Superprobe 733 equipped with four wavelength dispersive spectrometers and one energy dispersive spectrometer, and operated with a beam current of 15 kV at 5 nanoamps. Data were reduced using ZAF corrections. The remaining samples were analyzed with a JEOL JXA-50A microprobe with three wavelength dispersive spectrometers, operated at 15 kV and 22 nanoamps. Bence-Albee corrections were employed in data reduction. Accuracy and precision were evaluated by comparing microprobe analyses of amphibole standards K-HB and SC-HB:

	SC-HB			K-HB		
	Published value	Probe value	sd	Published value	Probe value	sd
SiO_2	40.60	40.63	0.25	40.37	41.57	0.22
TiO_2	4.70	4.89	0.03	4.72	4.51	0.04
Al_2O_3	13.70	12.91	0.07	14.90	14.06	0.11
FeO	15.77	15.70	0.23	10.92	10.60	0.09
MnO	0.28	0.19	0.02	0.09	0.08	0.02
MgO	9.84	9.58	0.18	12.80	12.56	0.09
CaO	10.10	10.27	0.07	10.30	10.08	0.08
Na_2O	3.11	2.98	0.04	2.05	2.01	0.04
K_2O	1.14	1.15	0.04	2.05	2.01	0.04
n =		5			9	

sd = one standard deviation

The concentrations of major elements (except FeO, determined by rapid chemical methods) and selected trace elements (Ba, Nb, Rb, Sr, Y, and Zr) were determined by X-ray fluorescence (XRF) dispersive analysis on fused pellets at the Analytical Chemistry Section of the Geological Survey of Canada, Ottawa. V, Cr, Ni, Cu, Ga, and Zn were determined by ICP-MS and/or by DCP. Ferric iron was estimated by using $Fe_2O_3 = Fe_2O_3$(total, XRF) -1.11134*FeO(volumetric).

For concentrations represented by the analyzed samples, absolute error (in wt. %), taken to be equivalent to the detection limit, is as follows: SiO_2 (0.40), TiO_2 (0.02), Al_2O_3 (0.40), Fe_2O_3 (0.10), FeO (0.20), MnO (0.01), MgO (0.10), CaO (0.10), Na_2O (0.50), K_2O (0.05), P_2O_5 (0.02), Ba (0.002), Nb (0.003), Rb (0.002), Sr (0.002), Y (0.003), and Zr (0.002). Detection limit (in ppm) for the remaining elements is as follows: Ga (1), La (0.1), and Yb (0.05).

Trace element concentrations reported for the Potato Hill pluton (Appendix III) were determined by XRF on fused pellets at Saint Mary's University (SMU), Halifax. Ba, Rb, Sr, Y and Zr were also determined for the same samples by the Geological Survey of Canada (GSC) laboratory. Considerable between-laboratory discrepancies exist for the two data sets. Compared with the GSC data, the SMU results are 10 % higher for Ba, and 20 to 30 % lower for Zr and Y. These results fall well outside the range of analytical error reported by both laboratories. Direct comparison of the trace element data for the Lake Michel intrusive suite and the Potato Hill pluton reported in Appendix III is therefore unwarranted. For this reason, analytical data for both complexes are not presented on the same diagrams in the text.

The results for Rb and Sr fall within the error limits reported by both laboratories.

APPENDIX II

Microprobe Mineral Analyses

The unit name is indicated after each sample number. "c" and "r" denote core and rim analysis, respectively. "m" denotes matrix phase, and "i" denotes mineral inclusion (in garnet). Abbreviations used here and in the text are: amph-amphibole, ap-apatite, bi-biotite, cd-cordierite, chl-chlorite, ct-carbonate (calcite and/or dolomite), cpx-clinopyroxene, ep-epidote, fo-forsterite, gd-gedrite, gp-graphite, gt-garnet, hc-hercynite, hbl-hornblende, ilm-ilmenite, Ksp-potassium feldspar, mt-magnetite, mu-muscovite, opx-orthopyroxene, ph-phlogopite, pl-plagioclase, qz-quartz, scp-scapolite, sil-sillimanite, sl-salite, sp-spinel, sph-sphene, ti-titanite, wol-wollastonite, zr-zircon. Total Fe as FeO.

VO-85-024 (Ppn-adjacent to Taylor Brook gabbro complex)

	cd(r)	cd(c)	gt(r)	gt(c)	bi(m)	opx(m)	cd(m)	sp	pl	mt
SiO_2	49.96	49.75	39.05	38.57	35.95	48.60	50.64	0.76	58.34	
TiO_2			0.07	0.04	5.30	0.20		0.07		0.64
Al_2O_3	31.34	31.35	21.02	20.73	14.96	4.68	31.57	52.98	24.72	0.53
FeO	6.67	7.81	31.30	32.09	21.02	31.64	9.20	38.30	0.80	92.33
MnO	0.17	0.20	2.68	2.45	0.11	1.04	0.37	0.41		0.06
MgO	9.59	9.05	5.71	6.07	9.35	14.16	8.43	3.44		
CaO			1.13	1.26		0.12			8.70	
Na_2O	0.04	0.10			0.12	0.03	0.01		6.79	
K_2O					9.66				0.42	
	97.8	98.3	100.9	101.2	96.5	100.5	100.2	95.9	99.8	93.6

VO-85-503 (garnetiferous Pgn)

	bi(m)	bi(i)	gt(c)	pl
SiO_2	37.03	37.86	39.50	63.64
TiO_2	2.77	2.77	0.03	0.08
Al_2O_3	16.71	16.39	22.14	24.66
FeO	18.75	16.51	30.55	
MnO	0.04	0.03	1.00	
MgO	11.87	14.13	8.15	
CaO			1.43	5.62
Na_2O	0.06	0.05		8.59
K_2O	9.85	9.57		0.29
	96.9	97.4	102.9	102.9

VO-85-574 (garnetiferous Pgn)

	bi(m)	bi(i)	gt(r)	gt(c)	pl
SiO_2	37.39	37.41	39.96	40.02	64.36
TiO_2	2.81	2.65	0.05	0.05	0.05
Al_2O_3	16.73	17.09	22.49	22.12	24.60
FeO	14.93	12.98	27.69	28.02	0.06
MnO	0.03		0.66	0.65	
MgO	13.80	15.66	10.23	10.37	
CaO		0.05	1.21	1.24	5.31
Na_2O	0.05	0.15		0.02	7.69
K_2O	9.22	9.12			0.20
	95.0	95.2	101.7	102.5	102.3

VO-85-617 (garnetiferous Pgn)

	gt(c)	gt(r)	bi	bi(m)	gt(m)	pl
SiO_2	38.28	37.66	34.67	35.12	38.13	63.23
TiO_2	0.05	0.05	4.33	4.58	0.04	
Al_2O_3	20.98	20.95	14.64	14.79	20.90	23.43
FeO	34.75	36.40	27.79	28.37	34.40	0.09
MnO	0.96	1.17	0.04	0.04	0.95	
MgO	2.62	1.21	5.62	4.91	2.38	
CaO	5.03	4.79	0.02	0.04	5.21	4.85
Na_2O		0.08		0.05	0.02	8.31
K_2O			8.28	8.19		0.19
	102.7	102.4	95.4	96.1	104.6	100.1

VO-85-659-1 (Ppn)

	gt(c)	bi(m)	gt(c)	bi(m)	sp	pl
SiO_2	40.06	36.35	39.95	36.63	0.03	61.65
TiO_2	0.02	5.19	0.05	5.23		0.02
Al_2O_3	22.48	17.07	22.25	16.93	58.71	25.52
FeO	30.73	17.34	31.65	16.86	32.97	0.05
MnO	0.50	0.02	0.56	0.04	0.12	
MgO	8.55	11.40	7.27	10.86	6.05	
CaO	1.18		1.30		0.02	6.83
Na_2O	0.02	0.14		0.06		7.43
K_2O		9.50		9.35		0.21
	103.6	97.1	103.1	96.1	97.9	101.4

VO-85-685 (garnetiferous Pgn)

	bi(m)	gt(c)	gt(r)	pl
SiO_2	38.95	39.94	39.21	67.13
TiO_2	2.78	0.05	0.04	0.03
Al_2O_3	16.86	22.30	21.94	23.50
FeO	14.37	28.38	33.48	0.13
MnO	0.02	0.49	0.58	
MgO	14.59	10.51	7.21	
CaO		1.04	0.85	3.86
Na_2O	0.05		0.04	7.99
K_2O	9.02			0.18
	96.7	102.8	103.4	102.8

VO-85-879 (garnetiferous Pgn)

	gt(c)	gt(r)	bi(m)	bi(m)	bi(m)	pl
SiO_2	40.20	39.07	37.78	37.65	37.54	60.24
TiO_2	0.08	0.06	4.60	5.27	5.45	0.02
Al_2O_3	22.39	21.67	15.91	15.35	15.58	25.96
FeO	28.91	31.22	17.25	17.56	17.84	0.07
MnO	0.66	1.11	0.02	0.03	0.03	
MgO	7.98	5.64	12.32	12.11	12.05	
CaO	2.79	2.93				7.79
Na_2O	0.04	0.02	0.07	0.05	0.02	7.01
K_2O			9.23	9.24	9.22	0.19
	103.1	101.8	97.2	97.4	97.7	101.3

VO-85-946 (Ptn)

	opx(c)	opx(r)	gt(c)	gt(r)	pl
SiO_2	48.20	50.98	39.19	39.31	58.63
TiO_2	0.07	0.02			
Al_2O_3	2.59	1.83	21.69	21.51	25.72
FeO	27.73	28.45	30.80	31.96	0.18
MnO	0.26	0.32	0.97	0.92	
MgO	16.93	17.70	6.38	6.00	
CaO	0.38	0.20	3.01	2.35	8.25
Na_2O	0.04	0.02	7.13		7.13
K_2O	0.09				0.09
	96.2	99.5	102.0	102.0	100.0

VO-86-110 (coronitic Ptn)

	matrix			corona			matrix			
	cpx	gt	cpx	gt(r)	cpx(r)	cpx(c)	pl(c)	pl(r)	opx	cpx
SiO_2	49.96	38.46	48.87	37.47	49.92	49.02	61.65	63.11	46.95	47.35
TiO_2	0.13		0.15		0.11	0.18			0.08	0.13
Al_2O_3	0.89	20.10	0.92	19.77	0.96	0.97	23.56	22.80	0.36	1.10
FeO	26.08	32.27	29.87	32.30	25.00	27.49	0.05	0.14	46.97	26.36
MnO	0.78	2.19	0.60	2.82	0.49	0.62			1.51	0.78
MgO	3.21	0.62	3.46	0.56	3.29	3.49			3.83	3.19
CaO	19.63	7.50	16.14	7.49	18.73	19.20	6.04	4.96	0.93	19.72
Na_2O	0.40		0.33		0.35	0.45	8.23	8.83	0.02	0.52
K_2O							0.27	0.12		
	101.1	101.1	100.4	100.4	98.6	101.4	99.8	100.0	100.6	99.1

VO-86-111 (Ptn)

	gt(c)	gt(r)	opx(r)	opx(c)	gt(c)	gt(r)	bi	bi(m)	pl
SiO_2	39.23	39.04	51.54	50.15	38.60	38.42	36.89	37.42	59.46
TiO_2		0.03	0.07	0.10			5.47	5.26	
Al_2O_3	21.47	21.04	1.25	2.14	21.43	20.99	14.37	14.21	24.79
FeO	32.20	32.90	30.50	30.81	32.33	32.35	18.35	18.77	0.04
MnO	1.02	1.16	0.30	0.39	1.03	1.06	0.04	0.03	
MgO	5.39	4.69	16.93	16.46	5.36	5.03	11.10	11.15	
CaO	2.60	3.00	0.25	0.38	2.67	2.88			7.34
Na_2O			0.06	0.04			0.13	0.08	7.55
K_2O							9.26	9.59	0.51
	101.9	101.8	100.9	100.5	101.4	100.7	95.6	96.5	99.7

VO-86-113-2 (Ptn)

	opx(c)	opx(r)	gt(c)	gt(r)	pl	bi
SiO_2	49.17	49.45	38.45	38.56	57.07	37.04
TiO_2	0.12	0.08	0.04			5.45
Al_2O_3	0.61	0.93	20.64	20.49	26.57	16.54
FeO	39.49	39.31	30.68	31.96	0.06	14.57
MnO	0.36	0.44	1.06	1.14		
MgO	10.31	10.24	2.60	1.86		11.97
CaO	1.60	0.99	6.69	7.55	9.40	
Na_2O	0.06	0.06			6.23	0.15
K_2O					0.20	9.26
	101.7	101.5	100.0	101.5	99.5	95.0

VO-86-115 (Ptn)

	gt(c)	gt(r)	opx(r)	opx(c)	pl
SiO_2	36.79	36.84	47.15	48.21	59.83
TiO_2			0.08	0.09	
Al_2O_3	20.40	20.31	0.52	0.52	24.26
FeO	34.00	33.80	38.81	41.11	0.07
MnO	1.49	1.29	0.42	0.48	
MgO	2.01	1.67	9.24	9.21	
CaO	5.17	5.82	0.74	0.75	6.35
Na_2O					7.79
K_2O					0.27
	99.9	99.8	97.0	100.4	98.6

VO-86-271 (Ppn)

	gt(c)	bi(m)	pl
SiO_2	39.42	37.27	60.16
TiO_2		4.88	
Al_2O_3	21.46	14.65	24.31
FeO	30.33	16.25	0.05
MnO	0.56		
MgO	7.78	12.49	
CaO	1.56		7.00
Na_2O		0.06	7.32
K_2O		9.56	0.26
	101.1	95.1	99.1

VO-86-279 (Ptn)

	bi	gt(c)	gt(r)	opx(r)	opx(c)	pl
SiO_2	37.29	38.99	39.83	49.71	50.02	62.72
TiO_2	4.45			0.06	0.10	
Al_2O_3	14.85	21.14	19.90	2.24	1.97	23.09
FeO	17.06	32.63	33.76	28.15	27.75	0.06
MnO		0.66	0.72	0.19	0.16	
MgO	12.02	6.23	5.33	17.21	17.88	
CaO		1.62	1.69	0.22	0.21	5.04
Na_2O	0.05				0.12	8.67
K_2O	9.24					0.16
	94.9	101.3	101.2	97.8	98.2	99.7

VO-86-291 (Ptn)

	opx	pl	bi	gt
SiO_2	50.63	60.51	36.81	38.21
TiO_2	0.06		3.88	
Al_2O_3	1.90	23.83	14.70	21.22
FeO	29.07	0.12	17.39	31.64
MnO	0.19			0.52
MgO	17.19		11.36	6.45
CaO	0.20	6.30		1.87
Na_2O		7.66		
K_2O		0.27	9.24	
	99.2	98.7	93.4	99.9

VO-86-164-3 (Ppn)

	gt(m)	bi(m)	pl	gt(r)	gt(c)
SiO_2	38.34	35.69	65.21	37.91	39.65
TiO_2		3.57			0.02
Al_2O_3	21.23	16.50	21.80	20.64	21.01
FeO	33.32	17.45	0.03	30.41	31.99
MnO	0.97	0.03		0.84	0.95
MgO	6.54	10.39		7.88	7.04
CaO	0.39		3.20	0.40	0.45
Na_2O		0.14	9.83		
K_2O		9.13	0.17		
	100.8	92.9	100.2	98.1	101.1

VO-86-355-1 (Ppn; pelites next to Hooping Harbour satellite pluton)

	gt(c)	gt(r)	bi(m)	gt(m)	mu
SiO_2	37.02	36.99	33.76	37.42	43.56
TiO_2			2.77		0.84
Al_2O_3	20.92	20.63	16.85	20.91	31.73
FeO	34.62	35.73	24.84	35.60	2.76
MnO	1.70	2.73	0.03	2.12	0.06
MgO	3.39	2.27	6.22	3.04	0.52
CaO	1.76	1.38		1.42	
Na_2O			0.14		0.38
K_2O			8.77		9.44
	99.4	99.8	93.4	100.51	89.3

VO-86-355-2A

	gt(m)	bi(m)	pl	mu
SiO_2	37.10	33.97	57.20	44.27
TiO_2		2.81		0.41
Al_2O_3	21.12	17.43	24.41	31.62
FeO	37.26	23.74	0.07	3.09
MnO	0.71			0.02
MgO	3.45	6.65		0.84
CaO	1.18		6.39	
Na_2O		0.11	8.89	0.27
K_2O		8.89	0.09	9.57
	100.8	93.6	97.1	87.0

VO-86-355-2B

	pl	gt(m)	gt(m)*	bi(m)
SiO_2	68.07	37.95	36.80	34.98
TiO_2		3.07		2.75
Al_2O_3	20.14	20.75	21.00	18.47
FeO		37.32	38.22	23.55
MnO		0.50	0.63	
MgO		3.04	2.11	6.33
CaO	0.38	1.36	1.26	
Na_2O	12.07			0.09
K_2O	0.11	9.11		9.19
	100.8	100.9	100.1	65.4

* core of xenomorphic matrix grain

VO-86-355-3

	pl(c)	bi(m)	mu
SiO_2	59.33	35.30	44.39
TiO_2		2.25	0.39
Al_2O_3	23.87	17.76	32.21
FeO	0.04	22.55	3.20
MnO		0.12	
MgO		7.14	0.57
CaO	5.99		
Na_2O	8.01	0.10	0.34
K_2O	0.16	8.80	9.66
	97.4	94.0	90.8

VO-86-355-6A (Ppn)

	pl	gt	bi
SiO_2	62.05	37.34	34.36
TiO_2			2.31
Al_2O_3	23.20	20.73	17.39
FeO	0.04	30.68	21.07
MnO		6.86	0.18
MgO		3.24	8.54
CaO	5.39	1.03	
Na_2O	8.92		0.11
K_2O	0.24		8.70
	99.8	99.9	92.7

VO-86-451-2 (Ppn)

	gt(c)	bi	cd	gt	opx	pl
SiO_2	37.83	36.20	48.84	37.45	49.11	65.97
TiO_2		3.13			0.09	
Al_2O_3	21.78	16.06	32.04	21.61	3.72	21.83
FeO	30.89	15.14	5.46	31.16	27.73	
MnO	0.91		0.06	0.95	0.25	
MgO	8.45	13.04	10.13	8.36	18.48	
CaO	0.29			0.45	0.03	2.47
Na_2O		0.10				10.84
K_2O		9.03				0.13
	100.2	92.7	96.5	100.0	99.4	101.2

VO-86-484-2 (Ppn)

	gt(c)	gt(r)	cd(r)	cd(c)	bi(m)	cd(m)	cd(c)	cd(r)	gt(r)	gt(c)
SiO_2	37.65	37.64	48.46	48.55	35.07	47.73	49.02	48.48	38.85	38.18
TiO_2					3.19					
Al_2O_3	20.77	20.60	31.56	31.52	17.59	31.89	31.75	31.73	20.90	20.98
FeO	35.78	35.70	7.48	8.36	19.66	9.13	9.41	8.56	36.94	37.45
MnO	0.51	0.47	0.03	0.03	0.03	0.03	0.06	0.04	0.51	0.45
MgO	4.06	4.06	8.75	8.40	9.43	8.04	7.58	8.17	3.60	3.54
CaO	1.08	1.05	0.04							
Na_2O			0.14	0.07	0.09	0.15	0.08	0.09		
K_2O					9.43					
	99.9	99.5	96.5	96.9	94.5	97.0	97.9	97.1	100.8	100.6

VO86-825-3 (Ppn)

	opx	pl	bi	gt
SiO_2	48.64	63.21	36.16	38.16
TiO_2	0.06		4.54	
Al_2O_3	1.48	23.25	14.75	21.19
FeO	34.06	0.04	20.87	33.34
MnO	0.55		0.05	1.24
MgO	14.27		9.61	5.07
CaO	0.15	4.61		1.32
Na_2O	0.02	8.69	0.11	
K_2O		0.20	9.52	
	99.2	100.0	95.6	100.3

VO-86-2277 (Ppn)

	gt(m)	gt(c)	gt(r)	bi(m)	pl
SiO_2	37.68	37.50	37.97	35.67	60.66
TiO_2		0.02	4.11		
Al_2O_3	21.29	21.09	20.92	16.80	23.91
FeO	34.84	35.01	35.95	19.94	0.03
MnO	1.73	1.80	2.12	0.04	
MgO	4.07	3.53	2.94	8.63	
CaO	1.30	1.22	1.22		5.76
Na_2O				0.07	8.40
K_2O				9.65	0.29
	100.9	100.2	101.1	94.9	99.1

VO-86-2279 (Ppn)

	gt(c)	bi(m)	pl
SiO_2	39.46	38.81	58.68
TiO_2		4.64	
Al_2O_3	21.86	14.91	24.57
FeO	28.27	13.80	0.07
MnO	0.36	0.02	
MgO	9.96	13.89	
CaO	1.00		6.54
Na_2O		0.17	
K_2O		9.66	0.14
	100.9	95.9	98.1

VO-87-157-2 (Ptn)

	gt	opx	pl	gt(m)	bi(m)
SiO_2	38.12	50.53	58.75	37.64	35.24
TiO_2		0.05			6.65
Al_2O_3	22.78	2.02	26.40	22.47	15.06
FeO	28.62	27.35		17.94	
MnO	0.91	0.15		0.92	
MgO	6.75	19.04		6.71	10.83
CaO	2.92	0.25	7.88	2.78	
Na_2O			6.70		0.11
K_2O			0.51		8.99
	100.1	99.4	100.2	100.2	94.8

VO-87-175 (Ptn)

	gt(c)	gt(r)	opx(r)	opx(c)	pl(c)	pl(r)
SiO_2	37.13	37.20	49.29	49.09	47.40	47.02
TiO_2			0.05	0.09		
Al_2O_3	22.15	22.25	1.04	0.95	33.09	33.72
FeO	28.03	28.51	30.32	30.81		0.19
MnO	0.59	0.67	0.10	0.09		
MgO	4.52	4.33	15.97	15.55		
CaO	6.55	6.73	0.70	0.80	16.31	16.61
Na_2O			0.02		2.27	2.13
K_2O						0.05
	99.0	99.7	97.5	97.4	99.1	99.7

VO-87-232 (Ptn)

	gt(c)	gt(r)	opx(r)	opx(c)	pl(c)	pl(r)	gt(m)	bi(m)
SiO_2	37.00	37.24	50.83	50.48	56.34	55.92	37.43	34.99
TiO_2		0.02						6.06
Al_2O_3	21.98	22.09	0.57	1.19	27.16	27.94	22.31	14.60
FeO	26.86	27.17	28.00	28.76		0.14	26.68	20.20
MnO	2.64	2.64	0.67	0.80			2.35	
MgO	4.05	3.72	18.54	17.92			4.42	9.84
CaO	6.66	6.79	0.42	0.60	9.47	9.87	6.75	0.08
Na_2O				0.02	5.91	5.94		0.01
K_2O					0.35	0.27		
	99.2	99.7	99.1	99.7	99.2	100.1	99.9	94.2

PE-85-157A (Ppn)

	cd(m)	gt(m)	pl	gt(m)	bi(m)	gt(m)
SiO_2	48.50	39.49	59.17	38.72	37.41	39.24
TiO_2					6.23	
Al_2O_3	32.94	22.10	25.63	22.17	15.70	22.24
FeO	4.45	28.65	0.11	27.83	12.46	29.19
MnO		0.27		0.30	0.10	0.31
MgO	10.75	9.63		9.22	13.77	9.23
CaO	0.02	1.25	7.31	1.20	0.04	1.22
Na_2O	0.07		8.36		0.06	
K_2O	0.01		0.17		9.95	
	96.8	101.4	100.8	99.5	95.7	101.5

BK-70-323A (Ppn)

	gt(c)	gt(r)	cd(r)	cd(c)	gt(m)	bi(m)	cd(m)	pl
SiO_2	38.50	38.30	48.91	49.30	39.12	35.72	48.85	62.25
TiO_2						3.48		
Al_2O_3	21.13	20.91	32.01	32.44	21.07	18.60	32.00	23.94
FeO	36.73	35.93	7.82	8.72	36.04	19.12	8.30	0.05
MnO	1.03	0.93			1.00			
MgO	3.67	3.34	8.55	7.65	3.39	8.73	8.29	
CaO	0.88	0.85			0.91			5.79
Na_2O			0.15	0.11		0.17	0.12	8.61
K_2O						9.08		0.14
	102.0	100.3	97.4	98.2	101.5	94.9	97.6	100.8

APPENDIX III

Major and trace element geochemistry of the Lake Michel intrusive suite. Trace elements in ppm. ns = not sought.

	unit Pxg									
	VO-86-050	802	887	1174	1188	910	811	PE108	PE100	1175
SiO_2	63.2	66.5	63.8	61.5	64.0	64.2	62.0	63.6	62.0	62.5
TiO_2	1.43	1.27	0.98	1.61	0.97	1.47	1.66	1.35	1.00	1.57
Al_2O_3	13.8	12.5	15.6	14.3	14.4	12.8	13.4	14.1	15.2	13.9
Fe_2O_3	2.6	2.5	2.4	3.5	2.3	3.0	4.2	1.9	1.0	3.2
FeO	4.3	3.2	4.0	4.6	4.0	3.7	3.6	5.5	6.0	4.7
MnO	0.10	0.08	0.13	0.13	0.12	0.11	0.12	0.11	0.12	0.13
MgO	1.30	1.30	0.80	1.40	1.00	1.40	1.70	1.20	1.00	1.30
CaO	3.97	3.04	4.52	4.75	3.84	3.28	3.57	3.82	3.81	4.52
Na_2O	3.00	2.60	3.40	3.20	2.90	2.90	2.80	3.10	3.60	3.00
K_2O	3.91	4.18	3.48	3.43	3.86	4.15	3.99	3.86	3.80	3.28
H_2O	1.20	0.70	0.50	0.50	1.20	0.80	1.00	0.70	1.10	0.50
P_2O_5	0.64	0.72	0.54	0.75	0.52	0.76	0.88	0.62	0.51	0.75
TOTAL	98.25	97.89	100.19	99.17	97.91	97.77	97.92	99.16	98.04	98.85
Ba	1203	2036	1638	1254	1519	1869	2307	1281	1549	1380
Nb	32	25	58	28	32	27	65	31	34	27
Rb	135	106	99	111	112	145	93	132	121	109
Sr	429	661	552	492	484	619	745	736	466	241
Y	81	78	57	80	75	67	63	66	71	78
Zr	784	611	796	659	873	689	731	678	871	349
Li	16	18	6	12	14	27	12	ns	ns	ns
Ga	28	21	29	28	17	26	ns	ns	ns	ns
Th	5	2	4	5	6	28	1	6	4	ns
Be	4	2	3.2	4.2	3.7	2.9	2.6	4.1	4.1	3.8
Co	14	12	10	12	10	14	10	12	10	14
Cr	15	18	12	15	12	22	19	31	27	11
Cu	17	20	12	15	16	18	18	30	32	16
La	100	90	92	91	99	120	110	89	95	85
Ni	46	67	56	47	50	65	76	49	52	42
V	57	53	22	60	22	61	65	49	19	48
Yb	7.2	6.5	5.6	6.6	6.5	6.3	5.5	6.2	6.4	6.5
Zn	140	140	180	130	220	180	190	140	150	140

	unit Pxgk						unit Pgr				
	059	093	PE102	PE103	4030	1217	062	068	076	079	1198
SiO_2	65.3	63.5	59.8	66.0	59.5	60.2	66.0	66.2	63.9	64.4	63.8
TiO_2	1.01	1.18	1.67	0.90	1.72	1.55	1.18	1.02	1.20	1.13	1.18
Al_2O_3	14.4	15.3	14.7	14.6	14.9	14.7	13.1	13.8	14.6	14.9	14.6
Fe_2O_3	1.6	1.9	1.3	1.5	2.7	2.1	2.6	2.7	4.3	2.5	3.1
FeO	3.7	4.0	7.5	4.0	6.2	5.2	2.5	2.4	1.8	2.9	2.6
MnO	0.08	0.09	0.12	0.07	0.12	0.11	0.08	0.08	0.08	0.08	0.09
MgO	1.10	1.20	1.90	0.80	2.10	1.64	0.90	1.00	1.40	1.10	1.20
CaO	3.26	3.80	4.69	2.75	5.03	4.30	2.94	3.06	3.24	3.72	3.94
Na_2O	3.50	3.90	3.70	3.20	3.60	3.46	2.80	3.00	3.40	3.40	3.20
K_2O	3.93	3.62	2.88	4.24	2.78	3.76	4.63	4.39	4.41	4.03	4.10
H_2O	0.90	0.60	1.00	1.20	0.50	0.54	0.80	0.80	1.20	0.90	0.60
P_2O_5	0.34	0.38	0.51	1.20	0.52	0.50	0.57	0.58	0.66	0.58	0.64
TOTAL	98.22	98.87	98.77	99.26	99.17	98.06	97.30	98.23	98.99	98.74	98.45

APPENDIX III: (continued): Lake Michel intrusive suite

	unit Pxgk						unit Pgr				
	059	093	PE102	PE103	4030	1217	062	068	076	079	1198
Ba	958	1295	980	1314	1001	1240	1301	1147	1310	1198	1505
Nb	60	51	64	34	55	40	44	37	27	28	32
Rb	107	82	62	84	48	5	233	233	203	186	167
Sr	352	427	403	414	404	410	434	467	472	575	632
Y	45	33	53	36	67	60	108	104	53	68	86
Zr	525	590	743	594	641	810	652	536	531	462	513
Li	12	8	ns	ns	ns	ns	25	24	16	20	20
Ga	21	28	ns	ns	ns	17	25	21	26	22	26
Th	7	3	4	2	ns	ns	46	34	29	20	17
Be	2.8	2.7	2.9	2.1	3.0	ns	4.2	4.9	5.6	4.4	4.6
Co	11	12	19	11	20	ns	11	9	11	10	12
Cr	13	14	31	26	18	46	17	11	12	11	18
Cu	12	13	34	22	22	7	12	8	11	9	12
La	67	61	76	56	75	ns	140	120	85	84	94
Ni	34	47	45	47	43	35	45	37	45	39	53
V	47	64	88	36	100	100	45	36	49	41	52
Yb	4.1	4.2	5.2	3.5	6.1	ns	11	8.9	6.1	6.6	8.2
Zn	83	94	150	56	130	120	95	89	110	100	110

	unit Pgr	unit Pgk								
	4330	044	207	443-1	864	2079	2182	4128	PE109	PE110
SiO_2	66.7	75.2	71.8	68.3	70.7	74.5	71.1	67.5	68.9	72.6
TiO_2	0.91	0.29	0.40	0.76	0.54	0.32	0.52	0.93	0.74	0.31
Al_2O_3	14.1	12.2	14.1	14.0	13.7	13.5	14.0	14.1	14.1	12.4
Fe_2O_3	2.7	0.7	1.2	1.7	1.6	0.9	1.3	2.5	0.7	2.9
FeO	2.4	0.6	1.0	2.5	1.4	0.6	2.1	1.7	3.5	ns
MnO	0.08	0.02	0.03	0.06	0.05	0.02	0.05	0.06	0.06	0.03
MgO	0.80	0.20	0.40	0.70	0.50	0.30	0.40	0.80	0.60	0.20
CaO	2.89	0.56	1.34	2.07	1.49	0.66	1.66	2.46	2.13	0.66
Na_2O	3.10	2.60	3.50	3.30	3.20	3.10	3.30	3.30	3.30	2.70
K_2O	4.75	5.97	5.18	4.64	5.53	5.35	4.93	5.01	5.16	5.82
H_2O	0.50	0.50	0.60	0.90	0.50	0.60	0.70	0.50	0.50	0.80
P_2O_5	0.51	0.18	0.20	0.26	0.26	0.16	0.21	0.46	0.36	0.20
TOTAL	99.45	98.52	99.35	98.29	98.97	99.41	99.57	99.28	99.55	97.82
Ba	1218	727	642	834	1138	568	631	1577	1421	575
Nb	34	17	ns	50	69	ns	24	26	23	15
Rb	245	174	173	145	215	220	178	186	217	180
Sr	403	215	223	279	316	200	226	571	473	199
Y	116	14	ns	36	69	4	67	74	67	28
Zr	658	212	283	461	453	204	406	556	486	220
Li	27	6	10	10	10	ns	2	16	ns	ns
Ga	17	14	19	21	18	ns	26	20	ns	ns
Th	28	52	39	30	31	16	67	12	54	49
Be	4.8	1.0	3.0	3.1	2.7	2.2	3.2	2.7	4.0	1.4
Co	10	2	4	8	6	3	7	9	8	3
Cr	12	7	9	11	11	13	10	11	30	34
Cu	9	3	1	8	10	18	7	11	24	22
La	130	41	170	110	140	75	130	110	100	68
Ni	40	23	20	28	39	21	22	50	48	26
V	31	7	17	31	23	13	20	40	30	9
Yb	11	2	1.2	3.1	7.1	1.8	2.9	7.4	7.1	2.3
Zn	110	20	58	90	93	35	77	100	75	21

APPENDIX III: (continued): Lake Michel intrusive suite

	unit **Pgk**		unit **Pgp**		unit **Ppg**		unit **Pg**			
	PE104	4345	445	469	209	4134	443-2	468	481	642
SiO_2	68.8	69.8	68.3	64.6	60.4	61.4	66.6	71.1	68.1	74.5
TiO_2	0.39	0.84	0.76	0.93	1.62	1.47	0.49	0.27	0.37	0.18
Al_2O_3	15.2	12.9	14.0	14.7	14.2	13.9	16.5	16.0	16.6	13.8
Fe_2O_3	3.2	2.6	1.7	2.4	4.3	5.4	0.7	0.5	1.1	0.6
FeO	ns	1.6	2.5	3.6	3.1	3.1	2.1	1.3	1.4	0.6
MnO	0.03	0.06	0.06	0.10	0.11	0.12	0.04	0.03	0.04	0.02
MgO	0.50	0.80	0.70	0.90	1.70	1.40	0.70	0.60	0.80	0.10
CaO	1.51	2.16	2.07	3.60	4.44	3.62	1.68	3.11	3.24	1.08
Na_2O	3.60	2.70	3.30	3.00	3.40	3.00	3.60	5.20	5.40	3.60
K_2O	5.55	4.79	4.64	4.18	3.92	4.30	6.51	1.30	1.33	4.88
H_2O	0.70	ns	1.20	0.70	0.60	0.70	0.70	0.50	0.60	0.30
P_2O_5	0.20	0.41	0.26	0.46	0.77	0.73	0.22	0.18	0.21	0.14
TOTAL	98.98	98.66	98.29	98.47	97.96	99.17	99.14	99.77	98.59	99.50
Ba	813	1016	834	1394	2020	2326	2017	286	547	429
Nb	13	29	50	29	27	50	5	ns	5	34
Rb	245	240	145	166	115	144	163	73	56	298
Sr	270	329	279	429	953	605	551	538	681	146
Y	ns	69	36	70	52	148	68	ns	ns	ns
Zr	382	520	461	697	659	1059	341	111	125	168
Li	ns	ns	10	11	8	14	10	14	16	18
Ga	ns	ns	21	24	25	20	21	20	21	21
Th	130	ns	30	19	4	22	17	3	3	56
Be	2.5	3.6	3.1	3.7	3.8	3.0	1.7	2.7	2.0	3.4
Co	5	9	8	9	16	15	9	6	7	3
Cr	28	12	11	12	15	12	12	11	15	6
Cu	20	12	8	8	19	20	15	5	4	3
La	100	140	110	100	96	230	140	20	22	65
Ni	31	34	28	44	66	69	65	16	24	15
V	18	35	31	22	76	51	38	19	25	6
Yb	0.8	7.2	3.1	6.4	5.3	11	3.1	0.9	0.8	1.2
Zn	77	100	90	120	140	200	67	50	63	37

	unit **Pg**			
	814	PE101	PE105	476
SiO_2	73.4	66.3	76.20	74.4
TiO_2	0.33	1.01	0.18	0.31
Al_2O_3	13.9	13.2	12.10	13.4
Fe_2O_3	1.3	1.4	3.20	1.4
FeO	0.8	5.5	ns	0.8
MnO	0.03	0.14	0.07	0.02
MgO	0.40	0.90	ns	0.30
CaO	0.73	2.61	0.84	1.18
Na_2O	3.60	3.00	4.50	4.10
K_2O	5.33	4.73	2.80	3.33
H_2O^+	0.50	0.70	0.30	0.50
P_2O_5	0.18	0.48	0.13	0.16
TOTAL	100.00	99.27	100.02	99.56

APPENDIX III: (continued): Lake Michel intrusive suite

	unit Pg			
	814	PE101	PE105	476
Ba	987	2092	672	665
Nb	19	62	ns	27
Rb	137	119	38	109
Sr	331	385	96	241
Y	45	78	78	78
Zr	287	712	235	349
Li	4	ns	ns	ns
Ga	19	ns	ns	ns
Th	13	54	2	ns
Be	1.5	2.9	1.4	2.1
Co	4	9	3	3
Cr	9	33	32	8
Cu	7	30	25	1
La	110	100	26	120
Ni	34	68	30	23
V	17	16	5	12
Yb	4.5	6.8	3.9	3.2
Zn	47	170	72	34

APPENDIX III: (continued)
Major and trace element geochemistry of the Potato Hill pluton.

	unit Pcg			unit Pgg			unit Phg				unit Phg	
VO-87-	040A1	040A2	051	041	041B	052	061	057	086	055	084	076
SiO_2	62.7	61.9	64.1	68.8	57.6	65.7	56.8	59.9	61.8	60.7	61.1	64.1
TiO_2	1.10	1.09	0.99	0.59	1.56	0.80	1.88	1.73	1.33	1.51	1.55	1.23
Al_2O_3	15.3	15.8	15.7	12.9	13.4	13.3	13.6	13.2	14.4	13.8	12.7	13.6
Fe_2O_3	1.7	1.3	1.0	0.8	4.2	1.7	2.2	2.2	2.1	1.9	2.7	1.3
FeO	5.4	4.8	5.0	4.4	10.7	5.9	9.8	8.3	6.3	7.8	7.6	6.4
MnO	0.15	0.12	0.14	0.13	0.40	0.14	0.23	0.20	0.15	0.19	0.19	0.14
MgO	0.57	0.47	0.45	0.39	1.16	0.71	1.61	1.29	0.98	1.28	1.31	0.97
CaO	4.28	4.13	3.67	2.10	3.98	2.61	4.69	4.06	4.49	4.39	4.05	3.67
Na_2O	3.10	3.80	3.00	2.40	2.00	2.50	2.70	2.80	3.20	3.10	2.40	2.90
K_2O	3.98	4.20	4.88	5.26	3.29	4.86	3.96	3.64	3.06	3.44	4.06	4.27
H_2O	0.34	0.32	0.27	0.09	0.17	0.21	0.48	0.44	0.43	0.44	1.20	0.90
P_2O_5	0.40	0.40	0.40	0.50	1.00	0.90	1.40	1.30	1.00	1.11	0.46	0.30
	99.0	98.3	99.6	98.4	99.5	99.3	99.4	99.1	99.2	99.7	99.3	99.8
Ba	3209	3418	3756	3922	2885	2945	1645	1676	1917	1876	1279	181
Nb	27	25	28	15	39	12	71	53	37	43	51	46
Rb	83	83	92	119	92	136	121	106	64	77	113	94
Sr	529	556	496	356	300	311	266	312	420	372	295	281
Y	62	62	51	34	61	70	152	111	93	92	111	129
Zr	1587	1268	1441	1278	1502	1593	1723	1497	1253	1307	1440	1191
Ga	24	25	26	23	23	23	25	26	25	27	28	21
Zn	115	223	210	141	387	261	323	302	233	265	240	205

MAPS
NOT
FILMED

CARTES
OMISES